

Table of Contents

Schedule At A Glance	2
Sponsors	2
Highlights of Student Research in Basic Science and Electronic Ceramics Student Symposium	3
Hotel Floorplan	3
Plenary Speakers	4-5
Symposia	6-7
Presenting Author List	8-10

Final Program

Wednesday Morning	11-12
Wednesday Afternoon	12-15
Thursday Morning	15-17
Thursday Afternoon	17-20
Friday Morning	20-21
Friday Afternoon	21-24
Abstracts	25
Author Index	76

Basic Science Division Officers

Chair: JianLuo
Chair-Elect: Wayne Kaplan
Vice Chair: Eduardo Saiz
Secretary: Bryan Huey

Programming Chairs:
Bryan Huey, Adam Scotch

Electronics Division Officers

Trustee: Dwight Viehland
Chair: Quanxi Jia
Chair-Elect: Steven C. Tidrow
Vice-chair: Tim J. Haugan
Secretary: Haiyan Wang
Secretary-Elect: Geoff Brennecka

Programming Chairs:
Quanxi Jia, Haiyan Wang

Schedule At A Glance

Wednesday – January 23, 2013

Registration	7:30 a.m. – 6 p.m.	Oceans Ballroom Foyer
Opening Comments	8:30 a.m. – 8:45 a.m.	Indian
Plenary Session I	8:45 a.m. – 9:30 a.m.	Indian
Coffee Break	9:30 a.m. – 10 a.m.	Oceans Ballroom Foyer
Concurrent Technical Sessions	10 a.m. – 12:30 p.m.	Indian, Pacific, Coral A, Coral B, Mediterranean B/C
Lunch On Own	12:30 p.m. – 2 p.m.	
Poster Session Set-Up	12 p.m. – 5 p.m.	Atlantic/Arctic
Concurrent Technical Sessions	2 p.m. – 5:30 p.m.	Indian, Pacific, Coral A, Coral B, Mediterranean B/C
Coffee Break	3:30 p.m. – 4 p.m.	Oceans Ballroom Foyer
Poster Session & Reception	5:30 p.m. – 7:30 p.m.	Atlantic/Arctic

Thursday – January 24, 2013

Registration	7:30 a.m. – 5:30 p.m.	Oceans Ballroom Foyer
Plenary Session II	8:30 a.m. – 9:30 a.m.	Indian
Coffee Break	9:30 a.m. – 10 a.m.	Oceans Ballroom Foyer
Concurrent Technical Sessions	10 a.m. – 12:30 p.m.	Indian, Pacific, Coral A,
Coral B, Mediterranean B/C		
Lunch On Own	12:30 p.m. – 2 p.m.	
Concurrent Technical Sessions	2 p.m. – 5:30 p.m.	Indian, Pacific, Coral A, Coral B, Mediterranean B/C
Coffee Break	3:30 p.m. – 4 p.m.	Oceans Ballroom Foyer
Conference Dinner	7 p.m. – 9 p.m.	Atlantic/Arctic

Friday – January 25, 2013

Registration	7:30 a.m. – 5:30 p.m.	Oceans Ballroom Foyer
Plenary Session III	8:30 a.m. – 9:30 a.m.	Indian
Coffee Break	9:30 a.m. – 10 a.m.	Oceans Ballroom Foyer
Concurrent Technical Sessions	10 a.m. – 12:30 p.m.	Indian, Pacific, Coral A, Coral B, Mediterranean B/C
Lunch On Own	12:30 p.m. – 2 p.m.	
Concurrent Technical Sessions	2 p.m. – 5:30 p.m.	Indian, Pacific, Coral A, Coral B, Mediterranean B/C
Coffee Break	3:30 p.m. – 4 p.m.	Oceans Ballroom Foyer

Special Thanks to Our Sponsors For Their Generosity

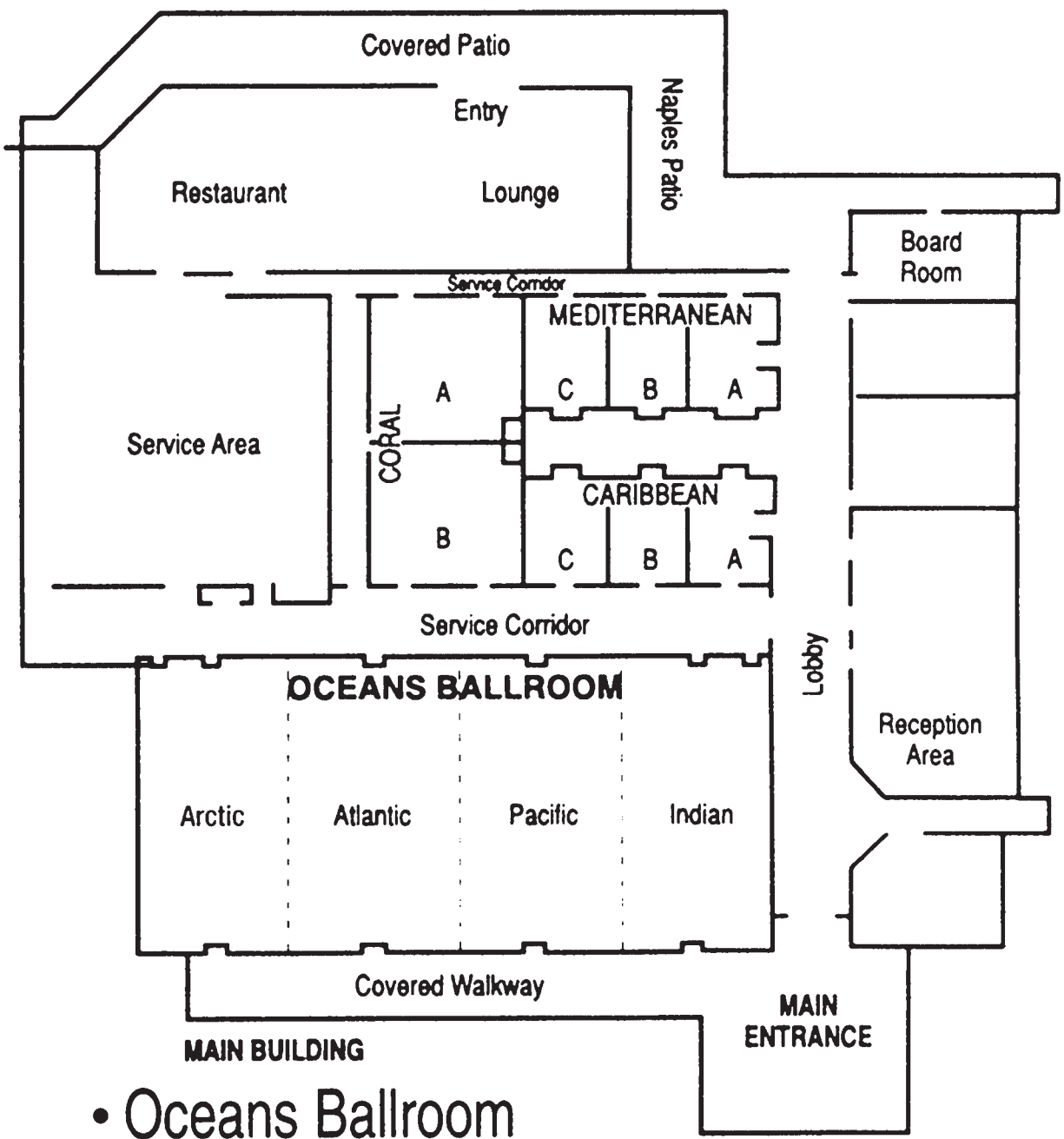


Highlights of Student Research in Basic Science and Electronic Ceramics – Student Symposium

Undergraduate student research is being conducted at universities all over the world, but rarely are these students allowed the opportunity to present their work at a meeting in front of their colleagues and esteemed professionals of the ceramics and materials community. This symposium will showcase undergraduate research to encourage innovation and involvement and to highlight the scientific contributions of undergraduate students to ceramics research.

Wednesday, January 23, 2013 – 12:15 p.m. – 1 p.m.

Doubletree by Hilton Floor Plan



- Oceans Ballroom

2013 EMA Plenary Speakers

Indian Room

Wednesday, January 23th

8:30 a.m. – 8:45 a.m. Opening Remarks



8:45 a.m. – 9:30 a.m.

Ramamoorthy Ramesh, Purnendu Chatterjee Chair Professor, Materials Science/Physics, University of California, Berkeley

Title: Pulsed Laser Deposition : God's Gift to Complex Oxides Creating New States of Matter with Oxide Heteroepitaxy

Ramesh graduated from the University of California, Berkeley with a PhD in 1987. Previously, he was Distinguished University Professor at the University of Maryland College Park. From 1989-1995, at Bellcore, he initiated research in several key areas of oxide electronics, including ferroelectric nonvolatile memories. His landmark contributions in ferroelectrics came through the recognition that conducting oxide electrodes are the solution to the problem of polarization fatigue, which for 30 years, remained an enigma and unsolved problem. His current research interests include thermoelectric and photovoltaic energy conversion in complex oxide heterostructures. He has published extensively on the synthesis and materials physics of complex oxide materials. He received the Humboldt Senior Scientist Prize and Fellowship to the American Physical Society (2001). In 2005, he was elected a Fellow of American Association for the Advancement of Science as well as the David Adler Lectureship of the American Physical Society. In 2007, he was awarded the Materials Research Society David Turnbull Lectureship Award, in 2009, he was elected Fellow of MRS and is the recipient of the 2010 APS McGroddy New Materials Prize. From December 2010 to August 2012 he served as the Founding Director of the SunShot Initiative at the U.S. Department of Energy, overseeing and coordinate the R&D activities of the U.S. Solar Program. In 2011, he was elected to the National Academy of Engineering.



Thursday, January 24th

8:30 a.m. – 9:30 a.m.

Rainer Waser, director, Institute of Solid State Research (IFF) at the HGF Research Center, Jülich, Germany

Title: Complexity at Work - Nanoionic Memristive Switches

Waser received his PhD in physical chemistry at the University of Darmstadt in 1984, and worked at the Philips Research Laboratory, Aachen, until he was appointed Professor at the faculty for Electrical Engineering and Information Technology of the RWTH Aachen University in 1992 and director of the Institute for Electronic Materials at the Forschungszentrum Jülich, in 1997. He is member of the Emerging Research Devices working group of the ITRS, and he has been collaborating with major semiconductor industries in Europe, the US, and the Far East. Since 2002, he has been the coordinator of the research program on nanoelectronic systems within the Germany national research centres in the Helmholtz Association. In 2007, he has been co-founder of the Jülich-Aachen Research Alliance, section Fundamentals of Future Information Technology (JARA-FIT). Together with Professor Wuttig, he heads a collaborative research center on resistively switching chalcogenides for future electronics (SFB 917) which comprises of 14 institutes within JARA-FIT and has been funded by the German national science foundation (DFG) since 2011.

2013 EMA Plenary Speakers

Indian Room



Friday, January 25th

8:30 a.m. – 9:30 a.m.

Kitt Reinhardt, Program Manager, Air Force Office of Scientific Research

Title: Material Science and Device Physics Challenges for Near-Real-Time Adaptive Monolithic Multimodal Sensing

Reinhardt holds a BS and MS in Electrical Engineering from the State University of New York at Buffalo (86,88). He received a doctorate degree in Engineering Physics from the Air Force Institute of Technology in 1994 for experimental research in high-energy space radiation interactions with surface and bulk electronic defects and junction current transport

phenomena in GaInP p/n junctions. Reinhardt joined the Air Force Research Laboratory in 1988 to pursue in-house research in sub- μm GaAs X-band microwave device and circuit design. Physics based modeling, simulation and characterization of GaAs, GaAs/Ge, and GaInP/GaAs/Ge p/n solar cells soon followed, before turning to electrical defect studies in diamond and SiC materials important for high-temperature power device applications. Returning to solar cells in the late 1990's, Reinhardt fostered a series of innovative multijunction solar cell research programs with industry and academia which ultimately resulted in today's world-record 30% efficient triple-junction GaInP/GaAs/Ge solar cells. This solar cell design is currently used on all U.S. Air Force and most commercial satellites launched today. For this contribution, Reinhardt and his AFRL research group was inducted into the U.S. Space Technology Hall of Fame in 2004. He received a Rotary National Stellar Award for Space Achievement in 2000 and led a definitive National Research Council study on NASA's Solar Power Program in 2001. Reinhardt was detailed to NASA GSFC in 2002 to coordinate collaborative research in remote sensing, power generation and radiation-hardened electronics. He returned in 2003 to lead AFRL's electronics space-radiation effects group employing in-house γ - and X-ray sources, 3D-poisson solver predictive tools and ab-initio and density functional modeling methods. In 2005, Reinhardt rotated to the Air Force Office of Scientific Research to establish a new basic research portfolio to address key solid-state materials science and device physics challenges preventing developments in adaptive monolithically integrated mixed-mode optical and infrared sensing.

Symposia

The 2013 Organizing Committee:

Quanxi Jia, Electronics Division
Bryan Huey, Basic Science Division
Tim Haugan, Electronics Division

S1: Functional and Multifunctional Electroceramics for Energy Storage, Conversion, and Harvesting, Detectors, Sensors, Frequency Agile Components, Packaging, Interconnects and Other Commercial Opportunities

Organizers: Steven C. Tidrow, The University of Texas – Pan American; Clive Randall, Pennsylvania State University; Shashank Priya, Virginia Polytechnic Institute and State University

S2: Multiferroic Materials and Multilayer Ferroic Heterostructures: Properties and Applications

Organizers: Melanie W. Cole, U.S. Army Research Laboratory; Ichiro Takeuchi, University of Maryland; Valanoor Nagarajan, The University of New South Wales; S. Pamir Alpay, University of Connecticut; Joseph V. Mantese, United Technologies Research Center

S3: Structure of Emerging Perovskite Oxides: Bridging Length Scales and Unifying Experiment and Theory

Organizers: Jacob L. Jones, University of Florida; David Cann, Oregon State University; Dragan Damjanovic, EPFL; Julia Glaum, UNSW; Simon R. Phillpot, University of Florida; Matthew Suchomel, Argonne National Laboratory; Xiaoli Tan, Iowa State University; Yu Wang, Michigan Tech

S4: LEDs and Photovoltaics Beyond the Light: Common Challenges and Opportunities

Organizers: Adam M. Scotch, OSRAM SYLVANIA; Erik D. Spoeerke, Sandia National Laboratories

S5: Structure and Properties of Interfaces in Electronic Materials

Organizers: John Blendell, Purdue University; R. Edwin García, Purdue University; Shen Dillon, University of Illinois

S6: Thermoelectrics: Defect Chemistry, Doping and Nanoscale Effects

Organizers: Alp Sehriioglu, Case Western Reserve University; Anke Weidenkaff, EMPA; Jon Ihlefeld, Sandia National Laboratories; Antoine Maignan, CRISMAT Laboratory

S7: Production Quality Ferroelectric Thin Films and Devices

Organizers: Ronald G. Polcawich US Army Research Laboratory; Glen Fox, Fox Materials Consulting; Geoff Brennecke, Sandia National Laboratories

S8: Advances in Memory Devices

Organizers: Bryan D. Huey, University of Connecticut; Glen Fox, Fox Materials Consulting

S9: Thin Film Integration and Processing Science

Organizers: Brady J. Gibbons, Oregon State University; Jon Ihlefeld, Sandia National Laboratories; Jon-Paul Maria, North Carolina State University

S10: Ceramic Composites for Defense Applications

Organizers: Edward P. Gorzkowski, Naval Research Laboratory; Ed Stutz, AFRL/RXPS, Wright-Patterson AFB; Ronald G. Polcawich, US Army Research Laboratory

Symposia

S11: Sustainable, Low Critical Material Use and Green Materials Processing Technologies

Organizers: Paul Clem, Sandia National Laboratories; Stephan Krohns, University of Augsburg

S12: Recent Developments in High Temperature Superconductivity

Organizers: Haiyan Wang, Texas A&M University; Timothy J. Haugan, The Air Force Research Laboratory; Quanxijia, Los Alamos National Laboratory

S13: Body Energy Harvesting for Intelligent Systems

Organizers: Wolfgang Sigmund, University of Florida, USA; Hanyang University; Seungbum Hong, Argonne National Laboratory

S14: Nanoscale Electronic Materials and Devices

Organizer: Michael Lilly, Sandia National Laboratories

S15: Failure-The Greatest Teacher

Organizers: Geoff Brenneka, Sandia National Laboratories; Jon Ihlefeld, Sandia National Laboratories; Jon-Paul Maria, North Carolina State University

S16: Highlights of Student Research in Basic Science and Electronic Ceramics

Organizers: Kelsey Meyer, New Mexico Institute of Mining and Technology; Troy Ansell, Oregon State University; Geoff Brenneka, Sandia National Laboratories

MEETING REGULATIONS

The American Ceramic Society is a nonprofit scientific organization that facilitates the exchange of knowledge meetings and publication of papers for future reference. The Society owns and retains full right to control its publications and its meetings. The Society has an obligation to protect its members and meetings from intrusion by others who may wish to use the meetings for their own private promotion purpose. Literature found not to be in agreement with the Society's goals, in competition with Society services or of an offensive nature will not be displayed anywhere in the vicinity of the meeting. Promotional literature of any kind may not be displayed without the Society's permission and unless the Society provides tables for this purpose. Literature not conforming to this policy or displayed in other than designated areas will be disposed. The Society will not permit unauthorized scheduling of activities during its meeting by any person or group when those activities are conducted at its meeting place in interference with its programs and scheduled activities. The Society does not object to appropriate activities by others during its meetings if it is consulted with regard to time, place, and suitability. Any person or group wishing to conduct any activity at the time and location of the Society meeting must obtain permission from the Executive Director or Director of Meetings, giving full details regarding desired time, place and nature of activity.

During oral sessions conducted during Society meetings, **unauthorized photography, videotaping and audio recording is prohibited**. Failure to comply may result in the removal of the offender from the session or from the remainder of the meeting.

The American Ceramic Society plans to take photographs and video at the conference and reproduce them in educational, news or promotional materials, whether in print, electronic or other media, including The American Ceramic Society's website. By participating in the conference, you grant The American Ceramic Society the right to use your name and photograph for such purposes. All postings become the property of The American Ceramic Society.

Registration Requirements: Attendance at any meeting of the Society shall be limited to duly registered persons.

Disclaimer: Statements of fact and opinion are the responsibility of the authors alone and do not imply an opinion on the part of the officers, staff or members of The American Ceramic Society. The American Ceramic Society assumes no responsibility for the statements and opinions advanced by the contributors to its publications or by the speakers at its programs; nor does The American Ceramic Society assume any liability for losses or injuries suffered by attendees at its meetings. Registered names and trademarks, etc. used in its publications, even without specific indications thereof, are not to be considered unprotected by the law. Mention of trade names of commercial products does not constitute endorsement or recommendations for use by the publishers, editors or authors.

Final determination of the suitability of any information, procedure or products for use contemplated by any user, and the manner of that use, is the sole responsibility of the user. Expert advice should be obtained at all times when implementation is being considered, particularly where hazardous materials or processes are encountered.

Copyright © 2013. The American Ceramic Society (www.ceramics.org). All rights reserved.

Presenting Author List

Oral Presenters

Name	Date	Time	Room	Page Number	Name	Date	Time	Room	Page Number
A					G				
Ahn, C.	23-Jan	2:00PM	Coral A	13	Gao, P.	23-Jan	10:30AM	Coral A	12
Allendorf, M.D.	24-Jan	12:45PM	Mediterranean B/C	17	Gao, P.	23-Jan	4:30PM	Mediterranean B/C	14
Amani, M.	23-Jan	11:45AM	Coral B	12	Ghosh, D.	23-Jan	2:30PM	Mediterranean B/C	14
Amemiya, N.	24-Jan	10:30AM	Indian	17	Gibbons, B.J.	24-Jan	3:15PM	Mediterranean B/C	19
Andrew, J.S.	24-Jan	3:00PM	Coral A	18	Glaum, J.	24-Jan	10:15AM	Pacific	16
Annappagada, S.	25-Jan	3:30PM	Coral A	22	Gorzowski, E.	25-Jan	4:30PM	Pacific	23
Ansell, T.	25-Jan	4:15PM	Coral B	22	Goyal, A.	23-Jan	2:00PM	Indian	14
Aoyagi, R.	24-Jan	3:00PM	Coral B	18	Graham, J.T.	25-Jan	10:30AM	Coral B	20
Appelhans, L.N.	25-Jan	3:00PM	Pacific	23	Grasso, G.	25-Jan	10:00AM	Indian	21
Armistead, P.	25-Jan	2:00PM	Pacific	23	Grin, Y.	24-Jan	2:00PM	Pacific	18
B					H				
Backhaus-Ricoult, M.	25-Jan	10:00AM	Pacific	20	Han, Y.	25-Jan	3:15PM	Coral B	22
Barrett, C.A.	23-Jan	10:45AM	Coral A	12	Harris, D.T.	24-Jan	4:45PM	Mediterranean B/C	19
Berbano, S.S.	23-Jan	3:15PM	Coral B	13	Haruyama, J.	23-Jan	4:30PM	Indian	14
Berry, J.J.	24-Jan	11:55AM	Mediterranean B/C	17	Haugan, T.	25-Jan	3:45PM	Indian	24
Bhalla, A.	24-Jan	4:00PM	Coral B	18	Hebert, S.	24-Jan	3:00PM	Pacific	18
Bock, J.A.	25-Jan	11:15AM	Pacific	21	Hellstrom, E.	25-Jan	11:30AM	Indian	21
Booth, J.	25-Jan	11:30AM	Coral A	20	Hishinuma, Y.	25-Jan	5:00PM	Coral A	22
Bosse, J.	23-Jan	11:15AM	Coral B	11	Hoffmann, M.J.	23-Jan	2:00PM	Mediterranean B/C	14
Brogli, G.	23-Jan	11:30AM	Coral B	12	Huey, B.D.	23-Jan	10:30AM	Coral B	11
Brown-Shaklee, H.J.	24-Jan	2:45PM	Coral B	18	Huey, B.D.	23-Jan	3:00PM	Coral A	13
Bux, S.	24-Jan	11:00AM	Pacific	17	Huey, B.D.	24-Jan	11:40AM	Mediterranean B/C	17
C					I				
Caillat, T.	24-Jan	11:15AM	Pacific	17	Ilhfeld, J.	25-Jan	11:45AM	Pacific	21
Cantoni, C.	24-Jan	4:30PM	Indian	19	Ilhfeld, J.	25-Jan	2:45PM	Mediterranean B/C	23
Carman, G.	23-Jan	4:30PM	Coral A	13	Izumi, T.	23-Jan	10:30AM	Indian	12
Carter, J.J.	23-Jan	12:15PM	Coral A	12	J				
Chan, H.M.	23-Jan	10:00AM	Mediterranean B/C	11	Jia, Q.X.	23-Jan	11:00AM	Coral A	12
Chen, C.	23-Jan	4:00PM	Coral A	13	Jia, Q.X.	24-Jan	5:00PM	Indian	19
Chen, L.	24-Jan	5:45PM	Indian	20	Jin, Y.M.	23-Jan	10:45AM	Coral B	11
Christen, H.M.	25-Jan	10:45AM	Mediterranean B/C	21	Jin, Y.M.	24-Jan	12:00PM	Coral A	16
Civale, L.	24-Jan	4:00PM	Indian	19	Jones, J.L.	25-Jan	10:00AM	Coral A	20
Clem, P.	23-Jan	5:00PM	Mediterranean B/C	14	Joyce, D.	25-Jan	5:00PM	Pacific	23
Coll, M.	23-Jan	2:30PM	Indian	14	Jung, J.	23-Jan	3:15PM	Mediterranean B/C	14
Coll, M.	25-Jan	12:00PM	Mediterranean B/C	21	K				
Cruz-Campa, J.L.	24-Jan	11:15AM	Mediterranean B/C	17	Kakimoto, K.	24-Jan	10:30AM	Coral B	16
Culp, S.	24-Jan	10:30AM	Pacific	17	Kalem, V.	24-Jan	4:45PM	Coral A	18
D					Kaplan, W.D.	23-Jan	11:00AM	Mediterranean B/C	11
Damjanovic, D.	24-Jan	3:30PM	Coral B	18	Karlicek, R.F.	24-Jan	10:00AM	Mediterranean B/C	16
Daniels, J.	23-Jan	4:15PM	Pacific	13	Kato, K.	24-Jan	2:00PM	Mediterranean B/C	19
Deepak, N.	24-Jan	3:15PM	Coral A	18	Kim, J.	23-Jan	2:45PM	Mediterranean B/C	14
Deepak, N.	25-Jan	11:45AM	Coral B	20	Kim, S.	23-Jan	4:45PM	Coral B	13
Denis, L.M.	23-Jan	12:30PM	Coral A	12	Kim, S.	25-Jan	4:30PM	Indian	24
DiAntonio, C.	25-Jan	3:15PM	Pacific	23	Kiss, T.	23-Jan	11:30AM	Indian	12
Dias, A.	24-Jan	5:15PM	Coral B	18	Kodumudi Venkataraman, L.	25-Jan	4:45PM	Coral B	22
Dillon, S.J.	23-Jan	10:30AM	Mediterranean B/C	11	Kolte, J.	24-Jan	4:15PM	Coral A	18
E					Korobova, N.	25-Jan	5:15PM	Mediterranean B/C	23
Eblen, M.	23-Jan	12:00PM	Mediterranean B/C	11	Kowalski, B.	23-Jan	5:15PM	Coral B	13
Edwards, D.	25-Jan	10:45AM	Pacific	21	Kral, K.	23-Jan	10:00AM	Coral A	12
Ehmke, M.C.	23-Jan	2:30PM	Pacific	13	Kreisel, J.	23-Jan	10:00AM	Pacific	11
Eshita, T.	25-Jan	4:00PM	Coral A	22	Krohns, S.	25-Jan	12:15PM	Coral A	20
Evans, J.T.	23-Jan	12:00PM	Coral B	12	Kumakura, H.	25-Jan	10:30AM	Indian	21
F					Kumar, N.	24-Jan	10:00AM	Pacific	16
Fancher, C.M.	25-Jan	12:00PM	Coral B	20	Kutnjak, Z.	24-Jan	2:45PM	Coral A	18
Ferekides, C.	24-Jan	10:25AM	Mediterranean B/C	16	Kutnjak, Z.	25-Jan	3:45PM	Coral A	22
Ferguson, I.	24-Jan	10:50AM	Mediterranean B/C	16	L				
Finkel, P.	25-Jan	2:00PM	Coral B	21	Larbalestier, D.	24-Jan	10:00AM	Indian	17
Fjeld, H.	24-Jan	2:30PM	Pacific	18	Laudenslager, M.	23-Jan	4:45PM	Mediterranean B/C	14
Foley, B.M.	25-Jan	11:30AM	Pacific	21	Lee, J.	23-Jan	4:15PM	Coral A	13
Foley, B.M.	25-Jan	2:30PM	Coral B	22	Lee, S.	25-Jan	12:00PM	Indian	21
Forrester, J.S.	25-Jan	4:00PM	Coral B	22	Lee, Y.	24-Jan	12:20PM	Mediterranean B/C	17
Fox, A.	25-Jan	5:00PM	Mediterranean B/C	23	Levin, G.A.	24-Jan	12:00PM	Indian	17
Freer, R.	24-Jan	2:45PM	Pacific	18	Levin, I.	23-Jan	2:45PM	Pacific	13
Funahashi, R.	24-Jan	12:00PM	Pacific	17	Li, J.	23-Jan	5:00PM	Pacific	14
Furman, E.	25-Jan	4:45PM	Pacific	23	Li, J.	24-Jan	3:00PM	Mediterranean B/C	19

Oral Presenters

Name	Date	Time	Room	Page Number	Name	Date	Time	Room	Page Number
Li, Q.	25-Jan	2:00PM	Indian	23	Schaefer, B.	23-Jan	12:45PM	Coral A	12
Liu, C.	24-Jan	11:15AM	Coral B	16	Seidel, J.	23-Jan	2:30PM	Coral A	13
Liu, Y.	23-Jan	3:15PM	Pacific	13	Seifkar, S.	25-Jan	10:30AM	Mediterranean B/C	21
Luo, J.	23-Jan	11:30AM	Mediterranean B/C	11	Selvamanickam, V.	23-Jan	11:00AM	Indian	12
M					Seo, I.	25-Jan	12:15PM	Coral B	20
Mackey, J.	24-Jan	11:30AM	Pacific	17	Seshadri, S.B.	25-Jan	4:30PM	Coral B	22
MacManus-Driscoll, J.	23-Jan	10:00AM	Indian	12	Shelton, C.T.	23-Jan	3:00PM	Mediterranean B/C	14
Mader, W.	23-Jan	10:15AM	Coral A	12	Sinclair, D.	24-Jan	2:00PM	Coral B	17
Maier, R.	25-Jan	2:45PM	Coral B	22	Singh, A.K.	23-Jan	11:15AM	Coral A	12
Maignan, A.	24-Jan	11:45AM	Pacific	17	Singh, G.	23-Jan	2:30PM	Coral B	12
Maiorov, B.	24-Jan	5:15PM	Indian	19	Singh, K.C.	24-Jan	12:15PM	Coral B	16
Mardilovich, P.	25-Jan	3:00PM	Mediterranean B/C	23	Smith, A.	25-Jan	3:00PM	Coral B	22
Maso, N.	23-Jan	11:00AM	Coral B	11	Solovyov, V.	23-Jan	3:00PM	Indian	14
Maso, N.	24-Jan	4:00PM	Coral A	18	Song, X.	24-Jan	4:00PM	Pacific	19
Maso, N.	24-Jan	4:30PM	Coral A	18	Spoerke, E.	23-Jan	8:00PM	Coral A	14
Medlin, D.L.	24-Jan	4:15PM	Pacific	19	Srinivasan, G.	24-Jan	2:30PM	Coral A	18
Meletis, E.I.	23-Jan	4:45PM	Coral A	13	Stemmer, S.	25-Jan	11:00AM	Coral A	20
Mirsaneh, M.	23-Jan	5:00PM	Coral B	13	Sumption, M.D.	25-Jan	11:00AM	Indian	21
Mitic, V.	25-Jan	2:15PM	Coral B	21	Sun, N.	25-Jan	2:00PM	Coral A	22
Moballeggh, A.	25-Jan	10:30AM	Pacific	21	Suu, K.	25-Jan	4:30PM	Coral A	22
N					T				
Nahm, S.	25-Jan	11:15AM	Coral B	20	Tagantsev, A.K.	24-Jan	11:00AM	Coral A	16
Nakamura, T.	25-Jan	3:00PM	Indian	24	Takato, M.	23-Jan	2:45PM	Coral B	12
Nakhmanson, S.	24-Jan	10:00AM	Coral A	16	Takeuchi, I.	24-Jan	2:30PM	Mediterranean B/C	19
Newman, N.	25-Jan	3:15PM	Coral A	22	Talvacchio, J.	23-Jan	2:00PM	Coral B	12
Nishi, T.	24-Jan	12:00PM	Coral B	16	Tan, X.	23-Jan	3:00PM	Coral B	13
Nittala, K.	24-Jan	4:30PM	Mediterranean B/C	19	Tan, X.	23-Jan	4:45PM	Pacific	13
O					Tang, M.	23-Jan	3:30PM	Mediterranean B/C	14
Ogino, H.	24-Jan	2:30PM	Indian	19	ten Elshof, J.E.	25-Jan	11:15AM	Mediterranean B/C	21
Onuta, T.	25-Jan	3:00PM	Coral A	22	Thomas, P.A.	23-Jan	11:00AM	Pacific	11
P					Tompa, G.S.	24-Jan	4:45PM	Pacific	19
Pamidi, S.V.	24-Jan	11:30AM	Indian	17	Tomsic, M.	24-Jan	11:00AM	Indian	17
Pan, X.	24-Jan	4:00PM	Mediterranean B/C	19	Triamnak, N.	24-Jan	2:30PM	Coral B	17
Paul Antony, A.	25-Jan	4:15PM	Indian	24	Trolier-McKinstry, S.	25-Jan	10:00AM	Coral B	20
Poepplmeier, K.	23-Jan	10:30AM	Pacific	11	Tsai, C.	23-Jan	5:00PM	Indian	14
Pojprapai, S.	24-Jan	11:00AM	Coral B	16	Tsuda, M.	25-Jan	2:30PM	Indian	23
Pokale, G.B.	24-Jan	5:00PM	Coral B	18	Tsurumi, T.	23-Jan	4:00PM	Coral B	13
Polcawich, R.G.	25-Jan	2:00PM	Mediterranean B/C	22	U				
Ponomareva, I.	24-Jan	11:30AM	Coral A	16	Usher, T.	24-Jan	10:45AM	Coral B	16
Q					V				
Qiao, Q.	23-Jan	12:15PM	Mediterranean B/C	11	Veber, A.	25-Jan	4:45PM	Mediterranean B/C	23
Qing, R.	23-Jan	4:30PM	Coral B	13	W				
R					Wada, S.	25-Jan	2:30PM	Pacific	23
Raengthon, N.	24-Jan	3:15PM	Coral B	18	Walenza-Slabe, J.	25-Jan	2:30PM	Mediterranean B/C	22
Ramesh, R.	23-Jan	8:45AM	Indian	11	Wang, H.	25-Jan	4:00PM	Mediterranean B/C	23
Ramprasad, R.	24-Jan	10:30AM	Coral A	16	Wang, Y.U.	23-Jan	12:00PM	Pacific	11
Randall, C.	23-Jan	8:30PM	Coral A	14	Wang, Y.U.	24-Jan	11:30AM	Coral B	16
Randall, C.	25-Jan	4:00PM	Pacific	23	Wardle, B.	25-Jan	5:00PM	Indian	24
Rao, B.	23-Jan	12:15PM	Pacific	11	Waser, R.	24-Jan	8:30AM	Indian	15
Reaney, I.M.	25-Jan	10:30AM	Coral A	20	West, A.R.	25-Jan	11:00AM	Pacific	21
Reinhardt, K.	25-Jan	8:30AM	Indian	20	Whatmore, R.W.	24-Jan	2:00PM	Coral A	18
Ren, X.	23-Jan	2:00PM	Pacific	13	Wu, J.	23-Jan	4:00PM	Indian	14
Ren, X.	24-Jan	4:45PM	Coral B	18	Wu, M.	25-Jan	2:45PM	Coral A	22
Rey, C.	25-Jan	3:30PM	Indian	24	X				
Rijnders, G.	25-Jan	10:00AM	Mediterranean B/C	21	Xi, X.	24-Jan	3:00PM	Indian	19
Rodriguez, J.	23-Jan	10:00AM	Coral B	11	Y				
Roedel, J.	24-Jan	10:00AM	Coral B	16	Yamamoto, H.	24-Jan	2:00PM	Indian	19
Roelofs, A.	25-Jan	11:30AM	Mediterranean B/C	21	Yan, Y.	23-Jan	3:30PM	Coral B	13
Rogers, M.	25-Jan	11:00AM	Coral B	20	Yang, H.	25-Jan	12:00PM	Coral A	20
Rossetti, G.A.	23-Jan	11:30AM	Pacific	11	Z				
S					Zhu, J.	24-Jan	4:30PM	Coral B	18
Sachet, E.	25-Jan	10:45AM	Coral B	20	Zou, G.	24-Jan	5:00PM	Mediterranean B/C	19
Sanchez, L.M.	25-Jan	4:30PM	Mediterranean B/C	23					
Sbrockey, N.M.	25-Jan	2:30PM	Coral A	22					

Presenting Author List

Poster Presenters

<u>Name</u>	<u>Date</u>	<u>Time</u>	<u>Room</u>	<u>Page Number</u>	<u>Name</u>	<u>Date</u>	<u>Time</u>	<u>Room</u>	<u>Page Number</u>
Akhtar, M.	23-Jan	5:30PM	Atlantic/Arctic	15	Kumar, N.	23-Jan	5:30PM	Atlantic/Arctic	15
Albuquerque, E.	23-Jan	5:30PM	Atlantic/Arctic	15	Mitic, V.	23-Jan	5:30PM	Atlantic/Arctic	15
Amani, M.	23-Jan	5:30PM	Atlantic/Arctic	15	Nolan, M.M.	23-Jan	5:30PM	Atlantic/Arctic	15
Brown-Shaklee, H.J.	23-Jan	5:30PM	Atlantic/Arctic	15	Okamoto, T.	23-Jan	5:30PM	Atlantic/Arctic	15
Brunke, L.	23-Jan	5:30PM	Atlantic/Arctic	15	Pierce, B.	23-Jan	5:30PM	Atlantic/Arctic	15
Burch, M.J.	23-Jan	5:30PM	Atlantic/Arctic	15	Prasertpalichat, S.	23-Jan	5:30PM	Atlantic/Arctic	15
Chu, B.	23-Jan	5:30PM	Atlantic/Arctic	15	Pudasaini, P.	23-Jan	5:30PM	Atlantic/Arctic	15
Drew, D.	23-Jan	5:30PM	Atlantic/Arctic	15	Rhee, K.	23-Jan	5:30PM	Atlantic/Arctic	15
Haugan, T.J.	23-Jan	5:30PM	Atlantic/Arctic	15	Song, J.	23-Jan	5:30PM	Atlantic/Arctic	15
Hayakawa, N.	23-Jan	5:30PM	Atlantic/Arctic	15	Thomas, E.L.	23-Jan	5:30PM	Atlantic/Arctic	15
Henriques, A.J.	23-Jan	5:30PM	Atlantic/Arctic	15	Tidrow, S.	23-Jan	5:30PM	Atlantic/Arctic	15
Kim, H.	23-Jan	5:30PM	Atlantic/Arctic	15	Yoon, S.	23-Jan	5:30PM	Atlantic/Arctic	15
Kim, S.	23-Jan	5:30PM	Atlantic/Arctic	15					

Wednesday, January 23, 2013

Plenary Session I

Room: Indian

8:30 AM

Opening Remarks

Organizing Committee: Quanxi Jia, Bryan Huey, Timothy Haugan

8:45 AM

(EMA-PL-001-2013) Pulsed Laser Deposition : God's Gift to Complex Oxides Creating New States of Matter with Oxide Heteroepitaxy (Invited)

R. Ramesh*, University of California, Berkeley, USA

9:30 AM

Break

S3: Structure of Emerging Perovskite Oxides: Bridging Length Scales and Unifying Experiment and Theory

Session 1

Room: Pacific

Session Chairs: John Daniels, University of New South Wales; Julia Glaum, The University of New South Wales

10:00 AM

(EMA-S3-001-2013) The local and average structure in lead-free BaTiO₃-based perovskites (Invited)

J. Kreisel*, CRP Lippmann & Luxembourg University, Luxembourg

10:30 AM

(EMA-S3-002-2013) Noncentrosymmetric Oxyfluoride Compounds (Invited)

K. Poeppelmeier*, Northern University, USA

11:00 AM

(EMA-S3-003-2013) Intermediate Phases at MPBs and analogous Temperature-driven Phase Transitions (Invited)

P. A. Thomas*, R. Beanland, University of Warwick, United Kingdom; S. Gorfman, University of Siegen, Germany; D. Keeble, University of Warwick, United Kingdom; J. Kreisel, Centre de Recherche Publique Gabriel Lippmann, Luxembourg; D. Woodward, University of Warwick, United Kingdom

11:30 AM

(EMA-S3-004-2013) Polar Anisotropy in Ferroelectric Perovskites: Theory and Experiment (Invited)

G. A. Rossetti*, University of Connecticut, USA

12:00 PM

(EMA-S3-005-2013) Nanodomain Structures, Mechanisms and Diffraction Effects in Morphotropic Phase Boundary Ferroelectrics

Y. U. Wang*, W. Rao, T. Cheng, J. Zhou, Michigan Tech, USA

12:15 PM

(EMA-S3-006-2013) Electric field induced structural transformation in Na_{1/2}Bi_{1/2}TiO₃

B. Rao*, R. Ranjan, Indian Institute of Science, India

S5: Structure and Properties of Interfaces in Electronic Materials**Grain Boundary Structure Dependent Properties**

Room: Mediterranean B/C

Session Chair: John Blendell, Purdue University

10:00 AM

(EMA-S5-001-2013) Alumina properties – pushing the (grain) boundaries (Invited)

H. M. Chan*, Q. Wu, M. Kracum, Z. Yu, J. M. Rickman, M. P. Harner, Lehigh University, USA

10:30 AM

(EMA-S5-002-2013) Orientation Dependence of Grain Boundary Thermal Conductance in Alumina (Invited)

S. J. Dillon*, K. Tai, University of Illinois Urbana-Champaign, USA

11:00 AM

(EMA-S5-003-2013) Structure and Energy of Equilibrated Ni-Alumina Interfaces (Invited)

H. Meltzman, W. D. Kaplan*, Technion - Israel Institute of Technology, Israel

11:30 AM

(EMA-S5-004-2013) Grain Boundary Complexion Diagrams: An Interfacial Counterpart to Bulk Phase Diagrams (Invited)

N. Zhou, Y. Zhang, J. Luo*, UCSD, USA

12:00 PM

(EMA-S5-005-2013) Thermal Conductivity of Thick Film Tungsten Metallization used in High-Alumina Ceramic Microelectronic Packages

M. Eblen*, Kyocera America, Inc., USA

12:15 PM

(EMA-S5-006-2013) 80 kV study of the Atomic Structure and Bonding at SrTiO₃/GaAs Hetero-interfaces

Q. Qiao*, S. Ogut, R. F. Klie, University of Illinois at Chicago, USA; R. Droopad, R. Contreras-Guerrero, Texas State University, USA

S8: Advances in Memory Devices**Fundamentals and Reliability**

Room: Coral B

Session Chair: Bryan Huey, University of Connecticut

10:00 AM

(EMA-S8-001-2013) Reliability of Ferroelectric Memory Embedded in 130nm CMOS (Invited)

J. Rodriguez*, Texas Instruments, USA

10:30 AM

(EMA-S8-002-2013) Improved Power Consumption for Ferroelectric Switching based on Nanoscale Switching Dynamics

N. Polomoff, S. Lee, J. Bosse, V. Palumbo, V. Vyas, M. Rivas, J. Leveillee, B. D. Huey*, University of Connecticut, USA

10:45 AM

(EMA-S8-003-2013) Generation and Storage of 360° Domain Walls for Magnetic Devices

Y. M. Jin*, L. D. Geng, Michigan Technological University, USA

11:00 AM

(EMA-S8-004-2013) Non-Ohmic Phenomena in BaTiO₃, SrTiO₃ and CaTiO₃

M. Prades, H. Beltran, E. Cordoncillo, Universitat Jaume I, Spain; N. Maso*, A. R. West, The University of Sheffield, United Kingdom

11:15 AM

(EMA-S8-005-2013) Nanoscale Dynamics in Phase Change Switching

J. Bosse*, University of Connecticut, USA; I. Grishin, O. Kolosov, Lancaster University, United Kingdom; B. D. Huey, University of Connecticut, USA

11:30 AM**(EMA-S8-006-2013) Preliminary Computational Approach to the Study of Oxygen Diffusion in HfO₂-x**

G. Broglia*, M. Montorsi, L. Larcher, University of Modena and Reggio Emilia, Italy

11:45 AM**(EMA-S8-007-2013) Effect of electrode materials on the performance of ZCAN/TiO₂/M resistive memory cells**

M. Chin, M. Amani*, T. O'Regan, A. Birdwell, M. Dubey, US Army Research Laboratory, USA

12:00 PM**(EMA-S8-008-2013) An autonomous nonvolatile memory latch (Invited)**

J. T. Evans*, Radiant Technologies, Inc., USA

S12: Recent Developments in High Temperature Superconductivity**YBCO Coated Conductors I-Processing**

Room: Indian

Session Chair: Haiyan Wang, Texas A&M University

10:00 AM**(EMA-S12-006-2013) YBCO CCs From A European Perspective (Invited)**

J. MacManus-Driscoll*, M. Bianchetti, A. Kursumovic, University of Cambridge, United Kingdom

10:30 AM**(EMA-S12-002-2013) Present Status and Future Prospect of R&D on Coated Conductors and Applications in Japan (Invited)**

T. Izumi*, M. Yoshizumi, Y. Shiohara, ISTECSRL, Japan

11:00 AM**(EMA-S12-003-2013) Progress in development of coated conductors for coil applications in high magnetic fields at low temperatures (Invited)**

V. Selvamanickam*, University of Houston, USA; Y. Chen, SuperPower Inc., USA; Y. Liu, N. D. Khatri, J. Liu, Y. Yao, A. Xu, C. Lei, E. Galtsyan, G. Majkic, University of Houston, USA

11:30 AM**(EMA-S12-005-2013) Recent Progress of Electromagnetic Characterization Techniques to Realize High Performance RE-123 Coated Conductors (Invited)**

T. Kiss*, K. Higashikawa, M. Inoue, Kyushu University, Japan; H. Tobita, T. Machi, M. Yoshizumi, T. Izumi, ISTECSRL, Japan; Y. Iijima, T. Saito, Fujikura Ltd., Japan; K. Ohmatsu, Sumitomo Electric Industries Ltd., Japan; S. Awaji, K. Watanabe, Tohoku University, Japan

S14: Nanoscale Electronic Materials and Devices**Nanoscale Electronic Materials and Devices**

Room: Coral A

Session Chair: Michael Lilly, Sandia National Laboratories

10:00 AM**(EMA-S14-001-2013) Nonexponential decay of photoluminescence intensity of small InAs quantum dots**

K. Kral*, Institute of Physics, Acad. Sci. of Czech Republic, v.v.i., Czech Republic; M. Mensik, Institute of Macromolecular Chemistry, Acad. Sci. of CR, v.v.i., Czech Republic

10:15 AM**(EMA-S14-002-2013) Preparation and characterization of ferroelectric lithium niobate pseudo nanocubes**

W. Mader*, M. Mueller, University of Bonn, Germany

10:30 AM**(EMA-S14-003-2013) Perovskite Nanoparticle enhanced Nanorod Array based Gas Sensors at High Temperature**

P. Gao*, H. Lin, H. Gao, University of Connecticut, USA

10:45 AM**(EMA-S14-004-2013) Engineering Tetragonal Barium Titanate in Freestanding Nanosheets**

C. A. Barrett*, T. T. Salguero, University of Georgia, USA

11:00 AM**(EMA-S14-005-2013) Strain-driven control of functionalities in complex metal-oxide films**

L. Yan, E. M. Choi, Los Alamos National Laboratory, USA; O. Lee, University of Cambridge, United Kingdom; Z. Bi, Los Alamos National Laboratory, USA; A. Chen, Texas A & M University, USA; J. Xiong, Los Alamos National Laboratory, USA; S. A. Harrington, University of Cambridge, United Kingdom; H. Wang, Texas A & M University, USA; J. L. MacManus-Driscoll, University of Cambridge, United Kingdom; Q. X. Jia*, Los Alamos National Laboratory, USA

11:15 AM**(EMA-S14-006-2013) Tuning the Sensitivity of Toxic Gas Detection Using Back Gate Bias in CVD Graphene Field Effect Transistors**

A. K. Singh*, M. Uddin, J. T. Tolson, University of South Carolina, USA; G. S. Tompa, N. Sbrockey, Structured Materials Industries Inc., USA; M. G. Spencer, Cornell University, USA; T. S. Sudarshan, G. Koley, University of South Carolina, USA

S16: Highlights of Student Research in Basic Science and Electronic Ceramics**Highlights of Student Research**

Room: Coral A

Session Chair: Troy Ansell, Oregon State University

12:15 PM**(EMA-S16-001-2013) Crystallographic and Electrical Properties of (Na_{0.5-x}Bi_{0.5+x})TiO_{3-3x}, where (-0.01 ≤ x ≤ 0.01)**

J. J. Carter*, E. Aksel, J. S. Forrester, J. L. Jones, University of Florida, USA

12:30 PM**(EMA-S16-002-2013) Mechanical Depoling and Piezoelectricity Loss in the Region of the Morphotropic Phase Boundary of NBT-BT**

L. M. Denis*, University of Florida, USA; J. Glaum, M. Hoffman, University of New South Wales, Australia; J. Forrester, J. L. Jones, University of Florida, USA

12:45 PM**(EMA-S16-003-2013) Stability and dewetting of Au on Ti, TiO_x, and ZnO**

B. Schaefer*, University of Florida, USA; J. Cheung, University of New South Wales, Australia; J. F. Ihlefeld, Sandia National Laboratories, USA; J. L. Jones, University of Florida, USA; N. Valanoor, University of New South Wales, Australia

S1: Functional and Multifunctional Electroceramics**Material Applications including Energy Storage, Conversion and Harvesting**

Room: Coral B

Session Chairs: Takaaki Tsurumi, Tokyo Institute of Technology; John Talvacchio, Northrop Grumman

2:00 PM**(EMA-S1-001-2013) Arrays of Superconducting SQUIDs as Antennas and Amplifiers (Invited)**

J. Talvacchio*, J. X. Przybysz, D. L. Miller, Northrop Grumman, USA

2:30 PM**(EMA-S1-002-2013) Comparative Study On Magentodielectric And Dielectric Substrate Based Rectangular Patch Antenna In UHF And SHF**

G. Singh*, S. Parashar, S. Sahu, KIIT University, India

2:45 PM**(EMA-S1-003-2013) Fabrication of Micro Wireless Power Transfer System by Multilayer Ceramic Coil**

M. Takato*, K. Saito, F. Uchikoba, Nihon University, Japan

3:00 PM

(EMA-S1-004-2013) Maximizing the Energy Storage Density with Antiferroelectric Ceramics through Mechanical Confinement
X. Tan*, S. E. Young, J. Zhang, Iowa State Univ, USA; W. Hong, Iowa State University, USA

3:15 PM

(EMA-S1-005-2013) Enhanced Ionic Transport in High Density, Pressure Formed $0.70\text{Li}_2\text{S} + 0.30\text{P}_2\text{S}_5$ Lithium Thiophosphate Solid Electrolytes
S. S. Berbano*, M. Mirsaneh, M. T. Lanagan, C. A. Randall, The Pennsylvania State University, USA

3:30 PM

(EMA-S1-048-2013) Development of High-Energy-Density Textured Piezoelectric Materials for Vibration Energy Harvesting (Invited)
S. Priya, Y. Yan*, Virginia Tech, USA

4:00 PM

(EMA-S1-006-2013) Microscopic Mechanism and Material Design of Electro-optic effect in Perovskite Ferroelectrics (Invited)
T. Tsurumi*, K. Takeda, T. Hoshina, H. Takeda, Tokyo Institute of Technology, Japan

4:30 PM

(EMA-S1-007-2013) Electrospun TiO₂ fiber as anode materials for lithium ion batteries
R. Qing*, W. Sigmund, University of Florida, USA

4:45 PM

(EMA-S1-008-2013) Photophysical and photocatalytic water splitting performance of Stibiotantalite type-structure compounds, SbMO_4 ($M = \text{Nb}, \text{Ta}$)
S. Kim*, S. Park, C. Lee, B. Han, S. Seo, J. Kim, Seoul National University, Republic of Korea; I. Cho, Stanford University, USA; K. Hong, Seoul National University, Republic of Korea

5:00 PM

(EMA-S1-009-2013) Enhanced energy storage capacities in solid state nanocomposite dielectrics
M. Mirsaneh*, A. Baker, W. Qu, S. Lee, E. Dorjpalam, R. Rajagopalan, C. A. Randall, The Pennsylvania State University, USA

5:15 PM

(EMA-S1-010-2013) Ternary $\text{Bi}(\text{B}'\text{B}'')\text{O}_3 - \text{PbTiO}_3$ Solid Solutions for High Temperature Piezoelectrics
B. Kowalski*, A. Sehrioglu, Case Western Reserve University, USA

S2: Multiferroic Materials and Multilayer Ferroic Heterostructures: Properties and Applications

Interfaces, Domain Phenomena and Transport

Room: Coral A

Session Chair: Melanie Cole, U.S. Army Research Laboratory

2:00 PM

(EMA-S2-001-2013) Interfacial coupling at multifunctional oxide interfaces (Invited)
C. Ahn*, Yale University, USA

2:30 PM

(EMA-S2-002-2013) Domain wall functionality in complex oxides (Invited)
J. Seidel*, University of New South Wales, Australia

3:00 PM

(EMA-S2-003-2013) Temporally Resolved Switching Steps During Polarization Reversal in Multiferroics
L. Ye, J. Bosse, A. Llubes, University of Connecticut, USA; J. Ihlefeld, Sandia National Laboratories, USA; B. D. Huey*, University of Connecticut, USA

3:30 PM

Break

4:00 PM

(EMA-S2-004-2013) Interface Engineered Ferroelectric Heterostructures (Invited)
C. Chen*, University of Texas San Antonio, USA

4:15 PM

(EMA-S2-005-2013) Tuning of Conduction at Domain Walls of BiFeO_3 Thin Films (Invited)
J. Lee*, A. Bhatnagar, Y. Kim, D. Hesse, M. Alexe, Max Planck Institute of Microstructure Physics, Germany

4:30 PM

(EMA-S2-006-2013) Multiferroic Modulation of Superparamagnetism (Invited)
G. Carman*, H. Kim, L. Schelhas, S. Tolbert, UCLA, USA

4:45 PM

(EMA-S2-007-2013) Interface Structure Evolution in Perovskite Oxide Epitaxial Thin Films (Invited)
E. I. Meletis*, J. Jiang, J. He, The University of Texas at Arlington, USA

S3: Structure of Emerging Perovskite Oxides: Bridging Length Scales and Unifying Experiment and Theory

Session 2

Room: Pacific

Session Chairs: Yu Wang, Michigan Tech; David Cann, Oregon State University

2:00 PM

(EMA-S3-007-2013) Triple-point type morphotropic phase boundary and high-performance Pb-free piezoelectrics (Invited)
X. Ren*, National Institute for Materials Science, Japan; D. Xue, J. Gao, C. Zhou, W. Liu, Frontier Institute of Science and Technology, China

2:30 PM

(EMA-S3-008-2013) The Effect of Poling and Stress on Switching in $\text{Ba}(\text{Zr}_{0.2}\text{Ti}_{0.8})\text{O}_3-x(\text{Ba}_{0.7}\text{Ca}_{0.3})\text{TiO}_3$ Piezoelectrics
M. C. Ehmke*, Purdue University, USA; J. Glaum, J. Daniels, M. Hoffman, The University of New South Wales, Australia; J. E. Blendell, Purdue University, USA; K. J. Bowman, Illinois Institute of Technology, USA

2:45 PM

(EMA-S3-009-2013) Nano/Mesoscale Structure and Pseudo-Symmetry in $\text{Na}_0.5\text{Bi}_0.5\text{TiO}_3$ and its Solid Solutions (Invited)
I. Levin*, NIST, USA

3:15 PM

(EMA-S3-010-2013) Local microstructure evolution of bismuth sodium titanate-based lead free piezoelectric systems across the morphotropic phase boundary region (Invited)
Y. Liu*, L. Noren, R. L. Withers, Y. Guo, J. Wang, the Australian National University, Australia; A. J. Studer, Bragg Institute, The Australian Nuclear Science and Technology Organization, Australia

3:45 PM

Break

4:15 PM

(EMA-S3-011-2013) Multi-length-scale scattering studies of actuation mechanisms in the $(1-x)\text{Bi}_0.5\text{Na}_0.5\text{TiO}_3-(x)\text{BaTiO}_3$ solid solution (Invited)
J. Daniels*, The University of New South Wales, Australia

4:45 PM

(EMA-S3-012-2013) Creation and Destruction of Morphotropic Phase Boundaries through Electrical Poling in Lead-Free $(\text{Bi}_{1/2}\text{Na}_{1/2})\text{TiO}_3-\text{BaTiO}_3$
C. Ma, H. Guo, X. Tan*, Iowa State University, USA

5:00 PM

(EMA-S3-013-2013) Phase Transition and Property Enhancement in (K,Na)NbO₃-based Ceramics (Invited)
J. Li*, Tsinghua University, China

S5: Structure and Properties of Interfaces in Electronic Materials

Transport, Structure and Composition of Interfaces

Room: Mediterranean B/C

Session Chair: Edwin Garcia, Purdue University

2:00 PM

(EMA-S5-007-2013) Microstructural Evolution in Perovskite Ceramics (Invited)
W. Rheinheimer, M. Bäurer, M. J. Hoffmann*, KIT, Germany

2:30 PM

(EMA-S5-008-2013) In situ diffraction reveals the dependence of domain wall motion on BaTiO₃ grain size and relation to macroscopic properties

D. Ghosh*, A. Sakata, J. Carter, University of Florida, USA; P. A. Thomas, University of Warwick, United Kingdom; H. Han, J. C. Nino, J. L. Jones, University of Florida, USA

2:45 PM

(EMA-S5-009-2013) Improvement of the silicon to silicon dioxide interface as Revealed by random telegraph signal noise analysis
J. Kim*, J. Kim, C. Lee, J. Lee, D. Kim, K. Yoo, H. Park, Dongbu Hitek., Co. Ltd, Republic of Korea

3:00 PM

(EMA-S5-010-2013) Control of ZnO thin film polarity through interface chemistry

C. T. Shelton*, E. Sachet, P. A. Elizabeth, J. Maria, NCSU, USA

3:15 PM

(EMA-S5-011-2013) Effect of Gas Adsorption in Electrode-Semiconductor Interface

S. Lee, J. Jung*, Kyungnam University, Republic of Korea

3:30 PM

(EMA-S5-012-2013) Stress-enhanced phase transformation kinetics in olivine battery electrodes (Invited)

M. Tang*, Lawrence Livermore Nat. Lab, USA

S11: Sustainable, Low Critical Material Use and Green Materials Processing Technologies

Materials for Sustainability: Optimized Material Choice and Performance for Low Critical Materials Use

Room: Mediterranean B/C

Session Chair: Paul Clem, Sandia National Laboratories

4:30 PM

(EMA-S11-002-2013) Ultra-efficient, Robust and Well-defined Nano-Array based Catalytic Devices for Emission Control

P. Gao*, Y. Guo, Z. Ren, University of Connecticut, USA

4:45 PM

(EMA-S11-003-2013) Electric field enhancement of photocatalysis

M. Laudenslager*, W. M. Sigmund, University of Florida, USA

5:00 PM

(EMA-S11-004-2013) Thermochromic windows for control of thermal heat gain: tuning and optimization of VO₂ coating metal-insulator transition temperature

P. Clem*, C. Edney, Sandia National Laboratories, USA

S12: Recent Developments in High Temperature Superconductivity

YBCO Coated Conductors II-Pinning

Room: Indian

Session Chair: Timothy Haugan, Air Force Research Laboratory

2:00 PM

(EMA-S12-007-2013) Engineered nanoscale defects for enhanced vortex-pinning in coated conductors (Invited)

A. Goyal*, S. Wee, Oak Ridge National Laboratory, USA

2:30 PM

(EMA-S12-008-2013) Novel vortex pinning mechanism of solution-derived YBCO nanocomposites driven by local lattice strains (Invited)

M. Coll*, A. Palau, J. Gazquez, A. Lordés, S. Ye, R. Guzmán, V. Rouco, R. Vlad, J. Arbiol, S. Ricart, ICMAB-CSIC, Spain; G. Deutscher, Tel Aviv University, Israel; C. Magen, Universidad Zaragoza, Spain; E. Bartolomé, T. Puig, X. Obradors, ICMAB-CSIC, Spain

3:00 PM

(EMA-S12-009-2013) New pinning strategies for the second-generation wires (Invited)

V. Solovoyov*, Q. Li, Brookhaven National Laboratory, USA

3:30 PM

Break

4:00 PM

(EMA-S12-010-2013) Strain-mediated self-assembly of secondary phase nanostructures in YBCO thick films via interfacial strain engineering (Invited)

J. Wu*, J. Shi, R. Emergo, J. Baca, X. Wang, University of Kansas, USA; T. Haugan, U.S. Air Force Research Laboratory, USA

4:30 PM

(EMA-S12-036-2013) Rare-metal-free Magnetism and Spintronics arising from Graphene Edges (Invited)

J. Haruyama*, Aoyama Gakuin University, Japan

5:00 PM

(EMA-S12-011-2013) Tunable Flux Pinning Properties in YBa₂Cu₃O_{7-δ} Thin Films by Functional Fe₂O₃:CeO₂ Vertically Aligned Nanocomposites

C. Tsai*, H. Wang, L. Chen, Texas A&M University, USA

S15: Failure: The Greatest Teacher

Failure: The Greatest Teacher

Room: Coral A

Session Chair: Geoff Brennecke, Sandia National Laboratories

8:00 PM

(EMA-S15-001-2013) Embracing Failure in Energy-Based Materials Research (Invited)

E. Spoerke*, D. V. Gough, J. Wheeler, N. Hudak, N. Bell, C. Edney, Sandia National Laboratories, USA; B. Aguirre, University of Texas, El Paso, USA; D. Frank, Sandia National Laboratories, USA

8:30 PM

(EMA-S15-002-2013) Surprises and Failures (Invited)

C. Randall*, Penn State University, USA

Poster Session

Room: Atlantic/Arctic

5:30 PM**(EMA-S1-P001-2013) Flexoelectricity in Dielectrics and Design of Flexoelectric Piezoelectric Composites of High Piezoelectric Response**

B. Chu*, University of Science and Technology of China, China; L. Cross, Pennsylvania State University, USA; D. R. Salem, South Dakota School of Mines and Technology, USA

(EMA-S1-P002-2013) Electromechanical Properties of Textured NKLNT Piezoelectric Ceramics

J. Song*, S. Kim, J. Jo, I. Kim, S. Jeong, M. Kim, Korea Electrotechnology Research Institute, Republic of Korea

(EMA-S1-P003-2013) Synthesis and dielectric properties of BaTiO₃-Bi(Ni_{0.5}Ti_{0.5})O₃ ceramics

N. Kumar*, D. P. Cann, Oregon State University, USA

(EMA-S1-P004-2013) Comparison of Goldschmidt's Tolerance Factor With Cubic and Tetragonal Ionic Radii Volume Constrained Perovskite Structures in the Design of Advanced Material

S. Tidrow*, The University of Texas - Pan American, USA

(EMA-S1-P005-2013) KFM Investigation about Electric Field Distribution of BaTiO₃ Layer in Degraded MLCC

T. Okamoto*, Pennsylvania State University, USA; S. Kitagawa, N. Inoue, A. Ando, H. Takagi, Murata Manufacturing Co., Ltd., Japan

(EMA-S1-P006-2013) Er₂O₃ Additive Influence on Microstructure and Dielectrical Properties of BaTiO₃-Ceramics

V. Mitic*, V. Paunovic, Faculty of Electronic Engineering, University of Nis, Serbia; M. Miljkovic, Center for Electron Microscopy, University of Nis, Serbia

(EMA-S2-P027-2013) Novel and Efficient Copolymer based quasi solid electrolyte for Dye Sensitized Solar Cells

M. Akhtar*, Z. Li, W. Lee, O. Yang, Chonbuk National University, Republic of Korea

(EMA-S3-P007-2013) Crystal structure and electrical properties of complex perovskite solid solutions based on NaNbO₃-Bi(Zn_{0.5}Ti_{0.5})O₃

S. Prasertpalichat*, D. P. Cann, Oregon State University, USA

(EMA-S4-P008-2013) Properties of undoped and Si-doped nonpolar a-plane GaN grown with different initial growth pressures

H. Kim*, Hanbat National University, Republic of Korea; K. Song, Korea Advanced Nano Fab Center, Republic of Korea

(EMA-S4-P009-2013) Radial Junction Nanostructured Plasmonics Silicon Solar Cells

P. Pudasaini*, A. Ayon, University of Texas at San Antonio, USA

(EMA-S6-P010-2013) Nanostructure Engineering and Combinatorial Solutions for Enhanced Nanotransport Behavior in Oxide-based Thermoelectric Materials for Power Generation

E. L. Thomas*, UDRI, USA; R. Snyder, AFRL, USA; X. Song, S. Chen, WVU, USA; W. Wong-Ng, NIST, USA

(EMA-S6-P011-2013) Thermoelectric behavior of SrTiO₃ solid solutions

H. J. Brown-Shaklee*, P. A. Sharma, M. A. Blea, Sandia National Laboratories, USA; P. E. Hopkins, University of Virginia, USA; J. F. Ihlefeld, Sandia National Laboratories, USA

(EMA-S6-P013-2013) Effect of amorphous phase on thermoelectric properties of B-doped Si film

N. Hayakawa*, K. Iwasaki, Toyota Boshoku Corporation, Japan

(EMA-S6-P014-2013) Mechanical and thermoelectric property analysis of simultaneously sintered segmented Bi₂Te₃/PbTe for thermoelectric module

S. Yoon*, O. Kwon, J. Han, J. Cho, Seoul National University, Republic of Korea; J. Kim, Korea Institute of Science and Technology, Republic of Korea; C. Park, Seoul National University, Republic of Korea

(EMA-S8-P015-2013) Memristor using metal to insulator transition of single VO₂ nanowire

S. Bae, Seoul National University, Republic of Korea; S. Lee, L. Lin, Georgia Institute of Technology, USA; J. Cho, S. Yoon*, H. Koo, Seoul National University, Republic of Korea; Z. Wang, Georgia Institute of Technology, USA; C. Park, C. Park, Seoul National University, Republic of Korea

(EMA-S9-P016-2013) Microstructural Characterization of Flux-Grown BaTiO₃ Thin Films

M. J. Burch*, D. T. Harris, J. Li, E. A. Dickey, J. P. Maria, North Carolina State University, USA

(EMA-S10-P017-2013) Effect of surface-treated MMT addition on the tensile behavior of MMT/glass/vinylester composites

J. Lee, Kyunghee University, Republic of Korea; Y. Jung, Philadelphia University, USA; K. Rhee*, Kyunghee University, Republic of Korea

(EMA-S12-P028-2013) Flux Pinning of YBa₂Cu₃O_{7-δ} Superconductor with Ultra-large Y₂BaCuO₅ Nanoparticle Additions

M. P. Sebastian, J. N. Reichart, M. M. Ratcliff, Air Force Research Laboratory, USA; J. L. Burke, University of Dayton Research Institute, USA; T. J. Haugan*, Air Force Research Laboratory, USA

(EMA-S12-P030-2013) Experimental investigation of the edge barrier pinning effect of bridged superconducting thin films

L. Brunke*, University of Dayton Research Institute, USA; W. Jones, M. Mullins, University of Dayton, USA; T. Haugan, Air Force Research Laboratory, USA

(EMA-S12-P031-2013) Search for superconductivity in doped carbon thin films

B. Pierce*, WPAFB, USA; J. L. Burke, L. B. Brunke, C. R. Ebbing, UDRI, USA; D. C. Vier, UCSD, USA; T. J. Haugan, WPAFB, USA

(EMA-S13-P024-2013) Effect of Nucleation time on Bending Response of Ionic Polymer-Metal Composites Actuators

S. Kim*, KAIST, Republic of Korea; S. Hong, Argonne National Laboratory, USA; G. Ahn, Y. Choi, Y. Kim, C. Oh, K. No, KAIST, Republic of Korea

(EMA-S14-P019-2013) Fabrication and characterization of metal-insulator-graphene (MIG) tunnel junctions

M. Amani*, M. L. Chin, B. M. Nichols, T. P. O'Regan, A. G. Birdwell, F. J. Crowne, M. Dubey, Army Research Laboratory, USA

(EMA-S14-P025-2013) Decay Mechanisms in Doped Silicon Nanocrystals

E. Albuquerque*, U. L. Fulco, L. R. da Silva, Universidade Federal do Rio Grande do Norte, Brazil

(EMA-S14-P026-2013) Structural and Electronic Properties of Cubic Barium Stannate

U. L. Fulco, E. Albuquerque*, Universidade Federal do Rio Grande do Norte, Brazil

(EMA-S16-P021-2013) Structural changes in Lead Zirconate Titanate due to High Neutron Radiation Exposure

A. J. Henriques*, J. S. Forrester, S. B. Seshadri, University of Florida, USA; D. Brown, Los Alamos National Laboratories, USA; J. T. Graham, S. Landsberger, University of Texas - Austin, USA; J. F. Ihlefeld, G. L. Brennecke, Sandia National Laboratories, USA; J. L. Jones, University of Florida, USA

(EMA-S16-P022-2013) A low-loss voltage actuated switch using metal-polymer nanocomposite

D. Drew*, Virginia Polytechnic Institute and State University, USA; A. Wang, F. Niroui, V. Bulovic, J. Lang, Massachusetts Institute of Technology, USA

(EMA-S16-P023-2013) Phase equilibria, crystallographic structure, and piezoelectric properties of tetragonal Pb(1-1.5x)SmxZr(1-y)TiyO₃

M. M. Nolan*, S. B. Seshadri, University of Florida, USA; B. Regadioli, Universidade de São Paulo, Brazil; J. S. Forrester, D. Lynch, J. L. Jones, University of Florida, USA

Thursday, January 24, 2013**Plenary Session II**

Room: Indian

8:30 AM**(EMA-PL-002-2013) Complexity at Work: Nanoionic Memristive Switches (Invited)**

R. Waser*, I. Valov, Forschungszentrum Jülich, Germany; E. Linn, RWTH Aachen University, Germany; S. Menzel, R. Dittmann, Forschungszentrum Jülich, Germany

9:30 AM**Break**

S1: Functional and Multifunctional Electroceramics

Piezoelectric and Pb-free Piezoelectric Materials, Devices and Applications I

Room: Coral B

Session Chairs: Yu Wang, Michigan Tech; Juergen Roedel, TU Darmstadt

10:00 AM

(EMA-S1-011-2013) Structure and Properties of BNT-based Lead-free Piezoceramics (Invited)

J. Roedel*, W. Jo, TU Darmstadt, Germany

10:30 AM

(EMA-S1-012-2013) Ferroelectric Property of (Li,Na,K)NbO₃ Piezoceramics on the Basis of Grain Size

K. Kakimoto*, R. Kaneko, I. Kagomiya, Nagoya Institute of Technology, Japan

10:45 AM

(EMA-S1-013-2013) Domain wall motion and electric-field-induced strains in NBT-xBT solid solutions from in situ neutron diffraction

T. Usher*, J. S. Forrester, E. Aksel, University of Florida, USA; A. Studer, Australian Nuclear Science and Technology Organisation, Australia; J. L. Jones, University of Florida, USA

11:00 AM

(EMA-S1-014-2013) The effect of tantalum dopant on ferroelectric fatigue behavior of lead-free ferroelectric potassium-sodium niobate

S. Pojprapai*, C. Uthaisar, Suranaree University of Technology, Thailand

11:15 AM

(EMA-S1-015-2013) Investigation of NaF doped NKN based lead-free ceramics at different sintering atmosphere

C. Liu*, The Pennsylvania State University, USA; P. Liu, Shaanxi Normal University, China; K. Kobayashi, C. A. Randall, The Pennsylvania State University, USA

11:30 AM

(EMA-S1-016-2013) Computational Study of Microstructure and Property Relations in Ferroelectric Polycrystals (Invited)

Y. U. Wang*, J. Zhou, Michigan Tech, USA

12:00 PM

(EMA-S1-017-2013) Crystal Structure of (Li,Na,K)NbO₃ Lead-free Piezoelectric Ceramics

T. Nishi*, K. Kakimoto, I. Kagomiya, Graduate School of Eng., Dept. Mater. Sci. & Eng., Nagoya Institute of Technology, Japan

12:15 PM

(EMA-S1-018-2013) Effect of tin content on electrical and piezoelectric properties of barium stannate titanate ceramics prepared from nanoparticles

K. C. Singh*, C. Jiten, R. Laishram, Sri Venkateswara College, India

S2: Multiferroic Materials and Multilayer Ferroic Heterostructures: Properties and Applications

Theory and Modeling

Room: Coral A

Session Chair: Melanie Cole, U.S. Army Research Laboratory

10:00 AM

(EMA-S2-008-2013) Ab initio design of ferroic materials with advanced functionalities: 2D ferroelectricity and Goldstone-like modes in perovskite-oxide layers (Invited)

S. Nakhmanson*, Argonne National Laboratory, USA

10:30 AM

(EMA-S2-009-2013) Computational Navigation Through the ABO₃ Chemical Space (Invited)

R. Ramprasad*, G. Pilania, V. Sharma, G. Rossetti, S. Alpay, University of Connecticut, USA

11:00 AM

(EMA-S2-010-2013) Charged Domain Walls in Proper and Improper Ferroelectrics (Invited)

A. K. Tagantsev*, Swiss Federal Institute of Technology, EPFL, Switzerland

11:30 AM

(EMA-S2-011-2013) Caloric effects in ferroelectric alloys from atomistic simulations (Invited)

I. Ponomareva*, S. Lisenkov, University of South Florida, USA

12:00 PM

(EMA-S2-012-2013) Phase Field Modeling of Multicomponent Multiferroic Composites

Y. M. Jin*, F. Ma, Y. U. Wang, S. L. Kampe, Michigan Technological University, USA; S. Dong, Peking University, China

S3: Structure of Emerging Perovskite Oxides: Bridging Length Scales and Unifying Experiment and Theory

Session 3

Room: Pacific

Session Chair: Jacob Jones, University of Florida

10:00 AM

(EMA-S3-014-2013) Relaxor Characteristics of Bi(Zn_{1/2}Ti_{1/2})O₃-based High-Strain Materials

N. Kumar*, D. Cann, E. Patterson, T. Ansell, Oregon State University, USA

10:15 AM

(EMA-S3-015-2013) Manipulation of the relaxor behaviour of BNT-BT ceramics due to Zr addition

J. Glaum*, The University of New South Wales, Australia; M. Acosta, TU Darmstadt, Germany; H. Simons, M. Hoffman, The University of New South Wales, Australia

S4: LEDs and Photovoltaics - Beyond the Light: Common Challenges and Opportunities

LEDs and Photovoltaics

Room: Mediterranean B/C

Session Chairs: Adam Scotch, OSRAM SYLVANIA; Erik Spoeke, Sandia National Laboratories

10:00 AM

(EMA-S4-001-2013) Possibilities for Smart Lighting and Smart Solar Integration (Invited)

M. H. Azzam, SolarOne Solutions, Inc., USA; R. F. Karlicek*, Rensselaer Polytechnic Institute, USA

10:25 AM

(EMA-S4-002-2013) Thin Film PV Technologies: Present Status and Challenges (Invited)

C. Ferekides*, University of South Florida, USA

10:50 AM

(EMA-S4-003-2013) ALD Sapphire, the Universal Substrate Technology for the Growth of Solid State Light Sources (Invited)

A. Melton, B. Kucukgoka, N. Lu, I. Ferguson*, University of North Carolina at Charlotte, USA

11:15 AM

(EMA-S4-004-2013) Selective Growth of ZnCdTe Graded Nanostructures for Enhanced Performance of CdTe Solar Cells (Invited)

J. L. Cruz-Campa*, Sandia National Laboratories, USA; D. Zubia, B. Aguirre, University of Texas at El Paso, USA; X. Zhou, D. Ward, C. A. Sanchez, Sandia National Laboratories, USA; J. J. Chavez, R. Ordonez, University of Texas at El Paso, USA; A. Pimentel, Sandia National Laboratories, USA; F. Anwar, University of Texas at El Paso, USA; J. Michael, Sandia National Laboratories, USA; E. Gonzales, The Center for Integrated Nanotechnologies, USA; D. Marrufo, University of Texas at El Paso, USA; E. Spoerke, C. Calvin, P. Lu, Sandia National Laboratories, USA; H. Prieto, J. C. McClure, University of Texas at El Paso, USA; G. N. Nielson, Sandia National Laboratories, USA

11:40 AM

(EMA-S4-005-2013) Nanoscale Photovoltaic Performance Based on AFM Investigations of Microstructured CdTe Islands

Y. Kutes, University of Connecticut, USA; J. Cruz-Campa, Sandia National Laboratories, USA; J. Bosse, L. Ye, A. Merkouriou, University of Connecticut, USA; B. A. Aguirre, D. Zubia, University of Texas at El Paso, USA; E. D. Spoerke, Sandia National Laboratories, USA; B. D. Huey*, University of Connecticut, USA

11:55 AM

(EMA-S4-006-2013) Oxide Semiconductors for photo-conversion technologies (Invited)

J. J. Berry*, P. F. Ndione, N. E. Widjonarko, A. K. Sigdel, P. A. Parilla, A. Zakutayev, J. D. Perkins, T. Genette, A. A. Dameron, D. C. Olson, D. S. Ginley, NREL, USA

12:20 PM

(EMA-S4-007-2013) Low Temperature Solution Processing of Inorganic Nanoparticles for Contact Layers in Organic Photovoltaics (Invited)

Y. Lee*, D. Barrera, J. Wang, G. F. Gao, S. R. Cheng, University of Texas at Dallas, USA; S. R. Ferreira, Sandia National Laboratories, USA; R. J. Davis, GE Global Research Center, USA; J. W. Hsu, University of Texas at Dallas, USA

12:45 PM

(EMA-S4-008-2013) Creating donor-acceptor interfaces for excitonic devices using nanoporous metal-organic frameworks (Invited)

M. D. Allendorf*, M. Foster, D. Gough, T. N. Lambert, K. Leong, S. Meek, E. Spoerke, V. Stavila, B. Wong, Sandia National Laboratories, USA

S6: Thermoelectrics: Defect Chemistry, Doping and Nanoscale Effects

Applications and Non-Oxide Thermoelectrics

Room: Pacific

Session Chair: Jon Ihlefeld, Sandia National Laboratories

10:30 AM

(EMA-S6-001-2013) Integration of Thermoelectric Materials at United Technologies Corporation (Invited)

S. Culp*, C. Lents, D. Jarmon, J. Turney, United Technologies Research Center, USA

11:00 AM

(EMA-S6-002-2013) Thermoelectric Properties of New High Temperature Material: $\text{Yb}_9\text{Mn}_{4+x}\text{Sb}_9$

S. Bux*, Jet Propulsion Laboratory/California Institute of Technology, USA; A. Zevelink, California Institute of Technology, USA; O. Janka, University of California Davis, USA; T. Vo, D. Uhl, Jet Propulsion Laboratory/California Institute of Technology, USA; J. Snyder, California Institute of Technology, USA; P. Von Allmen, Jet Propulsion Laboratory/California Institute of Technology, USA; S. Kauzlarich, University of California Davis, USA; J. Fleurial, Jet Propulsion Laboratory/California Institute of Technology, USA

11:15 AM

(EMA-S6-003-2013) Development of high-efficiency segmented thermoelectric couples

T. Caillat*, S. Firdosy, B. Li, C. Huang, V. Ravi, N. Keyawa, H. Anjunyan, J. Paik, J. Chase, L. Lara, J. Fleurial, Jet Propulsion Laboratory/Caltech, USA

11:30 AM

(EMA-S6-004-2013) Spark Plasma Sintering for High Temperature Thermoelectrics

J. Mackey*, University of Akron, USA; A. Sehirlioglu, Case Western Reserve University, USA; F. Dynys, NASA Glenn Research Center, USA

11:45 AM

(EMA-S6-005-2013) Thermoelectric chalcogenides: the case of chromium sulfides and selenides

A. Maignan*, E. Guilmeau, F. Gascoin, Y. Bréard, V. Hardy, LABORATOIRE CRISMAT / CNRS ENSICAEN, France

12:00 PM

(EMA-S6-006-2013) Thermoelectric materials for middle temperature application (Invited)

R. Funahashi*, National Institute of Advanced Industrial Science & Technology, Japan

S12: Recent Developments in High Temperature Superconductivity

Superconductor Applications I: High Field Magnet Development and Technologies

Room: Indian

Session Chair: Haiyan Wang, Texas A&M University

10:00 AM

(EMA-S12-012-2013) A round wire multifilament HTS conductor for high field magnet use – what stands in the way? (Invited)

D. Larbalestier*, NHMFL, USA

10:30 AM

(EMA-S12-013-2013) Development of Accelerator Magnets Using Coated Conductors (Invited)

N. Amemiya*, H. Otake, K. Goda, T. Nakamura, Kyoto University, Japan; T. Ogitsu, KEK, Japan; K. Koyanagi, T. Kurusu, Toshiba Corporation, Japan; Y. Mori, Kyoto University, Japan; Y. Iwata, K. Noda, National Institute of Radiological Sciences, Japan; M. Yoshimoto, Japan Atomic Energy Agency, Japan

11:00 AM

(EMA-S12-014-2013) Improvement Performance of MgB₂ and Nb₃Sn superconductors for MRI, NMR, Fault Current Limiters, and Wind Turbine Generators (Invited)

M. Tomsic*, M. Rindfleisch, C. J. Thong, X. Peng, Hyper Tech, USA; M. Sumption, Ohio State University, USA

11:30 AM

(EMA-S12-015-2013) AC Loss Measurements on 2G High Temperature Superconducting Coils (Invited)

S. V. Pamidi*, J. Kvitkovic, J. Kim, C. Kim, Florida State University-Meteorology, USA

12:00 PM

(EMA-S12-016-2013) AC Losses of Multifilament Coated Conductors and Coils

G. A. Levin*, J. Murphy, T. Haugan, M. Mullins, P. Barnes, M. Majoros, M. Sumption, T. Collings, M. Polak, P. Mazola, J. Šouc, J. Kováč, P. Kováč, UES, Inc., USA

S1: Functional and Multifunctional Electroceramics

Piezoelectric and Pb-free Piezoelectric Materials, Devices and Applications II

Room: Coral B

Session Chairs: Amar Bhalla; Derek Sinclair, University of Sheffield

2:00 PM

(EMA-S1-019-2013) The Defect Chemistry of ATiO₃ Perovskites by a combination of Atomistic Simulations and Experimentation (Invited)

J. Dawson, C. Freeman, M. Li, L. Ben, J. Harding, D. Sinclair*, University of Sheffield, United Kingdom

2:30 PM

(EMA-S1-020-2013) Relaxor characteristics of the phase transformation in $(1-x)\text{BaTiO}_3 - x\text{Bi}(\text{Zn}_{1/2}\text{Ti}_{1/2})\text{O}_3$ perovskite ceramics

N. Triamnak*, Oregon State University, USA; R. Yimnirun, Suranaree University of Technology, Thailand; D. P. Cann, Oregon State University, USA

2:45 PM

(EMA-S1-021-2013) Design of high energy density $(\text{Bi}_{0.2}, \text{Ba}_{0.8})(\text{Zn}_{0.1}, \text{Ti}_{0.9})\text{O}_3$ -based relaxor capacitors
H. J. Brown-Shaklee*, M. A. Blea, G. L. Brenneka, Sandia National Laboratories, USA

3:00 PM

(EMA-S1-022-2013) Synthesis and High-Temperature Electrical Properties of Bismuth Layer-Structured Oxide (Invited)
R. Aoyagi*, T. Kitahara, M. Maeda, T. Yokota, Nagoya Institute of Technology, Japan

3:15 PM

(EMA-S1-023-2013) Effect of Non-Stoichiometry on Electronic Properties of $\text{BaTiO}_3 - \text{Bi}(\text{Zn}_{1/2}, \text{Ti}_{1/2})\text{O}_3$ Ceramics
N. Raengthon*, Oregon State University, USA; H. J. Brown-Shaklee, G. L. Brenneka, Sandia National Laboratories, USA; D. P. Cann, Oregon State University, USA

3:30 PM

(EMA-S1-047-2013) Breaking of macroscopic centric symmetry in ceramics: implications for flexoelectric effect (Invited)
D. Damjanovic*, A. Biancoli, Swiss Federal Institute of Technology - EPFL, Switzerland

4:00 PM

(EMA-S1-024-2013) Multifunctionality of Ferroics and Multiferroics (Invited)
A. Bhalla*, USA

4:30 PM

(EMA-S1-025-2013) Influence of (Li,Ce,Pr) Ions doped on the Piezoelectric Properties of $\text{CaBi}_2\text{Nb}_2\text{O}_9$ Ceramics
J. Zhu*, S. Bao, Z. Peng, D. Liu, D. Xiao, Sichuan University, China

4:45 PM

(EMA-S1-026-2013) Large piezoelectricity and dielectric permittivity in a phase coexisting ceramic
Y. Yao, Y. Yang, X. Ren*, Xi'an Jiaotong University, China

5:00 PM

(EMA-S1-027-2013) Effect of Heating Rate and Ramp-Up Temperature on Microwave Dielectric Properties of $\text{Ba}_2\text{Ti}_9\text{O}_{20}$ Ceramics
G. B. Pokale*, S. P. Butee, S. S. Bashaiyah, K. Raju, College of Engineering Pune, India

5:15 PM

(EMA-S1-028-2013) Structure, vibrational spectroscopy and luminescence of LaSbO_4 ceramics prepared by solid-state reaction method
K. Siqueira, R. Borges, J. Soares, A. Dias*, UFOP, Brazil

S2: Multiferroic Materials and Multilayer Ferroic Heterostructures: Properties and Applications

Advanced Materials Synthesis and Characterization I

Room: Coral A

Session Chair: Melanie Cole, U.S. Army Research Laboratory

2:00 PM

(EMA-S2-013-2013) Multiferroic (ferroelectric/ferromagnetic) behaviour of $\text{Bi}_7\text{Ti}_3\text{Fe}_{2.1}\text{Mn}_{0.9}\text{O}_{21}$ Aurivillius Phase Thin Films (Invited)
L. Keeney, T. Maity, M. Schmidt, N. Deepak, S. Roy, A. Amann, M. E. Pemble, R. W. Whatmore*, Tyndall National Institute, Ireland

2:30 PM

(EMA-S2-014-2013) Functionalized Chemical Assembly of Ferrite-Ferroelectric Nanoparticles by "Click" reaction (Invited)
G. Sreenivasulu, F. Chavez, G. Srinivasan*, Oakland University, USA

2:45 PM

(EMA-S2-016-2013) New Spin Amplitude Modulation Driven Solid and Soft Composite Multiferroics
B. Rozic, Jozef Stefan Institute, Slovenia; M. Jagodic, Institute of Mathematics, Physics and Mechanics, Slovenia; S. Gyergyek, M. Drofenik, D. Arcon, Z. Kutnjak*, Jozef Stefan Institute, Slovenia

3:00 PM

(EMA-S2-017-2013) Janus-type Bi-phasic Multiferroic Nanofibers
J. S. Andrew*, J. D. Starr, M. Budi, University of Florida, USA

3:15 PM

(EMA-S2-018-2013) Growth of Aurivillius phase $\text{Bi}_5\text{Ti}_3\text{FeO}_{15}$ thin films by Atomic Vapour Deposition
N. Deepak*, P. Zhang, L. Keeney, M. E. Pemble, R. W. Whatmore, Tyndall National Institute, Ireland

3:30 PM

Break

4:00 PM

(EMA-S2-019-2013) Electrical properties of stoichiometric BiFeO_3 prepared by mechanosynthesis with either conventional or spark plasma sintering
A. Perejon, L. A. Perez-Maqueda, Instituto de Ciencia de Materiales de Sevilla, Spain; N. Maso*, A. R. West, The University of Sheffield, United Kingdom

4:15 PM

(EMA-S2-020-2013) Growth, structural and electrical characterization of heteroepitaxial multiferroic bismuth ferrite based thin films on Si (001) substrate
J. Kolte*, A. Daryapurkar, P. Gopalan, Indian Institute of Technology Bombay, India

4:30 PM

(EMA-S2-021-2013) Electrical properties of Ca-doped BiFeO_3 ceramics: from p -type semiconduction to oxide-ion conduction
N. Maso*, A. R. West, The University of Sheffield, United Kingdom

4:45 PM

(EMA-S2-022-2013) Effects of Sr- and La-doping on the piezoelectric, dielectric and microstructural properties of PZT
V. Kalem*, Selcuk University, Turkey; M. Timuçin, Middle East Technical University, Turkey

S6: Thermoelectrics: Defect Chemistry, Doping and Nanoscale Effects

Oxide Thermoelectrics I

Room: Pacific

Session Chair: Sabah Bux, Jet Propulsion Laboratory/California Institute of Technology

2:00 PM

(EMA-S6-007-2013) Preparation of oxide-based thermoelectric materials with spark-plasma techniques (Invited)
Y. Grin*, Max-Planck-Institut für Chemische Physik fester Stoffe, Germany

2:30 PM

(EMA-S6-008-2013) Defects and transport in thermoelectric calcium cobalt oxide
H. Fjeld*, M. Schrade, T. Norby, T. Finstad, University of Oslo, Norway

2:45 PM

(EMA-S6-009-2013) Transport Phenomena in CaMnO_3 : A Combined Experimental and Modelling Approach
R. Freer*, F. Azough, University of Manchester, United Kingdom; S. Parker, M. Molinari, University of Bath, United Kingdom; E. Combe, R. Funahashi, National Institute of Advanced Industrial Science and Technology, Japan

3:00 PM

(EMA-S6-010-2013) Thermoelectric properties of hollandite materials (Invited)
S. Hebert*, H. Takahashi, N. Raghavendra, F. Gascoin, D. Pelloquin, A. Maignan, CRISMAT, France

3:30 PM

Break

4:00 PM

(EMA-S6-011-2013) Enhancement of Thermoelectric Properties of Ceramic Ca₃Co₄O_{9+δ} through Doping and Addition of Nano-inclusions

X. Song*, Y. Chen, M. Torres, D. Palacio, E. Barbero, West Virginia University, USA; E. L. Thomas, University of Dayton Research Institute / Air Force Research Laboratory-WPAFB, USA; P. N. Barnes, Army Research Laboratory, USA

4:15 PM

(EMA-S6-012-2013) Atomic Scale Investigations of Interfacial Defect Structure in Thermoelectric Materials (Invited)

D. L. Medlin*, Sandia National Laboratories, USA

4:45 PM

(EMA-S6-013-2013) Thermoelectric assessment of silicon nanowire networks

A. J. Lohn, University of California Santa Cruz, USA; E. Coleman, Structured Materials Industries, Inc., USA; K. J. Norris, University of California Santa Cruz, USA; N. Sbrockey, Structured Materials Industries, Inc., USA; G. S. Tompa*, N. P. Kobayashi, University of California Santa Cruz, USA

S9: Thin Film Integration and Processing Science**Controlling Phase Assemblage and Stoichiometry I**

Room: Mediterranean B/C

Session Chair: Jon-Paul Maria, North Carolina State University

2:00 PM

(EMA-S9-001-2013) Supra Crystals Consisting of Nano-Sized Perovskite Single Crystals in Cube Shape (Invited)

K. Kato*, National Institute of Advanced Industrial Science and Technology, Japan; K. Mimura, National Institute of Advanced Industrial Science and Technology, Japan; F. Dang, National Institute of Advanced Industrial Science and Technology, Japan; H. Imai, Keio University, Japan; S. Wada, University of Yamanashi, Japan; M. Osada, H. Haneda, National Institute for Materials Science, Japan; M. Kuwabara, Kyushu University, Japan

2:30 PM

(EMA-S9-002-2013) Combinatorial thin film methodology for exploration of novel functional materials (Invited)

I. Takeuchi*, University of Maryland, USA

3:00 PM

(EMA-S9-003-2013) Highly Textured (K,Na)NbO₃ Pb-free piezoelectric films prepared by sol-gel process

J. Li*, Q. Yu, Tsinghua University, China

3:15 PM

(EMA-S9-004-2013) Bi-based Piezoelectric Thin Films via Chemical Solution Deposition

Y. Jeon, E. Patterson, Oregon State University, USA; P. Mardilovich, W. Stickle, Hewlett-Packard Corporation, USA; J. Ihlefeld, G. Brennecke, Sandia National Laboratories, USA; B. J. Gibbons*, Oregon State University, USA

3:30 PM

Break

In Situ Characterization and Novel Processing

Room: Mediterranean B/C

Session Chair: Jon Ihlefeld, Sandia National Laboratories

4:00 PM

(EMA-S9-005-2013) Effects of Interfaces and Surfaces on Domain Structure and Properties in Ferroelectric Thin Films (Invited)

X. Pan*, The University of Michigan, USA

4:30 PM

(EMA-S9-006-2013) In situ synchrotron X-ray diffraction based technique reveals the effect of adhesion layer on the texture of solution-derived PZT thin films

K. Nittala*, S. Mhin, J. L. Jones, University of Florida, USA; J. F. Ihlefeld, G. L. Brennecke, Sandia National Laboratories, USA

4:45 PM

(EMA-S9-007-2013) Flux-assisted growth of BaTiO₃ thin films

D. T. Harris*, M. Burch, P. G. Lamb, North Carolina State University, USA; J. F. Ihlefeld, Sandia National Laboratories, USA; E. C. Dickey, J. Maria, North Carolina State University, USA

5:00 PM

(EMA-S9-008-2013) Carbon Nanotubes Integrated with Superconducting NbC (Invited)

G. Zou*, Soochow University, China; H. Luo, New Mexico State U., USA; Y. Zhang, Tsinghua U., China; T. McCleskey, L. Civale, Los Alamos National Lab, USA; Y. Zhu, North Carolina State U., USA; A. Burrell, Argon National Lab, USA; Q. Jia, Los Alamos National Lab, USA

S12: Recent Developments in High Temperature Superconductivity**New Superconductors and MgB₂ I-Processing and Pinning**

Room: Indian

Session Chair: Timothy Haugan, Air Force Research Laboratory

2:00 PM

(EMA-S12-017-2013) Development of new superconductors tailored by MBE (Invited)

H. Yamamoto*, Y. Krockenberger, NTT Basic Research Labs., Japan; M. Naito, Tokyo Univ. of Agric. and Technol., Japan

2:30 PM

(EMA-S12-018-2013) Structural features and superconductivity in iron-based superconductors with thick blocking layers (Invited)

H. Ogino*, A. Yamamoto, K. Kishio, J. Shimoyama, The University of Tokyo, Japan

3:00 PM

(EMA-S12-019-2013) Properties of epitaxial Ba(Fe_{1-x}Cox)₂As₂ thin films on different substrates (Invited)

X. Xi*, Temple University, USA

3:30 PM

Break

4:00 PM

(EMA-S12-020-2013) Comparative analysis of vortex pinning and dynamics in oxide, iron-based and MgB₂ superconductors (Invited)

L. Civale*, Los Alamos National Laboratory, USA

4:30 PM

(EMA-S12-021-2013) Nanoscale phase inhomogeneities in Fe-based selenides: Implications on the electronic structure and magnetic ground state (Invited)

C. Cantoni*, A. F. May, M. A. Michael, A. Safa-Sefat, B. C. Sales, Oak Ridge National Laboratory, USA

5:00 PM

(EMA-S12-022-2013) Epitaxial growth of superconducting molybdenum nitride films by a chemical solution method

Y. Y. Zhang, Tsinghua University, China; H. M. Luo, New Mexico State University, USA; N. Haberkorn, Los Alamos National Laboratory, USA; G. Zou, Soochow University, China; F. Ronning, Los Alamos National Laboratory, USA; H. Wang, Texas A&M University, USA; L. Civale, E. Bauer, A. K. Burrell, T. M. McCleskey, Q. X. Jia*, Los Alamos National Laboratory, USA

5:15 PM

(EMA-S12-023-2013) Pinning landscape in Fe-based thin films Superconductors (Invited)

B. Maiorov*, Los Alamos National Laboratory, USA

5:45 PM

(EMA-S12-024-2013) Enhanced superconducting properties in Iron chalcogenide thin films

L. Chen*, C. Tsai, Y. Zhu, A. Chen, J. Lee, X. Zhang, H. Wang, TAMU, USA

Friday, January 25, 2013

Plenary Session III

Room: Indian

8:30 AM

(EMA-PL-003-2013) Material Science and Device Physics Challenges for Near-Real-Time Adaptive Monolithic Multimodal Sensing

K. Reinhardt*, USAF/AFRL

9:30 AM

Break

S1: Functional and Multifunctional Electroceramics**Integrated Homo-, Hetro-epitaxial Single and Multi-Layer Films and Device Structures**

Room: Coral B

Session Chairs: Susan Trolier-McKinstry; Sahn Nahm, Korea University

10:00 AM

(EMA-S1-029-2013) Low Temperature Deposition of Electroceramic Films (Invited)

S. Trolier-McKinstry*, A. Rajashekar, S. Bharadwaja, S. Ko, E. Dorpalam, Penn State, USA

10:30 AM

(EMA-S1-030-2013) Examining the effects of charge defects on domain switching in thin film PZT via controlled neutron irradiation

J. T. Graham*, University of Texas at Austin, USA; G. L. Brenneka, Sandia National Laboratories, USA; P. J. Ferreira, University of Texas at Austin, USA; L. Small, D. Duquette, Rensselaer Polytechnic Institute, USA; S. Landsberger, University of Texas at Austin, USA; J. F. Ihlefeld, Sandia National Laboratories, USA

10:45 AM

(EMA-S1-031-2013) Wide bandgap semiconductors supporting a tunable mid-IR surface plasmon resonance

E. Sachet*, S. Franzen, J. Maria, North Carolina State University, USA

11:00 AM

(EMA-S1-033-2013) Anti-ferroelectric behavior of lead-free thin film NBT-BT

M. Rogers*, C. Fancher, Z. Zhao, J. Blendell, R. Garcia, Purdue University, USA

11:15 AM

(EMA-S1-034-2013) Formation of (Na_{0.5}K_{0.5})NbO₃ Thin Films and Their Application to Piezoelectric Nanogenerators (Invited)

I. Seo, B. Kim, M. Jang, S. Nahm*, Korea University, Republic of Korea

11:45 AM

(EMA-S1-035-2013) X-ray diffraction analysis of out-of-phase boundaries in epitaxial bismuth titanate (Bi₄Ti₃O₁₂) thin films prepared by atomic vapour deposition

N. Deepak*, P. Zhang, L. Keeney, M. E. Pemble, R. W. Whatmore, Tyndall National Institute, Ireland

12:00 PM

(EMA-S1-036-2013) Crystallographic Texture Effect on the Electromechanical Response of K_{0.5}Na_{0.5}NbO₃ modified Bi_{0.5}Na_{0.5}TiO₃-BaTiO₃

C. M. Fancher*, Purdue University, USA; W. Jo, J. Rödel, Technische Universität Darmstadt, Germany; J. E. Blendell, Purdue University, USA; K. J. Bowman, Illinois Institute of Technology, USA

12:15 PM

(EMA-S1-032-2013) Structural and Electrical properties of the 0.95(Na_{0.5}K_{0.5})NbO₃-0.05CaTiO₃ Thin Film grown by RF Sputtering Method

I. Seo*, B. Kim, M. Jang, S. Nahm, Korea University, Republic of Korea

S2: Multiferroic Materials and Multilayer Ferroic Heterostructures: Properties and Applications**Advanced Materials Synthesis and Characterization II**

Room: Coral A

Session Chair: Melanie Cole, U.S. Army Research Laboratory

10:00 AM

(EMA-S2-023-2013) The role of Pt_xPb intermetallic phases in crystallization of solution-deposited PZT and PbTiO₃ thin films: Critical insight from in situ X-ray diffraction (Invited)

J. L. Jones*, K. Nittala, S. Mhin, T. Sanders, University of Florida, USA; D. Robinson, Argonne National Laboratory, USA; G. Brenneka, J. Ihlefeld, Sandia National Laboratories, USA

10:30 AM

(EMA-S2-024-2013) Defect Chemistry and Phase Transitions in Ti-doped Bi_{1-x}NdxFeO₃ ceramics (Invited)

I. M. Reaney*, University of Sheffield, United Kingdom

11:00 AM

(EMA-S2-025-2013) Electric field tunable (Ba,Sr)TiO₃ films grown by molecular beam epitaxy (Invited)

S. Stemmer*, E. Mikheev, A. Kajdos, A. Hauser, University of California, Santa Barbara, USA

11:30 AM

(EMA-S2-026-2013) Microwave Characterization of Multiferroic Materials (Invited)

J. Booth*, NIST, USA; N. D. Orloff, Stanford University, USA; I. Takeuchi, University of Maryland, USA

12:00 PM

(EMA-S2-027-2013) Oxygen vacancies effects on physical properties in multiferroic thin films

H. Yang*, Soochow University, China; H. Wang, Texas A&M University, USA; Y. Wang, Los Alamos National Laboratory, USA

12:15 PM

(EMA-S2-028-2013) Different Routes to Multiferroicity

S. Krohns*, P. Lunkenheimer, A. Ruff, F. Schrettle, University of Augsburg, Germany; J. Mueller, M. Lang, University of Frankfurt, Germany; A. Loidl, University of Augsburg, Germany

S6: Thermoelectrics: Defect Chemistry, Doping and Nanoscale Effects**Oxide Thermoelectrics II**

Room: Pacific

Session Chair: Alp Sehirlioglu, Case Western Reserve University

10:00 AM

(EMA-S6-014-2013) Oxides with crystallographic shear defects – potential thermoelectric materials? (Invited)

M. Backhaus-Ricoult*, Corning Inc., USA

10:30 AM

(EMA-S6-015-2013) Electric Field-Induced Point Defect Redistribution in TiO₂

A. Moballeggh*, E. Dickey, NC State University, USA

10:45 AM

(EMA-S6-016-2013) The effect of pO₂ on the thermoelectric properties of beta gallia rutile intergrowths

D. Edwards*, M. Alberga, Alfred University, USA

11:00 AM

(EMA-S6-017-2013) Semiconductor-insulator transition in rutile ceramics controlled by post-sinter cooling conditions

A. R. West*, Y. Liu, University of Sheffield, United Kingdom

11:15 AM

(EMA-S6-018-2013) The Influence, Role, and Property Variations in Ferroelectricity at the Edge of the Metal-Insulator Transition and Its Influence on Thermoelectric Properties

J. A. Bock*, S. Lee, C. A. Randall, S. Trolier-McKinstry, The Pennsylvania State University, USA

11:30 AM

(EMA-S6-019-2013) Measurement of Thermal Conductivity and Thermal Boundary Conductance of Nano-Grained SrTiO₃ Thin Films

B. M. Foley*, H. Brown-Shaklee, J. C. Duda, R. Cheaito, University of Virginia, USA; B. J. Gibbons, Oregon State University, USA; D. L. Medlin, J. F. Ihlefeld, Sandia National Laboratories, USA; P. E. Hopkins, University of Virginia, USA

11:45 AM

(EMA-S6-020-2013) Thermal conductivity and domain wall Kapitza conductance in epitaxial bismuth ferrite thin films

J. Ihlefeld*, Sandia National Laboratories, USA; P. E. Hopkins, University of Virginia, USA; C. Adamo, Cornell University, USA; L. Ye, B. Huey, University of Connecticut, USA; S. R. Lee, Sandia National Laboratories, USA; D. G. Schlom, Cornell University, USA

S9: Thin Film Integration and Processing Science

Epitaxial Growth and Strain Engineering

Room: Mediterranean B/C

Session Chair: Brady Gibbons, Oregon State University

10:00 AM

(EMA-S9-009-2013) Strain and composition effects in epitaxial Pb(Zr,Ti)O₃ thin films (Invited)

G. Rijnders*, University of Twente, Netherlands

10:30 AM

(EMA-S9-010-2013) Structural and magnetic properties of epitaxial (111) oriented NiFe₂O₄ thin film on (0001) c-plane sapphire via chemical solution processing

S. Seifkar*, North Carolina State University, USA; B. Calandro, Missouri University Science and Technology, USA; G. Rasic, North Carolina State University, USA; N. Bassiri-Gharb, Georgia Institute of Technology, USA; J. Schwartz, North Carolina State University, USA

10:45 AM

(EMA-S9-011-2013) Temperature-dependent diffraction and microscopy observations of phase transitions and domain formation in highly-strained BiFeO₃ (Invited)

H. M. Christen*, W. Siemons, C. Beekman, M. Chi, J. Howe, N. Balke, P. Maksymovych, M. Biegalski, Oak Ridge National Laboratory, USA; A. Vaillonis, Stanford University, USA; P. Gao, X. Pan, University of Michigan, USA; A. K. Farrar, J. Moreno, D. Tenne, Boise State University, USA

11:15 AM

(EMA-S9-012-2013) Langmuir-Blodgett Films of 2D Oxide Nanosheets as Seed Layers for Oriented Growth of SrRuO₃ on Si

J. E. ten Elshof*, M. Nijland, S. Kumar C. Palanisamy, R. Lubbers, S. A. Veldhuis, R. Besselink, G. Koster, G. Rijnders, University of Twente, Netherlands

11:30 AM

(EMA-S9-013-2013) Epitaxial Ferroelectric Thin Films for Micro-Electro-Mechanical-System Based Data Storage (Invited)

A. Roelofs*, Center for Nanoscale Materials, USA

12:00 PM

(EMA-S9-014-2013) Low temperature epitaxial CeO₂ ultrathin films and nanostructures by atomic layer deposition

M. Coll*, J. Gazquez, A. Palau, X. Obradors, T. Puig, ICMAB-CSIC, Spain

S12: Recent Developments in High Temperature Superconductivity

New Superconductors and MgB₂ II—Wires and Devices

Room: Indian

Session Chair: Haiyan Wang, Texas A&M University

10:00 AM

(EMA-S12-025-2013) Scaling up of ex-situ multifilamentary MgB₂ superconducting wire manufacturing (Invited)

G. Grasso*, A. Tumino, S. Brisigotti, R. Piccardo, M. Tropeano, D. Nardelli, V. Cubeda, Columbus Superconductors, Italy

10:30 AM

(EMA-S12-026-2013) Development of high performance MgB₂ wires by internal Mg diffusion process (Invited)

H. Kumakura*, S. Ye, A. Matsumoto, K. Togano, National Institute for Materials Science, Japan

11:00 AM

(EMA-S12-027-2013) Critical Current Density of Multifilamentary Second Generation MgB₂ Wires (Invited)

M. D. Sumption*, The Ohio State University, USA; G. Li, M. A. Rindfleisch, M. J. Tomsic, Hyper Tech Research Incorporated, USA; W. E. Collings, The Ohio State University, USA

11:30 AM

(EMA-S12-028-2013) Synthesis and Properties of High-Jc Bulk BaFe₂As₂ Superconductors (Invited)

E. Hellstrom*, J. Weiss, J. Jiang, F. Kametani, D. Larbalestier, A. Polyanski, C. Tarantini, Applied Superconductivity Center - Florida State University, USA

12:00 PM

(EMA-S12-029-2013) Epitaxial thin films and artificially engineered superlattices of BaFe₂As₂ (Invited)

S. Lee*, C. M. Folkman, C. B. Eom, University of Wisconsin, USA; C. Tarantini, J. Jiang, J. D. Weiss, F. Kametani, E. E. Hellstrom, D. C. Larbalestier, Florida State University, USA; P. Gao, Y. Zhang, Q. X. Pan, University of Michigan, USA

S1: Functional and Multifunctional Electroceramics

Piezoelectrics and Characterization of Materials, Interfaces, as well as Electrical, Mechanical, Electro-mechanical and Other Material Properties

Room: Coral B

Session Chairs: Peter Finkel, Naval Undersea Warfare Center; Vojislav Mitic, Faculty of Electronic Engineering

2:00 PM

(EMA-S1-037-2013) Investigation of ferroelectric phase transitions and large energy conversion in domain engineered ferroic crystals

P. Finkel*, Naval Undersea Warfare Center, USA; S. Lofland, Rowan University, USA; D. Viehland, Virginia Tech, USA

2:15 PM

(EMA-S1-038-2013) The statistical analysis vertical grain contacts surfaces influence on BaTiO₃ ceramics intergranular capacity

V. Mitic*, V. Paunovic, Faculty of Electronic Engineering, University of Nis, Serbia; S. Jankovic, Mathematical institute, SASA, Serbia; L. Kocic, Faculty of Electronic Engineering, University of Nis, Serbia

2:30 PM**(EMA-S1-039-2013) Measurement of the Thermal Conductivity of Single and Polycrystalline PZT Thin Films**

B. M. Foley*, University of Virginia, USA; H. J. Brown-Shaklee, J. F. Ihlefeld, Sandia National Laboratories, USA; P. E. Hopkins, University of Virginia, USA

2:45 PM**(EMA-S1-040-2013) Determination of the Dissociation Kinetics of Defect Complexes under dc Bias in Perovskite Materials using TSC and In-Situ EPR Techniques**

R. Maier*, J. Follman, C. Randall, The Pennsylvania State University, USA

3:00 PM**(EMA-S1-041-2013) Probing Low-level Radiation Damage Using Thin Film Capacitors and Dielectric Measurements**

A. Smith*, North Carolina State University, USA; Y. Zhang, W. J. Weber, University of Tennessee, USA; S. C. Shannon, J. Maria, North Carolina State University, USA

3:15 PM**(EMA-S1-042-2013) Relaxation Behavior of Oxygen Vacancies in A(Ti_{0.99}Mg_{0.01})O₃ Perovskite Ceramics (A=Ba, Sr, Ca)**

Y. Han*, G. Song, SungKyunKwan University, Republic of Korea

3:30 PM**Break****4:00 PM****(EMA-S1-043-2013) Crystallographic refinement yields point defect and lattice changes in PZT as a result of neutron irradiation**

J. S. Forrester*, A. J. Henriques, S. B. Seshadri, University of Florida, USA; D. Brown, Los Alamos National Laboratory, USA; J. T. Graham, S. Landsberger, University of Texas-Austin, USA; J. F. Ihlefeld, G. L. Brennecke, Sandia National Laboratories, USA; J. L. Jones, University of Florida, USA

4:15 PM**(EMA-S1-044-2013) Piezoelectric Properties of the High Temperature xPbTiO₃ - (1 - x)[BiScO₃ + Bi(Ni_{1/2}Ti_{1/2})O₃] Ternary Perovskite Ferroelectric System**

T. Ansell*, D. P. Cann, Oregon State University, USA

4:30 PM**(EMA-S1-045-2013) Cooperative strain accommodation and high piezoelectricity in Sm doped PZT**

S. B. Seshadri*, M. M. Nolan, J. S. Forrester, J. C. Nino, University of Florida, USA; P. A. Thomas, University of Warwick, United Kingdom; J. L. Jones, University of Florida, USA

4:45 PM**(EMA-S1-046-2013) On the origin of high piezoresponse in BiScO₃-PbTiO₃**

L. Kodumudi Venkataraman*, Indian Institute of Science, India; A. N. Fitsch, European Synchrotron Radiation Facility, France; R. Ranjan, Indian Institute of Science, India

S2: Multiferroic Materials and Multilayer Ferroic Heterostructures: Properties and Applications**Properties and Device Applications**

Room: Coral A

Session Chair: Melanie Cole, U.S. Army Research Laboratory

2:00 PM**(EMA-S2-029-2013) Voltage Control of Magnetism in Multiferroic Heterostructures and Low-Power Devices (Invited)**

N. Sun*, Northeastern University, USA

2:30 PM**(EMA-S2-030-2013) Voltage Tunable Acoustic Resonance in Perovskite Thin Films (Invited)**

N. M. Sbrockey*, G. S. Tompa, Structured Materials Industries, Inc., USA; T. S. Kalkur, University of Colorado at Colorado Springs, USA; M. W. Cole, U.S. Army Research Laboratory, USA; J. Zhang, S. P. Alpay, University of Connecticut, USA

2:45 PM**(EMA-S2-031-2013) Growth and Ferromagnetic Resonance Properties of Nanometer-Thick Yttrium Iron Garnet Films (Invited)**

M. Wu*, Colorado State University, USA

3:00 PM**(EMA-S2-032-2013) Nonlinear dynamics of multiferroic cantilevers (Invited)**

T. Onuta*, University of Maryland, USA

3:15 PM**(EMA-S2-033-2013) Mechanism of microwave loss in practical high performance dielectrics (Invited)**

N. Newman*, L. Liu, A. Matusevich, M. Flores, Arizona State University, USA

3:30 PM**(EMA-S2-034-2013) Material Advancement Needs for Efficient Pyroelectric Power Generation and Cooling (Invited)**

S. Annapragada*, J. V. Mantese, T. D. Radcliff, United Technologies Research Center, USA

3:45 PM**(EMA-S2-035-2013) Giant Electrocaloric Effect in Relaxor Ceramic Materials for Dielectric Refrigeration**

Z. Kutnjak*, B. Rozic, B. Malic, H. Ursic, J. Holc, M. Kosec, Jozef Stefan Institute, Slovenia; Q. M. Zhang, The Pennsylvania State University, USA

S7: Production Quality Ferroelectric Thin Films and Devices**Production Quality Ferroelectric Thin Films and Devices**

Room: Coral A

Session Chairs: Glen Fox, Fox Materials Consulting, LLC; Geoff Brennecke, Sandia National Laboratories; Ronald Polcawich, U.S. Army Research Laboratory

4:00 PM**(EMA-S7-001-2013) Development of PZT based ferroelectric capacitor for mass-production ferroelectric RAM (FRAM) (Invited)**

T. Eshita*, W. Wang, K. Nakamura, S. Mihara, FUJITSU SEMICONDUCTOR LIMITED, Japan; H. Yamaguchi, K. Nomura, FUJITSU LABORATORIES LIMITED, Japan

4:30 PM**(EMA-S7-002-2013) Development of Process Technology for Ferroelectric Thin Film Application (Invited)**

K. Suu*, ULVAC, Inc., Japan

5:00 PM**(EMA-S7-003-2013) Sputtered Nb-doped PZT Film with Giant Piezoelectricity for MEMS Applications (Invited)**

Y. Hishinuma*, Y. Li, J. Birkmeyer, FUJIFILM Dimatix, USA; T. Fujii, T. Naono, T. Arakawa, FUJIFILM Corporation, Japan

S9: Thin Film Integration and Processing Science**Novel Substrates**

Room: Mediterranean B/C

Session Chair: Glen Fox, Fox Materials Consulting, LLC

2:00 PM**(EMA-S9-015-2013) PZT based PiezoMEMS for RF Systems (Invited)**

R. G. Polcawich*, J. Pulskamp, T. Ivanov, S. Bedair, R. Proie, L. Sanchez, C. Meyer, US Army Research Laboratory, USA

2:30 PM**(EMA-S9-016-2013) Sputtered PZT Thin Films on Copper Foils**

J. Walenza-Slabe*, B. J. Gibbons, T. Ansell, Oregon State University, USA; R. G. Polcawich, U.S. Army Research Laboratory, USA

2:45 PM

(EMA-S9-017-2013) The roles of solution chemistry, substrate, and pyrolysis temperature on the chemical heterogeneity in PZT films
J. Inhefeld*, P. G. Kotula, B. D. Gauntt, G. L. Brennecke, D. V. Gough, E. D. Spoerke, Sandia National Laboratories, USA

3:00 PM

(EMA-S9-018-2013) Alternative Adhesion Layers for Noble Metal/Si substrates - Impact on PZT Thin Films for MEMS Devices (Invited)

P. Mardilovich*, J. Abbott, Hewlett-Packard Company, USA; C. Shelton, North Carolina State University, USA; W. Stickle, G. Long, Hewlett-Packard Company, USA; E. Patterson, K. Brookshire, B. Maack, S. Freyand, B. Gibbons, Oregon State University, USA

3:30 PM**Break**

Controlling Phase Assemblage and Stoichiometry II

Room: Mediterranean B/C

Session Chair: Christopher Shelton, NCSU

4:00 PM

(EMA-S9-019-2013) Role of boundaries on the low-field magnetotransport properties of (La_{0.7}Sr_{0.3}MnO₃)_{1-x}(ZnO)_x nanocomposite thin films (Invited)

A. Chen, W. Zhang, Texas A&M University, USA; Z. Bi, Q. Jia, Los Alamos National Laboratory, USA; J. L. MacManus-Driscoll, University of Cambridge, United Kingdom; H. Wang*, Texas A&M University, USA

4:30 PM

(EMA-S9-020-2013) Effects of Pb-excess in Pb(Zr_{0.52}, Ti_{0.48})O₃, PZT(52/48), Thin Films for Use in Multilayer Actuators

L. M. Sanchez*, Army Research Laboratory, USA; G. Fox, Fox Materials Consulting LLC, USA; I. Takeuchi, University of Maryland, USA; R. G. Polcawich, Army Research Laboratory, USA

4:45 PM

(EMA-S9-021-2013) Influence of the precursor chemistry on the formation of the perovskite phase in PMN-PT thin films

A. Veber*, Institut "Jozef Stefan", Slovenia; S. Kunej, Institut "Jozef Stefan", Slovenia; M. Spreitzer, Institut "Jozef Stefan", Slovenia; A. Vorobiev, S. Gevorgian, Chalmers University of Technology, Sweden; D. Suvorov, Institut "Jozef Stefan", Slovenia

5:00 PM

(EMA-S9-022-2013) Control of Crystallographic Texture and Surface Morphology of Pt/TiO₂ Templates for Enhanced PZT Thin Film Performance

A. Fox*, Oregon State University, USA; G. Fox, Fox Materials Consulting LLC, USA; B. Gibbons, Oregon State University, USA; S. Trolier-McKinstry, Penn State University, USA

5:15 PM

(EMA-S9-023-2013) Peculiarities of PZT Films Produced by Different Technologies for MEMS

N. Korobova*, S. Timoshenkov, V. Vodopyanov, National Research University of Electronic Technology, Russian Federation

S10: Ceramic Composites for Defense Applications

Nano-composites

Room: Pacific

Session Chair: Edward Gorzkowski, Naval Research Laboratory

2:00 PM

(EMA-S10-001-2013) Dielectric Film Development for Naval Pulse Power Applications (Invited)

P. Armistead*, Office of Naval Research, USA

2:30 PM

(EMA-S10-002-2013) Piezoelectric and Dielectric Enhancement of New Nano-structured Ceramics with High Density of Heteroepitaxial Interface by MPB Engineering (Invited)

S. Wada*, University of Yamanashi, Japan

3:00 PM

(EMA-S10-003-2013) Polymer-MOF Composites for Dielectric Materials

L. N. Appelhans*, Sandia National Laboratory, USA

3:15 PM

(EMA-S10-004-2013) Synthesis and Characterization of Nanoparticle/Nanocrystalline Barium Titanate and PLZT for Functional Nanoparticle-Polymer Composites

C. DiAntonio*, T. Monson, M. Winter, T. Chavez, P. Yang, Sandia National Laboratories, USA

3:30 PM**Break**

Piezo-composites/Extreme Environments

Room: Pacific

Session Chair: Charles Stutz, AFRL/MLPS

4:00 PM

(EMA-S10-005-2013) Composite Electronic Materials for Capacitive Devices (Invited)

C. Randall*, Penn State University, USA

4:30 PM

(EMA-S10-006-2013) Bi(Zn_{0.5}Ti_{0.5})O₃ - BaTiO₃ Composites for Pulsed Power Applications

E. Gorzkowski*, M. Pan, Naval Research Laboratory, USA; G. Brennecke, H. Brown-Shaklee, Sandia National Laboratories, USA

4:45 PM

(EMA-S10-007-2013) Investigation of Tunable Bulk Microwave Dielectrics

E. Furman*, B. A. Jones, S. E. Perini, M. T. Lanagan, Pennsylvania State University, USA; S. Kwon, W. Hackenberger, R. Sahul, TRS Technologies, Inc, USA

5:00 PM

(EMA-S10-008-2013) Bio-dielectric Hybrid Films for Capacitor Applications

D. Joyce*, Air Force Research Laboratory, USA; F. Ouchen, N. Venkat, S. R. Smith, University of Dayton Research Institute, USA; K. M. Singh, UES, Inc., USA; J. G. Grote, Air Force Research Laboratory, USA

S12: Recent Developments in High Temperature Superconductivity

Superconductor Applications II—Large-Scale and Hybrid Energy Storage and Machine Technologies

Room: Indian

Session Chair: Haiyan Wang, Texas A&M University

2:00 PM

(EMA-S12-030-2013) Superconductivity: Rising to the Energy Challenges (Invited)

Q. Li*, Brookhaven National Lab, USA

2:30 PM

(EMA-S12-031-2013) Compensation for Fluctuating Output of Solar Photovoltaic and/or Wind Power with a Hybrid Energy Storage System Composed of MgB₂ SMES and Hydrogen Storage Systems (Invited)

M. Tsuda*, D. Miyagi, Tohoku University, Japan; T. Hamajima, Hachinohe Institute of Technology, Japan; T. Shintomi, Nihon University, Japan; Y. Makida, KEK, Japan; T. Takao, Sophia University, Japan; M. Kajiwara, Iwatani Corporation, Japan

3:00 PM

(EMA-S12-032-2013) Winding Technology of Fully-Superconducting Induction/Synchronous Machine for Next Generation Automobile Application (Invited)

T. Nakamura*, S. Misawa, H. Kitano, H. Shimura, T. Nishimura, N. Amemiya, Kyoto University, Japan; Y. Itoh, M. Yoshikawa, T. Terazawa, IMRA Material R&D Co., Ltd, Japan; N. Okumura, IASIN SEIKI Co.,Ltd., Japan

3:30 PM

(EMA-S12-033-2013) Applications Using High Temperature Superconducting Tapes

C. Rey*, Tai-Yang Research Co., USA

3:45 PM

(EMA-S12-034-2013) Development of Superconducting and Cryogenic Power Systems and Impact for Aircraft Propulsion (Invited)

T. Haugan*, Air Force Research Laboratory, USA; D. Latypov, BerrieHill Research Co., USA

4:15 PM

(EMA-S12-035-2013) SMES for Wind Energy Systems

A. Paul Antony*, D. T. Shaw, State University of New York at Buffalo, USA

S13: Body Energy Harvesting for Intelligent Systems

Body Energy Harvesting

Room: Indian

Session Chairs: Wolfgang Sigmund, University of Florida; Seungbum Hong, Argonne Nat Lab

4:30 PM

(EMA-S13-001-2013) A New Approach to Multifunctional Lead-free Piezoelectric Films Coupled with Ultra-Thin Flexible Metal Foil Substrates for Implantable Smart Medical Devices; Sensors and Energy Harvesters (Invited)

S. Kim*, A. Leung, E. Greenstein, Brown University, USA; S. Kim, D. Kim, Auburn University, USA; A. I. Kingon, Brown University, USA

5:00 PM

(EMA-S13-002-2013) Piezoelectric and Electroactive Strain Harvesters for Wearable and Implantable Sensor Applications (Invited)

B. Wardle*, Massachusetts Institute of Technology, USA; M. Kim, KRISS, Republic of Korea; Q. Zhang, Pennsylvania State University, USA

Wednesday, January 23, 2013

Plenary Session I

Room: Indian

8:45 AM

(EMA-PL-001-2013) Pulsed Laser Deposition : God's Gift to Complex Oxides Creating New States of Matter with Oxide Heteroepitaxy (Invited)

R. Ramesh*, University of California, Berkeley, USA

The advent of high temperature superconductivity in cuprates was a global trigger point for a comprehensive revisit to all transition metal oxides that exhibit a rich spectrum of functional responses, including magnetism, ferroelectricity, highly correlated electron behavior, superconductivity, etc. The basic materials physics of such materials provide the ideal playground for interdisciplinary scientific exploration. By far, one of the most important elements of this resurgence of worldwide interest in these materials has been, and continues to be, pulsed laser deposition (PLD). Since its introduction to the field of oxides by Venkatesan and co-workers at Bellcore/Rutgers, it has taken the world by storm. I have personally been one of the major beneficiaries of this explosion. Its relative simplicity and the ability to transfer the stoichiometry of complex oxides onto a substrate with unprecedented perfection has been one of the key reasons for the proliferation. The technique has evolved significantly since the early days in the late eighties; several surface tools have now become standard in PLD and I am sure they will continue to evolve even more.

S3: Structure of Emerging Perovskite Oxides: Bridging Length Scales and Unifying Experiment and Theory

Session 1

Room: Pacific

Session Chairs: John Daniels, University of New South Wales; Julia Glaum, The University of New South Wales

10:00 AM

(EMA-S3-001-2013) The local and average structure in lead-free BaTiO₃-based perovskites (Invited)

J. Kreisel*, CRP Lippmann & Luxembourg University, Luxembourg

BaTiO₃-based relaxors such as BaTi_{1-x}Zr_xO₃ (BTZ) present a homovalent Zr⁴⁺/Ti⁴⁺ substitution and its properties have attracted a significant interest [1], more recently namely in the light of reports on large piezoelectric effects [2]. Here, we will first recall our experimental results from X-ray absorption [3] and neutron pair distribution functions (PDFs) [4] before putting emphasis on insight that can be gained from ab-initio calculations [5]. We will show that the type of a Ti displacement is entirely determined by the local Ti/Zr distribution in the adjacent unit cells. We show that the underlying mechanism involves local strain effects that ensue from the difference in size between the Ti⁴⁺ and Zr⁴⁺ cations. Interestingly, the local strain effects induce distortions of the octahedra but not their rotation (tilting). Finally, we will put our observations in the light of the report of a large piezoelectric effect in Ca-doped BTZ (BCTZ) [2], discuss phase transitions that we have recently observed in BCTZ and discuss possible origins why such a large response is observed in BCTZ but not in BTZ. [1] A. Simon et al JPCM 16, 963 (2004). [2] W. Liu, X. Ren, PRL 103, 257602 (2009). [3] C. Laulhé, F. Hippert, J. Kreisel, et al. PRB 74, 014106 (2006) & Phase Transitions 84, 438 (2011). [4] C. Laulhé, et al. , PRB 79, 064104 (2009). [5] C. Laulhé, A. Pasturel, F. Hippert, J. Kreisel, PRB 82, 132102 (2010).

10:30 AM

(EMA-S3-002-2013) Noncentrosymmetric Oxyfluoride Compounds (Invited)

K. Poeppelmeier*, Northeastern University, USA

This talk will present analyses we have performed upon oxyfluoride compounds and their relationship with noncentrosymmetric materials such as lithium niobate and potassium titanyl phosphate. Synthesis of noncentrosymmetric materials – materials that lack an inversion center – has been a long-standing and difficult goal of inorganic chemistry. Noncentrosymmetric crystals are used for their piezoelectric, ferroelectric, and second-harmonic generation (SHG) properties. Recently, nanolithography has sought UV lasers to create increasingly small lithographic features. To pursue UV lasers, scientists have sought new SHG active crystals to double the frequency of laser light to higher energies. One such material is the oxyfluoride KBe₂BO₃F₂; we seek to develop similar materials for use as SHG-active crystals. Efficient SHG-active crystals often have anions with aligned polar moments in the solid state. Therefore, to synthesize highly-efficient SHG crystals, a promising strategy is to utilize anions that inherently contain polar moments to establish principles and guidelines to target syntheses of SHG-active materials.

11:00 AM

(EMA-S3-003-2013) Intermediate Phases at MPBs and analogous Temperature-driven Phase Transitions (Invited)

P. A. Thomas*, R. Beanland, University of Warwick, United Kingdom; S. Gorfman, University of Siegen, Germany; D. Keeble, University of Warwick, United Kingdom; J. Kreisel, Centre de Recherche Publique Gabriel Lippmann, Luxembourg; D. Woodward, University of Warwick, United Kingdom

Extensive research has been devoted to the crystal symmetry at the MPB, first in lead-based compounds (PZT) and latterly in lead-free piezoelectrics (NBT-BT-KNN). Broadly, the interpretations are: Bridging of symmetrically unrelated phases such as R3m (R) and P4mm (T) by a lower symmetry phase; Transition by shrinkage of domain-size and nanodomain formation. How the transformation across an MPB occurs is a challenge to experiment and theory. Investigation of the structures of inherently chemically disordered materials without identically-repeating unit cells pushes the limits of experimental techniques and First Principles modelling to gain insights into messy behaviour, often dominated by extrinsic factors rather than intrinsic, is non-trivial. We present a multi-technique and length-scale study of NBT-based materials. On the nanoscale (<10nm), we show NBT is disordered rhombohedral, an observation we reconcile with earlier evidence of monoclinicity from methods that probe larger-scale features. In the region between R and T phases, either temperature- or composition-driven, we analyse pseudo-cubic intermediate regions and reveal a critical point. We examine the peculiar tetragonal symmetries (eg P4bm) that appear and explain their competition-mediated formation. We discuss in the context of the close energetic relationships of different phases often invoked for the enhancement of piezoelectricity.

11:30 AM

(EMA-S3-004-2013) Polar Anisotropy in Ferroelectric Perovskites: Theory and Experiment (Invited)

G. A. Rossetti*, University of Connecticut, USA

The thermodynamic theory of polar anisotropy is applied to several perovskite-structured ferroelectric solid solutions. The theory produces excellent qualitative agreement with experimentally determined phase diagrams and electromechanical properties, and also accounts for triple and tricritical points, monoclinic bridging phases, miniaturized domain states, and phase coexistence. The theory predicts that despite topological distinctions, the diffusionless phase diagrams of the 'shifting' type, 'pinching' type and 'morphotropic' type all share a common feature: a line in composition-

temperature plane along which the crystallographic anisotropy of polarization vanishes. To investigate this prediction experimentally, the specific heat for barium titanate and for compositions in the morphotropic solid solutions lead zirconate-titanate, lead zinc niobate-lead titanate, and lead magnesium niobate-lead titanate was measured at temperatures 100K to 1000K. The excess enthalpies and entropies of the paraelectric to ferroelectric and inter-ferroelectric phase transitions were determined. The results show that the discontinuities in entropy and polarization at the inter-ferroelectric boundaries are uniformly quite small, confirming weak anisotropy of polarization at these transitions. Similarities and contrasts between the mixing of anisotropy energies in lead-based and lead-free solid solutions will be highlighted.

12:00 PM

(EMA-S3-005-2013) Nanodomain Structures, Mechanisms and Diffraction Effects in Morphotropic Phase Boundary Ferroelectrics

Y. U. Wang*, W. Rao, T. Cheng, J. Zhou, Michigan Tech, USA

Phase field modeling is employed to study the nanodomain structures and mechanisms responsible for enhanced electromechanical properties near morphotropic phase boundaries (MPBs) in ferroelectric solid solutions. Computer simulations provide insights into phase coexistence, domain wall contribution, field-induced inter-ferroelectric phase transformation and their relations to the superior piezoelectric properties around MPB. The modeling and simulation show that extrinsic domain mechanisms play important roles in the strong piezoelectricity around MPBs, and crystallographic domain engineering is effective to exploit the domain mechanisms for property enhancement. The coherent scattering, interference and adaptive diffraction effects of nanodomains and diffuse scattering associated with heterogeneous lattice distortions are discussed. While the computational studies are performed for lead-based MPB ferroelectrics, the findings also provide insights into other MPB systems and help develop lead-free materials.

12:15 PM

(EMA-S3-006-2013) Electric field induced structural transformation in $\text{Na}_{1/2}\text{Bi}_{1/2}\text{TiO}_3$

B. Rao*, R. Ranjan, Indian Institute of Science, India

$\text{Na}_{1/2}\text{Bi}_{1/2}\text{TiO}_3$ (NBT) and its solid solutions have been extensively investigated as a potential lead free piezoelectric ceramic. The complex structure and phase transition of pure NBT has not been clearly understood yet. In this work we have carried out XRD structural analysis of unpoled and electrically poled specimens of this compound. Using Rietveld refinement, we show that NBT undergoes irreversible monoclinic (*Cc*) to rhombohedral (*R3c*) structural transition after application of electric field. This phenomenon has been analyzed using two alternative models. In the polarization rotation model the compound is thought to intrinsically possess *Cc* structure, and the electric field induces the polarization vector to rotate in the pseudocubic (1-10) plane to the $\langle 111 \rangle_{\text{pc}}$ direction thereby yielding the *R3c* structure. The second model is based on additional interference effects caused due to existence of nanoscale twin domains whose size is less than coherence length of X-rays. This gives rise to coherent and adaptive diffraction effects causing the rhombohedral structure to appear as monoclinic. Comparing the observed monoclinic lattice parameters with those derived using the adaptive phase theory. Our results provide an ideal foundation to understand the role of monoclinic distortion and nanodomains in influencing the property of NBT.

S5: Structure and Properties of Interfaces in Electronic Materials

Grain Boundary Structure Dependent Properties

Room: Mediterranean B/C

Session Chair: John Blendell, Purdue University

10:00 AM

(EMA-S5-001-2013) Alumina properties – pushing the (grain) boundaries (Invited)

H. M. Chan*, Q. Wu, M. Kracum, Z. Yu, J. M. Rickman, M. P. Harmer, Lehigh University, USA

Recently, a new framework for understanding atomic-scale, grain boundary interphases (or complexions) has emerged. These interphases exist only at grain boundaries, and can display a rich diversity of structures and properties. The talk will discuss strategies for achieving unique combinations of material properties. Examples where selected additives such as copper and rare earth elements (Y, Hf) have resulted in modifications to grain boundaries in polycrystalline alumina, together with the corresponding enhancements in the mechanical and transport behavior will be discussed.

10:30 AM

(EMA-S5-002-2013) Orientation Dependence of Grain Boundary Thermal Conductance in Alumina (Invited)

S. J. Dillon*, K. Tai, University of Illinois Urbana-Champaign, USA

While significant effort has been made to characterize the interfacial thermal conductance of grain boundaries and interphase boundaries, few studies have treated the effects of interfacial anisotropy. This presentation will report recent measurements of the grain boundary thermal conductance of (0001) twist boundaries in alumina. The results will be rationalized in the context of interfacial dislocation density.

11:00 AM

(EMA-S5-003-2013) Structure and Energy of Equilibrated Ni-Alumina Interfaces (Invited)

H. Meltzman, W. D. Kaplan*, Technion - Israel Institute of Technology, Israel

Understanding the structure, chemistry and energy of metal-ceramic interfaces is important for both fundamental science and technological applications. Metal-ceramic interfaces for fundamental studies are often produced by diffusion bonding or thin film deposition, although both techniques can result in a metastable interface state rather than a thermodynamically equilibrated state. The minimum energy configuration of an interface is a significant driving force for microstructural evolution of interfaces. The goal of this work was to determine the solid-solid interface energy and structure for Ni- Al_2O_3 (0001) interfaces. Samples were based on pure thin Ni films which were dewetted in the solid-state (under controlled oxygen partial pressure) to reach equilibrium, from which both the interface structure and energy was determined. For interface structural and energy analysis, TEM samples were characterized using a monochromated and aberration corrected TEM. Winterbottom analysis was used to determine the interface energy, and exit wave reconstruction of TEM data was used to construct an atomistic model of the interface. From the TEM analysis it was found that the interface structure is incoherent, and reconstructed to form a 2-D interface Bravais lattice of $2.5\sqrt{3}R30$. The concept of interfacial reconstruction as an alternative mechanism to semi-coherent interfaces for absorbing strain energy will be discussed.

11:30 AM

(EMA-S5-004-2013) Grain Boundary Complexion Diagrams: An Interfacial Counterpart to Bulk Phase Diagrams (Invited)

N. Zhou, Y. Zhang, J. Luo*, UCSD, USA

Bulk phase diagrams are one of the most useful tools for materials science. Materials researchers have long recognized that grain bound-

aries (GBs) can exhibit phase behaviors; for example, the classical Fowler adsorption isotherm already implied the existence of first-order transitions. Following the seminal Cahn model (for critical-point wetting), various grain boundary (premelting and prewetting types) phase diagrams have been constructed by Straumal, Carter, Mishin, Wynblatt and others. Furthermore, recent studies using advanced microscopy directly observed a series of discrete GB interfacial phases (which were also named “complexions”). After a brief review of some historical aspects, this talk will discuss our recent efforts on developing GB diagrams as a useful tool for materials science, which include both the less rigorous — yet robustly useful — GB lambda diagrams and more rigorous GB phase diagrams with well-defined transition lines and critical points. Recent studies demonstrated that such GB diagrams are useful in solving old scientific mysteries, predicting new phenomena, and designing optimal fabrication recipes. Several recent examples will be discussed. We suggest that GB diagrams can be a useful component for the Materials Genome project.

12:00 PM

(EMA-S5-005-2013) Thermal Conductivity of Thick Film Tungsten Metallization used in High-Alumina Ceramic Microelectronic Packages

M. Eblen*, Kyocera America, Inc., USA

In a conventional high temperature co-fired multilayer 90~96% alumina microelectronic package, the thick film refractory metallization traces used for electrical signal routing also play a role in thermal conduction. This is seen in the electronics space with the common use of a thermal via array. What is less known is the quantitative thermal dissipation improvement due to the metallization. Answering this question poses experimental challenges as the co-fired metallization properties cannot be measured independently due to the sintering process interaction with the ceramic body. A quick inspection of the metallization electrical resistivity or sheet resistance when compared to that of pure tungsten provides evidence of this dramatic change in physical properties. Therefore, we are constrained to characterize the entire metallization/ceramic composite in a more or less homogenized manner. In the present study, directional normal and in-plane thermal diffusivity measurements were conducted on a geometrically simple periodic laminate metallization/alumina structure. The rear surface transient temperature response curve was then correlated to a finite element model by varying the metallization thermal conductivity until the low frequency component of the residual error was minimized.

12:15 PM

(EMA-S5-006-2013) 80 kV study of the Atomic Structure and Bonding at SrTiO₃/GaAs Hetero-interfaces

Q. Qiao*, S. Ogut, R. F. Klie, University of Illinois at Chicago, USA; R. Droopad, R. Contreras-Guerrero, Texas State University, USA

We examined ultra-thin SrTiO₃ films deposited on As-terminated GaAs (100) using molecular beam epitaxy under various O₂ partial pressures. Atomic-resolution Z-contrast images of different SrTiO₃ films were obtained using the aberration-corrected JEOL JEM-ARM200CF operated at 80 kV. Using atomic-column resolved EELS, our analysis of the Ti and O near-edge fine structure reveals different bonding configurations at the interface resulting from different growth methods. These results strongly suggest that although it does not affect the cationic arrangement at the interface, a Ti pre-layer deposition alleviates the oxidation of the substrate and consequently the Fermi level pinning at the interface, as reported before. The relationship between interfacial oxidation and Fermi level pinning is further studied by examining SrTiO₃ films grown with oxygen plasma and molecular oxygen. We will present the atomic-resolution Z-contrast images, annular bright field images and EELS studies to confirm the effects of oxidation states in inducing the Fermi level pinning. Using first-principles DFT calculations, we analyze the formation energies

of Ti-related impurity defects in the bulk and surface regions of GaAs to help in the interpretation of electron microscopy experiments.

S8: Advances in Memory Devices

Fundamentals and Reliability

Room: Coral B

Session Chair: Bryan Huey, University of Connecticut

10:00 AM

(EMA-S8-001-2013) Reliability of Ferroelectric Memory Embedded in 130nm CMOS (Invited)

J. Rodriguez*, Texas Instruments, USA

Ferroelectric random access memory (FRAM) offers unique capabilities which make it an attractive non-volatile memory for many applications. The low voltage operation, low write power, and fast write capability is of specific interest for ultra low power mobile and wireless electronics, battery powered measurement applications, and emerging applications including intelligent, battery-less sensors. The ability of the FRAM to operate as both a data and code-storage memory provides flexibility for embedded microcontroller and system on chip devices. Non-volatile information storage coupled with high endurance enables FRAM to be a replacement for battery-backed SRAM, as in data logging systems. Together with advantageous features the reliability of the memory must be demonstrated. We present results of a comprehensive reliability evaluation of a 2T-2C, 4Mb, FRAM embedded within a standard 130 nanometer CMOS platform with 5 layers of Cu metallization. Endurance to >10¹⁵ data cycles and data retention equivalent of 10 years at 85°C is demonstrated.

10:30 AM

(EMA-S8-002-2013) Improved Power Consumption for Ferroelectric Switching based on Nanoscale Switching Dynamics

N. Polomoff, S. Lee, J. Bosse, V. Palumbo, V. Vyas, M. Rivas, J. Leveillee, B. D. Huey*, University of Connecticut, USA

High Speed SPM studies of ferroelectric switching dynamics have revealed a strong but nonlinear influence of voltage pulsing conditions on domain nucleation versus growth mechanisms. In particular, high voltages beyond the coercive field favor nucleating new domains, while lower voltages promote domain growth instead. As a result, the possibility exists to engineer switching pulses for nucleating a high density of switching sites, which can then efficiently grow and overlap to rapidly complete the switching process even with much lower sustained poling biases. The overall energy consumption is improved in this process, providing a route for enhanced switching efficiencies in ferroelectric devices.

10:45 AM

(EMA-S8-003-2013) Generation and Storage of 360° Domain Walls for Magnetic Devices

Y. M. Jin*, L. D. Geng, Michigan Technological University, USA

360° domain walls in planar magnetic nanowires attract attentions for their potential new functionalities in miniaturized devices, such as sensor application in patterned magnetic films, magnetic random access memory cell in nanorings, and magnetic memory and logic device in multilayer stripes. For the applications of 360° domain walls, reliable production and accurate control of them are necessary. This talk presents a micromagnetic simulation study of 360° domain wall behaviors in planar nanowire loops. In particular, it is shown that a nanowire loop with a shape-isotropic wall generator at one end and a shape-anisotropic wall stopper at the other end functions like a data storage stack: 360° domain walls are generated and pushed into stack under rotating field before overflow, while popped out and annihilated when field rotating direction is inverted until underflow. The stack capacity is determined by the total length of the nanowire loop.

This simple nanowire design can be integrated into magnetic circuits as an operation unit for 360° domain wall generation and storage.

11:00 AM

(EMA-S8-004-2013) Non-Ohmic Phenomena in BaTiO₃, SrTiO₃ and CaTiO₃

M. Prades, H. Beltran, E. Cordocillo, Universitat Jaume I, Spain; N. Maso*, A. R. West, The University of Sheffield, United Kingdom

The bulk conductivity of *p*-type, acceptor-doped BaTiO₃, SrTiO₃ and CaTiO₃ increases by 1-2 orders of magnitude for temperatures in the range 200–700 °C on application of a small *dc* bias, e.g. 1–100 Vcm⁻¹. By contrast, the mirror image of the behaviour of acceptor-doped systems is observed in lightly reduced, *n*-type, Mn-doped BaTiO₃ whose conductivity decreases on application of a *dc* bias. With both *p*-type and *n*-type materials, the conductivity changes on application of a *dc* bias are rather similar to those observed on changing the oxygen partial pressure in the atmosphere during conductivity measurements. The partially ionised oxygens which must exist in many standard ceramic samples, especially at sample surfaces, can readily act as either electron traps or electron sources. For a *n*-type conductor, the trapping of electrons under the action of a small *dc* bias leads to an increase in sample resistance whereas for *p*-type materials, electrons are also trapped at the sample surface, but these arise from ionisation of underbonded oxide ions associated with the acceptor dopants, leading to an increase in hole concentration. The holes must be located on oxygen which, chemically, are equivalent to O⁻ ions.

11:15 AM

(EMA-S8-005-2013) Nanoscale Dynamics in Phase Change Switching

J. Bosse*, University of Connecticut, USA; I. Grishin, O. Kolosov, Lancaster University, United Kingdom; B. D. Huey, University of Connecticut, USA

Phase change materials are promising candidates for non-volatile memory systems. To assess the switching characteristics, combinatorial approaches are leveraged implementing a range of voltage pulse amplitudes, durations, and rise/fall times. Current maps with conductive AFM are interleaved to assess the amorphous or crystalline state. Threshold switching characteristics are thereby identified, with amorphous to crystalline phase transitions observed down to 30 nsec pulses. Investigations into high density data recording, the dynamics of the switching process, and switching stability are also underway.

11:30 AM

(EMA-S8-006-2013) Preliminary Computational Approach to the Study of Oxygen Diffusion in HfO_{2-x}

G. Broglia*, M. Montorsi, L. Larcher, University of Modena and Reggio Emilia, Italy

Hafnium oxide has been identified as one of the most promising materials for the fabrication of novel memory and logic devices. This work would be a preliminary investigation of the sub-stoichiometric effects on oxygen diffusion, which has been supposed one of the most influencing factors on resistive switching. Long time molecular dynamic simulations have been performed and the trajectory has been employed to assess the mean square displacement of oxygen ions. Both crystal and amorphous structures have been simulated in order to recreate the major number of possible scenario encountered in real devices. Especially a model to investigate sub-stoichiometric oxide has been implemented, in order to obtain preliminary information about the migration of oxygen ions in particular condition. The activation energy in sub-stoichiometric system is lower than the stoichiometric structure, possibly due to the instability of the system and the probability of formation of preferential path for the ions. The structural analysis shows the oxygen coordination increases with the vacancy percentage, because Hf tends to form higher number of bonds to stabilize the structures. Thus, at lower vacancy percentage the diffusion activation is favoured because the local environment around oxygen atoms is not saturated and the atom movement is easier.

11:45 AM

(EMA-S8-007-2013) Effect of electrode materials on the performance of ZCAN/TiO₂/M resistive memory cells

M. Chin, M. Amani*, T. O'Regan, A. Birdwell, M. Dubey, US Army Research Laboratory, USA

The effect of the cathode material on non-volatile metal-insulator-metal resistive random access memory (RRAM) was investigated utilizing a Zr₄₀Cu₃₅Al₁₅Ni₁₀ (ZCAN) amorphous metal anode. Due to the atomically flat nature of the bottom metal contact, significant improvements in device reproducibility could be obtained relative to other crystalline metals, where the surface roughness is typically on the order of the dielectric thickness. TiO₂ grown by atomic layer deposition was used as the dielectric layer, and has previously been used with Pt electrodes to demonstrate RRAM devices with high on/off ratios. Several top contacts including Al, Ti, Zn, Nb, In, and Ag were deposited by various PVD techniques and their effect on device hysteresis was followed with I-V and C-V measurements. It was found that the choice of cathode metallization plays a critical role for the hysteresis and switching behavior in these devices. In order to better understand the interfacial reactions occurring in these devices, they were investigated utilizing Raman spectroscopy, energy-dispersive x-ray spectroscopy and x-ray photoelectron spectroscopy.

12:00 PM

(EMA-S8-008-2013) An autonomous nonvolatile memory latch (Invited)

J. T. Evans*, Radiant Technologies, Inc., USA

Ferroelectric memory circuits to date embed ferroelectric capacitors within a nest of control signals, clocks, and programming lines. This is true for both memory arrays and latch circuits. This universally implemented arrangement does not fully exploit the unique physical property of ferroelectric capacitors which hold their memory states in distortions of their crystal lattices with or without a circuit attached. A ferroelectric nonvolatile memory circuit that operates without clocks or control lines, depending only upon the information stored inside a ferroelectric capacitor to determine its state after the application of power, is autonomous. Truly autonomous memory uses as few as three connections: ground, power, and the output node. The output node provides the internal state of the latch to the outside world while the latch is powered. It also acts as the input. The state of the latch is changed by forcing the output node of the latch to the desired digital condition where it remains as long as power is applied. The circuit returns automatically to that state when power is removed and reapplied. An autonomous nonvolatile latch should be operable in any electrical circuit with or without control signals using the same voltage as the circuits or equipment with which it interacts. Other more complex configurations of the autonomous latch may use independent inputs and outputs or allow the write operation to take place with the supply voltage off.

S12: Recent Developments in High Temperature Superconductivity

YBCO Coated Conductors I-Processing

Room: Indian

Session Chair: Haiyan Wang, Texas A&M University

10:00 AM

(EMA-S12-006-2013) YBCO CCs From A European Perspective (Invited)

J. MacManus-Driscoll*, M. Bianchetti, A. Kursumovic, University of Cambridge, United Kingdom

In this talk, I will summarise our recent progress in CC research in the context of new European research efforts. In particular, I will highlight what I believe to be a way forward for fabrication of high performance conductor using rapid PLD growth protocols incorpo-

rating compositions which produce self-assembled, segmented nanorods of complex double perovskite additions, combined with particles which give rise to pinning from oxygen disordering.

10:30 AM

(EMA-S12-002-2013) Present Status and Future Prospect of R&D on Coated Conductors and Applications in Japan (Invited)

T. Izumi*, M. Yoshizumi, Y. Shiohara, ISTEC-SRL, Japan

Through the several national projects, long coated conductors with high I_c performance could stably be fabricated. Then, the trend of the R&D of coated conductors has been moved to develop the typical characteristics for applications such as high in-field I_c , low ac loss, high mechanical strength etc. A number of progresses on the development of coated conductors have been achieved in M-PACC project. For example, the BaHfO₃ doped REBCO coated conductors fabricated by PLD process revealed extremely high I_c values under magnetic fields, such as typically value over 80A at 77K under 3T. According to the progress of the development of coated conductors, the development of three electric power applications using C.C. was started at 2008. The proto-type devices of "Transmission Cable", "Transformer" and "SMES" have been developed to show the advantages of applications using coated conductors. In the cable project, two different types of the cable using coated conductors were already produced, one is "High Current Type of Cable" (5kA-66kV) and the other is "High Voltage Type" (3kA-275kV). Expected performances on both types were confirmed through the operation tests. Additionally, the 2MVA transformer was set up and the performance will be evaluated soon. This work was supported by NEDO as the project for Development of Materials & Power Applications of Coated Conductors.

11:00 AM

(EMA-S12-003-2013) Progress in development of coated conductors for coil applications in high magnetic fields at low temperatures (Invited)

V. Selvamanickam*, University of Houston, USA; Y. Chen, SuperPower Inc., USA; Y. Liu, N. D. Khatri, J. Liu, Y. Yao, A. Xu, C. Lei, E. Galtsyan, G. Majkic, University of Houston, USA

Prototypes of superconducting devices have been made by several institutions world-wide using coils of coated conductors. In order to achieve cost-performance metric for employment of coated conductors in applications such as wind generators and superconducting magnetic energy storage (SMES), we are working on achieving dramatic improvement of critical current at the operating conditions of these applications i.e. in magnetic fields of 2 to 30 T at temperatures of 4.2 K to 50 K. Our results show the importance of optimization of coated conductor fabrication process for superior performance not just in low magnetic fields at 77 K but at the operating conditions of low temperatures and high magnetic fields that are of interest most coil applications. Additionally, the mechanical properties of these conductors are being improved for robustness in these applications. Recent progress in processing and characterization of coated conductors to meet the performance requirements at operating conditions of interest to coil applications in high fields and low temperatures will be discussed in this presentation. This project was partly funded by Advanced Research Projects Agency-Energy (ARPA-E) award DE-AR0000196.

11:30 AM

(EMA-S12-005-2013) Recent Progress of Electromagnetic Characterization Techniques to Realize High Performance RE-123 Coated Conductors (Invited)

T. Kiss*, K. Higashikawa, M. Inoue, Kyushu University, Japan; H. Tobita, T. Machi, M. Yoshizumi, T. Izumi, ISTEC-SRL, Japan; Y. Iijima, T. Saito, Fujikura Ltd., Japan; K. Ohmatsu, Sumitomo Electric Industries Ltd., Japan; S. Awaji, K. Watanabe, Tohoku University, Japan

Important issues surrounding the development of rare-earth (RE-123) based superconducting wires intended for practical applications mainly involve, 1) problems associated with weak grain boundary

coupling, 2) elimination of current blocking obstacles, and 3) introducing effective magnetic flux pinning centers. A major reason for the difficulties is that phenomena need to be effectively controlled over a spatial region spanning 12-decades, i.e., a nano-scale structural control for effective magnetic flux pinning, a control of grain boundary characteristics over sub-micron to several tens of microns, in addition to eliminating defects affecting current flow. On the other hand, the production of wires on an industrial scale with lengths of several 100's of meters to several kilometres require defect detection methods over the entire wire lengths to establish homogeneity from both reproducibility and quality management points of view. In order to solve these issues and to realize high performance RE-123 based coated conductors, we have developed multi-functional and multi-scale characterization techniques. In this talk, we will review insights from these analysis including in-field current transport properties, spatially resolved local flux flow dissipation and critical current.

S14: Nanoscale Electronic Materials and Devices

Nanoscale Electronic Materials and Devices

Room: Coral A

Session Chair: Michael Lilly, Sandia National Laboratories

10:00 AM

(EMA-S14-001-2013) Nonexponential decay of photoluminescence intensity of small InAs quantum dots

K. Kral*, Institute of Physics, Acad. Sci. of Czech Republic, v.v.i., Czech Republic; M. Mensik, Institute of Macromolecular Chemistry, Acad. Sci. of CR, v.v.i., Czech Republic

We present a theoretical interpretation of the photoluminescence decay in samples of small InAs quantum dots. Small nanoparticles of InAs are supposed to behave as a semiconducting material with indirect band gap. This property causes the main reason for the slowing down of the photoluminescence decay. We show that the light emission is made possible thanks to the non-adiabatic process of the promotion of electron to the Gamma valley with the help of the inter-valley multiple scattering of electron on lattice vibrations. Using quantum kinetic equations it is shown numerically that in accordance with experiment the photoluminescence intensity decays as a power-law function of time.

10:15 AM

(EMA-S14-002-2013) Preparation and characterization of ferroelectric lithium niobate pseudo nanocubes

W. Mader*, M. Mueller, University of Bonn, Germany

Lithium niobate LiNbO₃ is ferroelectric and has non-linear and double refracting optical properties below 1210 °C. Crystals of LiNbO₃ have a number of technical applications as band-pass filters and optical modulators and are intensively studied and used in laser optics for phase modulation and generation of second harmonics (SHG). It is expected that nanocrystals of LiNbO₃ with a narrow size distribution refine the commonly used technique of quasi phase-matching through periodic domain structures in the submicron range. We successfully prepared LiNbO₃ nanocrystals by thermal decomposition of metal-organic niobium alkoxide and lithium alkoxide precursors in a non-polar solvent using the 'heating-up' method. X-ray diffraction and electron diffraction proved the product as phase pure LiNbO₃. TEM imaging displays a narrow size distribution of well-faceted nanocrystals in the range of 7 - 10 nm. The LiNbO₃ crystals exhibit the six possible R-face {1-102} facets and hence appear as slightly distorted cubes or pseudo cubes. The suspension of the nanocrystals clearly shows SHG at 516 nm by applying a 1033 nm laser beam which proves the nanoparticles being ferroelectric. Raman spectroscopy and piezo force microscopy reveals further information on the nanocrystals properties.

10:30 AM

(EMA-S14-003-2013) Perovskite Nanoparticle enhanced Nanorod Array based Gas Sensors at High Temperature

P. Gao*, H. Lin, H. Gao, University of Connecticut, USA

Using a combination of solution deposition and post-annealing, well-aligned semiconductor metal oxide nanorod arrays have been fabricated on oxidized silicon substrates. Through magnetron sputtering, perovskite-type ABO₃ nanoparticles were deposited onto the surface of individual metal oxide nanorods to form core-shell nanorod arrays. X-ray diffraction analysis, electron microscopy and spectroscopy have been used to characterize and identify the structure, morphology, chemical compositions and distribution on the nanorod surfaces and interfaces. Similar to the noble metal sensitization effect, the decoration of perovskite nanoparticles was found to significantly enhance the fabricated sensor sensitivity and stability at high temperature up to 1000 °C. The electrical sensing mechanism has been investigated by electrical and electrochemical methods to unravel the carrier transport routes and kinetics involving both electronic and ionic defects, associated with the detected gaseous species such as O₂, CO and NO_x. In addition to good sensitivity, the fabricated core-shell nanorod sensors have shown faster response and recovery compared to pristine nanorod sensors to both CO and NO_x gases. These perovskite nanoparticle enhanced semiconductor nanorod based sensors could find potential application in various high temperature energy and environmental devices and systems.

10:45 AM

(EMA-S14-004-2013) Engineering Tetragonal Barium Titanate in Freestanding Nanosheets

C. A. Barrett*, T. T. Salguero, University of Georgia, USA

From both a commercial and academic standpoint, barium titanate (BTO) is one of the most important ferroelectric materials in the perovskite family, triggering numerous fields of study and industrial applications. However, BTO's continued level of usage may hinge upon the development of fabrication techniques that can achieve sub-10 nm features, paving the way for size reduction and ultimately increased performance in devices like multilayered ceramic capacitors. In general, ferroelectric characteristics in perovskites are size dependant, with shrinking dimensions leading to weaker dielectric properties and reduced transition temperatures. The cause of these phenomena has been linked to a suppression of the intrinsic Curie temperature of a dielectric material when subjected to finite dimensions. One possible way of circumventing this problem is to limit the number of quantum-confined dimensions, thus reducing the size-dependent decay of polar order while still achieving nanoscale thicknesses. In this contribution, we introduce a method of preparing free-standing BTO nanosheets with sub-2 nm thicknesses and micron-sized lateral dimensions. The topochemical reaction of alkaline earth precursors with colloidal titania nanosheets will be discussed. In addition, we present our findings on the evolving morphology of BTO nanosheets and the contributed effect on their long range and local crystallographic characteristics.

11:00 AM

(EMA-S14-005-2013) Strain-driven control of functionalities in complex metal-oxide films

L. Yan, E. M. Choi, Los Alamos National Laboratory, USA; O. Lee, University of Cambridge, United Kingdom; Z. Bi, Los Alamos National Laboratory, USA; A. Chen, Texas A & M University, USA; J. Xiong, Los Alamos National Laboratory, USA; S. A. Harrington, University of Cambridge, United Kingdom; H. Wang, Texas A & M University, USA; J. L. MacManus-Driscoll, University of Cambridge, United Kingdom; Q. X. Jia*, Los Alamos National Laboratory, USA

Epitaxial nanocomposites, in which much enhanced functionalities can be achieved through interfacing different strongly correlated ma-

terials at the nanoscale, provide a new design paradigm to produce novel properties that cannot be obtained in the individual constituents. Recent experimental results have shown that much improved functionalities in complex metal-oxides can be obtained through constituent interactions on micro-, meso-, and/or nanoscales. In this talk, I will discuss our effort to control the functionality in hybrid complex metal-oxide nanostructures, namely, vertically aligned epitaxial nanocomposites. We have demonstrated that it is possible to control the strain and to dramatically improve the physical properties or functionalities of complex meta-oxide films by using epitaxial nanocomposites.

11:15 AM

(EMA-S14-006-2013) Tuning the Sensitivity of Toxic Gas Detection Using Back Gate Bias in CVD Graphene Field Effect Transistors

A. K. Singh*, M. Uddin, J. T. Tolson, University of South Carolina, USA; G. S. Tompa, N. Sbrockey, Structured Materials Industries Inc., USA; M. G. Spencer, Cornell University, USA; T. S. Sudarshan, G. Koley, University of South Carolina, USA

We have investigated the tuning of the sensitivity and selectivity of chemical vapor deposition (CVD) graphene sensors, towards toxic gases such as NH₃ and NO₂ using a global back-gate. The multi-layer graphene (MLG) used in this work was grown by cracking CH₄ in presence of H₂ at 1000 °C on copper foils. Field effect transistors (FETs) were fabricated on the transferred MLG on 100 nm thick SiO₂/Si substrate. Preliminary sensing studies on these devices showed 20 % increase (10 % decrease) in conductivity for 20 ppm NO₂ (550 ppm NH₃). The ambipolar current-voltage transfer characteristics of CVD graphene FETs have Dirac point in the range of 6-12 V. This indicates p-type doping of the graphene, and explains conductivity increase (decrease) for electron withdrawing (donating) NO₂ (NH₃). For 20 ppm NO₂, graphene's sensitivity (defined as fractional change in conductivity) increases from 6% to 13% as back-gate bias (V_{bg}) changes from -8 to 8V. The opposite trend is observed with 500 ppm NH₃ where the conductivity decreases from 26% to 10% as V_{bg} changes from -8 to 8V. These results can be explained with appropriate band diagrams, and demonstrate that appropriate V_{bg} can be utilized to tune the sensitivity and selectivity toward various analyte molecules in back-gated graphene FET based sensors. Initial field testing of sensors in automotive applications are also reviewed.

S16: Highlights of Student Research in Basic Science and Electronic Ceramics

Highlights of Student Research

Room: Coral A

Session Chair: Troy Ansell, Oregon State University

12:15 PM

(EMA-S16-001-2013) Crystallographic and Electrical Properties of (Na_{0.5-x}Bi_{0.5+x})TiO_{3±δ}, where (-0.01≤x≤0.01)

J. J. Carter*, E. Aksel, J. S. Forrester, J. L. Jones, University of Florida, USA

(Na_{0.5}Bi_{0.5})TiO₃ (NBT) is a material of interest in various ferroelectric solid solutions for piezoelectric applications. In this perovskite structure, the A-site is equally shared by Na⁺ and Bi³⁺ ions. Stoichiometric variation in NBT commonly occurs during processing due to various causes such as the volatility of sodium and bismuth at high temperatures. These changes have been shown to affect the structure and performance of the material. This work examines the crystallographic structure changes in NBT, as well as some of the piezoelectric property changes that occur when the ceramics are prepared with non-stoichiometric A-site compositions. Changes to the bismuth and sodium proportions were made in five steps from

($\text{Na}_{0.51}\text{Bi}_{0.49}$) $\text{TiO}_{3\pm\delta}$ to ($\text{Na}_{0.49}\text{Bi}_{0.51}$) $\text{TiO}_{3\pm\delta}$. High resolution X-ray diffraction data were modeled using the Rietveld method in order to understand crystal structure differences. As the compositions deviated further from stoichiometric, the measured lattice parameters are indicative of a less distorted monoclinic structure. The cubic phase fraction remained relatively constant. Ferroelectric polarization and strain hysteresis loops were measured in order to examine the effect of non-stoichiometry on piezoelectric performance. The bismuth rich/sodium deficient samples exhibited a higher d_{33} value and broke down at a higher electric field than the other compositions.

12:30 PM

(EMA-S16-002-2013) Mechanical Depoling and Piezoelectricity Loss in the Region of the Morphotropic Phase Boundary of NBT-BT

L. M. Denis*, University of Florida, USA; J. Glaum, M. Hoffman, University of New South Wales, Australia; J. Forrester, J. L. Jones, University of Florida, USA

The highest piezoelectric coefficients of (1-x)(Na_{0.5}Bi_{0.5})TiO₃-xBaTiO₃ (NBT-BT) are often found at compositions near the morphotropic phase boundary ($0.06 \leq x \leq 0.07$). However, high piezoelectric coefficients are often associated with high electromechanical coupling, meaning compositions near the MPB may be subject to depoling during mechanical stress. The present work investigated this interrelationship between piezoelectric properties and mechanical depoling. Ferroelectric coercive field amplitude was determined from polarization and strain hysteresis loops of NBT-xBT compositions (x=.04,.06,.07,.09,.13) at field amplitude 4.5 kV/mm. Poled samples of the same compositions were depoled while measuring the converse piezoelectric coefficient by superposing static compressive offset stresses of increasing amplitude (ranging from 0 to 115 MPa) with a cyclic measurement signal (5 MPa, 0.1 Hz). From these measurements, the mechanical coercive stress was extracted. These two measurements show that both ferroelectric coercive field and mechanical coercive stress increase in compositions further from the MPB. At NBT-7BT, the minimum ferroelectric coercive field and mechanical coercive stress were observed. It has therefore been shown that although compositions near the MPB exhibit the highest piezoelectric coefficients, they also undergo mechanical depoling at lower stresses.

12:45 PM

(EMA-S16-003-2013) Stability and dewetting of Au on Ti, TiO_x, and ZnO

B. Schaefer*, University of Florida, USA; J. Cheung, University of New South Wales, Australia; J. F. Ihlefeld, Sandia National Laboratories, USA; J. L. Jones, University of Florida, USA; N. Valanoor, University of New South Wales, Australia

Stable metal-dielectric contacts are essential for ferroelectric and multiferroic applications, where high processing temperatures can affect the structure and effectiveness of electrodes. Choice of electrode adhesion layer is therefore essential for stability. 40 nm Au electrodes with three different 40 nm buffer layers (Ti, TiO_x, and ZnO) on oxidized Si substrates were studied using high-temperature confocal laser scanning microscopy (HT-CLSM) and scanning electron microscopy (SEM) to characterize their stability at high temperatures. HT-CLSM is a unique technique that allows for the capture of real-time video data at elevated temperatures, and SEM was used to further characterize the Au layer after processing. The HT-CLSM data revealed time- and temperature-dependent dewetting (delamination) of the Au layer, and SEM revealed the shape of the delaminated surface features. The time dependence of this dewetting could be modeled by the JMAK kinetic equation, which typically describes isothermal phase transformations but could be applied quite well to this situation. From the video data and JMAK plots, Au was found to delaminate from the ZnO buffer at the quickest rate, followed by TiO_x and Ti. This can be paralleled and contrasted with an earlier study, which showed the reverse effect using Pt as the electrode material.

S1: Functional and Multifunctional Electroceramics

Material Applications including Energy Storage, Conversion and Harvesting

Room: Coral B

Session Chairs: Takaaki Tsurumi, Tokyo Institute of Technology; John Talvacchio, Northrop Grumman

2:00 PM

(EMA-S1-001-2013) Arrays of Superconducting SQUIDs as Antennas and Amplifiers (Invited)

J. Talvacchio*, J. X. Przybysz, D. L. Miller, Northrop Grumman, USA

Superconducting Quantum Interference Filters (SQIFs) are series-parallel connections of SQUIDs designed to (a) increase output voltage and dynamic range, (b) control response linearity and output impedance, (c) improve sensitivity to weak signals, and (d) make the voltage vs. magnetic-field response robust to variations in junction critical currents normally obtained with high-T_c oxide Josephson junctions. SQIF designs implemented in high-T_c superconductors permit packaging with small cryocoolers at ~70K. We are interested in SQIFs as combined antennas and LNAs that are (a) electrically small, (b) extremely wideband, 1 kHz to 1 GHz, (c) extremely low noise, and able to sense and amplify the magnetic field component of RF plane waves with full preservation of amplitude and phase information. We explored scaling of SQIFs with N parallel junctions and M series junctions. Most of the important performance parameters – output voltage, power gain, signal-to-noise dynamic range, spur-free dynamic range (SFDR), noise temperature, and sensitivity to variations in I_c – improve with larger M and N. In experiments to increase SFDR, we employed differential SQIF pairs to greatly reduce even-order spurs and created a triangle-wave periodic response to reduce third-order spurs. We compare the resulting SFDR with other LNA technologies.

2:30 PM

(EMA-S1-002-2013) Comparative Study On Magnetodielectric And Dielectric Substrate Based Rectangular Patch Antenna In UHF And SHF

G. Singh*, S. Parashar, S. Sahu, KIIT University, India

The development of novel magnetodielectric material based antennas has emerged as the area of intense research. Since, it's been a difficult task to achieve self biased magnetic materials for antenna substrate applications at frequencies >600MHz range. Here, we have focused on the simulation based comparative results between Magnetodielectric (Zinc Ferrite) and dielectric based substrate in the Rectangular Patch Antenna. The simulation has been done using ADS in the frequency range of 1-30GHz. The simulation has been done to compare all the parameters related to antenna. The bandwidth was found to be nearly 3.5 GHz in case of magnetodielectric substrate for its applications in ultra wide band whereas 1GHz bandwidth in dielectric substrate showing its application in the field of narrow band width. The detail study will be discussed focusing on application in microwave frequency ranges.

2:45 PM

(EMA-S1-003-2013) Fabrication of Micro Wireless Power Transfer System by Multilayer Ceramic Coil

M. Takato*, K. Saito, F. Uchikoba, Nihon University, Japan

Micro wireless power transfer system by multilayer ceramic coils is proposed. Technology of the wireless power transfer has been remarked as one of a strong method of noncontact power transmis-

sion. Magnetic induction type transfer has been used widely within small distance. The advantage of this type is high efficiency. Also, the long distance transfer by the electromagnetic resonance type has been studied. On the other hand, there is strong demand of noncontact power supply to extremely small space, for instance, MEMS devices. However, it is difficult to apply the conventional method for the small devices. The reason is that the size of those power transfer system is too big to apply for the small device. The problem is a structure of the transmission coil. Usually, the coil has been composed of a magnetic core and a winding wire. This structure is difficult to miniaturize. In this paper, miniaturized wireless power transfer system making use of multilayer magnetic ceramic inductor composed of monolithic structure is proposed. Also, the fabrication process and the transmission evaluation are discussed. The turn number of the coil was twenty. The coil was formed inside the magnetic material. The permeability of ferrite used as the magnetic material was 900. The dimensions of the fabricated multilayer ceramic inductor were 3, 3, 1.3 [mm] width, length, and height, respectively.

3:00 PM

(EMA-S1-004-2013) Maximizing the Energy Storage Density with Antiferroelectric Ceramics through Mechanical Confinement

X. Tan*, S. E. Young, J. Zhang, Iowa State Univ, USA; W. Hong, Iowa State University, USA

Antiferroelectric ceramics can be forced by electric fields to transition to a ferroelectric phase. This phase transition is manifested by expansions in both longitudinal and transverse directions and double polarization vs. electric field hysteresis loops. Compared to linear dielectrics and normal ferroelectrics, antiferroelectric materials display a much higher electrical energy storage density. The properties of the antiferroelectrics play a decisive role for the energy density in capacitor applications. The electric field-induced phase transition is investigated under mechanical confinements in bulk samples of antiferroelectric perovskite oxides at room temperature. Profound impacts of mechanical confinements on the phase transition are observed due to the interplay of ferroelasticity and the volume expansion at the transition: The uniaxial compressive pre-stress delays while the radial compressive pre-stress suppresses it. This corresponds to the enhancement of the electrical energy storage density under mechanical confinement. Such confinement is also realized through partially electroding the ceramic disk samples. The experimental results are rationalized with a phase field model which describes the impact of mechanical confinements on the phase transition.

3:15 PM

(EMA-S1-005-2013) Enhanced Ionic Transport in High Density, Pressure Formed $0.70\text{Li}_2\text{S} + 0.30\text{P}_2\text{S}_5$ Lithium Thiophosphate Solid Electrolytes

S. S. Berbano*, M. Mirsaneh, M. T. Lanagan, C. A. Randall, The Pennsylvania State University, USA

Solid electrolytes are safer alternatives to liquid electrolytes, especially for higher temperature energy storage applications. This work focuses on lithium thiophosphates, which can be synthesized using the non-vacuum technique of mechanical milling, do not contain germanium, and exhibit a low glass transition temperature ($\sim 215^\circ\text{C}$). High density $0.70\text{Li}_2\text{S} + 0.30\text{P}_2\text{S}_5$ (mole fraction) pellets were prepared by pressing mechanically milled powders at $\sim 225^\circ\text{C}$. Percent relative densities up to 94% of the $\text{Li}_7\text{P}_3\text{S}_{11}$ crystalline phase were obtained without detectable crystallinity in x-ray diffraction patterns (collected using $\text{Cu-K}\alpha$ x-rays). Rather than impedance spectroscopy above room temperature, where only electrode polarization effects are seen, ion dynamics were investigated below room temperature where conduction relaxations can be observed. As density increased, the ionic conductivity, determined using impedance spectroscopy, increased. This talk will describe the mechanisms for enhanced ionic conduction in terms of mixing laws and ion mobility.

3:30 PM

(EMA-S1-048-2013) Development of High-Energy-Density Textured Piezoelectric Materials for Vibration Energy Harvesting (Invited)

S. Priya, Y. Yan*, Virginia Tech, USA

Vibration energy harvesting has gained tremendous attention in last decade. In most common approach, piezoelectric transduction mechanism is used to convert vibration energy into electrical energy. Among various methodologies, the piezoelectric mechanism has been shown to provide advantages at micro-to-meso scale. For energy harvesting under off-resonance conditions, the choice of piezoelectric materials is governed by the transduction coefficient ($d \times g$). Textured piezoelectric ceramic provide an effective way to achieve the high transduction coefficient. By using templated grain growth (TGG) method, we have investigated a series of $\langle 001 \rangle$ textured PMN-PT/PZT piezoelectric ceramics with high d and k values having transduction coefficient magnitude comparable to that of $\langle 001 \rangle$ oriented single crystals. For on-resonance energy harvesting, high power textured Mn doped PMN-PZT piezoelectric materials were synthesized, which possess excellent "hard and soft" combinatory characteristics. To further improve the energy harvesting efficiency of these materials, multilayer structure via low-temperature co-firing were synthesized. In this presentation, we will provide the experimental results on energy generation efficiency from textured ceramics and co-fired multilayers. Analytical model explaining the observed variation in output power in terms of material coefficients will be provided.

4:00 PM

(EMA-S1-006-2013) Microscopic Mechanism and Material Design of Electro-optic effect in Perovskite Ferroelectrics (Invited)

T. Tsurumi*, K. Takeda, T. Hoshina, H. Takeda, Tokyo Institute of Technology, Japan

Optical modulators (OM) using electro-optic (EO) effect will be a key device for realizing next generation network. Lithium niobate (LN) single crystals are currently used for OM in large or local area networks but the EO-coeff. of LN is too low to make miniaturized OM used in the home network. PLZT was a candidate for this purpose but the EO-coeff. of PLZT drastically decreased above 1GHz and the toxicity of lead also gives a limitation for a wide range of applications. A new lead-free material showing excellent EO-effect is therefore highly desired at present. To develop a new material, understanding of a microscopic mechanism of material properties should be required. However, the origin of EO-effect has not been fully elucidated so far. In this study, it was the elucidated for perovskite ferroelectrics by studying relationships with piezoelectric, dielectric and photo-elastic properties. The EO coefficient g should be employed as intrinsic parameter to describe the EO effect. We found that the EO coefficient g was determined as a product of the photo-elastic and electrostrictive coefficient. Based on this mechanism, we have proposed a new EO crystal of Bi-based relaxors and found that the crystal exhibited the highest Kerr coefficient in lead-free crystals.

4:30 PM

(EMA-S1-007-2013) Electrospun TiO_2 fiber as anode materials for lithium ion batteries

R. Qing*, W. Sigmund, University of Florida, USA

TiO_2 is one of the most attractive anode materials for lithium ion batteries due to their structural stability, long cycling life, low cost, wide availability, decent charging/discharging capacity and environmental benignity. They are also considered to be ideal material for plug-in electric vehicles coupled with high voltage cathodes. Here we present our latest results on fabrication and electrochemical testing of TiO_2 nanofibers synthesized via electrospinning method.

Fibers with diameter below 200 nm could be achieved with a post heat-treatment on the electrospun fiber mats. Good cycleability is obtained for the synthesized fibers. The impact of calcination condition on material structure and activity are reported. Composite fiber synthesis with functionalized Carbon nanotubes will also be mentioned.

4:45 PM

(EMA-S1-008-2013) Photophysical and photocatalytic water splitting performance of Stibiotantalite type-structure compounds, $SbMO_4$ ($M = Nb, Ta$)

S. Kim*, S. Park, C. Lee, B. Han, S. Seo, J. Kim, Seoul National University, Republic of Korea; I. Cho, Stanford University, USA; K. Hong, Seoul National University, Republic of Korea

Ferroelectric materials are considered to be a new family of efficient photocatalysts. Here, we investigate stibiotantalite type-structure compounds, $SbMO_4$ ($M = Nb, Ta$), with ferroelectric properties and layered crystal structures as photocatalysts for hydrogen evolution from water. Both compounds were synthesized by a conventional solid-state method, and their optical properties, electronic band structure, and photocatalytic properties were evaluated. Diffuse reflectance analysis showed that $SbNbO_4$ and $SbTaO_4$ have a band gap of 3.1 eV and 3.7 eV, respectively. From the electronic band structure calculations, it was found that the NbO_6 and TaO_6 octahedra mainly contributed to the formation of valence and conduction bands of $SbNbO_4$ and $SbTaO_4$, respectively. Mott-Schottky analysis reveals that their conduction-band edge potentials are higher than the water reduction (hydrogen evolution) potential (0 V vs. RHE), indicating both compounds can generate hydrogen from water. The photocatalytic water splitting performance was conducted by using pure water and UV-light irradiation, and photocatalytic H_2 production was confirmed for both compounds. The photocatalytic activity difference in both compounds was discussed with regard to electronic band structure and dipole moment difference, resulting from their crystal structures.

5:00 PM

(EMA-S1-009-2013) Enhanced energy storage capacities in solid state nanocomposite dielectrics

M. Mirsaneh*, A. Baker, W. Qu, S. Lee, E. Dorjpalam, R. Rajagopalan, C. A. Randall, The Pennsylvania State University, USA

Over the last decade, solid state nanocomposite materials have been progressively studied with the aim of increasing the capacity of energy storage devices. Nanometer size particles possess much higher surface area with an enhanced interfacial effect, resulting in an exceptional impact on the electric field distribution and therefore on the transportation of charge carriers. This would affect the electrical properties including breakdown strength in these materials. Preferred distribution of particles as well as particle shape and size are known to be the critical parameters of these systems. We will present our recent data on the effect of inorganic nanoparticle fillers in composites in a variety of devices including electrostatic capacitors, supercapacitors and batteries where the conduction of charge carriers is affected by the presence of nanoparticles. Our results show at least 3-fold increase in the energy density of the device as a result of the addition of nanoparticles. Within this article, we study microstructure, electrical, electrochemical and dielectric properties of the nanocomposites and propose our analytical view on the possible physical phenomena for such an extraordinary behavior.

5:15 PM

(EMA-S1-010-2013) Ternary $Bi(B'B'')O_3 - PbTiO_3$ Solid Solutions for High Temperature Piezoelectrics

B. Kowalski*, A. Sehirlioglu, Case Western Reserve University, USA

High temperature piezoelectric materials are sought after for fuel and gas modulation in engines, ultrasonic drilling on the surface of

Venus, and power generation in space applications such as thermoacoustic engines. The operating temperature for most widely used commercial piezoelectrics, usually based on $Pb(Zr,Ti)O_3$ (PZT), is $\sim 200^\circ C$, severely limiting its high temperature capabilities. In the early 2000's, Eitel et al demonstrated an inverse relationship between tolerance factor and Curie temperature (T_c) that has spurred interest in $Bi(B'B'')O_3 - PbTiO_3$ (PT) systems due to the increased T_c at the morphotropic phase boundary near which the electromechanical properties are enhanced. In this work, binary and ternary solid solutions are built from the combination of PT with perovskite end members $BiScO_3$, $BiInO_3$, and $Bi(Zn_{0.5},Zr_{0.5})O_3$. Further aliovalent doping for the B-site cations is also being explored. The operating temperatures are investigated both in terms of phase transformation temperatures and increased ac and dc conductivity. The dielectric and electromechanical properties will be presented as a function of frequency, electric field and temperature. Results have shown T_c 's in excess of $425^\circ C$ and piezoelectric coefficients (d_{33}) between (420-600) pC/N.

S2: Multiferroic Materials and Multilayer Ferroic Heterostructures: Properties and Applications

Interfaces, Domain Phenomena and Transport

Room: Coral A

Session Chair: Melanie Cole, U.S. Army Research Laboratory

2:00 PM

(EMA-S2-001-2013) Interfacial coupling at multifunctional oxide interfaces (Invited)

C. Ahn*, Yale University, USA

Complex oxide materials exhibit a strong interplay between spin, charge, and lattice effects. The possibility of integrating these different kinds of behavior together with nanoscale precision has motivated the development of new, artificially structured complex oxide-based materials systems. In certain cases, the atomic-scale interface of these structures dominates the observed behavior, with new physical properties emerging. We describe the structure-property relationship of complex oxide interfaces studied using a variety of techniques, including high resolution synchrotron scattering, to determine the interplay between new interfacial structural motifs and the resulting electronic function.

2:30 PM

(EMA-S2-002-2013) Domain wall functionality in complex oxides (Invited)

J. Seidel*, University of New South Wales, Australia

Interfaces and topological boundaries in complex oxide materials, such as domain walls, have recently received increasing attention due to the fact that their properties, which are linked to the inherent order parameters of the material, its structure and symmetry, can be completely different from that of the bulk material [1]. I will present an overview of recent results on electronic and optical properties of ferroelectric phase boundaries, domain walls, and topological defects in multiferroic $BiFeO_3$ [1, 2] and $ErMnO_3$ [3]. The origin and nature of the observed confined nanoscale properties is probed using a combination of nanoscale transport measurements, high resolution transmission electron microscopy and first-principles density functional computations. I will also give an outlook on how these special properties can be found in other material systems and discuss possible future applications [4]. 1. J. Seidel, et al., Nature Materials 8, 229 (2009). 2. J. Seidel, et al., Phys. Rev. Lett. 107, 126805 (2011). 3. D. Meier, J. Seidel et al., Nature Materials 11, 284 (2012). 4. G. Catalan, J. Seidel, R. Ramesh, and J. Scott, Rev. Mod. Phys. 84, 119 (2012). Presenting author's email: jan.seidel@unsw.edu.au

3:00 PM

(EMA-S2-003-2013) Temporally Resolved Switching Steps During Polarization Reversal in Multiferroics

L. Ye, J. Bosse, A. Lluberes, University of Connecticut, USA; J. Ihlefeld, Sandia National Laboratories, USA; B. D. Huey*, University of Connecticut, USA

Multiferroic domain stability and switching speeds can be strongly dependent upon the local domain configuration. With multiple possible polarization orientations, ferroelastic and ferroelectric switching, and substrate/electrode effects as well, even epitaxial films can exhibit complex textures of domains with nearly 50 μm of domain wall per μm^2 of film. Based on PFM and extensive image analysis, the local domain orientation is mapped, domain boundary types are identified, and their charging is calculated. These routines are then applied to movies of the polarization reversal process, enabling mapping and statistical analysis of the initial and overall switching directions, angles, and switching order. These reveal domains influencing the behavior of their nearest neighbors, backswitching, and a surprisingly high fraction of switching perpendicular to the applied field instead of along the easy axis.

4:00 PM

(EMA-S2-004-2013) Interface Engineered Ferroelectric Heterostructures (Invited)

C. Chen*, University of Texas San Antonio, USA

Interface engineered ferroelectric heterostructures were epitaxially grown on crystal substrate surfaces, such as single (001) MgO, (001) LaAlO₃, polycrystalline metal types, and semiconductors surfaces by pulsed laser deposition. Microstructural characterizations by x-ray diffraction and transmission electron microscopy indicate that the as-grown heterostructures are c-axis oriented with an atomic sharp interface. The multilayered ferroelectric BaTiO₃/SrTiO₃ and Mn-doped (Ba,Sr)TiO₃//Ba(Zr,Ti)O₃ heterostructures on single crystalline (001) MgO have excellent epitaxial quality. The microwave dielectric measurements (~18 GHz) reveal that the dielectric constants, dielectric tunability, and dielectric losses of the heterostructures are highly dependent upon the stacking period number (N) and layer thickness (di). The optimized dielectric performance was determined with the best value for the loss tangent (0.02) and the dielectric constant (1320) with a very large of dielectric tunability of >60%, which suggests that both BTO/STO and Mn-doped (Ba,Sr)TiO₃//Ba(Zr,Ti)O₃ heterostructures can be used for the development of room temperature tunable microwave elements, supercapacitance applications, structural health monitoring system, and various energy harvest device developments. Details will be discussed in the talk.

4:15 PM

(EMA-S2-005-2013) Tuning of Conduction at Domain Walls of BiFeO₃ Thin Films (Invited)

J. Lee*, A. Bhatnagar, Y. Kim, D. Hesse, M. Alexe, Max Planck Institute of Microstructure Physics, Germany

Domain walls in ferroic materials may be regarded as two dimensional nanoscale objects comprising natural interfaces that are embedded in the host material. An increased magnetoelectric coupling at the domain walls of multiferroic materials, associated with the breaking of the ferroic order parameter, has been already revealed. Among all multiferroics, BiFeO₃ (BFO) is one of the rare intrinsic multiferroics at room temperature. Lately the domain wall properties in this intriguing material have been intensively explored. Recent studies, many of them being conducted by scanning probe microscopy, showed the presence of a number of effects such as enhanced conductivity, abnormal photovoltaic effect, giant magnetoresistance. Among these effects the enhanced electrical conductivity at domain walls is most relevant for potential applications. But until now there was no attempt to tune the physical properties of these domain walls in a designed way. The pres-

ent talk will address the issue of tuning and controlling the enhanced conductivity of domain walls in BFO. We will show different approaches to achieve this goal, for instance by incorporation of foreign atoms (chemical doping) or increasing the density of point defects at the domain walls. Macroscopic as well as AFM-based microscopic investigations were used to unveil the transport mechanism as well as the photoelectric properties of the domain walls.

4:30 PM

(EMA-S2-006-2013) Multiferroic Modulation of Superparamagnetism (Invited)

G. Carman*, H. Kim, L. Schelhas, S. Tolbert, UCLA, USA

Multiferroic materials have received considerable attention over the last decade with a focus on strain mediated composites evaluate at the "bulk" level. More recently there has been an effort to electrically manipulate single magnetic domains at the nanoscale with considerable success both in Ni nanoscale elliptical elements as well as Ni nanoring structures. In this work, we report experimental results showing electric field-induced magnetoelastic anisotropy in Ni nanocrystals alters the blocking temperature and controls the Ni nanocrystals superparamagnetic behavior. The sample consists of 16 nm diameter Ni nanocrystals on a (011) oriented PMN-PT single crystal substrate. Zero field cooling curves shows that the blocking temperature can be changed by 40 K using an electric field. Prior to the electric field, the particles are superparamagnetic while following the application of the electric field the particles exhibit single domain behavior, as measured using a SQUID magnetometer. These results indicate a multiferroic system that can be electrically switched between a superparamagnetic and single domain state.

4:45 PM

(EMA-S2-007-2013) Interface Structure Evolution in Perovskite Oxide Epitaxial Thin Films (Invited)

E. I. Meletis*, J. Jiang, J. He, The University of Texas at Arlington, USA

Perovskite oxides are an important class of materials due their excellent dielectric, ferroelectric, and piezoelectric properties. Furthermore, their thin film form exhibits enhance properties compared to their bulk counterpart and are highly desirable for advanced device applications. It has been shown that the physical properties of the films are strongly affected by their microstructure and interface structure. We have also shown that processing parameters and the substrate/film misfit strain are two critical parameters that can be manipulated to grow a variety of structural architectures in these films (self-assembled structures, 1-D nanocolumns, etc.). An overview will be presented of recent developments in BaTiO₃-based epitaxial thin films and their microstructures and interface structures. We will focus on the (i) synthesis of 1-D and 2-D interface structures in (Ba,Sr)TiO₃ epitaxial films grown on miscut MgO substrates and their effect on properties; (ii) growth of nanofinger structures in Ba(Zr,Ti)O₃-based epitaxial thin films formed via twin-coupling by sharing their {111}/{110} planes with respect to the epitaxial layer and the structure evolution mechanism from the epilayer to nanofingers; and (iii) our recent discovery and structure determination of two monolithic superstructures Ba₁₀Ti₈O₂₆ and Ba₈Ti₈O₂₄ in epitaxial thin films deposited on (001) MgO substrate using RF magnetron sputtering.

S3: Structure of Emerging Perovskite Oxides: Bridging Length Scales and Unifying Experiment and Theory

Session 2

Room: Pacific

Session Chairs: Yu Wang, Michigan Tech; David Cann, Oregon State University

2:00 PM

(EMA-S3-007-2013) Triple-point type morphotropic phase boundary and high-performance Pb-free piezoelectrics (Invited)

X. Ren*, National Institute for Materials Science, Japan; D. Xue, J. Gao, C. Zhou, W. Liu, Frontier Institute of Science and Technology, China

Morphotropic phase boundary (MPB) is a central concept for high piezoelectricity. It normally refers to a “compositional phase boundary that separates two different ferroelectric phases”, and maximum piezoelectricity appears at such a boundary. However, it has been found that the MPB of different piezoelectric systems show very different piezoelectric performance. MPB of Pb-based systems shows high piezoelectricity, whereas MPB of Pb-free systems like KNN-based systems exhibits much lower piezoelectricity. It is of interest to understand such a difference, because such understanding may provide important insight into how to develop high-performance Pb-free piezoelectrics. Here we show that whether a MPB can result in high piezoelectricity depends on whether it starts from a “triple-point”, i.e., a three-phase coexistence point in the temperature-composition phase diagram. Systems having a triple-point type MPB exhibit high piezoelectricity in both Pb-containing and Pb-free systems. The triple point appears to be a tricritical point with vanishing polarization anisotropy. The MPB starting from such a point also possesses low polarization anisotropy and thus facilitates polarization rotation between different polarization states, thus achieving high-piezoelectricity. Triple-point type MPB may be a useful guideline for designing high-performance Pb-free piezoelectric materials.

2:30 PM

(EMA-S3-008-2013) The Effect of Poling and Stress on Switching in $\text{Ba}(\text{Zr}_{0.2}\text{Ti}_{0.8})\text{O}_3\text{-x}(\text{Ba}_{0.7}\text{Ca}_{0.3})\text{TiO}_3$ Piezoelectrics

M. C. Ehmke*, Purdue University, USA; J. Glaum, J. Daniels, M. Hoffman, The University of New South Wales, Australia; J. E. Blendell, Purdue University, USA; K. J. Bowman, Illinois Institute of Technology, USA

The lead-free $\text{Ba}(\text{Zr}_{0.2}\text{Ti}_{0.8})\text{O}_3\text{-x}(\text{Ba}_{0.7}\text{Ca}_{0.3})\text{TiO}_3$ (BZT-BCT) system has been demonstrated to show attractive piezoelectric performance at the morphotropic phase boundary (MPB), and is a possible alternative to lead based piezoceramics. A significant characteristic of the BZT-BCT system is a strong temperature dependence of the MPB, at which a phase mixture or a lower symmetry phase exists. Compositions across the MPB from rhombohedral to tetragonal symmetry including a MPB composition have been studied for their poling behavior to elucidate the mechanisms present in the different compositions. We show that poling at room temperature and very high electric fields allows for significant improvement of the piezoelectric coefficient of over 50% for rhombohedral and MPB compositions, while electrically harder tetragonal compositions exhibit only moderate improvements. Moreover, the mechanical depoling behavior under a uniaxial compressive stress is investigated, which demonstrates limitations for this material system for applications, particularly for the soft rhombohedral and MPB compositions. The results are discussed in terms of crystallographic structure, microstructural processes, a defect charge carrier model and the switching processes determined from small signal electric experiments.

2:45 PM

(EMA-S3-009-2013) Nano/Mesoscale Structure and Pseudo-Symmetry in $\text{Na}_{0.5}\text{Bi}_{0.5}\text{TiO}_3$ and its Solid Solutions (Invited)

I. Levin*, NIST, USA

$\text{Na}_{0.5}\text{Bi}_{0.5}\text{TiO}_3$ -based piezoelectrics are promising alternatives to PZT. $\text{Na}_{0.5}\text{Bi}_{0.5}\text{TiO}_3$ (NBT) crystallizes with a perovskite-like structure and exhibits a complex interplay between various modes of octahedral rotations and polar cation displacements superimposed onto Na/Bi chemical disorder. This intricate displacive behavior extends into the NBT-based solid solutions with $\text{K}_{0.5}\text{Bi}_{0.5}\text{TiO}_3$ (KBT), BaTiO_3 , etc. Despite intense studies of NBT and related systems, a comprehensive understanding of their crystal and domain structures remains elusive. Therefore, we revisited several controversial aspects of structural behavior in NBT and NBT-KBT solid solutions using various techniques of transmission electron microscopy combined with high-resolution X-ray powder diffraction. The results were used to develop a model that reconciles the nanoscale and average structures in these systems.

3:15 PM

(EMA-S3-010-2013) Local microstructure evolution of bismuth sodium titanate-based lead free piezoelectric systems across the morphotropic phase boundary region (Invited)

Y. Liu*, L. Noren, R. L. Withers, Y. Guo, J. Wang, the Australian National University, Australia; A. J. Studer, Bragg Institute, The Australian Nuclear Science and Technology Organization, Australia

Morphotropic phase boundary (MPB) containing piezoelectric systems generally exhibit enhanced piezoelectric performance at compositions within, or close to, the MPB region. The mechanism/s underlying such enhancement, however, are still contentious due to complex micro/nano-structure and apparently inherent local structural variability associated with octahedral tilt disorder/platelet precipitates in such piezoelectric materials. This work reports some recent structural analysis results from $\text{Bi}_{0.5}\text{Na}_{0.5}\text{TiO}_3$ (BNT) and its binary, lead free, piezoelectric materials systems derived from it via electron diffraction and in situ neutron diffraction. The results suggest that intrinsically existing local microstructure in BNT essentially continues across the MPB region. The local microstructure, originating from inherent octahedral tilt disorder, is strongly electric field- and chemical composition-dependent, and may help to explain a series of phenomena observed in BNT-based binary materials systems, including the enhanced piezoelectric effect in the region of the MPB.

4:15 PM

(EMA-S3-011-2013) Multi-length-scale scattering studies of actuation mechanisms in the $(1-x)\text{Bi}_{0.5}\text{Na}_{0.5}\text{TiO}_3\text{-}(x)\text{BaTiO}_3$ solid solution (Invited)

J. Daniels*, The University of New South Wales, Australia

Using a combination of high-energy x-ray and neutron scattering techniques, it is shown that the structural response of $(1-x)\text{Bi}_{0.5}\text{Na}_{0.5}\text{TiO}_3\text{-}(x)\text{BaTiO}_3$ solid solutions to applied electric fields is a coupling of multiple processes over different length scales. At the atomic to nanometer scale, diffuse x-ray scattering from single crystals is used to investigate variations in local atomic offsets and movement of stacking fault structures under field. Neutron diffraction is used to measure the bulk average symmetry and field-induced lattice and ferroelastic strains. Novel techniques such as 3DXRD then allow us to probe individual grains within the polycrystal matrix. This presentation will explore the ability of such in-situ scattering techniques to quantitatively explain the observed macroscopic electro-mechanical behaviour of these and other future materials.

4:45 PM

(EMA-S3-012-2013) Creation and Destruction of Morphotropic Phase Boundaries through Electrical Poling in Lead-Free $(\text{Bi}_{1/2}\text{Na}_{1/2})\text{TiO}_3\text{-BaTiO}_3$

C. Ma, H. Guo, X. Tan*, Iowa State University, USA

Piezoelectric materials, which enable the conversion between mechanical and electrical energies, are crucial in numerous applications including energy harvesting, medical imaging, and minimally invasive surgery. Superior piezoelectricity emerges at the morphotropic phase boundary (MPB), where multiple ferroelectric phases coexist. The basic rule for developing high-performance piezoelectrics, which has been closely followed since 1950s, is to identify ferroelectric compositions at MPBs, and then pole them with strongest possible electric fields. Our in-situ transmission electron microscopy observations and piezoelectricity measurements on $(1-x)(\text{Bi}_{1/2}\text{Na}_{1/2})\text{TiO}_3\text{-xBaTiO}_3$ ceramics indicate that this long-standing guiding rule is questionable. The real-time evolution of crystal structure and domain morphology during the poling-induced phase transitions in compositions of $x = 0.055, 0.06, \text{ and } 0.07$ demonstrates that poling fields can either destroy or create MPBs and the associated strong piezoelectric property. Therefore, even the previously ignored single-phase materials could exhibit superior piezoelectricity if stable MPBs form during poling. Such fundamental alterations to the universal guideline add a new dimension to the development of next generation high-performance piezoelectrics.

5:00 PM

(EMA-S3-013-2013) Phase Transition and Property Enhancement in $(\text{K,Na})\text{NbO}_3$ -based Ceramics (Invited)

J. Li*, Tsinghua University, China

Sodium potassium niobate (KNN) based ceramics have received much attention as a promising candidate of lead-free piezoelectric materials because of its high piezoelectric properties. Chemical modification such as Li doping to KNN can remarkably enhance its piezoelectric properties by significantly shifting downward the tetragonal to orthorhombic transition point to room temperature, resulting in a state of two-phase coexistence in favor for enhancing piezoelectric response. This talk will give an example that a high piezoelectric coefficient d_{33} up to 324 pC/N can be obtained in Li-modified KNN ceramics without Ta and Sb doping, when tetragonal and orthorhombic phases coexist at room temperature, which enables domain engineering by re-poling treatment after aging. However, the challenge still remaining for the KNN system is design and realization of its morphotropic phase boundary (MPB) like that in $\text{Pb}(\text{Zr,Ti})\text{O}_3$ system to improve its temperature stability of enhanced piezoelectricity. For this purpose, we tried two approaches. One is utilization of the phase boundary of two kinds of tetragonal phases, and another is incorporating a rhombohedral BiFeO_3 compound to tetragonal Li/Ta-modified KNN. Finally, as one application example, this presentation will introduce the development of microscale 1-3 type piezoceramic composites using KNN-based ceramics for high-frequency medical imaging transducers.

S5: Structure and Properties of Interfaces in Electronic Materials

Transport, Structure and Composition of Interfaces

Room: Mediterranean B/C

Session Chair: Edwin Garcia, Purdue University

2:00 PM

(EMA-S5-007-2013) Microstructural Evolution in Perovskite Ceramics (Invited)

W. Rheinheimer, M. Bäurer, M. J. Hoffmann*, KIT, Germany

Perovskite ceramics are commonly used in electronic devices as sensors, actuators and passive devices and the properties of the grain

boundaries strongly influence the macroscopic behaviour. From a materials point of view perovskite materials have in common that the crystal structure is a stable ABO_3 structure that has low capability for the solution of either A or B excess. A deeper understanding of the influence of grain boundary properties on grain growth is necessary in order to tailor the microstructure as needed for best performance. Strontium Titanate has been used as a model system to study grain growth in perovskite systems in the absence of a liquid phase. It has been found that grain growth does not follow a classical Arrhenius type behaviour over the complete temperature range examined but shows two distinct drops in grain boundary mobility. The effect is reversible meaning that with step changes in temperature grain growth rate can be lowered and raised by orders of magnitude in temperature intervals as small as 40°C . This counterintuitive behaviour is discussed on the background of relative surface energies extracted from pore shapes, grain boundary morphology and growth studies on embedded single crystals. All findings during grain growth experiments have been backed up by HR- and analytical (S-) TEM work.

2:30 PM

(EMA-S5-008-2013) In situ diffraction reveals the dependence of domain wall motion on BaTiO_3 grain size and relation to macroscopic properties

D. Ghosh*, A. Sakata, J. Carter, University of Florida, USA; P. A. Thomas, University of Warwick, United Kingdom; H. Han, J. C. Nino, J. L. Jones, University of Florida, USA

Relative permittivity of barium titanate (BaTiO_3) peaks at grain sizes of approximately $1\ \mu\text{m}$. While two widely accepted theories attribute either internal residual stress or 90-degree domain wall contribution as the origin of the superior properties for grain sizes close to $1\ \mu\text{m}$, a complete and quantitative account for domain wall dynamics as a function of grain size is yet to be presented. Using an in situ high-energy X-ray diffraction (XRD) technique in transmission mode during application of high external electric fields, we show conclusive and direct evidence that 90-degree domain wall motion in BT is present under high electric fields across the grain size range $0.21\ \mu\text{m}$ to $3.52\ \mu\text{m}$, though peaks around the grain size of $2\ \mu\text{m}$ where macroscopic properties are also higher. Measurement of the unit cell volume and spontaneous lattice strain evidences that the degree of residual internal stress due to changing domain wall density is measurable though small. The current investigation thus conclusively attributes 90-degree domain wall motion to the superior properties in fine-grain BT ceramics.

2:45 PM

(EMA-S5-009-2013) Improvement of the silicon to silicon dioxide interface as Revealed by random telegraph signal noise analysis

J. Kim*, J. Kim, C. Lee, J. Lee, D. Kim, K. Yoo, H. Park, Dongbu Hitek., Co. Ltd, Republic of Korea

In MOSFET, $1/f$ is reduced by 1 to 2 orders of magnitude by incorporating fluorine at the silicon dioxide to silicon interface. This is attributed to a lower interface state density by fluorine, as confirmed by charge pumping. HRTEM micrographs show the presence of a transition layer at the interface without fluorine. This layer is not observed with fluorine. Instead, a smooth interface is between single crystal and amorphous Silicon dioxide is observed. Random Telegraph Signal [RTS] noise with MOSFETs of dozens nano size is believed to be the origin of $1/f$ noise and is known to provide insight into the nature of trapping and de-trapping sites at the interface. Discrete switching of drain current is observed between a low level at an average time and a high level at an average time in each state. The characteristic average times increase with incorporation of fluorine. Since the probabilities of electron capture and emission are, respectively, inversely proportional to average time of high state and low state, this trend agrees with a reduction in $1/f$ noise. An effect which supports the assumption of an electron capture, as explained by the band diagram. Interface states of silicon to silicon dioxide can explain continuously

within the band gap near the silicon to silicon dioxide interface. This appears to be caused by screening of the trap potential.

3:00 PM

(EMA-S5-010-2013) Control of ZnO thin film polarity through interface chemistry

C. T. Shelton*, E. Sachet, P. A. Elizabeth, J. Maria, NCSU, USA

When grown epitaxially on sapphire substrates, ZnO thin films exhibit oxygen, or c-, polarity. Insertion of a few nm of MgO as a buffer layer, however, causes the polarity to switch to zinc-polar or c+. Other researchers have surmised that the polarity switching observed in ZnO with increasing buffer layer thickness is the result of a change in the crystal structure of the MgO buffer from an intermediate wurtzite phase to the more stable rock-salt structure. Previously, we demonstrated that the overriding effect regulating ZnO polarity is coverage. Dual AC resonance tracking piezoresponse force microscopy (DART-PFM) was used to observe the polarity of ZnO films as a function of buffer layer thicknesses over a range spanning island nucleation and coalescence. Additionally, since the structure factor of opposite polar faces in wurtzite materials is different, differential absorption of x-rays may be used to establish polarity. The absolute polarity of ZnO thin films was confirmed using the anomalous dispersive behavior of X-rays around Zn K-edge absorption energies. Both methods confirm the existence of mixed polarity films at intermediate buffer layer thicknesses. Collectively this research suggests that an interface chemistry, as opposed to epitaxy, provides a predominate influence on ZnO polarity.

3:15 PM

(EMA-S5-011-2013) Effect of Gas Adsorption in Electrode-Semiconductor Interface

S. Lee, J. Jung*, Kyungnam University, Republic of Korea

The current flows in an electrode-semiconductor interface because of charge transport from the semiconductor to the metal or in the reverse direction. This mechanism includes thermionic emission, carrier recombination in the depletion region over, carrier recombination in the neutral region of the semiconductor and tunneling through the barrier. When gas atoms are adsorbed in the interface, however, the adsorbed atoms should play the important role in determining the characteristics of the interface because the adsorbed atoms change the work function of the metal surfaces. The gas atom permeates sometimes through the bulk lattice toward the metal/semiconductor, causing a perturbation at this interface that gives rise to a change in the output signal. In this study, the effect of charge transport by the gas adsorption in metal-semiconductor interface is discussed qualitatively. Thermionic field emission and gas ionic field emission tunneling through a barrier of the interface are simulated in a heavy doping system.

3:30 PM

(EMA-S5-012-2013) Stress-enhanced phase transformation kinetics in olivine battery electrodes (Invited)

M. Tang*, Lawrence Livermore Nat. Lab, USA

Many electrode materials for lithium-ion batteries undergo one or multiple phase transitions during battery charge/discharge, and their performance are profoundly influenced by the phase transformation kinetics. One such example is the LiMPO₄ (M=Fe, Mn, Ni, Co) olivine cathode, which transforms between a Li-poor and Li-rich phase upon cycling. Transformation between crystalline phases with a misfit strain often incurs significant elastic stress, which is usually considered as an energy penalty to slow down the transformation process. However, our recent phase-field simulations of the Li intercalation in LiFePO₄ surprisingly shows that the presence of misfit stress can considerably enhance the Li (de-)insertion kinetics by one order of magnitude at large applied overpotentials. Further analysis shows that this counter-intuitive phenomenon is the result

of 1) the suppression of phase separation and elimination of phase boundary in LiFePO₄ by coherency stress, and 2) the increase in effective Li diffusivity due to the stress contribution to the Li diffusion potential. Our results suggest that "stress engineering" of electrode materials might provide a fruitful approach to improving battery performance.

S11: Sustainable, Low Critical Material Use and Green Materials Processing Technologies

Materials for Sustainability: Optimized Material Choice and Performance for Low Critical Materials Use

Room: Mediterranean B/C

Session Chair: Paul Clem, Sandia National Laboratories

4:30 PM

(EMA-S11-002-2013) Ultra-efficient, Robust and Well-defined Nano-Array based Catalytic Devices for Emission Control

P. Gao*, Y. Guo, Z. Ren, University of Connecticut, USA

Constructed with parallel or honeycomb channels micrometer to millimeter in diameter, monolithic catalysts and reactors have been utilized in various business sectors ranging from mechanical, automotive, fine chemicals, pharmaceutical, to biotechnology industries. Exemplified by the catalytic after-treatment devices in automobiles, monolithic catalysts and reactors generally integrate the bare monolith with highly porous catalyst support and catalysts with high surface area and activity. However, the state-of-art monolithic catalysts in industry suffers from some long-standing problems such as mediocre-uniformity, need for high catalyst loading, low materials utilization, random catalytic sites, poor washcoat adhesion, short lifetime, degradation tendency, all of which lead to much compromised and less-than desirable catalytic performance. Herein, by directly integrating the bare 3D monoliths with well-defined nanostructure arrays (nano-arrays), the nano-array monolithic catalysts significantly reduce the precious metal and metal oxide usages by an order of magnitude, while demonstrating good thermal stability and catalytic activity. The 3D nano-array catalysts represent a new and effective class of model devices for catalytic emission control in combustion engines and turbines.

4:45 PM

(EMA-S11-003-2013) Electric field enhancement of photocatalysis

M. Laudenslager*, W. M. Sigmund, University of Florida, USA

Photocatalysts harness the power of the sun to degrade pollutants that are resistant to breakdown in the environment. These semiconductor materials generate electron-hole pairs when they absorb photons with energy greater than their bandgap. These electron-hole pairs go on to generate free radicals, which are effective at degrading the unwanted compounds into environmentally benign material. Several studies have demonstrated that electrodes placed inside a photocatalytic system can improve performance, but state the effect levels off after very small DC voltages. In this work, the effect of a DC external electric field is investigated, which prevents photolysis from occurring at higher voltages. When the reactor is placed inside an electric field instead of placing electrodes into the liquid itself, the effect continues to improve the performance as the voltage increases. At the highest electric field strength, the degradation time of Procion Red dye using P25 powder was reduced to half. This increase in photocatalytic reaction rate corresponds to the Poole-Frenkel equation, which describes electron motion in semiconductors with applied electric fields. The effect appears to be greater in P25 than pure rutile, which indicates it might help electrons overcome the energy barrier between phases. Therefore, electric fields could be used to make other materials interesting photocatalysts that would not be under normal conditions.

5:00 PM

(EMA-S11-004-2013) Thermochromic windows for control of thermal heat gain: tuning and optimization of VO₂ coating metal-insulator transition temperature

P. Clem*, C. Edney, Sandia National Laboratories, USA

The intriguing semiconductor-metal transition of vanadium dioxide has been investigated for many years with regards to electrical properties and band structure, and has recently been analyzed as a promising candidate for smart thermochromic windows. We will present results of an investigation of solution-deposited and sputtered VO₂ films, and influence of doping, grain size, and process atmosphere on film transition uniformity, electrical properties, and optical properties. The complicated band structure of VO₂ is influenced by stress, doping, oxygen vacancy concentration, and compositional uniformity, and impacts of these effects on film quality will be discussed. Films with transition temperatures tunable from 25C to 80 C, and semiconductor/metal resistance ratios of up to 100,000 will be shown, as well as initial modeling of impact of tunable optical properties on candidate solar gain applications. Sandia National Laboratories is a multi-program laboratory managed and operated by Sandia Corporation, a wholly owned subsidiary of Lockheed Martin Corporation, for the U.S. Department of Energy's National Nuclear Security Administration under contract DE-AC04-94AL85000.

S12: Recent Developments in High Temperature Superconductivity

YBCO Coated Conductors II-Pinning

Room: Indian

Session Chair: Timothy Haugan, Air Force Research Laboratory

2:00 PM

(EMA-S12-007-2013) Engineered nanoscale defects for enhanced vortex-pinning in coated conductors (Invited)

A. Goyal*, S. Wee, Oak Ridge National Laboratory, USA

Engineered nanoscale defects within REBa₂Cu₃O_{7-δ} (REBCO) based coated conductors are of great interest for enhancing vortex-pinning, especially in high-applied magnetic fields. We have conducted extensive research to optimize vortex-pinning and enhance J_c via controlled introduction of various types of nanoscale defects ranging from simple rare-earth oxides and Ba-based perovskites (BaMO₃, M=Zr, Sn, etc.) to double perovskite rare-earth tantalates and niobates (Ba₂RETaO₆ and Ba₂RENbO₆). This talk will summarize our results on how density, morphology, and composition of these engineered nanoscale defects affects vortex-pinning in different temperature, field and angular regimes. Detailed microstructural and superconducting properties coated conductors with these engineered defects will be presented.

2:30 PM

(EMA-S12-008-2013) Novel vortex pinning mechanism of solution-derived YBCO nanocomposites driven by local lattice strains (Invited)

M. Coll*, A. Palau, J. Gazquez, A. Llordés, S. Ye, R. Guzmán, V. Rouco, R. Vlad, J. Arbiol, S. Ricart, ICMAB-CSIC, Spain; G. Deutscher, Tel Aviv University, Israel; C. Magen, Universidad Zaragoza, Spain; E. Bartolomé, T. Puig, X. Obradors, ICMAB-CSIC, Spain

Vortex pinning landscape engineering is foreseen as the route to high performance YBCO coated conductors at high fields. Solution-derived YBCO nanocomposites with spontaneously segregated oxide second phase nanoparticles were shown to be an excellent low cost processing option with huge isotropic pinning forces. We will report on TFA-YBCO nanocomposites with BaZrO₃, Y₂O₃, BaCeO₃ and Ba₂YTaO₆ second phase nanoparticles, which evi-

dence that these nanocomposites do experience a highly effective novel pinning mechanism, coupling superconducting pairing to lattice strain. The presence of randomly oriented nanoparticles generate incoherent interfaces with the epitaxial YBCO matrix causing localized nanostrained regions that has been correlated with a strong enhancement of vortex pinning and a vanishing anisotropy. Still we demonstrated that the YBCO intrinsic mass anisotropy is preserved as was evidenced by high field H_{c2}(T) measurements. STEM investigation shows a ramified shape of inhomogeneously distributed nanostrained regions associated to a highly dense defect structure (mainly extra Cu-O chains and partial dislocations interacting with twin boundaries). We propose that the inhomogeneously distributed nanostrained regions locally suppress Cooper pair formation according to a Bond Contraction Pairing model.

3:00 PM

(EMA-S12-009-2013) New pinning strategies for the second-generation wires (Invited)

V. Solovyov*, Q. Li, Brookhaven National Laboratory, USA

In the last several years the second generation (2G) superconducting wires are considered as promising alternatives to rare-earth based permanent magnets (PM) in rotating machines operating at a temperature of 20 – 40K in a magnetic field of 1-3 T. It is becoming clear, however, that the pinning strategies developed and studied for 77 K applications are less effective at lower temperatures. Here we outline several new strategies for improving the low-temperature performance by utilizing in-plane strain of thick YBCO layers manufactured by reel-to-reel metal-organic deposition (MOD). First we show that the strain-induced pinning mechanism analysis, based on the Eshelby model of the elastically strained composites, predicts that small YBCO grain size is a critical component of a strong pinning architecture that can enable critical current density values approaching the depairing limit. Second, we will describe how the in-plane strain can be controlled by processing parameters. Systematic changes of the in-plane structure and YBCO grain size are mapped with respect to the YBCO stability line and the Cu₂O-CuO line on the Bormann-Hammond diagram. It is demonstrated that the optimum critical current density is the result of a trade-off between YBCO grain coupling and the strain-induced pinning. This work has been performed under contract with ARPA-E, U. S. Department of Energy.

4:00 PM

(EMA-S12-010-2013) Strain-mediated self-assembly of secondary phase nanostructures in YBCO thick films via interfacial strain engineering (Invited)

J. Wu*, J. Shi, R. Emergo, J. Baca, X. Wang, University of Kansas, USA; T. Haugan, U.S. Air Force Research Laboratory, USA

Controllable generation of nanostructures of secondary phases in epitaxial primary matrix films can provide a unique pathway to new functionality. Thick-film YBa₂Cu₃O_{7-δ} (YBCO) coated conductors are such an example in which 3-dimensional nanostructured pinning landscape can significantly enhance the critical current density J_c in magnetic fields. Interfacial strains play a critical role in strain-mediated self-assembly of secondary-phase nanostructures and a quantitative study of interfacial strain at microscopic scale is important to design and assembling 3-dimensional pinning landscape in YBCO. In this work, a theoretical model based on the elastic strain theory was developed to understand the strain at the coherent or semi-coherent interface between secondary phase and YBCO matrix, and that between the YBCO matrix film and substrate. We show the interplay of these two interfacial strains could result in a variety of nanostructure morphology and some have been demonstrated experimentally. This study suggests engineering the interfacial strains may provide a viable method towards design functional secondary phase nanostructures in nanocomposite films.

4:30 PM

(EMA-S12-036-2013) Rare-metal-free Magnetism and Spintronics arising from Graphene Edges (Invited)

J. Haruyama*, Aoyama Gakuin University, Japan

The graphene, an ultimate two-dimensional molecule sheet with thickness as thin as one carbon atom size, is attracting significant attention. Although a variety of exciting phenomena has been experimentally reported in graphenes, none has experimentally reported on edgerelated phenomena. Basically, there are two kinds of atomic structures in graphene edges; the so-called arm chair and zigzag edges. Theoretically, zigzag edge yields a flat energy band, which makes electrons localize around the edge. The localized electrons are spontaneously spin-polarized due to strong electron interaction arising from extremely high electron density of states. It allows research of spin-based phenomena and applications to novel spintronic devices, in spite of a material consisting of only carbon atoms with sp² orbitals. None has, however, reported on experimental observation of edge-related phenomena, because lithographic fabrication of graphene edges easily introduces disorder. In the talk, I will present that the nanomeshes with hydrogen-terminated zigzag pore edges exhibit magnetic-critical-metal-free large-amplitude ferromagnetism, anomalous magnetoresistance oscillations, and also some spin-related phenomena, which are strongly associated with the polarized electron spins localizing at the pore edges.

5:00 PM

(EMA-S12-011-2013) Tunable Flux Pinning Properties in YBa₂Cu₃O_{7-x} Thin Films by Functional Fe₂O₃:CeO₂ Vertically Aligned Nanocomposites

C. Tsai*, H. Wang, L. Chen, Texas A&M University, USA

(Fe₂O₃)_x:(CeO₂)_{1-x} vertically aligned nanocomposite (VAN) with different compositions are decorated in YBa₂Cu₃O_{7-x} (YBCO) thin films as cap layers by a pulsed laser deposition method. The composition of Fe₂O₃ dopants in the VAN cap layers is controlled as 10%, 30% and 50% to achieve different densities and arrangements of Fe₂O₃ and CeO₂ nanopillars and to change the flux pinning landscapes in YBCO thin films. The microstructure and defect analysis including XRD, high resolution XTEM and STEM are conducted to investigate the morphology variation of the VAN structures with various compositions. In order to study the effect of pinning landscapes on the superconducting performance, the superconducting properties of both self-field and in-field critical current density (J_c^{sf} and $J_c^{in-field}$ ($H//c$)) and transition temperature (T_c) are measured. The results show all doped samples obtain T_c above 90 K and the J_c^{sf} measured at 65K increased up to 9.2 MA/cm² for 30% Fe₂O₃ doped sample. As the measurement temperature decreases to 5K, the sample with 50% Fe₂O₃ VAN show the best result. This work provides a new route for achieving magnetic pinning with well controlled density and diameter to as effective pinning centers in YBCO coated conductors.

S15: Failure: The Greatest Teacher**Failure: The Greatest Teacher**

Room: Coral A

Session Chair: Geoff Brenneka, Sandia National Laboratories

8:00 PM

(EMA-S15-001-2013) Embracing Failure in Energy-Based Materials Research (Invited)

E. Spoecker*, D. V. Gough, J. Wheeler, N. Hudak, N. Bell, C. Edney, Sandia National Laboratories, USA; B. Aguirre, University of Texas, El Paso, USA; D. Frank, Sandia National Laboratories, USA

Benjamin Franklin once proclaimed, "I didn't fail the test, I just found 100 ways to do it wrong." The sentiment of this comment reflects a well-understood, if not often articulated, approach to scientific research. Revealing how, and just as importantly why, "not" to do some-

thing is instrumental to discovering critical advances in emerging technologies. In this talk I will highlight a number of recent examples of "failure" in our group's materials-based research, spanning fields ranging from electrical energy storage to photovoltaics to carbon dioxide sequestration. I will describe the motivation and design of each program, where the research deviated from expectations, and the value of the lessons we have taken away from each effort moving forward. Learning from the failures of these programs not only stands to advance research in these select areas, but extension of the principles uncovered may also lead to progress in other developing technological systems. Sandia National Laboratories is a multi-program laboratory managed and operated by Sandia Corporation, a wholly owned subsidiary of Lockheed Martin Corporation, for the U.S. Department of Energy's National Nuclear Security Administration under contract DE-AC04-94AL85000.

8:30 PM

(EMA-S15-002-2013) Surprises and Failures (Invited)

C. Randall*, Penn State University, USA

Scientific process is always a balance of predicting and testing hypothesis and theory. Often new insights are gained through these experiences and curiosities. During this talk, we will consider some recent examples of such insights, as related to unusual observations in electroceramics and the learning process gained from such observations.

Poster Session

Room: Atlantic/Arctic

(EMA-S1-P001-2013) Flexoelectricity in Dielectrics and Design of Flexoelectric Piezoelectric Composites of High Piezoelectric Response

B. Chu*, University of Science and Technology of China, China; L. Cross, Pennsylvania State University, USA; D. R. Salem, South Dakota School of Mines and Technology, USA

Flexoelectricity is an electromechanical physical phenomenon which describes the linear relationship between strain gradient (or electric field gradient) and electric polarization (or stress). Piezoelectric composites, in which none of the components is piezoelectric, can be designed by exploiting flexoelectricity of one or more components in the composites. The flexoelectricity in various materials including ceramics and polymers will be first shown and discussed in this presentation. Design of flexoelectric piezoelectric composites with giant piezoelectric response will be also presented. Factors that affect the piezoelectric response of flexoelectric piezoelectric composites will be further discussed. Our results suggest that flexoelectric piezoelectric composites could be a new class of functional materials with excellent piezoelectric properties,

(EMA-S1-P002-2013) Electromechanical Properties of Textured NKLNT Piezoelectric Ceramics

J. Song*, S. Kim, J. Jo, I. Kim, S. Jeong, M. Kim, Korea Electrotechnology Research Institute, Republic of Korea

Na_{0.5}K_{0.5}NbO₃ (NKN) has drawn greater attention owing to their ultrasonic applicability and is also considered to be promising candidates for a lead-free piezoelectric system. However, it was also found that sintering NKN ceramics under atmospheric pressure is difficult, in general, and their piezoelectric properties are insufficient for practical applications. To improve the sinterability and piezoelectric properties, various dopants have been investigated. Among them, 1mol% Li₂O excess (Na_{0.51}K_{0.47}Li_{0.02})(Nb_{0.8}Ta_{0.2})O₃ (NKLNT) ceramics were reported to have excellent electromechanical responses by controlling the microstructure. In addition, many researchers have developed textured ceramics by using reactive template grain growth (RTGG) processing. The piezoelectric properties of the textured NKN-based ceramics were comparable to those of unmodified PZT. RTGG is believed to be an effective process to improve the piezoelectric properties of the ceramics. In this study, 1mol% Li₂O excess NKLNT textured ceramics with high piezoelectric properties were investigated.

Plate-like perovskite NaNbO_3 template crystals synthesized by a topochemical reaction method were used. The effects of template on sinterability, texturing and piezoelectric properties in the ceramics were investigated.

(EMA-S1-P003-2013) Synthesis and dielectric properties of $\text{BaTiO}_3\text{-Bi}(\text{Ni}_{0.5}\text{Ti}_{0.5})\text{O}_3$ ceramics

N. Kumar*, D. P. Cann, Oregon State University, USA

Ceramics of the composition $(1-x)\text{BaTiO}_3\text{-xBi}(\text{Ni}_{0.5}\text{Ti}_{0.5})\text{O}_3$ ($0.025 \leq x \leq 0.6$) were prepared by solid state synthesis. The x-ray diffraction data showed a perovskite structure with pseudo-cubic symmetry for most compositions ($0.1 \leq x \leq 0.55$). The optimum dielectric properties were observed for a 2% Ba-deficient composition at $x=0.2$ with a relative permittivity close to 1000 and a dielectric loss below 0.05 up to 450 °C. It was also highly insulating with a resistivity of 0.4 G Ω -cm at 400 °C which was more than twice the resistivity value for the stoichiometric composition at the same temperature. While the room temperature hysteresis loops were slightly non-linear and broad for the stoichiometric composition at $x=0.2$, they became extremely linear and slim with introduction of Ba-deficiencies. On the whole, Ba-deficient compositions showed great potential for high temperature capacitor applications and the role of Ba-deficiencies in suppressing the dielectric losses became increasingly pronounced as amount of $\text{Bi}(\text{Ni}_{0.5}\text{Ti}_{0.5})\text{O}_3$ in the ceramics increased.

(EMA-S1-P004-2013) Comparison of Goldschmidt's Tolerance Factor With Cubic and Tetragonal Ionic Radii Volume Constrained Perovskite Structures in the Design of Advanced Material

S. Tidrow*, The University of Texas - Pan American, USA

Goldschmidt's tolerance factor has provided guidance for development of new perovskite materials for decades. Unfortunately, there are increasing numbers of publications and reports in which Goldschmidt's tolerance factor has not provided and does not provide an adequate model for understanding material parameters. In this presentation, we continue to develop the recently presented volume constrained simple "ideal" cubic perovskite model as compared with Goldschmidt's tolerance factor by extending the visual illustrations to include tetragonal perovskite structures. Using this new approach, a mapping transformation into ionic radii space, yields some results similar with Goldschmidt's tolerance factor and yet provides a more accurate, although still insufficient, physical model for understanding of material parameters. This material is based upon work supported by, or in part by, the U.S. Army Research Laboratory and the U.S. Army Research Office under contract/grant number W911NF-08-1-0353.

(EMA-S1-P005-2013) KFM Investigation about Electric Field Distribution of BaTiO_3 Layer in Degraded MLCC

T. Okamoto*, Pennsylvania State University, USA; S. Kitagawa, N. Inoue, A. Ando, H. Takagi, Murata Manufacturing Co., Ltd., Japan

The suppression of insulation degradation in the applied dc voltage is increasingly important in thin dielectric layers in multilayer ceramic capacitors (MLCCs). To clarify the mechanism of insulation degradation, it is essential to characterize directly the changes in electric field distribution within the dielectric layers as a function of time. The electric field distributions of degraded dielectric layers were investigated by Kelvin probe force microscopy (KFM) under the applied dc field of 1.3 kV/mm at room temperature in a cross sectional view. The KFM study conducted here found that the local electric field in the dielectric layers strengthens near the cathodes at the initial stage of the degradation, and in the highly degraded stage the local field became strong near the anodes. Furthermore, this concentrated field on the anode was found easily alternating polarity of the applied voltage under such mild conditions that the oxygen vacancies are essentially immobile, in contrast to a homogeneous distribution found throughout the layers of the fresh MLCC. These results indicate the relative local resistivity in dielectric layer decrease from the vicinities of the

anode at initial stage of degradation. However, at the highly degraded layers, barrier layers near the anode could control the current.

(EMA-S1-P006-2013) Er₂O₃ Additive Influence on Microstructure and Dielectrical Properties of BaTiO_3 -Ceramics

V. Mitic*, V. Paunovic, Faculty of Electronic Engineering, University of Nis, Serbia; M. Miljkovic, Center for Electron Microscopy, University of Nis, Serbia

Doped BaTiO_3 -ceramics is very interesting for its application as resistors with PTCR, multilayer ceramics capacitors, thermal sensors etc. Er doped BaTiO_3 -ceramics, with different Er_2O_3 content, ranging from 0.01 to 1.0 wt% Er, were investigated regarding their microstructural and dielectric characteristics. The samples were prepared by the conventional solid state reaction and sintered at 1350°C in an air atmosphere for 4 hours. The grain size and microstructure characteristics for various samples and their phase composition was carried out using a scanning electron microscope SEM equipped with EDS system. SEM analysis of Er/ BaTiO_3 doped ceramics showed that in samples doped with a low level of rare-earth ions, the grain size ranged from 10-40 μm , while with the higher dopant concentration the abnormal grain growth is inhibited and the grain size ranged between 2-10 μm . Dielectric measurements were carried out as a function of temperature up to 180°C. The low doped samples sintered at 1350°C, display the high value of dielectric permittivity at room temperature, 2300 for 0.01Er/ BaTiO_3 . A nearly flat permittivity-response was obtained in specimens with higher additive content. Using a modified Curie-Weiss law the Curie constant (C) and a critical exponent γ were calculated. The obtained values of γ pointed out the diffuse phase transformation in heavily doped BaTiO_3 samples.

(EMA-S2-P027-2013) Novel and Efficient Copolymer based quasi solid electrolyte for Dye Sensitized Solar Cells

M. Akhtar*, Z. Li, W. Lee, O. Yang, Chonbuk National University, Republic of Korea

The quasi or solid polymer electrolyte have recently attracted electrolyte materials owing to their advantages including high ionic conductivities which are achieved by "trapping" a liquid electrolyte in polymer cages formed in a host matrix, good contacting and filling properties of the nanostructured electrode and counter electrode. In this work, the copolymer of Polybutyl acrylate (PBA) and polyacrylonitrile (PAN) was prepared by thermal polymerization of butyl acrylate and acrylonitrile monomers at 80°C under vacuum condition. The prepared PAN-co-PBA was further heated at 100°C to avoid any impurities in the copolymer and used as gel polymer electrolyte for dye sensitized solar cells (DSSCs). Importantly, the presence of carboxylate group in copolymer was acted as superabsorbent to organic liquid/solvent in the redox electrolyte which significantly improved the physical, mechanical and ionic conductivity properties of gel polymer electrolytes. The obtained gel polymer electrolyte presented the highest ionic conductivity of 3.86 x 10⁻³ S/cm, resulting in the good support in the charge transportation from electrolyte layer and conduction layer of cells and improved the interfacial contact with working electrode to electrolyte layers.

(EMA-S3-P007-2013) Crystal structure and electrical properties of complex perovskite solid solutions based on $\text{NaNbO}_3\text{-Bi}(\text{Zn}_{0.5}\text{Ti}_{0.5})\text{O}_3$

S. Prasertpalichat*, D. P. Cann, Oregon State University, USA

Perovskite solid solutions based on $(1-x)\text{NaNbO}_3\text{-xBi}(\text{Zn}_{0.5}\text{Ti}_{0.5})\text{O}_3$ were prepared using conventional solid state synthesis. The crystal structure and electrical properties were examined using x-ray diffraction and dielectric spectroscopy. A pure orthorhombic perovskite phase was identified up to a composition of $x=0.09$ that suggests a solubility limit of approximately 9 mol%. For the $x = 0.09$ composition, an in-situ high energy x-ray analysis technique was performed and no changes in the crystal structure were observed during the application of an electric field ranging from 0-25 kV/cm. The dielectric properties were characterized by a dielectric permittivity maximum

(T_m) that decreased as the BZT content increased. Furthermore, the phase transition became increasingly diffuse and frequency-dependent at compositions with $x > 0.05$ (5 mol%) which corresponded to the observation of a change from orthorhombic to pseudo-cubic symmetry in the XRD data. The polarization hysteresis data was characterized by a slim linear loop across the whole set of solid solutions. The trend in optical band gap near the solubility limit correlated to the observed change in perovskite symmetry.

(EMA-S4-P008-2013) Properties of undoped and Si-doped nonpolar a-plane GaN grown with different initial growth pressures

H. Kim*, Hanbat National University, Republic of Korea; K. Song, Korea Advanced Nano Fab Center, Republic of Korea

Despite the progress in nonpolar light emitting diodes (LEDs), the growth of nonpolar a- or m-plane GaN is complex and still produces high densities of threading dislocations (TDs) and basal stacking faults (BSFs). To achieve high performance nonpolar GaN LEDs, the properties of nonpolar GaN films need to be understood thoroughly. Here, we grew Si-doped GaN films with different silane (SiH₄) flow rates on two undoped GaN templates prepared by modulating the initial growth pressure. The dominant photoluminescence (PL) peaks were observed at 3.42 eV (3.27 eV: donor-acceptor pair (DAP)) for the undoped GaN sample grown with higher (lower) initial growth pressure. For all Si-doped GaN samples, the dominant PL peak at 3.42 eV was observed, which was related with excitons bound to BSFs. The intensity ratio of the 3.42 eV band to near band edge (NBE) emission was reduced with increasing doping concentration, associated with the decrease in the density of BSFs. The intensity of the DAP-longitudinal optical (LO) phonon replica was found to exceed the DAP emission above 50 K, probably due to the structural defect-related emission in heavily Si-doped a-plane GaN samples. Based on the emission at 3.36 eV, it was concluded that the improved crystalline quality was obtained through Si doping.

(EMA-S4-P009-2013) Radial Junction Nanostructured Plasmonics Silicon Solar Cells

P. Pudasaini*, A. Ayon, University of Texas at San Antonio, USA

A new solar cells design concept having radial p-n junction is presented with the possibility of lower cost and higher efficiency. The proposed solar cells consist of sub-wavelength nanotextured surface in combination with noble metal nanoparticles array. COMSOL multiphysics simulation indicates that the ultimate efficiency of the silicon nanotextured array surface in combination with gold (Au) nanoparticles is found to be 38.58%, which compares favorably well with the ultimate efficiency of 31.11% to its counterpart without plasmonic Au nanoparticles. The metal assisted electroless chemical etching along with nanosphere lithography is used to fabricate the silicon nanopillar (SiNP) textured surface. Low cost Spin on Dopant technique is used to fabricate the radial p-n junction. The power conversion efficiency (PCE) for the radial junction SiNP array textured solar cell with nanopillar height 800 nm is found to be 10.67%, while the PCE of the planar silicon solar cells is 8.65%, despite of its higher VOC of 574 mV. The PCE decreased with the further increase in nanopillar height. This is because of the increased front surface recombination due to the increased surface area. With the inclusion of front side plasmonic metal nanoparticles the PCE of the solar cells is decreased to 7.31%, which is due to the reduced open circuit voltage due to increased surface recombination.

(EMA-S6-P010-2013) Nanostructure Engineering and Combinatorial Solutions for Enhanced Nanotransport Behavior in Oxide-based Thermoelectric Materials for Power Generation

E. L. Thomas*, UDRI, USA; R. Snyder, AFRL, USA; X. Song, S. Chen, WVU, USA; W. Wong-Ng, NIST, USA

Thermoelectric (TE) materials directly inter-convert temperature differentials to electrical energy, and vice versa, and can potentially solve many energy demands faced by various high temperature applica-

tions. However, there are several hurdles encountered in the making of practical TE devices, including known materials' low inter-conversion efficiency and temperature stability. Here, we target oxide-based materials for high temperature power generation applications that overcome the traditional barriers faced by low-dimensional materials during scale-up productions, and can assist other systems by waste-heat scavenging. This presentation highlights our doping, nanostructured and combinatorial approaches to fostering TE property enhancements in calcium cobaltite (Ca₃Co₄O₉) and its derivatives. Regarding the temperature and environment of a particular application, a variety of TE material compositions are needed. Our recently developed combinatorial mapping techniques and state-of-the-art screening methods are positioned to accelerate the selection and introduction of novel TE materials into manufacturing processes.

(EMA-S6-P011-2013) Thermoelectric behavior of SrTiO₃ solid solutions

H. J. Brown-Shaklee*, P. A. Sharma, M. A. Blea, Sandia National Laboratories, USA; P. E. Hopkins, University of Virginia, USA; J. F. Ihlefeld, Sandia National Laboratories, USA

Lanthanum doped strontium titanate (STO) is a promising semiconductor for thermoelectric applications. In this work, we explore the electrical and thermal properties of lanthanum and bismuth doped STO bulk ceramics produced by solid state and chemical synthesis methods. Reduced pO₂ annealing of doped STO was required to develop the carrier concentrations required for favorable thermoelectric performance. Processing in these highly reducing atmospheres, however, formed bismuth-rich inclusions and A-site vacancies. Surprisingly, the A-site deficient STO that contained bismuth inclusions exhibited higher power factors than the site balanced, n-doped La-STO due to the apparent increase in thermopower. The thermoelectric behavior of doped STO will be fully discussed. This work was supported by the Laboratory Directed Research and Development program at Sandia National Laboratories. Sandia National Laboratories is a multi-program laboratory managed and operated by Sandia Corporation, a wholly owned subsidiary of Lockheed Martin Corporation, for the U.S. Department of Energy's National Nuclear Security Administration under contract DE-AC04-94AL85000.

(EMA-S6-P013-2013) Effect of amorphous phase on thermoelectric properties of B-doped Si film

N. Hayakawa*, K. Iwasaki, Toyota Boshoku Corporation, Japan

Crystalline Si-based compound is known to show high thermoelectric properties due to the Si-Si network formed by sp³ hybridization. However, thermoelectric properties of compounds having amorphous and clathrate Si-Si network have not been studied in detail. We prepare B-doped Si film consisting of amorphous and crystalline mixed-phase by RF magnetron sputtering. The volume fraction of amorphous phase is from 46 to 100%. Seebeck coefficient of the film at room temperature decreases from 300 to 180 $\mu\text{V K}^{-1}$ with an increase in the volume fraction of amorphous phase. Meanwhile, the electrical conductivity is not dependent on the volume fraction of amorphous phase, and is about 1 S cm^{-1} . These results are attributed to an increase in carrier concentration from 1.3×10^{19} to $1.4 \times 10^{20} \text{ cm}^{-3}$ and a decrease in carrier mobility from 0.23 to 0.05 $\text{cm}^2 \text{ V}^{-1} \text{ s}^{-1}$ with the increase in amorphous phases. The thermal conductivity, 1 $\text{W m}^{-1} \text{ K}^{-1}$, is lower than that of crystalline Si because of enhancement of phonon-scattering by atomic arrangement of amorphous. The figure of merit Z is in less than $1.0 \times 10^{-5} \text{ K}^{-1}$ due to low electrical conductivity.

(EMA-S6-P014-2013) Mechanical and thermoelectric property analysis of simultaneously sintered segmented Bi₂Te₃/PbTe for thermoelectric module

S. Yoon*, O. Kwon, J. Han, J. Cho, Seoul National University, Republic of Korea; J. Kim, Korea Institute of Science and Technology, Republic of Korea; C. Park, Seoul National University, Republic of Korea

Thermoelectric materials have specific temperature region where they have highest ZT value. In order to obtain high efficiency in

wide temperature range, the segmented thermoelectric elements, which consist of several layers of different thermoelectric materials, can be used. The segmented Bi₂Te₃/PbTe thermoelectric elements were fabricated by a simultaneous sintering method with Spark Plasma Sintering (SPS). Bond strength of the segmented sample was evaluated by Tensile test. The diffusion behaviors at the interface of the segmented elements were investigated with FESEM and EDS. Also XRD measurements were performed to observe the possible presence of second phases. Thermoelectric properties of the segmented elements, Bi₂Te₃ and PbTe were measured and compared. Finally the electromotive force were measured under the condition of $\Delta T > 300^\circ\text{C}$. Based on the result, the effect of the segmentation of thermoelectric material on thermoelectric property was confirmed.

(EMA-S8-P015-2013) Memristor using metal to insulator transition of single VO₂ nanowire

S. Bae, Seoul National University, Republic of Korea; S. Lee, L. Lin, Georgia Institute of Technology, USA; J. Cho, S. Yoon*, H. Koo, Seoul National University, Republic of Korea; Z. Wang, Georgia Institute of Technology, USA; C. Park, C. Park, Seoul National University, Republic of Korea

VO₂ which shows metal-insulator transition near room temperature ($T_c=68^\circ\text{C}$) possesses unique electrical and optical properties, which can lead to a wide variety of applications, including all-optical switches, electro-optical switches, smart windows, and memristor devices. Memristors are passive circuit elements which behave as resistors with memory; the resistance state can depend on other state variables which include temperature, structural properties, and electrical bias. The memristive property of VO₂ thin film has been reported [1]. In this study, the electrical properties of single VO₂ nanowire were measured when various electrical bias voltages were applied. The VO₂ nanowires were synthesized by hydrothermal process which was followed by thermal annealing at 400°C in N₂ atmosphere. The phase transition of single VO₂ nanowire was driven by 0.35V bias. When bias voltage pulse was applied, the resistances of the nanowire changed to various values which depend on the amount of bias voltage and the number of pulse. 1. Driscoll T, Kim HT, Chae BG, Di Ventra M, Basov DN., Phase-transition driven memristive system, Appl. Phys. Lett. 95 (2009), 043503 This research was supported by a grant from Construction Technology Innovation Program (CTIP) funded by Ministry of Land, Transport and Maritime Affairs (MLTM) of Korean Government, 12CCTI-B050622-05-000000.

(EMA-S9-P016-2013) Microstructural Characterization of Flux-Grown BaTiO₃ Thin Films

M. J. Burch*, D. T. Harris, J. Li, E. A. Dickey, J. P. Maria, North Carolina State University, USA

The role of the BaO•B₂O₃ (BBO) fluxing agent on the microstructural development of pulsed-laser deposited (PLD) BaTiO₃ thin films were studied. Transmission electron microscopy (TEM) was utilized to study grain size, secondary phase formation, and twin boundary occurrence of the BaTiO₃ as a function of flux composition. The samples were deposited at 400°C and subsequently annealed at 900°C on sapphire substrates. The films were prepared for TEM by the use of a focused ion beam (FIB). The films grown with BBO flux were highly crystalline with grain sizes varying from 0.1 to 0.5 μm , whereas the films grown with no fluxing agent showed an average grain size less than 0.1 μm and a much higher porosity. The improved microstructure of the flux-grown BaTiO₃ films lead to enhanced dielectric properties. Pockets of a secondary phase containing aluminum have been observed at the interface between the sapphire and the BBO doped BaTiO₃ thin films, with no secondary phase present in the un-fluxed samples. This phase has been verified to be BaAl₂O₄ by x-ray and electron diffraction, as well as electron energy loss spectroscopy. In addition, twin boundaries have been found to be prevalent in the large grains of the BBO fluxed films.

(EMA-S10-P017-2013) Effect of surface-treated MMT addition on the tensile behavior of MMT/glass/vinylester composites

J. Lee, Kyunghee University, Republic of Korea; Y. Jung, Philadelphia University, USA; K. Rhee*, Kyunghee University, Republic of Korea

It is known that addition of carbon nanotubes (CNTs) can improve the mechanical properties of conventional fiber reinforced polymer matrix, and many studies have been made to investigate the mechanical behavior of CNT/fiber/polymer matrix composites. However, compared to CNTs, only few research results on the mechanical properties of MMT (Montmorillonite) reinforced fiber/polymer matrix composites have been reported. In this study, MMT was surface-treated using 3-aminopropyltriethoxysilane and mixed with vinylester resin. Then chopped strand glass was impregnated into a vinylester resin mixed with clay. Tensile tests have been performed to determine the effect of surface-treated MMT addition on the tensile properties of MMT/glass/vinylester composites. The concentration ratios of MMT applied in the composites were 0.5, 1.0, 1.5, and 2.0 wt% respectively. The results showed that the tensile strength and elastic modulus of surface-treated MMT/glass/vinylester composites were higher than those of untreated MMT/glass/vinylester composites for each concentration ratio. The improvement occurred due to the increase of intercalation and dispersion of MMT in the matrix. The improvement also occurred due to the improved interfacial bonding strength between the MMT and the vinylester resin by the surface-treatment of the MMT.

(EMA-S12-P028-2013) Flux Pinning of YBa₂Cu₃O_{7- δ} Superconductor with Ultra-large Y₂BaCuO₅ Nanoparticle Additions

M. P. Sebastian, J. N. Reichart, M. M. Ratcliff, Air Force Research Laboratory, USA; J. L. Burke, University of Dayton Research Institute, USA; T. J. Haugan*, Air Force Research Laboratory, USA

Addition of nanophase defects to YBa₂Cu₃O_{7- δ} (YBCO) superconductor thin films is known to enhance flux pinning and increase current densities (J_{c1}). The addition of Y₂BaCu₅ (Y211) was studied previously in (Y211/YBCO)_N multilayer structures, and in Y211+YBCO films deposited from pie-shaped targets. This paper systematically studies the effect of Y211 addition in thin films deposited by pulsed laser deposition from YBCO_{1-x}Y_{211_x} ($x = 0-20$ vol%) single targets, at temperatures of $775-840^\circ\text{C}$. Interestingly, the resulting size of Y211 particles is 20-40 nm, in contrast to 10-15 nm in previous studies, and the number density is reduced. A slight increase of $J_{c1}(H,T)$ was achieved. Results and comparisons of flux pinning, intrinsic stresses, current densities, critical temperatures, and microstructures will be presented.

(EMA-S12-P030-2013) Experimental investigation of the edge barrier pinning effect of bridged superconducting thin films

L. Brunke*, University of Dayton Research Institute, USA; W. Jones, M. Mullins, University of Dayton, USA; T. Haugan, Air Force Research Laboratory, USA

Recent combined theoretical investigation and experimental evidence suggests that edge-barrier pinning is an intrinsic mechanism that can alter the critical current density (J_c) in bridged superconducting films. However; the experimental evidence for bridge widths < 10 microns has been limited thus far, because of the difficulties of making 1-2 micron size bridges without edge damage, de-oxygenation, or burning out upon going normal. In this study, a large number of samples of varying bridge width from 1-100 micron size were measured and compared, with careful focus on 1-2 micron bridges. Films of YBa₂Cu₃O_{7-x} (YBCO) were deposited by evaporation method and by pulsed laser deposition also with nanosize BaZrO₃ or Y₂BaCuO₅ additions, to compare different microstructures and effects of flux pinning. Several sets of YBCO films were coated with 300 nm thick layer of Au to increase quench protection. The bridges were made by photolithography and focused ion beam (FIB) etching. Systematic experimental studies and analysis of varying bridge-widths will be presented.

(EMA-S12-P031-2013) Search for superconductivity in doped carbon thin films

B. Pierce*, WPAFB, USA; J. L. Burke, L. B. Brunke, C. R. Ebbing, UDRI, USA; D. C. Vier, UCSD, USA; T. J. Haugan, WPAFB, USA

There have been significant studies to induce superconductivity and increase transition temperatures (T_c) in the different allotropes of carbon. Doping of diamond films with boron = 0.5–5 Vol% achieved T_c up to 7K, and superconductivity was achieved in Cs₃C₆₀ 'buckyballs' with a maximum T_c of 38K under pressure. However, so far $T_c > 20K$ has not been measured in any form of carbon, which is needed for wire applications. Herein we attempt to achieve a high T_c measured resistively in amorphous carbon, diamond-like carbon(DLC), graphite thin films, and carbon fiber films doped with promising elements including Boron, Phosphorus, and Sulfur. Carbon films were prepared by pulsed laser deposition (PLD) with doped or un-doped single-element targets. Graphite films were created from graphite rods and DLC was deposited on Pyrex through CVD to form the crystalline structure. Ion implantation was also used to add gaseous dopants very difficult to incorporate by PLD. Ion implantation energies and dosing times were varied to achieve different doping depths and profiles. Initial results with P implantation show a dramatic decrease of resistivity by a factor of 10^5 at $T < 50K$, with the carbon film changing from semi-conducting to metallic. There is some evidence of bulk superconductivity in a small volume fraction, as detected by microwave absorption methods. Further investigation must be done with graphite, DLC, and dopants.

(EMA-S13-P024-2013) Effect of Nucleation time on Bending Response of Ionic Polymer-Metal Composites Actuators

S. Kim*, KAIST, Republic of Korea; S. Hong, Argonne National Laboratory, USA; G. Ahn, Y. Choi, Y. Kim, C. Oh, K. No, KAIST, Republic of Korea

Ionic polymer metal composites (IPMCs) are electro-active polymers (EAPs) that show the electromechanical transduction. IPMCs are promising materials as soft actuators in many applications because IPMCs in hydrated state show relatively large displacement under small electric voltage (<5V). The conventional metal electrode of IPMCs is noble metal such as platinum and gold. Because noble metal is expensive, the non-noble metal such as copper and nickel could be substituted for noble metal. Furthermore, the autocatalytic electroless plating of nickel could reduce the processing time less than 14 hrs as compared with the conventional processing time (more than 48hrs). Depending on the fabrication condition such as time, temperature and concentration, the bending response may differ. The bending response depends on not only the electrode properties but also the morphology of interfacial area between the electrode and polymer layer because the interfacial morphology affects capacitance of IPMCs. Among many fabrication conditions, nucleation time effect on the bending response of IPMCs did not investigated. Therefore, we investigated how nucleation time of nickel electro-less plating have influence on the electrode properties, interfacial morphology and bending response of IPMC.

(EMA-S14-P019-2013) Fabrication and characterization of metal - insulator - graphene (MIG) tunnel junctions

M. Amani*, M. L. Chin, B. M. Nichols, T. P. O'Regan, A. G. Birdwell, F. J. Crowne, M. Dubey, Army Research Laboratory, USA

Due to its extremely high carrier mobility and ballistic electron conduction, graphene has attracted significant interest for next generation, high-speed electronics. However, there has been difficulty in fabricating many types of devices since pristine single layer graphene has a band gap of zero, and bi-layer or nano-ribbon material, where a small band gap (typically less than 0.25 eV) can be opened, have significantly degraded carrier mobilities. On the other hand, graphene is very well suited as an electrode material for ultra-high frequency tunneling electronic devices. Graphene has previously been shown to have a work function which can be electrostatically adjusted by as much as 0.5 eV. In this research, we fabricate tunable metal-insulator-graphene (MIG) tunnel junctions, and compare the electrical characteristics with our macroscopic model. The MIG tunnel junctions are

fabricated utilizing CVD-grown graphene on SiO₂ with Al₂O₃ or HfO₂ insulator layers deposited via ALD on top of the graphene. Varying top metal contacts were reviewed and characterized. The quality of the transferred graphene was followed by Raman spectroscopy and AFM, and the electrical properties of these devices were characterized by I-V and C-V curves mapped as a function of the back-gated bias.

(EMA-S14-P025-2013) Decay Mechanisms in Doped Silicon Nanocrystals

E. Albuquerque*, U. L. Fulco, L. R. da Silva, Universidade Federal do Rio Grande do Norte, Brazil

Doped Si nanocrystals (NCs) have been synthesized and investigated by means of photoluminescence and electron spin resonance measurements. In the case of p-type doped NCs, absorption in the infrared region was observed, accompanied by quenching of the exciton photoluminescence. Simultaneous n- and p-type doping was also probed to provide further control on the photoluminescence properties of the Si NCs. These interesting findings opened up new opportunities to circumvent the drawbacks of pure Si NCs, with exciting potential applications. In view of that, we propose here a three-state model to explain the decay mechanisms of doped Si NCs modeled as nearly spherical, whose set up consists of one atom surrounded by its nearest neighbors forming a tetrahedral geometrical structure. We calculate the transition rates between conduction to valence band decay process, taking into account an impurity-intermediated decay. Our theoretical model is based on the first-principles density-functional calculations to evaluate the NCs electron states, and on the Fermi's golden rule to determine the transition rates. Although previous works have shown that the most probable position of the impurity is on the surface, we also investigate the role of the impurity position in the radiative transitions.

(EMA-S14-P026-2013) Structural and Electronic Properties of Cubic Barium Stannate

U. L. Fulco, E. Albuquerque*, Universidade Federal do Rio Grande do Norte, Brazil

Alkaline earth stannates A₂SnO₃ (A = Ca, Sr and Ba) are important materials for the electronic industry, mainly due to the easy modifications of their electric properties by the selection of an adequate cation, generating a variety of interesting magnetic, ferroelectric, metallic, semiconducting and superconducting properties. In particular, Barium stannate (BaSnO₃) has found increasing applications in materials technology as a constituent in perovskite solid solutions with complex compositions, been used in optical applications as capacitors, in ceramic boundary layers, and as a promising material to produce gas phase sensors for the detection of carbon monoxide and dioxide. In this work, the electronic band structure, density of states, dielectric function, optical absorption, and infrared spectrum of cubic BaSnO₃ were simulated using density functional theory, within both the local density (LDA) and generalized gradient (GGA) approximations. Dielectric optical permittivities and polarizabilities were also estimated, as well as its indirect band gaps. The effective masses of electrons and holes were computed by parabolic fittings along different directions at the conduction band minimum and valence band maximum, being anisotropic for both electrons and holes. Finally, its vibrational normal modes and the infrared spectrum were obtained and assigned.

(EMA-S16-P021-2013) Structural changes in Lead Zirconate Titanate due to High Neutron Radiation Exposure

A. J. Henriques*, J. S. Forrester, S. B. Seshadri, University of Florida, USA; D. Brown, Los Alamos National Laboratories, USA; J. T. Graham, S. Landsberger, University of Texas - Austin, USA; J. F. Ihlefeld, G. L. Brennecke, Sandia National Laboratories, USA; J. L. Jones, University of Florida, USA

Piezoelectric materials can be used as sensors in high radiation environments. However, such use requires knowledge of the struc-

tural response in the material to radiation exposure. The present work evaluates the change in the structure of a variety of technologically significant lead zirconate titanate (PZT) compositions. PZT based materials of the following three compositions were investigated: (1) undoped, (2) Fe-doped, and (3) Nb-doped PZT. Samples of all three compositions were synthesized using solid state processing. Laboratory X-ray diffraction was used to determine the initial phase purity of the materials. Half of all the samples were irradiated in a TRIGA reactor to a 1 MeV equivalent neutron fluence of $1.7 \times 10^{15} \text{ cm}^{-2}$ relative to the control group. After irradiation, neutron diffraction from the SMARTS diffractometer was used to analyze the crystal structures of each sample using Rietveld refinement. This approach allowed quantitative assessment of point defect concentrations. It was found that undoped and Fe-doped samples were phase pure tetragonal, whereas the Nb-doped samples were a mixture of tetragonal and rhombohedral phases. Most importantly, in each composition the unit cell expanded and the atomic positions and occupancies measurably changed with irradiation.

(EMA-S16-P022-2013) A low-loss voltage actuated switch using metal-polymer nanocomposite

D. Drew*, Virginia Polytechnic Institute and State University, USA; A. Wang, F. Niroui, V. Bulovic, J. Lang, Massachusetts Institute of Technology, USA

The electronics industry faces a serious challenge as it attempts to decrease transistor size following Moore's law; the extremely high energy usage per bit of information manipulated has already placed practical limits on device design and currently stands as the one of the largest obstacles towards further miniaturization of electronics. A zero-leakage switch on the nano-scale would help to decrease the amount of energy lost per cycle as we escape from basic transistor physics in an effort to continue device scaling into the foreseeable future. This research focuses on a voltage actuated switch created using a polymer, PDMS, highly doped with nickel microparticles in order to make it piezoresistive. Previous work in this area saw issues with poor particle dispersion, high necessary strain, and low levels of repeatability. These problems were remedied via surface functionalization of the nickel with a methoxysilane, refined device design and fabrication techniques, and optimization of material proportions in the composite. The results show an overall positive outlook for the future of this approach in creating a nano-scale low loss switch.

(EMA-S16-P023-2013) Phase equilibria, crystallographic structure, and piezoelectric properties of tetragonal $\text{Pb}(1-1.5x)\text{Sm}x\text{Zr}(1-y)\text{Ti}y\text{O}_3$

M. M. Nolan*, S. B. Seshadri, University of Florida, USA; B. Bregadiolli, Universidade de São Paulo, Brazil; J. S. Forrester, D. Lynch, J. L. Jones, University of Florida, USA

Samarium-doped lead zirconate titanate (PZT) is of fundamental interest as it shows an uncharacteristic relaxation in its piezoelectric coefficient at a frequency of 0.1 Hz and has high temperature longitudinal piezoelectric coefficient values that are roughly twice as large as those exhibited by La- and Nb-doped PZT. It is also of commercial importance in SAW devices and hydrophone applications. In this work, a phase diagram of tetragonal Sm-doped PZT was developed. Solubility of Sm in PZT was found to increase with the fraction of the B-site occupied by Ti. Close to the morphotropic phase boundary, the solubility of Sm was found to be 4 mol%, whereas the solubility of Sm in lead titanate was found to be 8 mol%. For practical applications, lead titanate based materials are almost always used with Mn-doping to decrease conductivity and facilitate poling of the material. It was found that the solubility of Sm in Mn-doped lead titanate is 15%. Structural analysis was carried on high resolution neutron diffraction patterns using the Rietveld refinement method, and it was determined that Sm substitutes for the A-site in lead titanate. The behavior of the longitudinal piezoelectric coefficient as a function of frequency and field amplitude is discussed.

Thursday, January 24, 2013

Plenary Session II

Room: Indian

8:30 AM

(EMA-PI-002-2013) Complexity at Work: Nanoionic Memristive Switches (Invited)

R. Waser*, I. Valov, Forschungszentrum Jülich, Germany; E. Linn, RWTH Aachen University, Germany; S. Menzel, R. Dittmann, Forschungszentrum Jülich, Germany

A potential leap beyond the limits of Flash (with respect to write speed, write energies) and DRAM (with respect to scalability, retention times) emerges from nanoionic redox-based switching effects encountered in metal oxides (ReRAM). A range of systems exist in which highly complex ionic transport and redox reactions on the nanoscale provide the essential mechanisms for memristive switching. One class relies on mobile cations which are easily created by electrochemical oxidation of the corresponding electrode metal, transported in the insulating layer, and reduced at the inert counter-electrode (so-called electrochemical metallization memories, ECM, also called CBRAM). Another important class operates through the migration of anions, typically oxygen ions, towards the anode, and the reduction of the cation valences in the cation sublattice locally providing metallic or semiconducting phases (so-called valence change memories, VCM). The electrochemical nature of these memristive effects triggers a bipolar memory operation. In yet another class, the thermochemical effects dominate over the electrochemical effects in metal oxides (so-called thermochemical memories, TCM) which leads to a unipolar switching as known from the phase-change memories. In all systems, the defect structure turned out to be crucial for the switching process. The presentation will cover fundamental principles in terms of microscopic processes, switching kinetics and retention times, and device reliability of bipolar ReRAM variants. Passive memory arrays of ReRAM cells open up the paths towards ultradense and 3-D stackable memory and logic gate arrays. The selector issue of passive memories will be described, emphasizing complementary resistive switches as a potential solution. Despite exciting results obtained in recent years, several challenges have to be met before these physical effects can be turned into a reliable industrial technology.

S1: Functional and Multifunctional Electroceramics

Piezoelectric and Pb-free Piezoelectric Materials, Devices and Applications I

Room: Coral B

Session Chairs: Yu Wang, Michigan Tech; Juergen Roedel, TU Darmstadt

10:00 AM

(EMA-S1-011-2013) Structure and Properties of BNT-based Lead-free Piezoceramics (Invited)

J. Roedel*, W. Jo, TU Darmstadt, Germany

The structures of the non-ergodic relaxors BNT-BT and BNT-BKT will be contrasted to the structures of the ergodic relaxors BNT-BT-KNN and BNT-BKT-KNN and related to salient electrical properties. For structural investigations, in-situ field-dependent synchrotron and electron diffraction has been applied as well as TEM studies. Phase transitions have been characterized with determinations of permittivity (as well as piezoelectric coefficient) as function of both electric field and temperature. Further, thermally stimulated depolarization currents have been determined as function of temperature and electric field. These properties are aug-

mented by standard determinations of temperature dependent polarization and strain. Further, quenching studies from critical temperatures in BNT-BT afford observations of changes in permittivity. It is suggested that in BNT-based materials two types of polar nanoregions are responsible for the observed structure and properties. This knowledge affords tailoring of improved materials for lead-free piezoceramics as well as for high-temperature dielectrics. Materials can be envisaged as ergodic relaxors, nonergodic relaxors or as relaxor/ferroelectric composites. In the spirit of the symposium, this study necessitated collaboration with experts in numerous fields. All contributors and papers will be cited during the presentation.

10:30 AM

(EMA-S1-012-2013) Ferroelectric Property of (Li,Na,K)NbO₃ Piezoceramics on the Basis of Grain Size

K. Kakimoto*, R. Kaneko, I. Kagomiya, Nagoya Institute of Technology, Japan

Alkali niobate ceramics based on solid solutions in the NaNbO₃-KNbO₃ (NKN) pseudo-binary system have been regarded as leading candidates for lead-free piezoelectric ceramics in which a high Curie temperature and excellent piezoelectric properties can be expected. However, owing to the difficulty in sintering them, the literature on the grain-size-related properties of NKN-series ceramics has remained essentially insufficient to date, although this is a crucial subject for the further improvement of piezoelectric properties. In this study, a model experiment on the grain-size-related ferroelectric properties of lead-free Li_{0.04}(Na_{0.50}K_{0.50})_{0.96}NbO₃ piezoelectric ceramics has been carried out. Firstly, the size classification of calcined powders was achieved by a wet-type centrifugal separation technique to obtain size-classified powders with different mean particle sizes. Then, spark plasma sintering (SPS) was performed for the size-classified powder sources to synthesize dense ceramics and control their mean grain sizes so that they ranged from 500 nm to approximately 5 μm. The results clearly allowed the distinguishing of different dielectric and ferroelectric properties on the basis of grain size. By increasing the grain size from 0.5 to 2.8 μm, the remanent polarization *P_r* gradually increases from 4.2 to 16.8 μC/cm², while the coercive field *E_c* tends to increase with decreasing grain size.

10:45 AM

(EMA-S1-013-2013) Domain wall motion and electric-field-induced strains in NBT-xBT solid solutions from in situ neutron diffraction

T. Usher*, J. S. Forrester, E. Aksel, University of Florida, USA; A. Studer, Australian Nuclear Science and Technology Organisation, Australia; J. L. Jones, University of Florida, USA

Ferroelectric materials based on Na_{0.5}Bi_{0.5}TiO₃ (NBT) are the focus of much current research; in particular, the solid solution between NBT and BaTiO₃ (BT) is widely studied. This system has a morphotropic phase boundary (MPB) near 6-7 at% BT at which compositions exhibit improved piezoelectric properties. The current work investigates the response of three prototypical compositions (NBT-4BT, NBT-6BT, and NBT-13BT) to electric fields using in situ neutron diffraction. Diffraction patterns were recorded during application of incrementally increased static electric fields to investigate lattice strain and domain switching. Additionally, stroboscopic data were recorded during bipolar subcoercive (weak) electric fields at 1 Hz to compare to weak-field property coefficients. The MPB composition (NBT-6BT) exhibited the lowest coercive field and transformed to a two-phase rhombohedral and tetragonal structure after electric field application. The degree of domain switching in each of the rhombohedral and tetragonal phases was higher than that in the single phase compositions (NBT-4BT and NBT-13BT). It has been previously hypothesized that mixed-phase materials (e.g., co-existing rhombohedral and tetragonal phases) should allow for greater degrees of domain wall motion than single phase materials. The present work demonstrates experimental evidence of this concept.

11:00 AM

(EMA-S1-014-2013) The effect of tantalum dopant on ferroelectric fatigue behavior of lead-free ferroelectric potassium-sodium niobate

S. Pojprapai*, C. Uthaisar, Suranaree University of Technology, Thailand

Currently, lead-free piezoelectric ceramics have been investigated to replace lead-contained piezoelectric ceramics such as PZT. In this work, the effect of tantalum dopant on electrical fatigue behavior of potassium-sodium niobate ceramic (K_{0.50}Na_{0.46}Li_{0.04})(Nb_{0.96-x}Sb_{0.04}Ta_x)O₃, where x = 0, 0.04, 0.08, and 0.12, (NKN-LST) was studied. It was found that the ceramic showed a single phase of tetragonal at Ta = 0% while the mix phase between tetragonal and orthorhombic at Ta greater than 0.04%. The composition which Ta = 0.12% exhibited greater piezoelectric properties compared to other compositions. The electrical fatigue behavior of different Ta ratios is represented by the change of hysteresis loops. The change of microstructure before and after fatigue test is detected by SEM and X-ray diffraction technique. Moreover, the piezoelectric constant, permittivity, quality factors of ceramics before and after the test are reported.

11:15 AM

(EMA-S1-015-2013) Investigation of NaF doped NKN based lead-free ceramics at different sintering atmosphere

C. Liu*, The Pennsylvania State University, USA; P. Liu, Shaanxi Normal University, China; K. Kobayashi, C. A. Randall, The Pennsylvania State University, USA

Perovskite type (Na,K)NbO₃ (NKN) system, as a good candidate for lead-free piezoelectric applications, has attracted a large amount of attention due to its good characteristics. However, pure NKN ceramics are difficult to be densified by normal sintering due to the high volatility of alkaline elements at high sintering temperature. In addition, base-metal cofired multilayer structured piezoelectrics are desired due to the lower cost of base-metal inner-electrode than that of the noble-metals like platinum or silver/palladium. In this study, NaF doped Ta-modified NKN ceramics are prepared via traditional solid state reaction route. The specimens are sintered in air and low-pO₂ atmosphere, respectively. Compared with pure NKN ceramics, the piezoelectric properties of the air-fired samples are improved, showing a "soft" piezoelectric behavior with higher dielectric permittivity and good moisture resistance. The dielectric loss of the low-pO₂ fired samples is not increased compared with that of the air-fired specimens. Rayleigh method is adopted for analyzing the relative domain motion of the NaF doped specimens. It turns out that the extrinsic mechanism contributes to the improved piezoelectric properties. All these results suggest that NaF-doped NKN based lead-free ceramics are promising for practical piezoelectric applications.

11:30 AM

(EMA-S1-016-2013) Computational Study of Microstructure and Property Relations in Ferroelectric Polycrystals (Invited)

Y. U. Wang*, J. Zhou, Michigan Tech, USA

Effects of crystallographic texture, grain shape and template volume fraction on piezoelectric properties of ferroelectric polycrystals are investigated by phase field modeling. Domain evolutions and hysteresis loops are simulated. Piezoelectric properties are studied as functions of texture, grain shape and template volume fraction. It is found that grain shape plays a minor role, crystallographic texture significantly improves the piezoelectric properties, while a higher volume fraction of templates tends to erode away the advantage of texturing. Templated grain growth and texture development in ferroelectric polycrystals are also simulated to investigate the effects of template seed volume fraction and sizes on final grain structures and textures. It is found that reducing template size and shortening seed distance is an effective way to achieve higher texture at lower template volume fraction, desired for property improvement. The findings help optimize the design and processing of textured ferroelectric polycrystals.

12:00 PM

(EMA-S1-017-2013) Crystal Structure of (Li,Na,K)NbO₃ Lead-free Piezoelectric Ceramics

T. Nishi*, K. Kakimoto, I. Kagomiya, Graduate School of Eng., Dept. Mater. Sci. & Eng., Nagoya Institute of Technology, Japan

(Na,K)NbO₃-based solid solutions are considered to be an attractive lead-free piezoelectric ceramics because of their good piezoelectric properties and high Curie temperature (TC). Li-substituted (Na,K)NbO₃ solid solution (LNKN) has better piezoelectric properties and higher TC than NKN. In particular, it has been well known the TC shifted linearly toward higher temperature with increasing Li mole ratio. However, there have been only a few detailed reports on the fine crystal structure of LNKN ceramics. In order to obtain a better understanding for the structure of LNKN ceramics, high-resolution synchrotron x-ray powder diffraction was carried out using the BL-4B in the Photon Factory of the High Energy Accelerator Research Organization (PF-KEK), Tukuba, Japan. The local fine structure of LNKN ceramics has been studied by means of Nb-K edge EXAFS at the BL-12C in the PF-KEK. It was found that the crystal structure of LNKN ceramics was the mixed phase structure including monoclinic Pm phase. The proportion of the Pm phase in LNKN ceramics linearly increased with increasing the amount of Li content. On the other hand, the phase transition from orthorhombic Bmm2 to tetragonal P4mm drastically occurred when the Li content is 6 mol%.

12:15 PM

(EMA-S1-018-2013) Effect of tin content on electrical and piezoelectric properties of barium stannate titanate ceramics prepared from nanoparticles

K. C. Singh*, C. Jiten, R. Laishram, Sri Venkateswara College, India

Electrical and piezoelectric properties of Ba(Ti_{1-x}Sn_x)O₃ ceramics with x = 0.025, 0.045 and 0.065, prepared from 6-nm powders, were compared with those of the corresponding ceramics obtained from 86-nm powders to see the effect of tin content and particle size of the starting powders. Ba(Ti_{1-x}Sn_x)O₃ powders were synthesized by solid state reaction of BaCO₃, TiO₂ and SnO₂ at 1050°C. The powders were high-energy ball milled to produce 6-nm powders. The powders were sintered at 1350°C for 4h to yield ceramics. X-ray diffraction studies showed single phase perovskite structure of all the ceramics. For these ceramics, an increase in Sn content from x = 0.025 to 0.065 produces a decrease in (i) remnant polarization P_r from 3.1μC/cm² to 0.3μC/cm², (ii) coercive field E_c from 2.5kV/cm to 0.8kV/cm, (iii) unipolar strain level s from 0.084% to 0.027%, and (iv) electro-mechanical coupling factor k_p from 33.6% to 19.3%. However, the bulk density and piezoelectric charge constant d₃₃ exhibit an increase from 5.03g/cm³ to 5.84g/cm³ and 7pC/N to 110pC/N respectively, with increasing Sn content. Despite the general role of tin in degrading the ferroelectricity in the ceramics, the present study reveals a cooperative mechanism involving both the starting particle size of 6nm and optimum tin content which results in the observed enhancement of d₃₃ with tin content.

S2: Multiferroic Materials and Multilayer Ferroic Heterostructures: Properties and Applications

Theory and Modeling

Room: Coral A

Session Chair: Melanie Cole, U.S. Army Research Laboratory

10:00 AM

(EMA-S2-008-2013) Ab initio design of ferroic materials with advanced functionalities: 2D ferroelectricity and Goldstone-like modes in perovskite-oxide layers (Invited)

S. Nakhmanson*, Argonne National Laboratory, USA

With the help of first-principles-based computational techniques, we study and predict advanced electroactive behavior in layered-perovskite compounds of Ruddlesden-Popper (RP) type. Specifically, we show that Goldstone-like states (collective, close to zero frequency excitations, requiring practically no consumption of energy) can be induced in a -SrO-TiO₂-PbO-TiO₂-SrO- RP superlattice, manifesting themselves as “easy” rotations of the in-plane polarization vector. We connect the presence of such unusual excitations to the basic properties of the constitutive PbO, SrO and TiO₂ atomic planes, and the evolution of these properties as the planes are stacked together to form a crystal. Lone electron pair activity of the Pb²⁺ sites and bracing action of the SrO planes are found to be paramount for the emergence of the Goldstone-like states, while the RP structure, in principle, is not. We also examine a fictitious Ba₂TiO₄ RP compound, showing that, unlike better cation-size balanced Ca- or Sr-based structures, it exhibits a assortment of incommensurate distortions, including ones that induce in-plane polarization. A competition between various distortion trends can be influenced by an application of epitaxial strain.

10:30 AM

(EMA-S2-009-2013) Computational Navigation Through the ABO₃ Chemical Space (Invited)

R. Ramprasad*, G. Pilania, V. Sharma, G. Rossetti, S. Alpay, University of Connecticut, USA

The concept of rationally designing materials with novel properties through the effective use of computational methods and complementary experiments is an appealing notion, and forms the core of the recent U. S. White House Materials Genome Initiative. This paradigm for studying the materials and property space has the potential to mitigate the costs, risks and time involved in an Edisonian approach to the preparation and testing of potentially useful materials, and could yield valuable insights into the fundamental factors underlying materials behavior. In keeping with this philosophy, in this present effort, we seek to accomplish a comprehensive search of the chemical space occupied by perovskite-like complex oxides with chemical formula ABO₃. At this time, attention is restricted only to the unary perovskite compounds with A and B being any of 65 metallic elements of the Periodic Table. The stability of each compound occurring in this vast chemical space has been determined; the properties of the stable compounds have been computed, and interesting chemistry-structure-property correlations have been established. In a parallel direction, for the specific case of BaTiO₃, 65 metallic dopants at the A and B sites have been considered, and once again, stability-property maps have been established. It is expected that such an investigation could lead to the discovery of new compounds with attractive properties.

11:00 AM

(EMA-S2-010-2013) Charged Domain Walls in Proper and Improper Ferroelectrics (Invited)

A. K. Tagantsev*, Swiss Federal Institute of Technology, EPFL, Switzerland

A ferroelectric domain wall can carry net bound charge depending on its orientation with respect to the direction of polarization in adja-

cent domains. Many features of such walls, called charged walls, can substantially differ from those of walls which carry no bound charge. An essential feature of this kind of walls in proper ferroelectrics is that, practically, these can exist only when their bound charge is nearly fully screened by free carriers. Presence of charged domain walls in a material can essentially affect its dielectric, ferroelectric, and piezoelectric properties. This presentation gives an outlook on the current understanding of properties of these objects, as well as on the impact of charged domain walls on macroscopic properties of materials.

11:30 AM

(EMA-S2-011-2013) Caloric effects in ferroelectric alloys from atomistic simulations (Invited)

I. Ponomareva*, S. Lisenkov, University of South Florida, USA

As the need for efficient energy converting devices has been rapidly increasing, the materials that exhibit large or even giant caloric responses have emerged as promising candidates for solid-state refrigeration which is an energy-efficient and environmentally friendly alternative to the conventional refrigeration technology. However, despite recent ground breaking discoveries of giant caloric responses in some materials they appear to remain one of nature's rarities. Here we use first-principles-based simulations to study electrocaloric and elastocaloric effects in $\text{Ba}_{0.5}\text{Sr}_{0.5}\text{TiO}_3$ alloys. Our computational data reveal the intrinsic features of such caloric effects in ferroelectrics with multiple ferroelectric transitions and their potential to exhibit giant caloric effects. Some of the findings include the coexistence of negative and positive electrocaloric effects in one material and an unusual field-driven transition between them as well as the coexistence of multiple giant caloric effects in $\text{Ba}_{0.5}\text{Sr}_{0.5}\text{TiO}_3$ alloys. These findings could potentially lead to new paradigms for cooling devices.

12:00 PM

(EMA-S2-012-2013) Phase Field Modeling of Multicomponent Multiferroic Composites

Y. M. Jin*, F. Ma, Y. U. Wang, S. L. Kampe, Michigan Technological University, USA; S. Dong, Peking University, China

Phase field modeling is developed to investigate the relationships between microstructures and properties in multicomponent multiferroic composite materials. Multiple physical processes are considered, including elastic, electric and magnetic phenomena. For magnetoelectric composites, the domain mechanisms for coupling of ferromagnetic and ferroelectric order parameters are studied, and the effects of coherency strain and electric conductivity are investigated. For ferroelectric ceramic-reinforced metal-matrix composites, the energy dissipation mechanisms for mechanical damping capabilities by ferroelastic domain wall motion, ferroelectric polarization switching and electric current Joule heating are studied. For structural metal matrix composites reinforced by phase transforming ferroic inclusions, strain-induced crack arresting and self-healing behaviors are considered. The simulation results provide quantitative insights into the microstructure, property and mechanism relationships and help design multicomponent multiferroic composites with improved properties.

S3: Structure of Emerging Perovskite Oxides: Bridging Length Scales and Unifying Experiment and Theory

Session 3

Room: Pacific

Session Chair: Jacob Jones, University of Florida

10:00 AM

(EMA-S3-014-2013) Relaxor Characteristics of $\text{Bi}(\text{Zn}_{1/2}\text{Ti}_{1/2})\text{O}_3$ -based High-Strain Materials

N. Kumar*, D. Cann, E. Patterson, T. Ansell, Oregon State University, USA

Recently, a number of material systems have been shown to exhibit large electromechanical strains under large electric fields (typically greater than 50 kV/cm). This presentation will highlight recent findings on large electromechanical strains observed in a family of compounds based on binary and ternary compositions in the system $\text{Bi}(\text{Zn}_{1/2}\text{Ti}_{1/2})\text{O}_3$ - $(\text{Bi}_{1/2}\text{Na}_{1/2})\text{TiO}_3$ - $(\text{Bi}_{1/2}\text{K}_{1/2})\text{TiO}_3$. The effective piezoelectric d_{33}^* values in these compositions are typically greater than 500 pm/V. These compositions show very little remanence in the polarization versus electric field data and negligible low field d_{33} . From the wealth of data on $(\text{Bi}_{1/2}\text{Na}_{1/2})\text{TiO}_3$ - $(\text{Bi}_{1/2}\text{K}_{1/2})\text{TiO}_3$ it is clear that in these complex solid solutions, there are multiple perovskite phases with different crystallographic distortions all within a close range of free energy. This presentation will highlight the evolution of relaxor behavior for compositions with varying amounts of BZT. At low concentrations of BZT, these materials behave very much like a conventional ferroelectric, with well-saturated loops with high remanent polarization ($P_r \sim 35 \mu\text{C}/\text{cm}^2$). As the BZT content is increased, the dielectric behavior displays characteristics of relaxor behavior. Polarization hysteresis data at elevated temperatures and a thermal hysteresis in the dielectric maximum are evidence for a relaxor to ferroelectric transition.

10:15 AM

(EMA-S3-015-2013) Manipulation of the relaxor behaviour of BNT-BT ceramics due to Zr addition

J. Glaum*, The University of New South Wales, Australia; M. Acosta, TU Darmstadt, Germany; H. Simons, M. Hoffman, The University of New South Wales, Australia

In the search for lead-free functional ceramics the system bismuth-sodium-titanate-barium-titanate (BNT-xBT) gained considerable interest, as it is not a pure ferroelectric material, but exhibits characteristics of a relaxor. It has been shown that the piezoelectric properties of BNT-BT-based materials strongly depend on temperature. Exceptionally high strains can be achieved around the transition temperature between the ferroelectric and the relaxor state. Depending on composition the transition temperature for BNT-BT ceramics is found around 80°C. This study investigates the influence of Zr-addition to the system BNT-6BT. Zr is supposed to enhance the relaxor characteristics of BNT-BT, as the system barium-zirconate-titanate is known to show relaxor characteristics by itself already. The temperature dependency of polarization, strain and permittivity was measured to determine the ferroelectric to relaxor transition temperature. With increasing Zr content, the characteristic pinching of the polarization loops is found at lower temperatures. Additionally, the expected increase in permittivity and strain appears closer to room temperature. This indicates that Zr addition leads to a de-stabilization of the induced ferroelectric order, resulting in a lower transition temperature between ferroelectric and relaxor state and therefore stronger relaxor-like characteristics at lower temperatures.

S4: LEDs and Photovoltaics - Beyond the Light: Common Challenges and Opportunities

LEDs and Photovoltaics

Room: Mediterranean B/C

Session Chairs: Adam Scotch, OSRAM SYLVANIA; Erik Spoerke, Sandia National Laboratories

10:00 AM

(EMA-S4-001-2013) Possibilities for Smart Lighting and Smart Solar Integration (Invited)

M. H. Azzam, SolarOne Solutions, Inc., USA; R. F. Karlicek*, Rensselaer Polytechnic Institute, USA

The integration of energy efficient LEDs with solar panels for off-grid outdoor lighting applications is a natural marriage of green technologies with significant deployment advantages and energy savings relative to conventional grid-connected outdoor lighting. This is particularly true as cost reductions and performance advancements in LED fixtures, solar panels and energy storage technologies increasingly provide off-grid outdoor lighting solutions with an attractive value proposition when compared to conventional outdoor lighting solutions. Events like Hurricane Sandy, predicted to get more frequent over time, further highlight the benefits of grid-independent lighting solutions. There is an emerging focus on lighting, solar systems and energy storage with embedded intelligence. This includes new capabilities like mesh motion sensing, integrated power management for maximum on-time and battery life, integrated safety and light based signaling capabilities, management of lamp intensity for improved night time vision, and improved solar form factors for a wider range of lighting design possibilities. These up and coming features will make the combination of solid state lighting and solar energy for off-grid applications more attractive than ever. This talk will review the current state of off-grid lighting, emerging technology and market trends for smart systems integration, and describe some of the technology and market barriers that need to be overcome to make this technology combination a compelling option for outdoor lighting applications.

10:25 AM

(EMA-S4-002-2013) Thin Film PV Technologies: Present Status and Challenges (Invited)

C. Ferekides*, University of South Florida, USA

In recent years, the photovoltaics (PV) market has been growing at annual rates in the 35-40% range. Although Si-based PV remains the dominant technology with a market share on the order of approx. 85%, thin film PV has reached some astonishing milestones and it has emerged as a significant player in the PV market. CIGS solar cells have reached efficiencies of 20%, and CdTe modules have quickly become the lowest cost technology available. Despite these recent successes serious challenges remain as both industry and the scientific community continue to seek and develop solutions to further advance performance, improve reliability, and lower the manufacturing costs of thin film PV. The presentation will provide an overview of the two leading thin film PV materials - CIGS and CdTe - and will discuss key advantages and challenges for each material technology as well as the thin film PV area in general. Technology and product characteristics, industrial activity, field performance, cost, manufacturability, material and device issues are among the topics to be discussed.

10:50 AM

(EMA-S4-003-2013) ALD Sapphire, the Universal Substrate Technology for the Growth of Solid State Light Sources (Invited)

A. Melton, B. Kucukgoka, N. Lu, I. Ferguson*, University of North Carolina at Charlotte, USA

Solid state lighting using light emitting diodes has been promoted as the next generation lighting technology with potentials of large en-

ergy savings. This paper uses Si and ZnO substrates for GaN and InGaN growth by metalorganic chemical vapor deposition (MOCVD). Si is favored as a substrate for cost reasons and ZnO offers many advantages for GaN and InGaN due to its closely matched lattice constant. However, tensile stress between GaN and Si, a potential reaction between Si and Ga, H₂ etching of the ZnO substrate at high temperatures and Zn diffusion out of the substrate still cause many issues during MOCVD growth for these substrates. In this work a universal substrate technology has been created using Atomic Layer Deposited (ALD) Al₂O₃, was as the transition layer on these substrates before MOCVD growth.

11:15 AM

(EMA-S4-004-2013) Selective Growth of ZnCdTe Graded Nanostructures for Enhanced Performance of CdTe Solar Cells (Invited)

J. L. Cruz-Campa*, Sandia National Laboratories, USA; D. Zubia, B. Aguirre, University of Texas at El Paso, USA; X. Zhou, D. Ward, C. A. Sanchez, Sandia National Laboratories, USA; J. J. Chavez, R. Ordonez, University of Texas at El Paso, USA; A. Pimentel, Sandia National Laboratories, USA; F. Anwar, University of Texas at El Paso, USA; J. Michael, Sandia National Laboratories, USA; E. Gonzales, The Center for Integrated Nanotechnologies, USA; D. Marruffo, University of Texas at El Paso, USA; E. Spoerke, C. Calvin, P. Lu, Sandia National Laboratories, USA; H. Prieto, J. C. McClure, University of Texas at El Paso, USA; G. N. Nielson, Sandia National Laboratories, USA

II-VI semiconductors are very attractive for solar cell fabrication due to their direct bandgap, high absorption coefficient, and low manufacturing cost. One challenge with II-VI semiconductors is to form a defect-free p/n junction. CdS/CdTe heterojunctions form several defects at the interface due to the large lattice mismatch between CdS and CdTe. These defects act like traps to photo-generated carriers and diminish the overall performance of the solar cells. In this work, selective nucleation of graded Zn_xCd_{1-x}Te on patterned CdS substrates is used to avoid defect formation. By introducing Zn into the matrix, the lattice parameter difference is reduced and beneficial electric fields are created. With fewer defects present in the device, the current, voltage, fill factor, and efficiency will increase. CdS substrates were patterned with optical lithography, electron beam lithography and step and flash imprint lithography reversed tone. CdTe was subsequently grown using close space sublimation. SEM, FIB and EBSD showed positive CdTe selectivity on CdS patterned samples with fewer grains per window as the feature size is reduced to the nanometer regime. Preliminary JV measurements showed the feasibility of using micro-patterned CdS substrates for CdS/CdTe solar cell fabrication

11:40 AM

(EMA-S4-005-2013) Nanoscale Photovoltaic Performance Based on AFM Investigations of Microstructured CdTe Islands

Y. Kutes, University of Connecticut, USA; J. Cruz-Campa, Sandia National Laboratories, USA; J. Bosse, L. Ye, A. Merkouriou, University of Connecticut, USA; B. A. Aguirre, D. Zubia, University of Texas at El Paso, USA; E. D. Spoerke, Sandia National Laboratories, USA; B. D. Huey*, University of Connecticut, USA

Photovoltaics, solar cells, and LEDs are frequently micro- or nanostructured, either by design or due to manufacturing processes. Leveraging a combined conductive-AFM system and optical platform with a solar simulator light source, the open circuit potential, short circuit current, and intensity induced conductivity can all be assessed locally. Spatial resolution down to the nanoscale is demonstrated, for example with polycrystalline microstructured CdTe islands. Maps and statistical analyses of the results indicate that the photocurrent is clearly sensitive to optical illumination as expected, with subtle differences depending on the illumination spectrum. More significantly, however, is that the local photocurrent is strongly dependent on proximity to certain grains and grain boundaries. Such results can therefore inform the optimization of future PV, solar, and LED devices.

11:55 AM

(EMA-S4-006-2013) Oxide Semiconductors for photo-conversion technologies (Invited)

J. J. Berry*, P. F. Ndione, N. E. Widjonarko, A. K. Sigdel, P. A. Parilla, A. Zakutayev, J. D. Perkins, T. Genette, A. A. Dameron, D. C. Olson, D. S. Ginley, NREL, USA

The use of transparent conducting oxide materials is pervasive in photovoltaics and other optoelectronic devices. As the performance demands on these systems increase the use of more tailored and tunable semiconducting oxides in traditional device architectures is becoming more pervasive. Advances in material oxide fabrication, processing and design will be discussed in the context of their subsequent use in photo-conversion technologies. Specific cases of the use of traditional oxides such as ZnO and NiO will be compared and contrasted with more recently explored In-Zn-Sn and Ni-Zn-Co based oxides materials. Impact of the oxide selection on interfacial morphology, electronic properties and ultimate device performance will be presented for organic photovoltaics. Similar considerations for the use of oxides in other renewable technologies will also be discussed.

12:20 PM

(EMA-S4-007-2013) Low Temperature Solution Processing of Inorganic Nanoparticles for Contact Layers in Organic Photovoltaics (Invited)

Y. Lee*, D. Barrera, J. Wang, G. F. Gao, S. R. Cheng, University of Texas at Dallas, USA; S. R. Ferreira, Sandia National Laboratories, USA; R. J. Davis, GE Global Research Center, USA; J. W. Hsu, University of Texas at Dallas, USA

Organic photovoltaic (OPV) devices is a promising route for low cost solar energy conversion. Inorganic contact layers exhibit attractive properties such as tunable energy levels, mechanical strength, and environmental stability, and can improve OPV device efficiency and lifetime. However, high quality inorganic films typically require physical vapor deposition or high temperature annealing. Here, we describe ongoing work in our group on low temperature solution processing of nanoparticle (NP)-based thin films for contact layers in OPV devices. For example, we utilize a ZnO NP/sol-gel composite electron transport layer to significantly improve air stability of OPV devices, and explain this in terms of increased interfacial strength at the metal cathode. We also demonstrate microwave-assisted synthesis of stable suspensions of various metal oxide NPs. Modification of NP properties while in suspension allows us to separately optimize material property from device processing, leading to room temperature solution deposition of NP films with desired properties on organic layers without post-processing. The good performance of OPV devices using these nanoparticle films as contact layers is correlated to the improvement in film uniformity and desired work function. Applicability of low temperature solution processing of inorganic NPs to other areas will also be discussed.

12:45 PM

(EMA-S4-008-2013) Creating donor-acceptor interfaces for excitonic devices using nanoporous metal-organic frameworks (Invited)

M. D. Allendorf*, M. Foster, D. Gough, T. N. Lambert, K. Leong, S. Meek, E. Spörker, V. Stavila, B. Wong, Sandia National Laboratories, USA

Precise control of orientation and separation distance within donor-acceptor (DA) pairs is a critical aspect of improving the efficiency of excitonic devices such as OLEDs and organic photovoltaics. It is now clear that disorder at this interface, an inherent feature of bulk heterojunctions (BHJ), and within the surrounding environment is a major contributor to poor device performance. A considerable research effort is underway worldwide to minimize this, but controlling these factors is difficult and impedes rational design. We are using nanoporous Metal-Organic Frameworks (MOFs) as highly ordered templates for creating DA pairs. MOFs possess an exceptional degree of synthetic flexibility, allowing the effects of donor-acceptor orienta-

tion to be probed systematically. We will describe experiments and first-principles modeling of MOFs infiltrated with fullerenes and thiophenes, creating DA complexes that mimic molecular-scale phenomena in BHJ. The results provide insight into DA interactions involving the framework and guests, suggesting ways that MOFs could be used in devices that involve charge separation. We also show that MOFs can serve as active layers in OPV devices. The synthetic flexibility of the MOF not only facilitates incorporation of target D and A, but also enables rational, directed engineering of key device interfaces that influence power conversion efficiency.

S6: Thermoelectrics: Defect Chemistry, Doping and Nanoscale Effects**Applications and Non-Oxide Thermoelectrics**

Room: Pacific

Session Chair: Jon Ihlefeld, Sandia National Laboratories

10:30 AM

(EMA-S6-001-2013) Integration of Thermoelectric Materials at United Technologies Corporation (Invited)

S. Culp*, C. Lents, D. Jarmon, J. Turney, United Technologies Research Center, USA

Over the past several decades, considerable work has been conducted on the improvement of thermoelectric materials for power generation and cooling applications. In contrast, less attention has been given to resolving the challenges faced when integrating these materials into devices and systems while making them robust to the harsh environments that exist for many applications. Thermoelectric applications work at United Technologies Research Center combines physics-based, thermal, electrical, and structural modeling with experimental validation methods to identify and quantify key areas of parasitic losses within thermoelectric structures; directing research activities and enabling enhanced device performance through geometric optimization for a given TE materials system. These tools and methods have been applied to aerospace and terrestrial TE power generators where thermal stresses are large and environmental protection of the TE materials is critical, as well as, aerospace electronics cooling applications where high heat flux density and coefficient of performance (COP) are paramount. Many challenges for successful application of thermoelectric systems in harsh environments remain however, and UTC is developing the tools to identify and mitigate these challenges and enable rapid integration of advanced TE materials as they emerge.

11:00 AM

(EMA-S6-002-2013) Thermoelectric Properties of New High Temperature Material: $\text{Yb}_9\text{Mn}_{4+x}\text{Sb}_9$

S. Bux*, Jet Propulsion Laboratory/California Institute of Technology, USA; A. Zvelink, California Institute of Technology, USA; O. Janka, University of California Davis, USA; T. Vo, D. Uhl, Jet Propulsion Laboratory/California Institute of Technology, USA; J. Snyder, California Institute of Technology, USA; P. Von Allmen, Jet Propulsion Laboratory/California Institute of Technology, USA; S. Kauzlarich, University of California Davis, USA; J. Fleurial, Jet Propulsion Laboratory/California Institute of Technology, USA

High ZT values have been achieved in complex Zintl phases such as $\text{Yb}_{14}\text{MnSb}_{11}$. The high ZT in these materials is attributed to inherently low glass-like lattice thermal conductivity brought by structural complexity and unique covalent bonding. Since these materials possess small band gaps, the electronic properties can be tuned via structural modifications or by chemical substitutions. Although, many other complex Zintl crystal structures are known, the thermoelectric properties of these materials remain relatively unexplored. We present the high temperature thermoelectric properties of a new Zintl phase based upon Yb, Mn, and Sb: $\text{Yb}_9\text{Mn}_{4+x}\text{Sb}_9$ prepared by

mechanochemical synthesis of the elements. The lattice thermal conductivity of this new smaller crystal structure (44 atoms per unit cell versus 104 atoms per unit cell in $\text{Yb}_{14}\text{MnSb}_{11}$) structure is about 30% lower than that of $\text{Yb}_{14}\text{MnSb}_{11}$ at room temperature and approaches the glassy minimum value at high temperature. The combination of low lattice thermal conductivity and relatively high carrier concentration (10^{20}) leads to a maximum ZT of 0.8 at 1000 K.

11:15 AM

(EMA-S6-003-2013) Development of high-efficiency segmented thermoelectric couples

T. Caillat*, S. Firdosy, B. Li, C. H. Huang, V. Ravi, N. Keyawa, H. Anjunyan, J. Paik, J. Chase, L. Lara, J. Fleurial, Jet Propulsion Laboratory/Caltech, USA

Radioisotope Thermoelectric Generators have been successfully used to power spacecrafts for deep space missions. They have consistently demonstrated their extraordinary reliability and longevity (more than 30 years of life). NASA's Radioisotope Power Systems Technology Advancement Program is pursuing the development of more efficient thermoelectric technologies. Over the last few years, under the Advanced Thermoelectric Couples (ATEC) task, several advanced high-temperature thermoelectric materials, including n-type $\text{La}_3\text{-xTe}_4$, p-type $\text{Yb}_{14}\text{MnSb}_{11}$, and n- and p-type filled skutterudites, have been developed for integration into advanced power generation devices at the Jet Propulsion Laboratory (JPL). The stability of their thermoelectric properties has been demonstrated for over 10,000 hours up to 1323K. Suitable sublimation suppression barriers/coatings and stable skutterudite metallization have been successfully developed and validated. JPL is now focusing on developing segmented, long-lived couples based on these high-temperature materials. Test performance results have demonstrated 10 to 15% conversion efficiency values at beginning of life with couple cold- and hot-junction temperatures in the 423–473K and 973–1273K, respectively. A progress update is provided.

11:30 AM

(EMA-S6-004-2013) Spark Plasma Sintering for High Temperature Thermoelectrics

J. Mackey*, University of Akron, USA; A. Sehirlioglu, Case Western Reserve University, USA; F. Dynys, NASA Glenn Research Center, USA

High temperature thermoelectrics serve as a reliable electrical power source for NASA missions including the recent Curiosity, New Horizons, and Cassini probes. The Si/Ge based radioisotope thermoelectric generators (RTGs) convert the heat of a radioisotope core into kilowatts of useful electrical power. The development of next generation RTGs require improved materials designed to perform at temperatures up to 1000°C. Investigation into silicide systems has revealed several potential candidate materials suitable for novel device fabrication. Silicide systems such as $\text{WSi}_2\text{-Si}_{1-x}\text{Ge}_x$ are composed of elements in relatively high abundance and low toxicity. Nanoscale grains and precipitates in a thermoelectric matrix have been theoretically proven to reduce thermal conductivity by means of phonon scattering which works to decouple the thermal and electrical transport phenomena resulting in improved conversion efficiency. Nanoscale silicide precipitates have been introduced into a Si/Ge matrix through high energy mechanical alloying and spark plasma sintering. In an effort to advance the technology from material design to application, proof of concept devices composed of SPS derived silicide materials have been developed.

11:45 AM

(EMA-S6-005-2013) Thermoelectric chalcogenides: the case of chromium sulfides and selenides

A. Maignan*, E. Guilmeau, F. Gascoin, Y. Bréard, V. Hardy, LABORATOIRE CRISMAT / CNRS ENSICAEN, France

Among the metal-S binaries, the Cr-S one allows to go from semiconductor to metal behavior going from Cr-S to Cr_2S_3 . The physical properties of Cr_2S_3 and Cr_5S_6 ceramics, sintered by SPS, have been

investigated (1). By comparing with sulfides containing d0 cations, it is found that the magnetic scattering of the charge carriers is detrimental for the power factor values, $\text{PF}_{700\text{K}}=210\text{-}4\text{W}\cdot\text{m}^{-1}\cdot\text{K}^{-2}$ for Cr_5S_6 against $\text{PF}_{700\text{K}}=1.1\text{ }10^{-3}$ for $\text{Cu}_0.1\text{TiS}_2$. Nonetheless, the low PF values are not redhibitory: a very low thermal conductivity can be reached in layered selenides or sulfides based on Cr³⁺. ZT values reaching 0.8 at 700K have been reported for AgCrSe_2 (2) and CuCrS_2 (3). In the present contribution, a comparison between ceramics of sulfides and selenides will be given. A special attention will be paid to the layered materials offering a possible engineering of the phonons. (1) A. Maignan et al, Science and Technology of Advanced Materials (in press) (2) F. Gascoin and A. Maignan, Chemistry of Materials 23, 2150 (2011) (3) G.C. Tewari et al, arXiv:0901.0977

12:00 PM

(EMA-S6-006-2013) Thermoelectric materials for middle temperature application (Invited)

R. Funahashi*, National Institute of Advanced Industrial Science & Technology, Japan

The demand for primary energy in the world was 12,013 million tons of oil per year in 2007. The average total thermal efficiency of the systems utilizing this fuel is as low as 30%, with about 70% of the heat exhausted to the air as waste heat. It is clear that improving the efficiencies of these systems could have a significant impact on energy consumption. Thermoelectric conversion is attracting attention because it is the strongest candidate to generate electricity from dilute waste heat sources. A silicide material with a good n-type thermoelectric property has been discovered. This silicide possesses a composition of $\text{Mn}_{3-x}\text{Cr}_x\text{Si}_4\text{Al}_2$ ($0 < x < 0.7$) and hexagonal CrSi_2 structure. The absolute values of Seebeck coefficient and electrical resistivity increase by Cr substitution up to 573 K. The dimensionless thermoelectric figure of merit ZT reaches 0.3 at 573 K for a Cr substituted one with $x = 0.3$. Since oxide passive layer is formed around the surface, electrical resistivity measured at 873 K is constant for two days in air, which indicates good oxidation resistance in air of this material. A thermoelectric module consisting of 64 pairs of legs has been fabricated using $\text{MnSi}_{1.7}$ and non Cr substituted $\text{Mn}_x\text{Si}_4\text{Al}_2$ devices as p- and n-type legs, respectively. Output power reaches 9.4 W, which corresponds to 2.3 kW/m² of power density against surface area of the substrate, for a heat source temperature of 873 K in air.

S12: Recent Developments in High Temperature Superconductivity

Superconductor Applications I: High Field Magnet Development and Technologies

Room: Indian

Session Chair: Haiyan Wang, Texas A&M University

10:00 AM

(EMA-S12-012-2013) A round wire multifilament HTS conductor for high field magnet use – what stands in the way? (Invited)

D. Larbalestier*, NHMFL, USA

HTS coated conductors have generated more than 35 T (LTS can attain ~24 T). But HTS remain expensive, complex, and lack the flexibility of LTS conductors, which are flexible in design, size, filament count etc. and easily cabled. The two industrial conductors, $(\text{Bi,Pb})_2\text{Sr}_2\text{Ca}_2\text{Cu}_3\text{O}_{10-x}$ (Bi-2223) and $\text{REBa}_2\text{Cu}_3\text{O}_{7-x}$ (REBCO) are both high-aspect ratio tapes, Bi-2223 being multifilament and REBCO available only as single filament tapes that are hard to cable for magnets. Recently we have generated >30 T with $\text{Bi}_2\text{Sr}_2\text{CaCu}_2\text{O}_{8-x}$ (Bi-2212) in a round multifilament architecture at current densities that remove the J_c gap between REBCO and Bi-2212. What separates these different HTS is the behavior of their grain boundaries. At one extreme are in situ grown REBCO GBs where classical bicrystal studies on [001] tilt GBs clearly apply and at the other is Bi-2212 where high J_c is developed without macroscopic

texture but with strongly intertwined grains. Is it really impossible to generate less obstructive grain boundaries in REBCO and allow a multifilament round wire REBCO? The recent example of high J_c in fine-grain (Ba_{0.6}K_{0.4})Fe₂As₂ suggests that some pleasant surprises may await us. *Dmytro Abramov, Eric Hellstrom, Jianyi Jiang, Fumitake Kametani, Jan Jaroszynski, Peter Lee, Chiara Tarantini, Ulf Trociewitz, and Huub Weijers have all been vital to the development of this point of view.

10:30 AM

(EMA-S12-013-2013) Development of Accelerator Magnets Using Coated Conductors (Invited)

N. Amemiya*, H. Otake, K. Goda, T. Nakamura, Kyoto University, Japan; T. Ogitsu, KEK, Japan; K. Koyanagi, T. Kurusu, Toshiba Corporation, Japan; Y. Mori, Kyoto University, Japan; Y. Iwata, K. Noda, National Institute of Radiological Sciences, Japan; M. Yoshimoto, Japan Atomic Energy Agency, Japan

High T_c superconductors (HTSs) have various advantages over copper or low T_c superconductors (LTSs) for magnet applications: better cooling efficiency and, thus, less electricity consumption, when operated at higher temperature; tolerance against localized disturbances, which are critical in LTS magnets, when operated at high temperature; generating higher magnetic field than copper; generating very high magnetic field, which is not available by using LTS, when operated at 4.2 K. A project to develop the fundamental technologies for accelerator magnets using coated conductors is in progress in Japan. Its aim is to establish fundamental technologies for cryo-cooler-cooled accelerator magnets wound with coated conductors. Our target applications are carbon cancer therapy and accelerator-driven subcritical reactor (ADSR). Downsizing accelerator by increasing magnetic fields is attractive for the former, and reducing electricity consumption is attractive for the latter. First, the magnet designs which are compatible with the designs of accelerators for carbon cancer therapy and ADSR are presented. Second, development of winding technologies enabling designed magnets is reported. Third, experimental and numerical results on the influence of the magnetization of coated conductors on the field quality are reported.

11:00 AM

(EMA-S12-014-2013) Improvement Performance of MgB₂ and Nb₃Sn superconductors for MRI, NMR, Fault Current Limiters, and Wind Turbine Generators (Invited)

M. Tomic*, M. Rindfleisch, C. J. Thong, X. Peng, Hyper Tech, USA; M. Sumption, Ohio State University, USA

MgB₂ (4-30K) and Nb₃Sn (4-15K) superconductors have the potential to enable large conduction cooled superconducting magnets for several commercial applications. Greatly improved performance of MgB₂ superconductors has recently been demonstrated, J_e and J_c has more than doubled. The performance of Nb₃Sn superconductors in the last few years have more than doubled in performance at high magnetic fields. Conduction cooled MRI and NMR applications are being driven by the elimination of liquid helium bath cooling due to increase cost of liquid helium and predicted shortages. The market pull for fault current limiters is the desire to reduce fault currents which are increasing due to distributed energy and the aging grid. The development of 5MW and 10MW superconducting wind turbine generators enables the reduction of weight on the tower compared to scaling up conventional non-superconducting technology. These applications can now be enabled by the new performance levels demonstrated for MgB₂ and Nb₃Sn superconductors.

11:30 AM

(EMA-S12-015-2013) AC Loss Measurements on 2G High Temperature Superconducting Coils (Invited)

S. V. Pamidi*, J. Kvitkovic, J. Kim, C. Kim, Florida State University-Meteorology, USA

Second Generation High temperature Superconducting (2GHTS) tapes are now commercially available from multiple manufactures in

long enough lengths to fabricate medium size coils to understand coil fabrication, conductor insulation, AC losses, and heat transfer issues. AC losses are one of the outstanding challenges that need to be addressed to enable wide spread application of 2GHTS devices in electric power sector. Superconducting coils encounter AC transport current and/or AC magnetic field in rotating machinery applications. Total AC loss measurements involving simultaneous AC transport current and AC magnetic field on coils are difficult and hence little data is available on total AC losses in 2G superconducting coils. At Florida State University Center for Advanced Power Systems (FSU-CAPS), a couple of different techniques have been used to measure AC losses in superconducting coils. Several 2GHTS coils were fabricated and total AC loss measurements were carried out on them. The paper will present descriptions of the apparatus used and some experimental data on total AC losses in 2G superconducting coils. Implications of conductor insulation on potential coil degradation and thermal gradients will be addressed.

12:00 PM

(EMA-S12-016-2013) AC Losses of Multifilament Coated Conductors and Coils

G. A. Levin*, J. Murphy, T. Haugan, M. Mullins, P. Barnes, M. Majoros, M. Sumption, T. Collings, M. Polak, P. Mazola, J. Šouc, J. Kováč, P. Kováč, UES, Inc., USA

We will report the data on magnetization losses and critical current of experimental multifilament copper stabilized coated conductors. The AC losses were measured at different sweep rates of the magnetic field up to 14 T/s. Also, will be presented the design and operation protocols for a pair of calorimetric systems that measure the total power losses in small high temperature superconducting coils or wire. The basic calorimeter measures self-field losses, and an alternate version of the calorimeter is mounted in the stator environment of a generator/motor where a 0.6 Tesla alternating magnetic field is produced by an eighth pole rotor designed to provide frequencies up to 400 Hz. The systems allow samples to carry direct or alternating current with the ability to concurrently expose them to a variable frequency alternating magnetic field. The calorimetric technique used is based on the mass boil-off of liquid nitrogen.

S1: Functional and Multifunctional Electroceramics

Piezoelectric and Pb-free Piezoelectric Materials, Devices and Applications II

Room: Coral B

Session Chairs: Amar Bhalla; Derek Sinclair, University of Sheffield

2:00 PM

(EMA-S1-019-2013) The Defect Chemistry of ATiO₃ Perovskites by a combination of Atomistic Simulations and Experimentation (Invited)

J. Dawson, C. Freeman, M. Li, L. Ben, J. Harding, D. Sinclair*, University of Sheffield, United Kingdom

Here we focus on the influence of chemical doping and non-stoichiometry in two important ferroelectric perovskites (BaTiO₃ and Na_{1/2}Bi_{1/2}TiO₃) and demonstrate the dramatic role played by the A-site cations in defining their electrical properties. In the case of BaTiO₃, the experimental results will be verified by atomistic simulations using a recently updated potential set. The simulations offer an exciting tool for analysing local strain effects and provide the opportunity to observe the small, sometimes subtle, local alterations that occur in the BaTiO₃ lattice. In particular we will discuss: - i) why does A-site Ca-doping of BaTiO₃ result in an increase in T_c ; ii) the influence of Rare Earth, RE₃₊, size on the doping mechanism in BaTiO₃; iii) the influence of A-site RE (or so-called donor) doping on the conduction properties and variation in T_c (comment will be made regarding the implication of these results for preparation of commercial

positive temperature coefficient of resistance (ptcr) thermistors); iv) the remarkable influence of the Na:Bi ratio on the conduction properties of Na_{1/2}Bi_{1/2}TiO₃. Finally, we will comment on the influence of A-site vacancies in controlling the conduction properties of ATiO₃ perovskites.

2:30 PM

(EMA-S1-020-2013) Relaxor characteristics of the phase transformation in (1-x)BaTiO₃ - xBi(Zn_{1/2}Ti_{1/2})O₃ perovskite ceramics

N. Triamnak*, Oregon State University, USA; R. Yimnirun, Suranaree University of Technology, Thailand; D. P. Cann, Oregon State University, USA

The single phase solid solutions of the (1-x)BaTiO₃-(x)Bi(Zn_{1/2}Ti_{1/2})O₃ (BT-BZT) where x = 0.02-0.15 were prepared in order to investigate dielectric properties. Crystal structure of samples was obtained by using an x-ray diffraction technique. For compositions x ≤ 0.08, the solid solutions exhibited tetragonal symmetry and transitioned to pseudo-cubic symmetry as the content of BZT increased. The composition x = 0.08 is believed to be the morphotropic phase boundary (MPB) of this material which was confirmed by measurement of the dielectric properties as a function of temperature. The dielectric response exhibited a sharp phase transition within the BT-rich region and the composition 0.92BT-0.08BZT was characterized by the onset of relaxor characteristics. As the concentration of BZT increased, the phase transition exhibited broader and more diffuse behavior. The polarization as a function of electric field (P-E) of these solid solutions also exhibited the same trend. The BT-rich compositions showed a normal ferroelectric P-E response with a decrease in loop area as the BZT content increased. The composition at x = 0.08 exhibited a pinched hysteresis loop occurred and with further increase in BZT content, the P-E response was characterized by slim loops.

2:45 PM

(EMA-S1-021-2013) Design of high energy density (Bi_{0.2}Ba_{0.8})(Zn_{0.1}Ti_{0.9})O₃-based relaxor capacitors

H. J. Brown-Shaklee*, M. A. Blea, G. L. Brennecke, Sandia National Laboratories, USA

Reduction of permittivity with increased electric field is a phenomenon known as voltage tuning and limits the energy density that many commercial ceramic capacitors can achieve. Here, we compare the voltage tuning behavior of (Bi_{0.2}Ba_{0.8})(Zn_{0.1}Ti_{0.9})O₃ (BZT-BT) relaxors to that of traditional commercial capacitor dielectrics. The BZT-BT dielectrics maintained high permittivities (k>1000) at fields greater than 150 kv/cm in contrast to BST dielectrics that fell to k~600 at half the field. This combination of high permittivity and breakdown strength resulted in energy densities of >1.4 J/cm³ and makes the BZT-BT family of dielectrics attractive for high-energy multilayer capacitors. The properties of 200 nF BZT-BT multilayer capacitors designed to withstand >500 volts will be discussed. This work was supported through the Energy Storage Program managed by Dr. Imre Gyuk of the Department of Energy's Office of Electricity Delivery and Energy Reliability. Sandia National Laboratories is a multi-program laboratory managed and operated by Sandia Corporation, a wholly owned subsidiary of Lockheed Martin Corporation, for the U.S. Department of Energy's National Nuclear Security Administration under contract DE-AC04-94AL85000.

3:00 PM

(EMA-S1-022-2013) Synthesis and High-Temperature Electrical Properties of Bismuth Layer-Structured Oxide (Invited)

R. Aoyagi*, T. Kitahara, M. Maeda, T. Yokota, Nagoya Institute of Technology, Japan

Bismuth layer-structured oxides (BLSO) have been studied as high-T_C ferroelectric and piezoelectric materials. BLSO have the general formula (Bi₂O₂)²⁺-(A_{m-1}B_mO_{3m+1})²⁻, in which pseudo-perovskite (A_{m-1}B_mO_{3m+1})²⁻ layers are interleaved with (Bi₂O₂)²⁺ layers, where m is the

number of BO₆ octahedra in the pseudo-perovskite layers. Generally, Bi₄Ti₃O₁₂-type BLSO shows high dielectric loss at high-temperature due to high conductivity. This is because BLSO generate a lot of Bi deficient during sintering process. So it is difficult to use BLSO as high-temperature piezoelectric devices. In this study, we have focused BLSO as a thermoelectric material because they have high conductivity at high temperature and Bi-based materials show low thermal conductivity. In this work, we explored Bi₄Ti₃O₁₂-nA³⁺B³⁺O₃ (n=1-2) ceramics such as Bi₄Ti₃O₁₂-nBiFeO₃, Bi₄Ti₃O₁₂-nBiMnO₃, etc. The ceramic samples were synthesized by a conventional solid state reaction. The resistivity of the samples was determined from the current-voltage relationship at various temperatures up to 350 °C. Additionally, temperature dependences of the thermoelectric properties, Seebeck coefficient and electrical conductivity, are characterized from 650 K to 1100 K. Bi₄Ti₃O₁₂-BiFeO₃ and Bi₄Ti₃O₁₂-2BiFeO₃ showed high Seebeck coefficient of >500 μV/K at 900 K.

3:15 PM

(EMA-S1-023-2013) Effect of Non-Stoichiometry on Electronic Properties of BaTiO₃ - Bi(Zn_{1/2}Ti_{1/2})O₃ Ceramics

N. Raengthon*, Oregon State University, USA; H. J. Brown-Shaklee, G. L. Brennecke, Sandia National Laboratories, USA; D. P. Cann, Oregon State University, USA

Perovskite materials have been known to be utilized in many emerging technologies such as capacitors and piezoelectric devices. Such applications require a high insulation resistance because in many cases the device is required to operate under extreme conditions such as high electric field or high temperature. By controlling the stoichiometry of materials, the electronic properties and especially the conductivity can be altered which can lead to highly resistive or highly conductive materials. In this study, BaTiO₃ - Bi(Zn_{1/2}Ti_{1/2})O₃ ceramics were selected to investigate the effects of non-stoichiometry on the perovskite A-site and B-site on the dielectric properties and conduction mechanisms. It was found that the excess positive charge (donor-like doping) induced via cation non-stoichiometry on the A- and/or B-site significantly improved the resistivity of the materials especially at high temperature as well as altered their dielectric properties. A more detailed discussion of the relevant defect chemistry of these materials will be presented. This study will help advance the understanding of the role of non-stoichiometry in perovskite materials.

3:30 PM

(EMA-S1-047-2013) Breaking of macroscopic centric symmetry in ceramics: implications for flexoelectric effect (Invited)

D. Damjanovic*, A. Biancoli, Swiss Federal Institute of Technology - EPFL, Switzerland

We report on observation of breaking of macroscopic centric symmetry in a number of non-poled ferroelectric ceramics and in paraelectric phase of ferroelectric ceramics. Both pyroelectric and direct piezoelectric responses have been measured in macroscopic polycrystalline samples that have never been subjected to an electric field. The obtained signal is comparable in magnitude to what was recently reported in the literature for flexoelectric response in similar materials. Materials we investigated include ceramics of BaTiO₃, (Sr_{1-x}Bax)TiO₃, PZT, (Ba,Ca)(Zr,Ti)O₃, and single crystal and ceramics of SrTiO₃. A detailed account of these observations will be given and implications discussed.

4:00 PM

(EMA-S1-024-2013) Multifunctionality of Ferroics and Multiferroics (Invited)

A. Bhalla*, USA

Emergent functionality is a hallmark of a sensing ferroic material where as the Multiple functionality signifies its cross-response properties for different external fields. The field of multifunctional and novel composites at scales from macro to nanoscale is growing rapidly for designing of novel multifunctional sensors for a variety of ap-

plications such as; structural health and human health monitoring, energy harvesting techniques and designing novel electronic meta-materials. There are several questions and near term future research challenges, for example: how to obtain giant, direct and cross response for dielectric, magnetoelectric and various other properties? How to enhance and exploit nonlinear response through stoichiometric changes or through engineering interfaces and domains? Can the microscopic and mesoscopic modeling be sufficiently predictive and agile to guide synthesis and characterization on the fly, i.e. can we succeed in "materials co-design"? Finally, what can we learn from essentially an optimal design in biology to mimic it in multifunctional materials? This paper will present: (1) A brief overview of the multifunctional materials and the current status, (2) To provide description and perspectives of the important emerging applications. (3) Some specific examples for designing composites with specific properties, Non-Lead multiferroics and Bio composites.

4:30 PM

(EMA-S1-025-2013) Influence of (Li,Ce,Pr) Ions doped on the Piezoelectric Properties of CaBi₂Nb₂O₉ Ceramics

J. Zhu*, S. Bao, Z. Peng, D. Liu, D. Xiao, Sichuan University, China

CaBi₂Nb₂O₉ piezoceramics with (Li,Ce,Pr) multidoped were synthesized by the conventional solid state reaction method. The crystal structure was determined by the X-ray diffraction. Temperature dependence of dielectric constant revealed that the Curie-temperature of CBN-based ceramics was slightly influenced by the dopants contents and the TC points were above ~930 centigrade degree for all compositions. The piezoelectric coefficient (d₃₃) were found to be about 13.0pC/N for Ca_{0.92}(LiCe_{0.5}Pr_{0.5})_{0.04}Nb₂O₉, nearly twice larger than that of pure CBN ceramics (~6.0pC/N). The thermally depoling behaviors were also studied indicating that (Li,Ce,Pr) modified CBN ceramics were a promising candidate for ultra-high temperature piezoelectric applications.

4:45 PM

(EMA-S1-026-2013) Large piezoelectricity and dielectric permittivity in a phase coexisting ceramic

Y. Yao, Y. Yang, X. Ren*, Xi'an Jiaotong University, China

Quasi-quadruple point, a point where four phases (Cubic-Tetragonal-Orthorhombic-Rhombohedral) nearly coexist together in the temperature-composition phase diagram was found in Sn doped BaTiO₃. At this point, dielectric permittivity reaches ~75000, a 6~7 fold increase compared with that of pure BaTiO₃ at its Curie point; the piezoelectric coefficient d₃₃ reaches 697pC/N, 5-times higher than that of pure BaTiO₃. Clearly, phase coexisting is playing an important role to enhance the properties.

5:00 PM

(EMA-S1-027-2013) Effect of Heating Rate and Ramp-Up Temperature on Microwave Dielectric Properties of Ba₂Ti₉O₂₀ Ceramics

G. B. Pokale*, S. P. Butee, S. S. Bashaihah, K. Raju, College of Engineering Pune, India

Polycrystalline Barium Nonatitanate (Ba₂Ti₉O₂₀) ceramic samples were prepared by solid state reaction followed by sintering between 1200°C – 1300°C (in air) for 2h with heating rate varying from 2 to 6°C/min and ramp up temperature increasing from 900°C to 1100°C. The highest sintered density of 94.6 %TD was obtained for the samples sintered at 1240°C- 2h with 6°C/min heating rate and ramp-up temperature of 900°C. The XRD patterns of all the sintered samples revealed Ba₂Ti₉O₂₀ structure (*Cry. Str.: Monoclinic, Sp. gp.: P2_{1/m}*) as the major phase and TiO₂, BaTi₅O₁₁ and BaTi₄O₉ as the minor phases. Microwave measurements conducted on the sintered samples revealed a progressive rise in the resonant frequency from ~ 9 to 14 GHz, increase in the unloaded quality factor (Q_uf) from 18635 GHz to 32600 GHz and a marginal increase in dielectric constant (ε_r') from 32.6 to 35.2 for the increase in heating rate from 2°C/min to

6°C/min. The best dielectric properties of ε_r' = 35.2 and Q_uf = 32600 GHz were obtained for the sample sintered at 1240°C-2h (heating rate = 6°C/min, ramp up temperature = 1000°C) which showed a marginally lower sintered density of 94.3% TD. When the ramp-up temperature was increased from 900°C to 1100°C, an improvement by almost 5 % in the quality factor at 1000°C was noted as against the one noted at 900°C, which subsequently got reduced by 6% for 1100°C. The observed rise in ε_r' and Q_uf for 1000°C ramp up temperature was mostly attributed to the lowering in content of secondary phases, fairly uniform and well developed grains and a good sintered density.

5:15 PM

(EMA-S1-028-2013) Structure, vibrational spectroscopy and luminescence of LaSbO₄ ceramics prepared by solid-state reaction method

K. Siqueira, R. Borges, J. Soares, A. Dias*, UFOP, Brazil

This work investigates the thermal evolution of LaSbO₄ ceramics produced by solid-state method in the temperature range 700-1500°C, for 6 h. Besides the expected phase transitions, a thermal decomposition at high temperatures to La₃SbO₇ was observed and discussed. The results showed that the phase LaSbO₄ is formed only below 1450°C, while temperatures lower than 1100°C are not able to produce crystalline structures. The samples were submitted to X-ray diffraction and Raman scattering measurements aiming to determine the crystal structures. The LaSbO₄ sample exhibited monoclinic structure, space group P2₁/c (#14), with Z=4. It was verified that all the 36 Raman-active modes predicted by group-theory calculations were observed. Also, the symmetries could be discerned by using polarized Raman scattering, which allow us to assign the gerade modes. The luminescence properties of LaSbO₄ were investigated and the results showed that this compound exhibits sensitivity of the host lattice to UV excitation. The PL spectra excited at 360 nm have a blue emission band maximum at 428 nm, corresponding to the self-activated luminescence center of LaSbO₄.

S2: Multiferroic Materials and Multilayer Ferroic Heterostructures: Properties and Applications

Advanced Materials Synthesis and Characterization I

Room: Coral A

Session Chair: Melanie Cole, U.S. Army Research Laboratory

2:00 PM

(EMA-S2-013-2013) Multiferroic (ferroelectric/ferromagnetic) behaviour of Bi₇Ti₃Fe_{2,1}Mn_{0,9}O₂₁ Aurivillius Phase Thin Films (Invited)

L. Keeney, T. Maity, M. Schmidt, N. Deepak, S. Roy, A. Amann, M. E. Pemble, R. W. Whatmore*, Tyndall National Institute, Ireland

Room temperature multiferroic materials are interesting for various applications, e.g. spin-based memory/logic devices. Here we report Aurivillius-type (Av) layered materials showing ferroelectricity and ferromagnetism at room temperature. Others have reported ferroelectric / ferromagnetic behaviour in 4-layer (m=4) ceramics of Bi₇Ti₃Fe_{1-x}Co_xO₁₅ (x=0.5). However, we found that while thin films with x=0.3 were ferroelectric at room temperature, ferromagnetism originated from Fe-Co rich inclusions. To increase the concentration of magnetic cations, thin films of Bi₇Ti₃Fe_{2,1}Mn_{0,9}O₂₁ with m=6 were prepared by CSD on sapphire substrates. This work will report the structural, ferroelectric (PFM) and magnetic (SQUID magnetometry) properties of these films, which show ferroelectric and ferromagnetic behaviour at ambient temperature. Preliminary observations via simultaneous PFM and MFM experiments on magnetoelectric cross-coupling within the films will be presented. The results of a careful microstructural analysis of the materials will be

presented. No second phases were observed, and the use of statistical methods to place confidence bounds on the ferromagnetic properties being intrinsic to the main (Av) phase, and not due to an unwanted second phase, will be discussed. The support of SFI under the FORME SRC Award number 07/SRC/I1172 is gratefully acknowledged

2:30 PM

(EMA-S2-014-2013) Functionalized Chemical Assembly of Ferrite-Ferroelectric Nanoparticles by “Click” reaction (Invited)

G. Sreenivasulu, F. Chavez, G. Srinivasan*, Oakland University, USA

The ability to sense magnetic fields under ambient conditions could have many applications in information storage and medical imaging. Composite materials with piezoelectric and piezomagnetic phases have attracted considerable attention in this regard in recent years. In this work we have created ferromagnetic-ferroelectric nano-composite materials by coating nanoparticles with complementary coupling groups and allowing the materials to self-assemble. We employed barium titanate (BTO) (diameter = 50 nm) and nickel ferrite (NFO) (diameter = 10 nm) nanoparticles for the assemblies. In one strategy we have attached carboxylate groups bearing an alkyne functionality to BTO nanoparticles and attaching alkyl azide groups to NFO nanoparticles. Using the “click” reaction, the two groups condense into a triazole group linking the particles together. The distance between nanoparticles can be controlled by choosing the length of the organic linker. There are a variety of organic coupling reactions that can be used to effect this result. The results of this work confirm that the organic linkers have been attached to the nanoparticles and that the nanoparticles have been assembled into composites. The characterization of these composites will be described in this work.

2:45 PM

(EMA-S2-016-2013) New Spin Amplitude Modulation Driven Solid and Soft Composite Multiferroics

B. Rozic, Jozef Stefan Institute, Slovenia; M. Jagodic, Institute of Mathematics, Physics and Mechanics, Slovenia; S. Gyergyek, M. Drogenik, D. Arcon, Z. Kutnjak*, Jozef Stefan Institute, Slovenia

We report observation of a magnetoelectric effect in a new spin amplitude modulation driven multiferroic $\text{FeTe}_2\text{O}_5\text{Cl}$. The magnetic and ferroelectric properties of the layered geometrically frustrated cluster compound $\text{FeTe}_2\text{O}_5\text{Cl}$ were investigated with single-crystal neutron diffraction, NMR, and dielectric measurements. The magnetoelectric coupling is proposed to originate from the temperature dependent phase difference between neighboring amplitude modulation waves similar to $\text{FeTe}_2\text{O}_5\text{Br}$ [1,2]. The impact of large Cl/Br ions substitution on the magnetoelectric properties is discussed. Furthermore, magnetoelectric behavior in recently synthesized soft composite multiferroic mixtures of ferroelectric liquid crystals (LC) with magnetite magnetic nanoparticles (NPs) is reviewed. The impact of the electric field on the magnetization is confirmed via SQUID susceptometer proving the indirect magnetoelectric coupling between the NP magnetization and LC's polarization. [1] M. Pregelj et al., Phys. Rev. Lett. 103, 147202 (2009). [2] M. Pregelj et al., Phys. Rev. B vol. 86, 054402 (2012).

3:00 PM

(EMA-S2-017-2013) Janus-type Bi-phasic Multiferroic Nanofibers

J. S. Andrew*, J. D. Starr, M. Budi, University of Florida, USA

Multiferroic materials hold enormous potential for a variety of applications, including tunable microelectronics and multiphase memory. The development of novel complex oxide-based composite materials provides an opportunity to fabricate multiferroic materials with performance suitable for real-world applications. In composite multiferroics, the resultant magnetoelectric effect arises from coupling at the interface between a piezoelectric and a mag-

netostrictive phase. Therefore, it is desirable to assemble a composite such that the interfacial contact area between each phase is maximized for increased performance. Here, we present the first example of a composite nanostructured building block with a Janus-type morphology for multiferroic applications. This composite is composed piezoelectric BaTiO_3 and magnetostrictive CoFe_2O_4 in an architecture that simultaneously provides access to the bulk and surface properties of both phases. These Janus-type fibers combine the large contact area of a core-shell fiber with the segmented ordering of a thin film, and allow for the control of both composition and surface anisotropy, providing additional degrees of freedom in the design of composite materials. In this talk, we will present the effects of processing on the size, crystallinity and morphology of these novel composites. Results from magnetic, dielectric, and magnetoelectric measurements will also be presented.

3:15 PM

(EMA-S2-018-2013) Growth of Aurivillius phase $\text{Bi}_5\text{Ti}_3\text{FeO}_{15}$ thin films by Atomic Vapour Deposition

N. Deepak*, P. Zhang, L. Keeney, M. E. Pemble, R. W. Whatmore, Tyndall National Institute, Ireland

Multiferroic materials are highly desirable due their ability to convert an electric response into a magnetic response and vice-versa. However, room temperature multiferroics are rare. The layer-structure, Aurivillius ferroelectrics can accommodate various magnetic ions, opening the possibility of new room temperature multiferroics. In this study, single-phase highly *c*-axis oriented Aurivillius phase $\text{Bi}_5\text{Ti}_3\text{FeO}_{15}$ thin films were prepared by atomic vapour deposition on single crystal SrTiO_3 substrates in a layer-by-layer growth mode using $\text{Bi}(\text{thd})_3$, $\text{Ti}(\text{O-iPr})_2(\text{thd})_2$ and $\text{Fe}(\text{thd})_3$ precursors (thd = 2,2,6,6-tetramethyl-3,5-heptanedionate and O-iPr = iso-propoxide). The crystalline properties of films were characterized by XRD and TEM. The effect of the amount of titanium and iron precursors delivered to reactor was studied. It was found that the crystalline properties depend strongly on precursor injection volume and temperature, and it is possible to grow fractional-*n* Aurivillius phases by changing these parameters. The films' morphologies were characterized by atomic-force microscopy and scanning electron microscopy. The ferroelectric domain structure was characterized with piezo-force microscopy and strong in-plane polarization piezo-response was observed. The results of magnetic assessment of the films will be discussed.

4:00 PM

(EMA-S2-019-2013) Electrical properties of stoichiometric BiFeO_3 prepared by mechano-synthesis with either conventional or spark plasma sintering

A. Perejon, L. A. Perez-Maqueda, Instituto de Ciencia de Materiales de Sevilla, Spain; N. Maso*, A. R. West, The University of Sheffield, United Kingdom

Bismuth ferrite (BiFeO_3) is both ferroelectric and antiferromagnetic at room temperature but there is no consistency in reported values of its electrical conductivity; semiconducting ceramics with low electrical resistivity at room temperature are frequently obtained. In this presentation, we show the electrical properties of stoichiometric pure BiFeO_3 prepared by direct mechanochemical synthesis from pristine iron and bismuth oxides. Ceramics sintered by either conventional heating in air or spark plasma sintering (SPS) followed by oxidative anneal in air are highly insulating with conductivity e.g. $\sim 10^{-6} \text{ Scm}^{-1}$ at 300 °C and activation energy 1.15(2) eV, which are comparable to those of a good-quality BiFeO_3 single crystal. By contrast, the as-prepared SPS sample without the post-sinter anneal shows higher conductivity e.g. $\sim 10^{-6} \text{ Scm}^{-1}$ at 225 °C and lower activation energy 0.67(3) eV, indicating some reduction of the sample by the SPS process. Possible mechanisms for the origin of the low electrical resistivity reported for BiFeO_3 ceramics will be discussed.

4:15 PM

(EMA-S2-020-2013) Growth, structural and electrical characterization of heteroepitaxial multiferroic bismuth ferrite based thin films on Si (001) substrate

J. Kolte*, A. Daryapurkar, P. Gopalan, Indian Institute of Technology Bombay, India

Materials with a combination of ferroelectric, ferroelastic or ferromagnetic properties are called as multiferroic materials. BFO is a versatile material with various applications such as magnetoelectric sensor, actuator, magnetoelectric memory, optical, FeRAM and photovoltaic applications. BFO has large electric polarization making it a promising alternative to lead based memory devices. However for low cost and real device application one has to integrate BFO onto silicon structure. BFO reacts with Si and forms Iron silicide at the interface, so proper combination of buffer layers have selected. In this work, heteroepitaxial BFO thin films have been grown on Si (100) substrate by using CeO₂/YSZ buffer layers using pulsed laser deposition. An oxide electrode has been used as a bottom electrode. X-ray diffraction pattern with phi scan confirms the epitaxial nature of the film. Film has been characterized by AFM for surface study. Electrical characterization has been carried out to check reliability for memory application. Fatigue and retention tests confirm that films are almost fatigue free and can retain charge up to 10000 sec. Leakage current density does not deteriorate over prolonged use, thereby making BFO a preferred candidate for memory application.

4:30 PM

(EMA-S2-021-2013) Electrical properties of Ca-doped BiFeO₃ ceramics: from p-type semiconduction to oxide-ion conduction

N. Maso*, A. R. West, The University of Sheffield, United Kingdom

Bismuth ferrite (BiFeO₃) has attracted considerable attention in recent years since it exhibits both G-type antiferromagnetic order with a long-periodicity spiral below the Néel temperature (T_N) at ~640 K and ferroelectricity below the Curie temperature (T_C) at ~1100 K, which may allow fabrication of novel functional materials involving coupling between magnetic and electrical order. We show in this presentation that BiFeO₃ can also be either a good oxide ion conductor or a p-type semiconductor, depending on doping and oxygen partial pressure during processing and subsequent cooling. In particular, Bi_{1-x}Ca_xFeO_{3-(x/2)+δ} ceramics are mixed oxide ion/electron conductors at 800 °C, but the electron conduction can be suppressed in low oxygen partial pressure atmospheres; when sintered and cooled in N₂ from 800 °C, they are oxide ion conductors with activation energy ~0.82–1.04 eV and conductivity ~1x10⁻⁵ Scm⁻¹ at 300 °C, comparable to that of 8 mol% yttria-stabilised zirconia. When heated in O₂ at 125 bar, however, they are mainly p-type semiconductors with conductivity ~1x10⁻³–4x10⁻⁵ Scm⁻¹ at room temperature and activation energy ~0.27–0.40 eV. The oxygen stoichiometry varies over the range 0 < δ < ~0.016, depending on processing conditions. The semiconductivity is attributed to mixed valence Fe with < ~3.2% Fe⁴⁺.

4:45 PM

(EMA-S2-022-2013) Effects of Sr- and La-doping on the piezoelectric, dielectric and microstructural properties of PZT

V. Kalem*, Selcuk University, Turkey; M. Timuçin, Middle East Technical University, Turkey

The influences of Sr²⁺ and La³⁺ additions on microstructure, on phase constitution, and on the electrical properties of PZT were investigated in detail. Sr and La co-doped PZT based piezoelectric ceramics, designated as PSLZT, were fabricated by conventional processing techniques. X-ray diffractograms revealed that perovskite structure was completely formed in all PSLZT compositions and increasing Sr content increased the tetragonality. The results showed that a certain PSLZT composition having 5 at% Sr and 1 at% La ex-

hibited favorable properties; a peak piezoelectric strain coefficient of $d_{33} = 640$ pC/N with attending dielectric and electromechanical parameters $K = 1800$, $k_p = 0.56$, $Q_m = 70$, $\tan \delta = 1.55\%$ and $T_c = 272$ °C which make this system be a promising material for electromechanical applications where quick switching and high operation temperature are needed.

S6: Thermoelectrics: Defect Chemistry, Doping and Nanoscale Effects**Oxide Thermoelectrics I**

Room: Pacific

Session Chair: Sabah Bux, Jet Propulsion Laboratory/California Institute of Technology

2:00 PM

(EMA-S6-007-2013) Preparation of oxide-based thermoelectric materials with spark-plasma techniques (Invited)

Y. Grin*, Max-Planck-Institut für Chemische Physik fester Stoffe, Germany

Finding of fast, reproducible synthetic routes for production of new and known materials in the pre-specified shape is one of the key problems in the thermoelectric applications. Spark Plasma Sintering (SPS) - an advanced densification techniques developed in last decades - may offer a solution for this demand. Promising candidates for thermoelectric materials fulfilling in particular requirements of availability, low cost and low toxicity of constituting elements are oxides. The studies on oxide materials as potential thermoelectrics are continuously progressing. Synthesis and shaping of such materials may be achieved in one step by SPS techniques. From the chemical point of view, the titanium oxides have raised considerable interest in respect of thermoelectricity. As an example, spark-plasma technique has been successfully applied for one-step direct synthesis of titanium sesquioxide from mixture of titanium dioxide with titanium. The components react by diffusion through the grain boundaries forming locally several intermediate phases. The electrical and thermal transport properties of the SPS-prepared material reflect well the known transition from semiconductor-to-metal above 400 K. Advantages and challenges of the spark-plasma preparation of oxide materials are analyzed.

2:30 PM

(EMA-S6-008-2013) Defects and transport in thermoelectric calcium cobalt oxide

H. Fjeld*, M. Schrade, T. Norby, T. Finstad, University of Oslo, Norway

Misfit-layered calcium cobalt oxide - here denoted as $[\text{Ca}_2\text{CoO}_{3-\delta}]_x[\text{CoO}_2]$ - has been extensively studied the last ten years as a potential p-type thermoelectric oxide. The relevant papers show, however, an appreciable scatter in the reported thermoelectric properties for apparently similar samples. A possible reason might be oxygen non-stoichiometry δ and its influence on charge carrier concentration and mobility. In this study, δ , Seebeck coefficient α and electrical conductivity σ were determined under equilibrium conditions as a function of oxygen partial pressure $p\text{O}_2$ ($1 - 10^{-5}$ atm) and temperature (350 - 875 °C). From the thermogravimetric study, δ increased with decreasing $p\text{O}_2$ and increasing temperature, reaching 0.14 at 825 °C and $p\text{O}_2 = 0.01$ atm. From the transport measurements, α and σ were found to reversibly increase and decrease, respectively, with decreasing $p\text{O}_2$. These observations can be explained by a decreasing electron hole concentration resulting from the formation of positively charged oxygen vacancies. In this contribution we will discuss the defect chemistry and transport properties in $[\text{Ca}_2\text{CoO}_{3-\delta}]_x[\text{CoO}_2]$ by employing different models. In particular, the influence of the two different crystal subsystems, i.e. the rock salt and CoO_2 layers, will be addressed.

2:45 PM

(EMA-S6-009-2013) Transport Phenomena in CaMnO₃: A Combined Experimental and Modelling Approach

R. Freer*, F. Azough, University of Manchester, United Kingdom; S. Parker, M. Molinari, University of Bath, United Kingdom; E. Combe, R. Funahashi, National Institute of Advanced Industrial Science and Technology, Japan

CaMnO₃ is one of a range of oxides being investigated for high temperature thermoelectric applications. In order to improve material performance (by maximizing the thermoelectric Figure of Merit: Z) it is necessary to increase the Seebeck coefficient whilst reducing both thermal conductivity and electrical resistivity. One strategy is to utilise nanostructuring to reduce thermal conductivity and selective dopants to reduce electrical resistivity. We are employing a combination of experimental and modelling techniques to understand transport processes in CaMnO₃. A range of doped, calcium manganate ceramics have been prepared by solid state reaction methods; high density crack-free products have been achieved by slow cooling. As well as determining thermoelectric properties we are using high resolution TEM (SuperSTEM2) to define atom level structures. In parallel with the experimental work we are employing DFT and potential-based simulation methods to evaluate the effects of dopants, porosity and nanostructural features on thermal and electron transport to define the most effective strategies to enhance thermoelectric properties. We will calculate the transport coefficients using the BoltzTraP code but the first stage in the modelling has been to establish reliable models for the electronic and lattice structure using VASP and other codes.

3:00 PM

(EMA-S6-010-2013) Thermoelectric properties of hollandite materials (Invited)

S. Hebert*, H. Takahashi, N. Raghavendra, F. Gascoin, D. Pelloquin, A. Maignan, CRISMAT, France

Since the discovery of a large thermopower in the metallic Na_xCoO₂, different families of oxides have been investigated to find new thermoelectric oxides. So far, the best p type oxides belong to the family of Na_xCoO₂ or cobalt misfits, while the best n types are electron doped perovskites or transparent conducting oxides, with ZT reported to be close respectively to 1 (p type) and 0.4 (n type). For n type oxides, the transport properties can be described as for degenerate semi-conductors. On the contrary, for the p type oxides, the properties can generally not be described by standard Boltzmann theory, and it has been argued that the interesting thermoelectric properties can be explained by spin and orbital degeneracy effects. These unique properties seem to be related to the presence of cobalt in edge shared octahedra, leading to a specific filling of the t_{2g} orbitals. We will review here the results obtained in the case of two families of oxides, with the common parameter of edge shared octahedra : (1) layered compounds with CdI₂ type layers and different block layers, and (2) oxides with the hollandite structure. Also, to further enhance the ZT values (by decreasing the electrical resistivity), non oxide hollandite materials have been investigated. Their properties will be compared to the ones of the oxides.

4:00 PM

(EMA-S6-011-2013) Enhancement of Thermoelectric Properties of Ceramic Ca₃Co₄O_{9+δ} through Doping and Addition of Nano-inclusions

X. Song*, Y. Chen, M. Torres, D. Palacio, E. Barbero, West Virginia University, USA; E. L. Thomas, University of Dayton Research Institute / Air Force Research Laboratory-WPAFB, USA; P. N. Barnes, Army Research Laboratory, USA

We report the effect of impurity doping and nano-inclusion addition on the thermoelectric performance of ceramic Ca₃Co₄O_{9+δ}. Among the various dopants, it is found there is significant enhancement of the power factor of Ca₃Co₄O_{9+δ} through Yb doping. The

pellets were prepared by pressing under 0.5 GPa and 2 GPa. The highest power factor of 553 μWm⁻¹K⁻² due to the significant increase of electrical conductivity was obtained for Ca_{2.9}Yb_{0.1}Co₄O_{9+δ} pressed at 0.5 GPa. This is 2.3 times higher than that of Ca₃Co₄O_{9+δ} (246 μWm⁻¹K⁻²). Nanostructure examinations show that the pellets pressed at 0.5 and 2 GPa have different nano-lamella structures. This work suggests that Yb is an effective doping element for enhancing the electrical transport properties of Ca₃Co₄O_{9+δ}, and the optimum doping level is related to the nanostructure of the bulk pellets. Yb is found to be efficient in reducing the thermal conductivity. In order to further decrease the thermal conductivity, various nano-inclusions were added to ceramic Ca₃Co₄O_{9+δ}. The effect of nano-inclusions on the nanostructure and performance of Ca₃Co₄O_{9+δ} will be presented and discussed.

4:15 PM

(EMA-S6-012-2013) Atomic Scale Investigations of Interfacial Defect Structure in Thermoelectric Materials (Invited)

D. L. Medlin*, Sandia National Laboratories, USA

Interfaces strongly affect the thermal and electronic transport properties of thermoelectric materials. At present, however, the fundamental understanding of interfacial structure in thermoelectrics is in its infancy. Here, I will discuss our electron microscopic studies of the atomic structure of interfaces in telluride-based thermoelectric materials, considering both tetradymite structured materials, such as Bi₂Te₃, as well as heterophase interfaces between tetradymite and rock-salt structured tellurides, which have been investigated in the context of thermoelectric nanocomposites. A key theme throughout this work is to establish the underlying roles of interfacial line defects, such as dislocations and interfacial steps. I will begin with an analysis of low-angle grain boundaries in Bi₂Te₃, discussing the arrangement and core structure of the individual dislocations that accommodate small tilt misorientations in this material. Second, I will discuss the structure of high angle grain boundaries in Bi₂Te₃, considering in detail the (0001) basal twin and nature of defects at interfaces vicinal to this relatively simple and low energy interface. Finally, I will discuss the role of interfacial defects in controlling phase transformations and strain accommodation at tetradymite/rocksalt telluride interfaces.

4:45 PM

(EMA-S6-013-2013) Thermoelectric assessment of silicon nanowire networks

A. J. Lohn, University of California Santa Cruz, USA; E. Coleman, Structured Materials Industries, Inc., USA; K. J. Norris, University of California Santa Cruz, USA; N. Sbrockey, Structured Materials Industries, Inc., USA; G. S. Tompa*, N. P. Kobayashi, University of California Santa Cruz, USA

With materials altered at the nanometer-scale, the thermoelectric (TE) figure of merit has been pushed beyond 1. Such advanced TE devices, however, rely on expensive materials including uncommon semiconductors and toxic heavy metals, therefore abundant and environmentally friendly choices (e.g., silicon) are highly desired. In this study, TE devices based on "networks" of silicon nanowires (SNWs) were fabricated and tested. In our experiment, large area (~2 cm²) TE devices were fabricated with SNWs grown on steel and other metallic substrates eliminating the need for expensive semiconductor substrates. Although, a single SNW is one-dimensional by its nature, the network of SNWs provides a three-dimensional material platform through which electrical current travels while potentially offering large thermal resistance as a whole. The Seebeck coefficients were measured as a function of operation temperature. Temperature dependence of the Seebeck coefficient was found to be weak over the range of 20-80degrees C at approximately -400μV/K for the unintentionally doped devices and +50μV/K, and -50μV/K, for p-type and n-type devices, respectively, which is comparable to those of bulk silicon. However, to produce sufficient quantities of electrical power to achieve their promise of ubiquitous low-cost heat energy recovery, se-

ries electrical resistance must be greatly reduced to values near those made for bulk silicon processes.

S9: Thin Film Integration and Processing Science

Controlling Phase Assemblage and Stoichiometry I

Room: Mediterranean B/C

Session Chair: Jon-Paul Maria, North Carolina State University

2:00 PM

(EMA-S9-001-2013) Supra Crystals Consisting of Nano-Sized Perovskite Single Crystals in Cube Shape (Invited)

K. Kato*, National Institute of Advanced Industrial Science and Technology, Japan; K. Mimura, National Institute of Advanced Industrial Science and Technology, Japan; F. Dang, National Institute of Advanced Industrial Science and Technology, Japan; H. Imai, Keio University, Japan; S. Wada, University of Yamanashi, Japan; M. Osada, H. Haneda, National Institute for Materials Science, Japan; M. Kuwabara, Kyushu University, Japan

Bottom-up synthesis of electronic materials has attracted a great attention to lead innovation in the field of industrial technology. Nanometer-sized single crystals of BaTiO₃ and SrTiO₃ in cube shape were considered to be candidates as building blocks for dielectric devices. They were synthesized by the hydrothermal method using aqueous Ti complex and organic additives. Each 15 nm-sized single crystal had a cubic shape with sharp edges and high lattice coherence. The nanocubes were arranged into ordered structures by the capillary force assisted self-assembly method. In the BaTiO₃ nanocube assemblies, the ordered region was over a wide range in tens of micrometers. The nanocubes were attached each other in face to face so that the assembly was dense. The piezoresponse behavior was identified to be ferroelectric. In contrast, SrTiO₃ nanocube assemblies showed paraelectric linear relation, which was identical to the property of the constituent block. However, the mixture assemblies showed a distinguished behavior, which was a combination of non-linear and stepwise changes against the poling field. The results suggested that BaTiO₃/SrTiO₃ hetero-interfaces affected the dielectric properties. The grain and interface-designed structures consisting of cube-shaped dielectric building blocks have potentials to tune the properties and would be expected for future dielectric device applications.

2:30 PM

(EMA-S9-002-2013) Combinatorial thin film methodology for exploration of novel functional materials (Invited)

I. Takeuchi*, University of Maryland, USA

We have developed combinatorial thin film synthesis and characterization techniques in order to perform rapid survey of previously unexplored materials phase space in search of new inorganic functional materials. Various thin film deposition schemes including pulsed laser deposition, electron-beam deposition, and co-sputtering are implemented for fabricating massive arrays of compositionally varying samples on individual combinatorial libraries. A suite of high-throughput characterization tools are employed to screen the combinatorial libraries and map different physical properties of materials as a function of sweeping composition changes. They include room-temperature scanning SQUID microscopy, scanning MOKE system, micromachined MEMS device arrays, variable-temperature parallel 4-point probe set up, scanning microwave and other probe microscopy. Because mapping structural phase distribution across compositional phase diagrams is an integral part of materials exploration, we are developing analysis techniques where x-ray diffraction data from combinatorial libraries are rapidly separated using clustering methods and cross-referenced against existing entries in crystallographic databases. Recent examples of discoveries in multifunctional materials will be discussed.

3:00 PM

(EMA-S9-003-2013) Highly Textured (K,Na)NbO₃ Pb-free piezoelectric films prepared by sol-gel process

J. Li*, Q. Yu, Tsinghua University, China

Sodium potassium niobate (KNN) films have received increasing attention as KNN-based bulk materials have been extensively studied as a promising lead-free piezoelectric system. To develop high-performance KNN-based piezoelectric films by clarifying the crystallographic orientation dependence of electrical properties, sol-gel processed KNN-based thin films were fabricated on Nb-doped SrTiO₃ substrates with different crystallographic orientations through an alkoxide-based route. A peak remnant polarization value (Pr) of 17.3 $\mu\text{C}/\text{cm}^2$ was obtained along the [110] direction due to the coincidence between the spontaneous polarization and film orientation, which is significantly higher than 10.5 $\mu\text{C}/\text{cm}^2$ in [111]-oriented and 10.1 $\mu\text{C}/\text{cm}^2$ in [001]-oriented ones. However, a better piezoelectric response was achieved in the [001]-oriented films with an average local effective piezoelectric coefficient (d_{33}) of 50.5 pm/V, as compared with 45.1 pm/V and 39.7 pm/V in [110]- and [111]-oriented films, respectively. This work using highly textured films revealed the property and crystallographic orientation linkage in the KNN system, which should be also helpful for the development of textured KNN-based ceramics.

3:15 PM

(EMA-S9-004-2013) Bi-based Piezoelectric Thin Films via Chemical Solution Deposition

Y. Jeon, E. Patterson, Oregon State University, USA; P. Mardilovich, W. Stickle, Hewlett-Packard Corporation, USA; J. Ihlefeld, G. Brenneka, Sandia National Laboratories, USA; B. J. Gibbons*, Oregon State University, USA

Increased restrictions on the use of lead have resulted in a search for candidates to replace lead-based piezoelectric materials. One promising material is the solid solution of $(\text{Bi}_{0.5}\text{Na}_{0.5})\text{TiO}_3 - (\text{Bi}_{0.5}\text{K}_{0.5})\text{TiO}_3$ (BNT-BKT). Although good behavior has been observed in bulk materials, similar results have been elusive for thin films. Here, 0.8 BNT - 0.2 BKT thin films were synthesized on Pt/Si substrates via chemical solution deposition. Phase purity was confirmed by X-ray diffraction. Overdoping of Bi, K, and Na (addition of excess cation precursors) was introduced to compensate for volatilization during synthesis. Compositional analysis of films was performed with electron probe microanalysis and X-ray photoelectron spectroscopy. Data from both measurements indicated stoichiometric films were achieved. Dense, smooth, crack-free films were achieved with relative dielectric constants from 390 to 730 and low dielectric loss of 2 - 5% at 1 kHz. Maximum and remanent polarizations were 45 and 16 $\mu\text{C}/\text{cm}^2$ (200 Hz), respectively. The addition of $\text{Bi}(\text{Mg}_{0.5}\text{Ti}_{0.5})\text{O}_3$ (BMgT) was also explored. These films displayed very promising piezoelectric response with $d_{33,f}$ up to 90 pm/V and strain values of 0.35%. Sandia is a multiprogram laboratory operated by Sandia Corporation, a Lockheed Martin Company, for the United States Department of Energy's National Nuclear Security Administration under contract DE-AC04-94AL85000.

In Situ Characterization and Novel Processing

Room: Mediterranean B/C

Session Chair: Jon Ihlefeld, Sandia National Laboratories

4:00 PM

(EMA-S9-005-2013) Effects of Interfaces and Surfaces on Domain Structure and Properties in Ferroelectric Thin Films (Invited)

X. Pan*, The University of Michigan, USA

The ferroelectric switching occurs through the nucleation and growth of favorably oriented domains and is mediated by defects and interfaces. Dislocations, for example, are known to destroy ferroelectric order; neighboring grains and interfaces subject the fer-

roelectric to localized strain, electric fields, or the screening of electric fields. Thus, it is critical to understand how the ferroelectric domain forms, grows, and interacts with structural defects. This talk presents the atomic scale characterization of ferroelectric/electrode interfaces and domain walls in BiFeO₃ and PbZr_{0.2}Ti_{0.8}O₃ thin films using aberration-corrected transmission electron microscopy (TEM). Furthermore, we use in situ TEM techniques to follow the kinetics and dynamics of ferroelectric switching in real-time. We observed localized nucleation events at the electrode interface, domain wall pinning on point defects, the formation of ferroelectric domains localized to the ferroelectric/electrode interface, and domain wall pinning by dislocations. These results show how defects and interfaces impede full ferroelectric switching of a thin film.

4:30 PM

(EMA-S9-006-2013) In situ synchrotron X-ray diffraction based technique reveals the effect of adhesion layer on the texture of solution-derived PZT thin films

K. Nittala*, S. Mhin, J. L. Jones, University of Florida, USA; J. F. Ihlefeld, G. L. Brennecke, Sandia National Laboratories, USA

Initial crystallization events during thermal processing help to determine the final texture of solution-derived PZT thin films. To characterize nucleation and growth events during processing, an in situ measurement technique was used. In this technique, the high flux of the synchrotron X-ray sources and the area detector were combined to allow concurrent measurement of phase and texture of the thin films in times as low as 0.25 s. Continuous measurement of diffraction intensities during crystallization at fast heating rates allowed for tracking of the evolution of the perovskite phase. To identify the effect of the adhesion layer on the perovskite phase, PZT thin films were solution deposited onto platinumized silicon substrates with TiO_x or ZnO adhesion layers and crystallized at heating rates between 0.5°C/s - 70°C/s. In situ diffraction measurements performed during crystallization revealed different trends in the variation of final film texture with adhesion layer and these results are used to evaluate the existing mechanisms for texture selection in PZT thin films. Sandia National Laboratories is a multi-program laboratory managed and operated by Sandia Corporation, a wholly owned subsidiary of Lockheed Martin Corporation, for the U.S. Department of Energy's National Nuclear Security Administration under contract DE-AC04-94AL85000.

4:45 PM

(EMA-S9-007-2013) Flux-assisted growth of BaTiO₃ thin films

D. T. Harris*, M. Burch, P. G. Lamb, North Carolina State University, USA; J. F. Ihlefeld, Sandia National Laboratories, USA; E. C. Dickey, J. Maria, North Carolina State University, USA

In this presentation we demonstrate that by incorporating a low melting temperature flux into BaTiO₃ we can enhance grain growth, crystallization, and the nonlinear dielectric properties important for devices like ferroelectric varactors. BaTiO₃ films with BaO-B₂O₃ flux were grown on c-sapphire using PLD from ceramic target compositions containing between 1% and 5% of the borate-based flux. Films were prepared at room temperature, then annealed at temperatures above the flux melting temperature of 869 °C. TEM cross-section analysis, X-ray diffraction, and atomic force microscopy was used to verify grain size and to search for microstructural signatures resulting from flux incorporation. Average grain sizes of 0.3 μm were observed in samples grown with 3% flux, compared to < 0.1 μm for conventional material. Capacitance and polarization measurements reveal a dramatic enhancement of the nonlinear electromechanical response with flux incorporation, presumably associated with improved crystallinity and larger grain size. Capacitors with 3% flux exhibit 70% permittivity tuning at 35 V applied to a 3 μm gap with losses below 1%. Capacitance temperature measurements reveal a shift in the Currie temperature of 50

°C, in agreement with phenomenological theory and strain measurements. Current efforts are focused on incorporation of the flux through vapor phase and exploration of the applicability to epitaxial growth.

5:00 PM

(EMA-S9-008-2013) Carbon Nanotubes Integrated with Superconducting NbC (Invited)

G. Zou*, Soochow University, China; H. Luo, New Mexico State U., USA; Y. Zhang, Tsinghua U., China; T. McCleskey, L. Civale, Los Alamos National Lab, USA; Y. Zhu, North Carolina State U., USA; A. Burrell, Argon National Lab, USA; Q. Jia, Los Alamos National Lab, USA

The formation of carbon nanotube and superconductor composites makes it possible to produce new and/or improved functionalities that the individual material does not possess. In this talk, we will give a brief summary about carbon nanotubes integrated with superconducting niobium carbide (NbC) by a chemical solution process. Here, coating well-aligned carbon nanotubes with superconducting NbC does not destroy the microstructure of the nanotubes in two different ways. NbC also shows much improved superconducting properties such as a higher irreversibility and upper critical field. An upper critical field value of ~5 T at 4.2 K is much greater than the 1.7 T reported in the literature for pure bulk NbC. Furthermore, the aligned carbon nanotubes induce anisotropy in the upper critical field, with a higher upper critical field occurring when the magnetic field is parallel to the carbon nanotube growth direction. These results suggest that highly oriented carbon nanotubes embedded in superconducting NbC matrix can function as defects and effectively enhance the superconducting properties of the NbC.

S12: Recent Developments in High Temperature Superconductivity

New Superconductors and MgB₂ I-Processing and Pinning

Room: Indian

Session Chair: Timothy Haugan, Air Force Research Laboratory

2:00 PM

(EMA-S12-017-2013) Development of new superconductors tailored by MBE (Invited)

H. Yamamoto*, Y. Krockenberger, NTT Basic Research Labs., Japan; M. Naito, Tokyo Univ. of Agric. and Technol., Japan

The search for new superconductors with higher T_c is the most challenging subject in materials sciences. Early efforts of our research team on the development of novel superconducting materials bear fruits and culminating in our recent reports on superconductivity in end-member T'-cuprates. Our unique, multi-source, oxide MBE system together with a high precision rate control system lies beneath the successful development of new superconducting materials. Besides the superior crystalline quality of materials grown by MBE, the list of merits of our setup might be extended to (1) low temperature reaction by ultimately small reactants, (2) quasi-stable phase formation by epitaxy, (3) contamination free environment under UHV utilizing pure metal sources, (4) high throughput screening of synthesis conditions. In addition, key factors, e.g., surface-to-volume ratio, can be readily exploited in film materials as oxygen engineering plays a fundamental role in superconducting cuprates. Oxygen engineering requires a thorough screening of thermodynamic parameters and we installed a vacuum tubular furnace equipped with a high precision p_{O₂} controller. We are encouraged by the effectiveness of such unique material designing techniques in exploring new superconducting materials. In contrast to other synthesis methods, attractive materials tailored by our method may be readily implemented in large-scale applications, e.g., coated conductors.

2:30 PM

(EMA-S12-018-2013) Structural features and superconductivity in iron-based superconductors with thick blocking layers (Invited)

H. Ogino*, A. Yamamoto, K. Kishio, J. Shimoyama, The University of Tokyo, Japan

Discovery of superconductivity in LaFeAs(O,F)[1] indicate new approach to design high- T_c superconductors. So far, new compounds containing iron tetragonal lattice were developed. Large numbers of compound containing anti-fluorite type iron pnictide or chalcogenide layers have been found, including the compounds composed of antiferrotype iron pnictide layers and perovskite-type oxide layers. Such kind of compounds were discovered in several chemical systems, and especially in the cases of Fe-As-Ca-(Sc,Ti)-O, Fe-As-Ca-(Mg,Ti)-O and Fe-As-Ca-(Al,Ti)-O systems, iron-based superconductors with very thick blocking layers were found[2]. The interlayer distances of Fe planes in the compounds are the longest among layered iron pnictides, and even longer than those of any cuprate superconductors. Not only for the interlayer distances, the variation of a -axis lengths of such compounds are wider than other iron-based superconductors. Structure analysis revealed the relationship between T_c and the local structure at the FeAs layer is realized even these compounds. On the other hand, electronic phase diagrams of such compounds are still not established, though the T_c of some compounds are above 40 K. In this presentation we will present feature of these compounds and their physical properties.

3:00 PM

(EMA-S12-019-2013) Properties of epitaxial Ba(Fe $_{1-x}$ Cox) $_2$ As $_2$ thin films on different substrates (Invited)

X. Xi*, Temple University, USA

Superconducting epitaxial iron pnictide BaFe $_{1.82}$ Co $_{0.18}$ As $_2$ thin films were successfully deposited on SrTiO $_3$ (STO), LaAlO $_3$ (LAO), La,Sr(Al,Ta)O $_3$ (LSAT), and MgO substrates by pulsed laser deposition. Different values of T_c onset and T_{c0} were obtained on different substrates, with a T_c onset of 22 K and T_{c0} of 20 K in films on STO. Using a SrTiO $_3$ template layer, BaFe $_{1.82}$ Co $_{0.18}$ As $_2$ films were grown on piezoelectric PMN-PT substrate. The effects of strain on superconductivity were studied both by growing the films on different substrates and by applying an electric field on the PMN-PT substrate.

4:00 PM

(EMA-S12-020-2013) Comparative analysis of vortex pinning and dynamics in oxide, iron-based and MgB $_2$ superconductors (Invited)

L. Civale*, Los Alamos National Laboratory, USA

Vortex physics has been a topic of interest since the discovery of the oxide high temperature superconductors (HTS). The complex vortex phenomena in these materials arise from the strong thermal fluctuations, which result from the small coherence length (ξ) and the large crystalline anisotropy (γ). Although this behavior contrasts with the simpler physics in conventional low T_c superconductors, according to the present understanding there is no sharp boundary between them. However, modern vortex matter models been developed to describe the oxide HTS, thus it is important to test them in different materials. The iron-based superconductors provide a chance to "bridge the gap" and check the validity of vortex matter theories in a new family of materials with broad ranges of T_c and γ , where the small ξ in some of them results in large fluctuation effects. On the other hand, the multi-band superconductivity in the Fe-based compounds introduces a new level of complexity, requiring a re-evaluation of the concept of anisotropy in the vortex behavior. Valuable information can also be obtained from MgB $_2$, a chemically simpler two-band superconductor. I will discuss our recent studies of vortex matter in thin films and single crystals of these materials, and present a comparative

analysis of the vortex dynamics and the characteristics of the depinning excitations.

4:30 PM

(EMA-S12-021-2013) Nanoscale phase inhomogeneities in Fe-based selenides: Implications on the electronic structure and magnetic ground state (Invited)

C. Cantoni*, A. F. May, M. A. Michael, A. Safa-Sefat, B. C. Sales, Oak Ridge National Laboratory, USA

Years of experimental work on cuprates have led to a vast understanding of the effect of nanoscale strain on superconducting properties. Strain relief mechanisms at interfaces involve oxygen vacancies and structural defects, which have a large effect on T_c and J_c . In the newest class of Fe-based superconductors, A $_{1-y}$ Fe $_2$ -xSe $_2$ (A = alkali metal, alkaline-earth metal), there is considerable evidence that Fe vacancy order, nanoscale phase separation, and associated lattice strain might be necessary conditions for superconductivity to arise. This presentation will focus on nanoscale inhomogeneities and their implication on the electronic structure of high- T_c superconductors and parent compounds as revealed by aberration corrected STEM and EELS. Examples from cuprates and different Fe-based superconductor families will be discussed in an effort to identify key signatures of superconductivity and the interplay with magnetism. In particular, it will be shown that nanoscale phase separation in ordered and disordered vacancy regions leads to a different magnetic ground state than the ground state of single-phase counterparts in TlFe $_{1.6}$ Se $_2$, suggesting that magnetoelastic coupling between different phases is important for the emergence of superconductivity in A $_{1-y}$ Fe $_2$ -xSe $_2$. Research sponsored by US DOE Office of Science, Materials Science and Engineering Division.

5:00 PM

(EMA-S12-022-2013) Epitaxial growth of superconducting molybdenum nitride films by a chemical solution method

Y. Y. Zhang, Tsinghua University, China; H. M. Luo, New Mexico State University, USA; N. Haberkorn, Los Alamos National Laboratory, USA; G. Zou, Soochow University, China; F. Ronning, Los Alamos National Laboratory, USA; H. Wang, Texas A&M University, USA; L. Civale, E. Bauer, A. K. Burrell, T. M. McCleskey, Q. X. Jia*, Los Alamos National Laboratory, USA

MoN (hexagonal). Among these two phases, hexagonal MoN shows the highest superconducting transition temperature (T_c). In this presentation, we report the synthesis and characterization of epitaxial superconducting molybdenum nitride films with different crystal structures and chemical compositions grown by a chemical solution deposition technique or polymer-assisted deposition. Hexagonal MoN was stabilized on c-cut sapphire but cubic Mo $_2$ N on (001) SrTiO $_3$ even though exactly the same precursor solution and the processing parameters (such as the annealing temperature and environment) were used. Both MoN and Mo $_2$ N films were phase pure materials and showed sharp superconducting transition. In particular, the MoN film showed excellent superconducting properties, including a transition temperature of 13.0 K, a transition width of 0.3 K, an H_{c2} of 6.0 T, and an H_{irr} of 5.0 T at 4.2 K.

5:15 PM

(EMA-S12-023-2013) Pinning landscape in Fe-based thin films Superconductors (Invited)

B. Maiorov*, Los Alamos National Laboratory, USA

Vortex matter in iron-arsenide superconductors exhibits a rich phenomenology that is still largely unexplored. Many superconducting properties are affected by strong thermal fluctuation due to the small coherence length and relatively high critical temperature and anisotropy. Thin films of Fe- and Cu-based exhibit strong pinning with high J_c . Angular dependent critical current measurements are

extremely useful to determine the nature of the effective pinning center. As an example, J_c for Co-doped Ba122, show very similar angular dependence than those of YBCO with self-assembled columnar defects, despite their clear differences. In this work we explore the influence of the random point defects introduced by proton irradiation on the vortex pinning and dynamics of different Ba122 superconductors and compare it with similar experiments in YBCO. We contrast and compare the effects of proton irradiation in samples with a variety and type of pinning landscapes. We explore these effects on the critical current and in vortex dynamics, measured by transport and magnetization. We analyze the influence of random point defects on different regions of the temperature, and magnetic field strength and orientation vortex phase diagrams in superconductors with complex pinning landscapes. These comparisons allow us drawing important conclusion with respect of the vortex pinning and dynamics.

5:45 PM

(EMA-S12-024-2013) Enhanced superconducting properties in Iron chalcogenide thin films

L. Chen*, C. Tsai, Y. Zhu, A. Chen, J. Lee, X. Zhang, H. Wang, TAMU, USA

Superconducting $\text{FeSe}_x\text{Te}_{1-x}$ thin films were deposited by a pulsed laser deposition (PLD) technique on various substrates including SrTiO_3 (STO), MgO and glass substrates. The structure analysis was carried out using X-ray diffraction (XRD) and transmission electron microscopy (TEM). The superconducting properties were measured using physical property measurement system (PPMS). The critical transition temperature (T_c) was measured by the transport measurement. The critical current density (J_c) was measured by the vibrating sample magnetometer (VSM) along with the transport measurement for comparison. The T_c and J_c were optimized by substrate/film matching and inserting interlayers. The pinning properties were discussed. In addition the iron chalcogenide film on amorphous substrate demonstrates this system is promising for the coated conductors.

Friday, January 25, 2013

S1: Functional and Multifunctional Electroceramics

Integrated Homo-, Hetero-epitaxial Single and Multi-Layer Films and Device Structures

Room: Coral B

Session Chairs: Susan Trolier-McKinstry; Sahn Nahm, Korea University

10:00 AM

(EMA-S1-029-2013) Low Temperature Deposition of Electroceramic Films (Invited)

S. Trolier-McKinstry*, A. Rajashekhar, S. Bharadwaja, S. Ko, E. Dorpalam, Penn State, USA

Deposition of high dielectric permittivity or high piezoelectric response films at low substrate temperatures is an enabling technology for increased functionality in flexible electronics. This presentation will describe two different approaches to preparation of crystalline films at low temperatures: spin spray deposition and in situ laser assisted deposition and crystallization. Spin spray deposition is essentially a surface-controlled precipitation process. A variety of nanocrystalline spinel films can be deposited at substrate temperatures of 50 – 90 °C. This in turn, enables deposition on polymeric layers, as well as on patterned photoresist. In the latter case, the films can be subsequently lifted off. The second approach involves simultaneous pulsed laser deposition and laser annealing of a wide variety of film compositions at temperatures below 400 °C. It has been shown that $\text{PbZr}_{0.52}\text{Ti}_{0.48}\text{O}_3$ films with controlled orientations and excellent properties can be prepared by this route.

10:30 AM

(EMA-S1-030-2013) Examining the effects of charge defects on domain switching in thin film PZT via controlled neutron irradiation

J. T. Graham*, University of Texas at Austin, USA; G. L. Brennecke, Sandia National Laboratories, USA; P. J. Ferreira, University of Texas at Austin, USA; L. Small, D. Duquette, Rensselaer Polytechnic Institute, USA; S. Landsberger, University of Texas at Austin, USA; J. F. Ihlefeld, Sandia National Laboratories, USA

Domain wall reversibility and domain switching behavior were investigated in $\text{PbZr}_{0.52}\text{Ti}_{0.48}\text{O}_3$ films of varying initial quality subject to neutron irradiation. The films were irradiated in a research nuclear reactor up to a 1 MeV equivalent neutron fluence of $5.16 \times 10^{15} \text{ cm}^{-2}$. Changes in domain structure were assessed using a combination of Rayleigh analysis and first order reversal curves (FORC). The intrinsic/reversible and extrinsic contributions to the permittivity were found to decrease with dose suggesting an increase in domain wall pinning. Also, the formation of a double peak in the hysteron distribution indicates an increase in the concentration of defect dipoles upon irradiation. Observed differences in the rate of damage accumulation between both reversible and irreversible domain wall contributions were concomitant with initial film quality. Results of a simple phase field model are presented to help elucidate how irradiation induced charge defects alter the stable domain structure and how initial film quality relates to damage rate. Sandia National Laboratories is a multi-program laboratory managed and operated by Sandia Corporation, a wholly owned subsidiary of Lockheed Martin Corporation, for the U.S. Department of Energy's National Nuclear Security Administration under contract DE-AC04-94AL85000

10:45 AM

(EMA-S1-031-2013) Wide bandgap semiconductors supporting a tunable mid-IR surface plasmon resonance

E. Sacht*, S. Franzen, J. Maria, North Carolina State University, USA

Demonstrating surface plasmon resonance (SPR) at lower (IR) frequencies will open exciting new possibilities for system integration. The mid-IR is of particular interest since many mainstream semiconductors are transparent to these energies, which could ultimately lead to fully integrated SPR based technologies. We demonstrate SPR in the mid-IR on two wide bandgap semiconducting materials, CdO and ZnO. For both material systems, heteroepitaxial thin films have been prepared on c-plane sapphire using PLD. The SPR was characterized using a spectroscopic ellipsometer and a custom built stage. Angle and wavenumber dependent maps of the plasmonic response will be compared to simulated maps based on a free electron Drude model. We further demonstrate active control of the surface plasmon properties. Due to the band gap in the plasmonic medium, light with super-bandgap energies can be used to actively change the carrier concentration in the conduction band, thus shifting the resonance frequency of the surface plasmon. We will present mid-IR SPR data collected in situ to a second independent light source and demonstrate active plasmon tuning on ZnO and CdO samples. Light and dark SPR measurements for intrinsic ZnO and CdO films illustrate the ability to actively tune the surface plasmon. Comparison against simulations suggests that carrier densities are modulated by $+1 \times 10^{18} \text{ cm}^{-3}$ during illumination.

11:00 AM

(EMA-S1-033-2013) Anti-ferroelectric behavior of lead-free thin film NBT-BT

M. Rogers*, C. Fancher, Z. Zhao, J. Blendell, R. Garcia, Purdue University, USA

Due to environmental and health concerns lead-free piezoelectric systems are currently being evaluated for use as replacements for PZT-based ceramics. $\text{Na}_0.5\text{Bi}_0.5\text{TiO}_3 - x\text{BaTiO}_3$ (NBT-BT) is a promising alternative. Thin NBT-BT films are deposited on Pt/Ti/SiO₂/Si substrates at temperatures between 500-800°C in a 150-200 mTorr O₂ environment. We have locally imaged, manipulated domains and measured polarization response of individual grains using Piezoresponse Force Microscopy (PFM). Results show

that the NBT-BT films display spontaneous polarization after annealing as well as some remnant polarization that fades out over time. It is hypothesized that the films exhibit a transition to an anti-ferroelectric phase, induced by the electric field applied during polarization measurement. We will discuss how our results compare to predictions from Landau theory.

11:15 AM

(EMA-S1-034-2013) Formation of (Na_{0.5}K_{0.5})NbO₃ Thin Films and Their Application to Piezoelectric Nanogenerators (Invited)

I. Seo, B. Kim, M. Jang, S. Nahm*, Korea University, Republic of Korea

Amorphous (Na_{0.5}K_{0.5})NbO₃ (NKN) thin films were grown at 300°C and subsequently annealed at 800°C under Na₂O, K₂O and NKN atmospheres. A homogeneous NKN phase was developed in the film annealed under NKN atmosphere and these films showed a very low leakage current density of 2.6x10⁻⁹A/cm² at 0.2 MV/cm and had good ferroelectric and piezoelectric properties of $\epsilon_r=620$, $P_r=11.7 \mu\text{C}/\text{cm}^2$, $E_c=133.8 \text{ kV}/\text{cm}$ and $d_{33}=74 \text{ pm}/\text{V}$ at 50 kV/cm. The P_r and E_c decreased when the oxygen partial pressure (OPP) exceeded 25.0 Torr because of the low breakdown field and high leakage current. The NKN film annealed under air atmosphere exhibited a high leakage current density that decreased with increasing OPP because of the decreased number of oxygen vacancies. The leakage current of the Pt/NKN/Pt device was explained by Schottky emission and the obtained Schottky barrier height between the Pt electrode and NKN film was approximately 1.24 eV. A piezoelectric nanogenerator was produced using a NKN film by growing the film on a Pt/Ti/SiO₂/Si substrate and successfully transferring it onto a flexible polyimide (PI) substrate. A gold interdigitated electrode was deposited onto this film to synthesize the NKN nanogenerator. The NKN nanogenerator produced an output voltage of 1.9 V, output current of 38 nA, and a high power density of 2.9 mW/cm³ (0.090 $\mu\text{W}/\text{cm}^2$).

11:45 AM

(EMA-S1-035-2013) X-ray diffraction analysis of out-of-phase boundaries in epitaxial bismuth titanate (Bi₄Ti₃O₁₂) thin films prepared by atomic vapour deposition

N. Deepak*, P. Zhang, L. Keeney, M. E. Pemble, R. W. Whatmore, Tyndall National Institute, Ireland

Ferroelectrics are a valuable class of functional materials. In thin film form, their crystalline quality and functionality can be greatly enhanced by strain induced effects from substrates. High quality epitaxial ferroelectric thin films are required for a number of applications, but different types of defects such as line defects; out-of-phase boundaries (OPBs) etc. affect their properties. X-ray diffraction (XRD) is a powerful tool for the analysis of crystallinity, but has not been able to identify defects such as OPBs directly, to date. In contrast transmission electron microscopy (TEM) can directly observe such defects. In the present study, XRD analysis has been used to directly infer the presence of OPBs in thin films of high quality *c*-axis oriented thin films of the Aurivillius-family ferroelectric bismuth titanate (Bi₄Ti₃O₁₂) prepared by atomic vapour deposition. The presence of OPBs was directly inferred from splitting of the (004) and (00 $\bar{1}2$) peaks in XRD studies and a model has been developed to account for the observed splitting. TEM studies confirmed the presence of OPBs and allowed quantitative analysis for comparison with the model. The experimental conditions under which these OPBs occur are discussed.

12:00 PM

(EMA-S1-036-2013) Crystallographic Texture Effect on the Electromechanical Response of K_{0.5}Na_{0.5}NbO₃ modified Bi_{0.5}Na_{0.5}TiO₃-BaTiO₃

C. M. Fancher*, Purdue University, USA; W. Jo, J. Rödel, Technische Universität Darmstadt, Germany; J. E. Blendell, Purdue University, USA; K. J. Bowman, Illinois Institute of Technology, USA

High strain K_{0.5}Na_{0.5}NbO₃ modified Bi_{0.5}Na_{0.5}TiO₃-BaTiO₃ (BNT-BT-KNN) has received interest as a potential replacement for

Lead containing materials. Recent experiments have suggested the high maximum strain is a result of a reversible transformation from a paraelectric to a distorted ferroelectric state. Currently the effect crystallographic texture has on the electrical response has not been investigated. In this study, the effect crystallographic texture has on the electrical response was investigated for BNT-5BT-2KNN, BNT-6BT-2KNN, and BNT-7BT-2KNN. Effects of texture symmetry were investigated by applying the electric field both normal to the tape cast plane and perpendicular to the tape cast plane. Using a 5kV/mm maximum applied field textured ceramics achieved a higher maximum strain level compared to conventional bulk ceramics. Temperature dependent strain measurements show: BNT-5BT-2KNN reaches a maximum strain response as the long range ferroelectric ordering destabilizes, while the maximum strain of BNT-6BT-2KNN and BNT-7BT-2KNN degraded linearly with temperature.

12:15 PM

(EMA-S1-032-2013) Structural and Electrical properties of the 0.95(Na_{0.5}K_{0.5})NbO₃-0.05CaTiO₃ Thin Film grown by RF Sputtering Method

I. Seo*, B. Kim, M. Jang, S. Nahm, Korea University, Republic of Korea

An amorphous (Na_{0.5}K_{0.5})NbO₃(NKN) phase was formed for a film grown at 300°C. A crystalline NKN phase was developed in the films annealed at 800°C for 30 min under air atmosphere. However, the K_{5.75}Nb_{10.85}O₃₀ (KN) second phase was also observed in this film, probably due to the evaporation of Na₂O. The NKN film without the second phase was well formed when it was annealed at 800°C under NKN atmosphere. Moreover, this NKN film exhibited the good piezoelectric and dielectric properties: $d_{33}=74 \text{ pC}/\text{N}$. Using the same process, the 0.95(Na_{0.5}K_{0.5})NbO₃-0.05CaTiO₃(NKN-CT) thin film was also fabricated. Compare with the NKN thin film, during the annealing under air atmosphere, the Ca₆Ti₂Nb₈O₃₀ (CTN) second phase was observed due to the evaporation of alkali oxide. When the film was annealed under NKN atmosphere, the homogeneous NKN-CT thin film without second phase was well developed. And this NKN-CT thin film exhibited the better piezoelectric properties ($d_{33}=120 \text{ pC}/\text{N}$) than NKN thin film because of the existence of the polymorphic phase transition at room temperature. In this work, the effect of annealing atmosphere on formation of the NKN-CT films will be discussed in detail and the piezoelectric and structural properties of the NKN-CT films will be also presented.

S2: Multiferroic Materials and Multilayer Ferroic Heterostructures: Properties and Applications

Advanced Materials Synthesis and Characterization II

Room: Coral A

Session Chair: Melanie Cole, U.S. Army Research Laboratory

10:00 AM

(EMA-S2-023-2013) The role of Pt_xPb intermetallic phases in crystallization of solution-deposited PZT and PbTiO₃ thin films: Critical insight from in situ X-ray diffraction (Invited)

J. L. Jones*, K. Nittala, S. Mhin, T. Sanders, University of Florida, USA; D. Robinson, Argonne National Laboratory, USA; G. Brennecke, J. Ihlefeld, Sandia National Laboratories, USA

Solution deposition is an attractive method for synthesis of PZT and lead titanate (PT) thin films due to its low cost and easy scalability. However, this process involves heating of the amorphous films to high temperatures during which diffusion and chemical reactions may occur at the interface between the film and the bottom electrode/substrate. Known intermetallic phases that develop (Pt₃Pb) and the loss of Pb in the film have been suggested to influence both the crystallographic texture of the resultant thin film and degrade the film properties due to the resulting chemical inhomogeneity. Such suggestions have not yet been confirmed due to the

lack of in situ techniques that are capable of probing this interface during the crystallization process. Using such recently developed techniques, we provide the insight needed to assess the effects of this interdiffusion on the texture and, moreover, are able to determine the effects of processing conditions (e.g., heating rate between 0.5°C/s to 70°C/s, Pb excess, Zr:Ti ratio, etc.) on this process. Sandia National Laboratories is a multi-program laboratory managed and operated by Sandia Corporation, a wholly owned subsidiary of Lockheed Martin Corporation, for the U.S. Department of Energy's National Nuclear Security Administration under contract DE-AC04-94AL85000.

10:30 AM

(EMA-S2-024-2013) Defect Chemistry and Phase Transitions in Ti-doped Bi_{1-x}Nd_xFeO₃ ceramics (Invited)

I. M. Reaney*, University of Sheffield, United Kingdom

Structural and magnetic phase transitions are investigated in Ti doped Bi_{1-x}Nd_xFeO₃ ceramics. Paraelectric (PE) to ferroelectric (FE) transitions were observed for compositions with $x \leq 0.125$ which manifested themselves as peaks in permittivity. In contrast, PE to antiferroelectric (AFE) transitions for $0.15 \leq x \leq 0.20$ gave rise to a step-like change in the permittivity with $x = 0.25$ exhibiting no sharp anomalies and remaining PE until room temperature. The large volume change at the PE to FE/AFE transitions coupled with their first-order character constrain the transitions to occur uniformly throughout the material. Hence, anomalies in DSC, permittivity and thermal expansion occur over a narrow temperature interval. Aberration corrected scanning transmission electron microscopy revealed that Bi_{0.85}Nd_{0.15}Fe_{0.9}Ti_{0.1}O₃ ceramics contain coherent Nd-rich precipitates distributed throughout the perovskite lattice. At low concentrations, therefore, Ti⁴⁺ replace Fe²⁺ with the creation of 2/3VNd³⁺, and at higher concentrations (when Fe²⁺ have been eliminated and the conductivity suppressed), Fe³⁺ with the creation of 1/3VNd³⁺. The switch in ionic compensation mechanism from 2/3VNd³⁺ at low Ti concentrations (similar to 1%) to 1/3VNd³⁺ at higher concentrations (>1%) results in a decrease in the magnitude of $\Delta TC/\Delta x$, as the disruption of long range anti-polar coupling declines.

11:00 AM

(EMA-S2-025-2013) Electric field tunable (Ba,Sr)TiO₃ films grown by molecular beam epitaxy (Invited)

S. Stemmer*, E. Mikheev, A. Kajdos, A. Hauser, University of California, Santa Barbara, USA

We report on molecular beam epitaxy (MBE) and dielectric characterization of tunable (Ba,Sr)TiO₃ (BST) films grown on platinized substrates. BST films were grown using a hybrid MBE approach, which uses a combination of solid, gas and metal-organic sources; in particular a volatile metal-organic source (titanium tetra isopropoxide (TTIP)) is used to supply Ti. We show that through optimization of growth parameters and film stoichiometry, BST films with dielectric quality factors greater than 1000 and tunabilities greater than 1:7 can be obtained on platinized substrates. We also show that optimization of the surface quality of the Pt bottom electrodes is crucial to obtain high dielectric breakdown strengths required for high tunabilities. We will discuss the relationships between structure, composition and dielectric properties of the BST films.

11:30 AM

(EMA-S2-026-2013) Microwave Characterization of Multiferroic Materials (Invited)

J. Booth*, NIST, USA; N. D. Orloff, Stanford University, USA; I. Takeuchi, University of Maryland, USA

Multiferroic materials present challenges for characterization, particularly at microwave frequencies where many potential applica-

tion fall. In order to effectively characterize multiferroic materials, one must separate out inductive and capacitive effects from the measured device response, as well as the effects of electric and magnetic bias fields. Conversion of device-dependent quantities such as inductance and capacitance to material parameters such as the relative permittivity and permeability is necessary in order to compare different materials, and broadband frequency dependence gives additional information about domain size and interactions. We address these issues with probe-based measurements of planar test devices fabricated on multiferroic samples. We demonstrate the simultaneous extraction of the complex relative permittivity and permeability on thin-film materials over a wide range of frequencies in the microwave range. We also demonstrate the application of in-plane electric- and magnetic-field biases, which can be used to determine the field dependences of both permittivity and permeability. Finally we use these measurements to address the magneto-electric coupling in the microwave frequency response of thin-film multiferroics.

12:00 PM

(EMA-S2-027-2013) Oxygen vacancies effects on physical properties in multiferroic thin films

H. Yang*, Soochow University, China; H. Wang, Texas A&M University, USA; Y. Wang, Los Alamos National Laboratory, USA

Oxygen vacancies have been proved to effectively manipulate the physical properties of oxide thin films. It is important to investigate the relationship between the oxygen vacancies and the physical properties in multiferroic thin films, both for the understanding of the fundamental physics underlying these effects and also for potential technological applications. Success of the investigation critically relies on an accurate determination of oxygen vacancies in these thin films. Recently, a nuclear resonance backscattering spectrometry method has been used to detect the oxygen concentration in BiFeO₃ and (Eu,Ba)TiO₃ thin films. The oxygen vacancies have been accurately measured and their effects on strain, structural distortion, and electrical and magnetic properties have been investigated. An AFM-to-FM transition in (Eu,Ba)TiO₃ thin films based on the manipulation of oxygen vacancies has been revealed and analyzed by first-principle investigation. More details will be presented in the talk.

12:15 PM

(EMA-S2-028-2013) Different Routes to Multiferroicity

S. Krohns*, P. Lunkenheimer, A. Ruff, F. Schrettle, University of Augsburg, Germany; J. Mueller, M. Lang, University of Frankfurt, Germany; A. Loidl, University of Augsburg, Germany

In the last decade various mechanisms for the onset of multiferroicity, i. e. the appearance of ground states revealing concomitant polar and magnetic order, were proposed. Among the different routes to coupled polar and magnetic ordering, spin-driven ferroelectricity in LiCuVO₄, charge-order driven ferroelectricity in antiferromagnetic magnetite or improper ferroelectricity of antiferromagnetic YMnO₃, driven by a structural phase transition were found. Especially in case of strong magnetoelectric coupling, multiferroic systems can pave the way for new generations of sensors and actuators. But the strong magnetoelectric effects, e.g., of spin-driven multiferroics is often limited to very low temperatures. Therefore, mechanisms for multiferroicity, e.g. electric-dipole-driven magnetism or charge-order driven ferroelectricity, and new multiferroic systems, e.g. artificial heterostructures, are in the scientific focus to overcome this drawback. Dielectric spectroscopy and non-linear electrical measurements are powerful tools to analyze the electronic properties of multiferroic systems giving new insights into the underlying physics, which allows their optimization. Here, we thoroughly discuss the dielectric properties of charge-order driven multiferroics. In detail, we address the question, if LuFe₂O₄ is a multiferroic and we also show a recently discovered new multiferroic charge-transfer system.

S6: Thermoelectrics: Defect Chemistry, Doping and Nanoscale Effects

Oxide Thermoelectrics II

Room: Pacific

Session Chair: Alp Sehirlioglu, Case Western Reserve University

10:00 AM

(EMA-S6-014-2013) Oxides with crystallographic shear defects – potential thermoelectric materials? (Invited)

M. Backhaus-Ricoult*, Corning Inc., USA

Having high temperature stability, semiconducting oxides are of potential interest for thermoelectric power generation. However, they usually suffer from low carrier mobility at high carrier concentration and from more localized charge carriers, when compared to other high-performance thermoelectric materials. They typically exhibit rather small power factors, but offer small thermal conductivities. General approaches for enhancing the carrier concentration, such as donor doping, are applicable to oxides, but effective tuning of the electrical properties is more difficult than in other small band gap semiconductors. Reducing thermal conductivity in oxides is difficult due to the small mean free phonon path; crystallographic defects turn out to be more effective than nanograin size. In this presentation, we will provide a general analysis and show results for oxides with defective crystal structures. Titania is used as a model material for comparing the impact of grain size, doping and substitution, second phase nanodispersion and crystallographic defects on electronic and thermal properties. It is shown that crystallographic oxygen shear defects in the Magnéli phases are the key driver for low thermal conductivity. Oxides like niobium and tungsten oxide form similar shear defects in more complex planar and block structures. Their impact on thermoelectric properties is illustrated.

10:30 AM

(EMA-S6-015-2013) Electric Field-Induced Point Defect Redistribution in TiO_2

A. Moballegh*, E. Dickey, NC State University, USA

The present work addresses the impact of point defect redistribution on the electrode properties of TiO_2 . High-purity single crystal and polycrystalline rutile TiO_2 specimens were equilibrated at specific oxygen partial pressures and temperatures to control the initial point defect concentrations. The samples were then subjected to field stresses up to 500V/cm at a temperature of 200°C. The spatial distribution of point defects was studied as a function of field strength and time by cathodoluminescence. High-resolution scanning transmission electron microscopy and electron energy loss spectroscopy were utilized to study the coalescence of defects near the electrode interfaces. These microstructural/microchemical studies were used to explain the observed changes in the I-V characteristics of the materials. This work was supported by the National Science Foundation under grant number DMR-1132058.

10:45 AM

(EMA-S6-016-2013) The effect of pO₂ on the thermoelectric properties of beta gallia rutile intergrowths

D. Edwards*, M. Alberga, Alfred University, USA

Thermoelectric generators (TEGs) convert waste heat to useable electrical energy. The development of oxide materials with improved thermoelectric properties will enable the development of TEGs that can operate above 1000K. Oxides with layered crystal structures offer the opportunity to decouple the electrical and thermal properties and thereby increase the thermoelectric figure of merit, ZT. Beta-gallia rutile intergrowths are a series of homologous compounds with crystal structures containing rutile-type blocks separated by thin beta-gallia layers. The ZT values of BGR intergrowths, $\text{Ga}_4\text{Tin-4O}_{2n-2}$,

prepared by solid state reaction and combustion synthesis, range from 10^{-3} to 10^{-1} at 1000K depending on sintering conditions. The wide range of ZT values observed for samples of similar composition is thought to be caused by differences in the $\text{Ti}^{3+}/\text{Ti}^{4+}$ content of the samples. In this work, we have investigated the thermoelectric properties of $\text{Ga}_4\text{Ti}_{15}\text{O}_{36}$ ($n = 19$) equilibrated at different pO₂. The thermoelectric properties and underlying defect chemistry will be presented.

11:00 AM

(EMA-S6-017-2013) Semiconductor-insulator transition in rutile ceramics controlled by post-sinter cooling conditions

A. R. West*, Y. Liu, University of Sheffield, United Kingdom

Although rutile, TiO_2 , is an insulator under normal usage conditions with band gap ~ 3.2 eV, the electrical properties of ceramics depend critically on cooling conditions after firing at high temperatures. With increasing firing temperature, small amounts of oxygen loss, too small to be detected, occur and on rapid quenching, there is insufficient time for reoxidation to occur. Conductivities of quenched samples increase and activation energies decrease with increasing quench temperature until, for instance, ceramics quenched from 1400 °C have conductivity $\sim 0.1 \Omega^{-1} \text{cm}^{-1}$ with activation energy 0.01 eV over the temperature range 10 to 500 K. Small amounts of oxygen loss during firing may be a common feature of many oxide ceramics but the resulting electrical properties depend critically on the post-sinter cooling conditions.

11:15 AM

(EMA-S6-018-2013) The Influence, Role, and Property Variations in Ferroelectricity at the Edge of the Metal-Insulator Transition and Its Influence on Thermoelectric Properties

J. A. Bock*, S. Lee, C. A. Randall, S. Trolier-McKinstry, The Pennsylvania State University, USA

Over the years in the study of ferroelectricity, there have been a few reports that have debated a unique state of matter, the metallic ferroelectric. Here we consider the use of donor oxygen vacancies to increase the electronic conductivity to extremely high levels that are at and around the Mott Criterion. We consider that the ferroelectricity perturbs the transition from insulator to metallic (MIT)-like behaviour. At the phase transition in the BaTiO_3 family, this is closely related to ferroelectric-paraelectric transition. In the relaxor ferroelectrics, the MIT is associated closely with the Burns temperature. Relaxor-based ferroelectrics have been known to have intrinsic localized phonon modes and have so-called phonon-glassy behaviour. These processes give low thermal conductivity, and coupled with high thermopower performance, point to opportunities with ferroelectric oxides in thermoelectric based studies.

11:30 AM

(EMA-S6-019-2013) Measurement of Thermal Conductivity and Thermal Boundary Conductance of Nano-Grained SrTiO_3 Thin Films

B. M. Foley*, H. Brown-Shaklee, J. C. Duda, R. Cheaito, University of Virginia, USA; B. J. Gibbons, Oregon State University, USA; D. L. Medlin, J. F. Ihlefeld, Sandia National Laboratories, USA; P. E. Hopkins, University of Virginia, USA

We report on the thermal conductivity of nano-grained SrTiO_3 (ng- SrTiO_3) films grown on sapphire substrates, as well as the thermal boundary conductance at the Al/ng- SrTiO_3 interface measured via time-domain thermoreflectance (TDTR). The 170nm oxide films of various grain-sizes were prepared from a chemical solution deposition process using a chelate chemistry and is shown to be a scalable method for producing dense ng- SrTiO_3 films. It is shown that the thermal conductivity of the ng- SrTiO_3 decreases with decreasing average grain size due to grain boundary scattering. In addition, we show that the DMM with a phonon attenuation term works well for RMS roughness less than 10nm, but breaks down beyond this.

11:45 AM

(EMA-S6-020-2013) Thermal conductivity and domain wall Kapitza conductance in epitaxial bismuth ferrite thin films

J. Ihlefeld*, Sandia National Laboratories, USA; P. E. Hopkins, University of Virginia, USA; C. Adamo, Cornell University, USA; L. Ye, B. Huey, University of Connecticut, USA; S. R. Lee, Sandia National Laboratories, USA; D. G. Schlom, Cornell University, USA

The role of domain boundaries on the thermal conductivity of epitaxial BiFeO₃ thin films has been investigated using time-domain thermoreflectance. (001)-pseudocubic oriented BiFeO₃ films were prepared on (001)-oriented SrTiO₃ single crystalline substrates via reactive molecular-beam epitaxy. Substrate vicinality was used to engineer the domain structure to contain 4-, 2-, and a single-domain variant. Domain wall types and density (domain wall length/unit area) was measured using piezoforce microscopy. It will be shown that 71° domain walls in strained BiFeO₃ films effectively scatter phonons and can decrease the measured thermal conductivity by a factor of 2 at room temperature. Sandia National Laboratories is a multi-program laboratory managed and operated by Sandia Corporation, a wholly owned subsidiary of Lockheed Martin Corporation, for the U.S. Department of Energy's National Nuclear Security Administration under contract DE-AC04-94AL85000.

S9: Thin Film Integration and Processing Science

Epitaxial Growth and Strain Engineering

Room: Mediterranean B/C

Session Chair: Brady Gibbons, Oregon State University

10:00 AM

(EMA-S9-009-2013) Strain and composition effects in epitaxial Pb(Zr,Ti)O₃ thin films (Invited)

G. Rijnders*, University of Twente, Netherlands

Ferroelectric oxides, such as Pb(Zr,Ti)O₃ (PZT), are very useful for electronic devices, as well as piezomechanical actuators and sensors. The ferro- and piezoelectric properties are strongly related to the crystal orientation as well as the strain state of the PZT layer, since it will influence the domain configuration within the film. Successful integration of these devices into silicon technology is therefore not only dependent on the ability of epitaxial growth on silicon substrates, but also the control of the crystallographic orientation and the residual strain state of the deposited PZT thin film. I will present the effects of the residual strain in epitaxial PZT thin films, grown on different substrate-buffer-layer combinations by pulsed laser deposition, on the ferroelectric and piezoelectric properties. Compressive or tensile stress caused by the difference in thermal expansion of the clamped PZT film and substrate is found to influence the domain structure, and therefore the ferroelectric and piezoelectric properties. Ferroelectric and dielectric properties are compared to the Pertsev's and Kukhar's Landau-Devonshire model for biaxially strained thin films. We found that experiments are in good correspondence with the theoretical predictions. In this contribution, I will furthermore highlight the recent progress on the fabrication of all-oxide piezo-MEMS devices by pulsed laser deposition.

10:30 AM

(EMA-S9-010-2013) Structural and magnetic properties of epitaxial (111) oriented NiFe₂O₄ thin film on (0001) c-plane sapphire via chemical solution processing

S. Seifkar*, North Carolina State University, USA; B. Calandro, Missouri University Science and Technology, USA; G. Rasic, North Carolina State University, USA; N. Bassiri-Gharb, Georgia Institute of Technology, USA; J. Schwartz, North Carolina State University, USA

A chemical solution processing route is developed and optimized to grow epitaxial (111) oriented NiFe₂O₄ (NFO) thin films on c-plane

(0001) sapphire substrate. A high degree of out-of-plane orientation in the <111> direction is confirmed using θ -2 θ X-ray diffraction and pole figures. The in-plane epitaxial relationships between the NFO (111) and Al₂O₃ (0001) are also confirmed with X-ray ϕ -scanning and selected area electron diffraction patterning. These results indicate two variants in the NFO crystallographic structures, rotated by 180 degrees, as well as 30 degree rotation of the NFO (111) with respect to the sapphire (0001). The top view and cross-sectional microstructures are examined using a helium ion microscope. The out-of-plane magnetization exhibits improved Mr/Ms ratio by lowering the NFO film thickness. Compared to randomly oriented and uniaxial textured NFO films on silicon and platinized silicon substrates, the out-of-plane coercivity of the biaxial/epitaxial textured NFO is lower in the film with same thickness. The improved out-of-plane magnetic anisotropy is comparable to epitaxial NFO films of comparable thickness deposited by pulsed laser deposition and sputtering.

10:45 AM

(EMA-S9-011-2013) Temperature-dependent diffraction and microscopy observations of phase transitions and domain formation in highly-strained BiFeO₃ (Invited)

H. M. Christen*, W. Siemons, C. Beekman, M. Chi, J. Howe, N. Balke, P. Maksymovych, M. Biegalski, Oak Ridge National Laboratory, USA; A. Vailionis, Stanford University, USA; P. Gao, X. Pan, University of Michigan, USA; A. K. Farrar, J. Moreno, D. Tenne, Boise State University, USA

BiFeO₃ has been the focus of intense research not only because of the unique coexistence of robust ferroelectric and antiferromagnetic order at room temperature, but also because it responds to epitaxial strain with a structural phase transition akin to those otherwise observed only in lead-based perovskites. At room temperature, the polymorphic transition from a nearly-rhombohedral, low-strain ("R") structure to a highly-axial ("T") form has been well documented in the literature. Within this T' polymorph, we observe a monoclinic (M_C) – monoclinic (M_A) – tetragonal (T) sequence of phase transitions, and show that the high-temperature, purely tetragonal phase remains polar. Results from temperature-dependent electron microscopy, scanning probe microscopy, and x-ray diffraction, show the nature and temperature evolution of the mixed-phase "stripe patterns" that are commonly observed in T'-BiFeO₃ samples. Specifically, we find that these patterns form as a consequence of differences in thermal expansion between film and substrate, and that their presence is a prerequisite to piezoelectric switching in T'-BiFeO₃.

11:15 AM

(EMA-S9-012-2013) Langmuir-Blodgett Films of 2D Oxide Nanosheets as Seed Layers for Oriented Growth of SrRuO₃ on Si

J. E. ten Elshof*, M. Nijland, S. Kumar C. Palanisamy, R. Lubbers, S. A. Veldhuis, R. Besselink, G. Koster, G. Rijnders, University of Twente, Netherlands

Oxide nanosheets are the oxide equivalents of graphene. They have a thickness of ~1 nm and can have lateral sizes up to tens of micrometers. They are made by exfoliation of layered oxides in aqueous solution using an ion exchange process. The resulting colloidal nanosheets are single-crystalline. Langmuir-Blodgett films of nanosheets can be used as textured crystalline templates onto which epitaxial oxides can be grown. We studied the mechanism of exfoliation and restacking of lepidocrocite-type titanates into Ti_{0.87}O₂ nanosheets in solution by small angle x-ray scattering, and developed a new method to monitor the kinetics of exfoliation by differential scanning calorimetry. The conditions for Langmuir-Blodgett (LB) deposition of nanosheets to >99% monolayer coverage on glass and silicon were optimized. SrRuO₃ films were grown on Ca₂Nb₃O₁₀ and Ti_{0.87}O₂ nanosheet films by pulsed laser deposition. SrRuO₃ is ferromagnetic below 160 K and shows strong magnetic anisotropy. Depending on nature of the seed layer, [001] oriented films grew on Ca₂Nb₃O₁₀, and [110] oriented films on Ti_{0.87}O₂. The influence of the seed layer on magnetization and Curie temperature is discussed.

11:30 AM

(EMA-S9-013-2013) Epitaxial Ferroelectric Thin Films for Micro-Electro-Mechanical-System Based Data Storage (Invited)

A. Roelofs*, Center for Nanoscale Materials, USA

Ferroelectric thin films are of interest for potential memory applications such as micro-electro-mechanical-system (MEMS) based storage devices. These systems require homogeneous ferroelectric properties at the nano-scale and a fast and reliable method for determining the polarization state of the ferroelectric thin film. Epitaxial (001) oriented $\text{Pb}(\text{Zr}_x\text{Ti}_{1-x})\text{O}_3$ thin films have been investigated with piezo-response-force (PFM) microscopy and two new experimental techniques to determine the domain configuration. The first technique enables fast and accurate determination of the domain orientation in ferroelectric thin films using a movable non-sharp electrode. The polarization orientation is determined by applying a DC voltage between the moveable top-electrode and an extended bottom electrode and if the applied voltage is large enough to induce polarization reversal in the domains opposed to the applied voltage a displacement current is measured. This way of determining the original polarization pattern is obviously destructive but offers the advantages of simplicity and a high-speed measurement technique. In the second scheme a charge amplifier is employed to measure the electrical current generated due to the direct piezoelectric effect when running a metallic probe with a constant force over a ferroelectric surface. Thermal stability experiments showed excellent retention properties.

12:00 PM

(EMA-S9-014-2013) Low temperature epitaxial CeO_2 ultrathin films and nanostructures by atomic layer deposition

M. Coll*, J. Gazquez, A. Palau, X. Obradors, T. Puig, ICMAB-CSIC, Spain

Epitaxial growth of CeO_2 thin films has generated huge interest for silicon-on-insulator structures and also as buffer layer in functional oxide heterostructures. For most of these applications, slight changes in film thickness, composition, stoichiometry, ion motion, epitaxy or structural defects can dramatically affect its properties. The surface self-limiting Atomic Layer Deposition (ALD) characteristic growth offers great potential to ensure a nanoscale control of CeO_2 properties over other deposition techniques such as chemical solution deposition, pulsed laser deposition or sputtering. For the first time, we prepared highly epitaxial as-deposited ALD- CeO_2 thin films on several single crystal substrates (LAO, STO, YSZ) at temperatures below 300°C obtaining a growth per cycle of $\approx 0.2\text{\AA}/\text{cycle}$. This extremely low growth rate has been identified as a key parameter to ensure epitaxial growth at these low temperatures. XRD, AFM, X-ray photoelectron spectroscopy (XPS), and advanced scanning transmission electron microscopy (STEM) confirmed the formation of ultra-smooth, pure and epitaxial (001) CeO_2 films with a thickness range of 2 to 10 nm. We demonstrate that combining e-beam lithography and ALD it is feasible to obtain size-controlled CeO_2 nanostructures. Additionally, further tuning of ALD conditions for CeO_2 deposition allowed us to obtain conformal coatings on 3D substrates.

S12: Recent Developments in High Temperature Superconductivity**New Superconductors and MgB_2 II—Wires and Devices**

Room: Indian

Session Chair: Haiyan Wang, Texas A&M University

10:00 AM

(EMA-S12-025-2013) Scaling up of ex-situ multifilamentary MgB_2 superconducting wire manufacturing (Invited)

G. Grasso*, A. Tumino, S. Brisigotti, R. Piccardo, M. Tropeano, D. Nardelli, V. Cubeda, Columbus Superconductors, Italy

The flexibility of ex-situ MgB_2 route allows for a wide range of wire architectures including different materials. The applicability of our copper stabilized 12 filaments tape has been already demonstrated in commercial MRI systems and, recently, in the first prototype of hydrogen-cooled superconducting cable. Alternative solutions with respect to the tape layout are now proposed. Round wires with high filling factor and high number of filaments appear suitable for high current cables due to the possibility to have a more compact layout and larger overall current density. For this application optimised round wires are now produced in very long lengths, up to 6 Km in a single piece. For DC magnets, a sandwich-like MgB_2 wire solution is currently proposed: a central MgB_2 tape conductor with high filling factor well above 20%, is laminated with two OFHC copper tapes after the final sintering. Thanks to this solution, the copper fraction and the wire critical current can be independently selected by adjusting the respective size of the superconducting and copper tapes. Regarding AC applications, the ex-situ method has been made compatible with a Titanium and Copper-Nickel sheathed MgB_2 wire: the combination of non-magnetic materials and of fine filaments with good electrical decoupling, lead to conductors showing low AC losses and comparable transport properties to the standard wires.

10:30 AM

(EMA-S12-026-2013) Development of high performance MgB_2 wires by internal Mg diffusion process (Invited)

H. Kumakura*, S. Ye, A. Matsumoto, K. Togano, National Institute for Materials Science, Japan

Internal Mg diffusion (IMD) process produces high density MgB_2 layer and high critical current properties, which makes it a promising method for fabricating MgB_2 wires. However, many unreacted B particles remain in the reacted layer of IMD processed wires. This is due to the insufficiency of Mg supplied to the B layer, because long diffusion distance is required for Mg atoms. Therefore, the reduction of required diffusion distance of Mg is effective in reducing the unreacted B and in increasing J_c values. The reduction of MgB_2 filament size, which can be realized in multi-filamentary wires, is an effective method in decreasing the diffusion distance of Mg. Recently we have fabricated 37-filamentary wires and have obtained J_c of $76,000\text{A}/\text{cm}^2$ at 4.2K and 10T. Another interesting method to decrease the required diffusion distance of Mg atoms is Mg powder addition in the B powder layer. Twice as high J_c as that of no Mg-added wire was obtained by 6at%Mg powder addition to the B powder layer. This Mg powder addition to B powder is also effective in increasing volume fraction of MgB_2 in the wire and hence, in increasing engineering $J_c(J_e)$ values. Some kinds of organic material additions to B powder layer such as C_8H_{10} are effective in enhancing J_c values although very small amount of C substitution for B site is obtained. Co-doping of C_8H_{10} and SiC is more effective in enhancing J_c values.

11:00 AM

(EMA-S12-027-2013) Critical Current Density of Multifilamentary Second Generation MgB₂ Wires (Invited)

M. D. Sumption*, The Ohio State University, USA; G. Li, M. A. Rindfleisch, M. J. Tomsic, Hyper Tech Research Incorporated, USA; W. E. Collings, The Ohio State University, USA

Recent advances in MgB₂ conductors are leading to a new level of conductor performance. Based on the use of an internal Mg diffusion or Mg infiltration starting point, but also includes optimized powders, proper chemistry, and an improved architecture, dense MgB₂ structure with not only a high critical current density J_c, but also a high engineering critical current density, J_e, can be obtained. Such a conductor could be described as a second generation MgB₂ conductor. In this paper, a series of these conductors has been prepared using a 2% C doping level. Scanning electron microscopy and associated energy dispersive X-ray spectroscopy were applied to characterize the microstructure and composition of the wires, and a dense MgB₂ layer structure was observed. The best layer J_c for our monofilamentary samples is 1.07x10⁵ A/cm² at 10 T, 4.2 K. This is about 10 x higher than that seen in the best PIT strands, and consistent with the best IMD strands in the literature. Previous IMD strands had lower J_e values because of small reacted IMD layers. However, optimization of the layer design has led to monofilamentary J_e values substantially higher than the corresponding PIT strands — our best J_e is seen to be 1.67x10⁴ A/cm² at 10 T, 4.2 K (a factor of higher than the best PIT).

11:30 AM

(EMA-S12-028-2013) Synthesis and Properties of High-J_c Bulk BaFe₂As₂ Superconductors (Invited)

E. Hellstrom*, J. Weiss, J. Jiang, F. Kametani, D. Larbalestier, A. Polyanski, C. Tarantini, Applied Superconductivity Center - Florida State University, USA

We developed a method to synthesize BaFe₂As₂ (Ba-122) samples that have high phase purity with small, randomly-oriented, well-connected grains with clean grain boundaries. Bi-crystal studies of Ba-122 show that the critical current density J_c falls off with increasing grain boundary angle, yet our polycrystalline K-doped Ba-122 has a much J_c than expected for a randomly oriented, polycrystalline sample. In contrast, identically prepared Co-doped Ba-122, which has a microstructure at the TEM level that is essentially identical to K-doped Ba-122 has significantly lower J_c. We will report on recent studies of Ba-122 samples directed at understanding what causes this high J_c and if it can be pushed even higher by changing the doping or by modifying the processing procedures.

12:00 PM

(EMA-S12-029-2013) Epitaxial thin films and artificially engineered superlattices of BaFe₂As₂ (Invited)

S. Lee*, C. M. Folkman, C. B. Eom, University of Wisconsin, USA; C. Tarantini, J. Jiang, J. D. Weiss, F. Kametani, E. E. Hellstrom, D. C. Larbalestier, Florida State University, USA; P. Gao, Y. Zhang, Q. X. Pan, University of Michigan, USA

Since the discovery of iron-based superconductors, epitaxial thin films have significantly advanced potential device applications and the understanding of the fundamental physical properties of these new superconductors. In particular, we recently have grown high quality epitaxial Co-doped BaFe₂As₂ (Ba-122) thin films using template engineering which generated c-axis aligned, self-assembled, second phase nanorods. For high field applications of Co-doped Ba-122 thin films, very high critical current density (J_c) and irreversibility field (H_{irr}) are indispensable along all crystal directions. On the other hand the development of superconductor-based devices such as junctions, SQUIDs and integrated circuits requires multilayer deposition with atomically smooth and uniform barriers. We have achieved success in both aims. We show that artificially engineered undoped Ba-122 / Co-doped Ba-122 compositionally modulated superlattices structures produces ab-aligned nanoparticle arrays and self-assembled c-axis aligned defects that combine to produce very

large J_c and H_{irr} enhancements. We also demonstrate atomically sharp interfaces in a structurally modulated SrTiO₃ (STO) / Co-doped Ba-122 superlattice that can serve as the basis for electronic uses of Co-doped Ba-122.

S1: Functional and Multifunctional Electroceramics

Piezoelectrics and Characterization of Materials, Interfaces, as well as Electrical, Mechanical, Electro-mechanical and Other Material Properties

Room: Coral B

Session Chairs: Peter Finkel, Naval Undersea Warfare Center; Vojislav Mitic, Faculty of Electronic Engineering

2:00 PM

(EMA-S1-037-2013) Investigation of ferroelectric phase transitions and large energy conversion in domain engineered ferroic crystals

P. Finkel*, Naval Undersea Warfare Center, USA; S. Lofland, Rowan University, USA; D. Viehland, Virginia Tech, USA

It is well known that ferroelectric single crystals display both a linear piezoelectric effect and a non-linear electro-mechanically coupled phase transformations. Domain engineered ferroelectric single crystals deliver an order of magnitude improvement compared to conventional PZT, although fatigue remains a drawback in achieving reliable multiple domain switching crucial for memory storage. Another fundamental shortcomings of ferroelectrics are low induced strain and high electric field often required for practical application in actuation, sensors and acoustics. We demonstrate that under specially compressive stresses ferroelectric relaxors exhibit low field induced reversible and sustainable strain associated with ferroelectric-ferroelectric phase switching and unusual and unexpected lack of fatigue after several millions cycles is believed due to strain accommodation occurring in ferroics (Finkel et al, Phys. Status Solidi A, 10,1002 (2012)). These phase transformations result in extremely large changes in polarization in response to relatively small stress changes, a property that is well suited to enhancing mechanical energy conversion demonstrated in certain ternary ferroelectric relaxor single crystals. Polarized light microscopy and X-ray diffraction are in a very good agreement with macroscopic observation and phenomenological model confirming proposed transformational path. The phenomena presented in this work are envisioned to be universal in domain engineered ferroics enabling mechanical stress to be used for strain and polarization control of electromechanical energy conversion offering a significant opportunity to increase the efficiency of ferroelectric energy harvesters.

2:15 PM

(EMA-S1-038-2013) The statistical analysis vertical grain contacts surfaces influence on BaTiO₃ ceramics intergranular capacity

V. Mitic*, V. Paunovic, Faculty of Electronic Engineering, University of Nis, Serbia; S. Jankovic, Mathematical institute, SASA, Serbia; L. Kocic, Faculty of Electronic Engineering, University of Nis, Serbia

A new approach on correlation between microstructure and properties of doped BaTiO₃ -ceramics based on grain contact surfaces probability and fractals have been analyses and developed in this study. BaTiO₃ samples doped by different additives (Nb₂O₅, MnCO₃, Er₂O₃, Yb₂O₃, Ho₂O₃) have been prepared by using conventional solid state procedure and were sintered from 1320°C to 1380 °C A reconstruction of microstructure configurations, like grains shapes, contacts surfaces and intergranular contact, by using statistical mathematics and fractal modeling method have been successfully done. The area of grains surfaces were calculated using fractal correction which expresses the irregularity of grains surface through fractal dimension. For better and deeper characterization of the ceramics ma-

terial microstructure the mathematical statistics calculations and also applied the Voronoi model. For all of these microstructure analysis and characterization we applied the vertical fracture between two pieces or samples view. The presented results, indicate that statistical mathematics method are very important for establishing more precise relation $C \approx f(\epsilon, S, d)$ and final microstructure and dielectric properties BaTiO₃ ceramics prognosis.

2:30 PM

(EMA-S1-039-2013) Measurement of the Thermal Conductivity of Single and Polycrystalline PZT Thin Films

B. M. Foley*, University of Virginia, USA; H. J. Brown-Shaklee, J. F. Ihlefeld, Sandia National Laboratories, USA; P. E. Hopkins, University of Virginia, USA

Measurement of the thermal conductivity of single and polycrystalline Lead Zirconate Titanate (Pb(Zr(1-x)Ti(x))O₃, or PZT) thin films of various compositions is presented. The 300nm thick PZT films were spin cast from commonly used chelate chemistries onto SrRuO₃/SrTiO₃ and platinumized ZnO/Si substrates to produce the single and polycrystalline films, respectively. Measurement of the thermal conductivity was performed using time-domain thermoreflectance (TDTR). In the case of single-crystalline films, we find that there is a 45% reduction in the thermal conductivity at the morphotropic phase boundary (MPB, $x = 0.48$) compared to nearby compositions at $x = 0.40$ and $x = 0.60$, while for polycrystalline films, we see very little variation in the thermal conductivity for various compositions. In addition, temperature dependent measurements of the thermal conductivity were performed on the zirconate-rich samples to investigate any differences between the high and low-temperature rhombohedral states at these compositions. We use a minimum-limit model for the thermal conductivity of PZT thin films to evaluate the measured results.

2:45 PM

(EMA-S1-040-2013) Determination of the Dissociation Kinetics of Defect Complexes under dc Bias in Perovskite Materials using TSC and In-Situ EPR Techniques

R. Maier*, J. Follman, C. Randall, The Pennsylvania State University, USA

Measurement techniques are developed to determine the dissociation parameters of acceptor-oxygen vacancy defect complexes under dc bias in order to understand the kinetics of the dissolution of these complexes responsible for reliability related issues including resistance degradation and ferroelectric aging. Changes in the electron paramagnetic resonance (EPR) signal related to a single hop of an oxygen vacancy to a next nearest lattice position away from an acceptor dopant can be detected. This effect makes it possible to monitor the dissociation of complexes in-situ under applied bias. Thermally stimulated current (TSC) techniques are used to measure the same kinetic parameters by monitoring the dissociation by means of current relaxations. Dopants act as trap sites for oxygen vacancies and perturb the barrier height for vacancy migration. Field dependent dissociation energies related to these barrier heights will be presented for the case of doped strontium titanate crystals. The applicability of TSC will be discussed as a means to measure the same parameters in lieu of an EPR system. These results will suggest a reevaluation of the practice of extrapolating vacancy diffusion coefficients from high temperatures where association is minimal to device operating temperatures at which driving forces for association become important.

3:00 PM

(EMA-S1-041-2013) Probing Low-level Radiation Damage Using Thin Film Capacitors and Dielectric Measurements

A. Smith*, North Carolina State University, USA; Y. Zhang, W. J. Weber, University of Tennessee, USA; S. C. Shannon, J. Maria, North Carolina State University, USA

Sparse populations of point defects are the initial manifestations of irradiation, and provided they are charged with respect to the host lattice, will be easily detected electrically at PPB levels and lower. Thin film capacitor structures provide an appropriate geometry for quick

and uniform irradiation of the dielectric material and allow for post dose dielectric measurements. This study uses cerium oxide thin films as a dielectric that is prepared using magnetron sputtering and characterized using x-ray diffraction and AFM image analysis. The devices are metal-insulator-metal capacitor structures deposited on (001)silicon substrates. Dielectric characterization of these structures reveals highly insulating ceria with a relative permittivity of approximately 24 and negligible dispersion in the frequency range between 0.1 kHz and 100 kHz. The films could withstand electric fields of 500 kV/cm with no increase in dielectric loss. After exposure to MeV Si radiation, results show a 10x increase in dispersion over three decades of frequency. Dielectric loss increases after irradiation to 5x the pre-irradiated value at low applied field and increases to 30x at fields of 500kV/cm. These results demonstrate the ability to detect radiation damage using dielectric methods at defect levels that are at least two orders of magnitude lower than can be achieved through current conventional techniques.

3:15 PM

(EMA-S1-042-2013) Relaxation Behavior of Oxygen Vacancies in A(Ti_{0.99}Mg_{0.01})O₃ Perovskite Ceramics (A=Ba, Sr, Ca)

Y. Han*, G. Song, SungKyunKwan University, Republic of Korea

Relaxation behavior of oxygen vacancy in A(Ti_{0.99}Mg_{0.01})O₃ Perovskite ceramics was studied. When Ti ions are replaced by Mg, a negatively charged defect, Mg on Ti site will be formed and accompany the corresponding number of oxygen vacancies (Vo). Thus, the formation of defect complex would be possible between MgTi^{''} and Vo. Dielectric losses(tanδ) were measured as a function of frequency(10~1MHz) at various temperatures (150~450C) and the activation energies for the motion of oxygen vacancies were estimated. The activation energies for Ca(Ti_{0.99}Mg_{0.01})O₃ and Sr(Ti_{0.99}Mg_{0.01})O₃ were calculated to be 0.63eV and 0.75eV over the temperature range studied. However, the energies for Ba(Ti_{0.99}Mg_{0.01})O₃ were estimated to be 0.65eV at lower temperatures (<300C) and 1.12eV at >300C. This result implies that the behavior of oxygen vacancy would be different at higher temperatures in Ba(Ti_{0.99}Mg_{0.01})O₃. The distance between MgTi^{''} and Vo in Ba(Ti_{0.99}Mg_{0.01})O₃ cell would be greater than those in Ca(Ti_{0.99}Mg_{0.01})O₃ and Sr(Ti_{0.99}Mg_{0.01})O₃ because of the larger cell size of Ba(Ti_{0.99}Mg_{0.01})O₃. The Coulomb energy between MgTi^{''} and Vo will decrease with the increase in separation, leading to the easy dissociation of dipoles. At higher temperatures, the motion of oxygen vacancy will require more energy for dissociation of (MgTi^{''}-Vo) in addition to the swing motion.

4:00 PM

(EMA-S1-043-2013) Crystallographic refinement yields point defect and lattice changes in PZT as a result of neutron irradiation

J. S. Forrester*, A. J. Henriques, S. B. Seshadri, University of Florida, USA; D. Brown, Los Alamos National Laboratory, USA; J. T. Graham, S. Landsberger, University of Texas-Austin, USA; J. F. Ihlefeld, G. L. Brennecke, Sandia National Laboratories, USA; J. L. Jones, University of Florida, USA

Lead zirconate titanate (PZT) compositions with superior piezoelectric properties are those in the vicinity of the morphotropic phase boundary (MPB) at Pb(Zr_{0.52}Ti_{0.48})TiO₃. In this region, the structure is also at its maximum crystallographic instability due to the meeting of two different phases (rhombohedral and tetragonal). Here, the objective is to examine crystal structure changes that occur in compositions close to the MPB as a response to exposure to neutron irradiation. The possible use of PZT as sensors in high radiation areas will depend on whether the crystal structure damage is reversible (resulting in radiation-tolerant materials) or irreversible (radiation-sensitive materials). Undoped, 2% Fe-doped, and 2% Nb-doped PZT with a Zr/Ti ratio of 50:50 (nominally tetragonal) were irradiated in a TRIGA reactor to a 1 MeV equivalent neutron fluence of 1.7×10¹⁵cm⁻². Neutron diffraction patterns of non-irradiated (control group) and irradiated samples were recorded on the

SMARTS diffractometer at LANSCE. Analysis of these patterns using the Rietveld refinement program GSAS has allowed crystal structure changes due to irradiation to be observed. We will present changes in the lattice parameters leading to cell volume increases, atomic position movements, isotropic displacement parameter differences, and point defect increases as a result of irradiation.

4:15 PM

(EMA-S1-044-2013) Piezoelectric Properties of the High Temperature $x\text{PbTiO}_3 - (1-x)[\text{BiScO}_3 + \text{Bi}(\text{Ni}_{1/2}\text{Ti}_{1/2})\text{O}_3]$ Ternary Perovskite Ferroelectric System

T. Ansell*, D. P. Cann, Oregon State University, USA

There exist a number of perovskite solid solutions based on PbTiO_3 that form ferroelectric materials, including the ubiquitous ferroelectric $\text{PbTiO}_3\text{-PbZrO}_3$ (PZT), which has been extensively studied and exploited for its excellent piezoelectric properties and relatively high Curie temperature, T_C . However, due to the inability of researchers to increase T_C past 400 oC, new ferroelectric materials have been researched to meet the piezoelectric properties of PZT and exceed the 400C threshold. The solid solution $x\text{PbTiO}_3 - (1-x)[0.5\text{BiScO}_3 - 0.5\text{Bi}(\text{Ni}_{1/2}\text{Ti}_{1/2})\text{O}_3]$ where $x = 0.54$ is the morphotropic phase boundary composition, was studied for high temperature ferroelectric applications. The stoichiometry of MPB ceramics were adjusted by controlling A-site occupancy of Pb and Bi. It was found that the stoichiometric composition had dielectric permittivity and loss, at 1 kHz, of 1490 and 0.049 at room temperature respectively. Piezoelectric properties measured included: $\text{Pr} = 31.0 \mu\text{C}/\text{cm}^2$, $E_c = 25.0 \text{ kV}/\text{cm}$, $d_{33} = 340 \text{ pC}/\text{N}$, $d_{33}^* = 896 \text{ pm}/\text{V}$, and a bipolar electromechanical strain of 0.25%. From these data, $T_c = 370\text{C}$ and a depoling temperature of $T_d = 325\text{C}$ was measured. The addition of bismuth increased the piezoelectric properties while decreasing the transition temperatures while the opposite was true for the addition of lead.

4:30 PM

(EMA-S1-045-2013) Cooperative strain accommodation and high piezoelectricity in Sm doped PZT

S. B. Seshadri*, M. M. Nolan, J. S. Forrester, J. C. Nino, University of Florida, USA; P. A. Thomas, University of Warwick, United Kingdom; J. L. Jones, University of Florida, USA

It is well established that large piezoelectric properties are obtained in lead zirconate (PZT) ceramics by chemical substitution and by using a zirconium to titanium ratio close to the morphotropic phase boundary. In this work, we demonstrate a different method of obtaining large piezoelectric properties. New results are shown in the classic PZT system that evidence unexpectedly high values of the piezoelectric coefficients at elevated temperatures. It is shown that incorporation of 2 at% Sm alters the ferroelectric to paraelectric phase transition characteristics in PZT and gives rise to piezoelectric coefficients up to 915 pm/V. These values are around twice that observed when using other donor substitution schemes such as Nb and La (477 pm/V and 435 pm/V, respectively). High-resolution X-ray diffraction from a synchrotron source is used to study the structural changes that occur during the ferroelectric to paraelectric phase transitions in Sm doped PZT and these results are compared to doping with other donor dopants, Nb and La. The effects of thermal cycling on the temperature-dependent piezoelectric coefficients of these doped PZT compositions are also studied, and provide insight into the nature of the origin of the effect.

4:45 PM

(EMA-S1-046-2013) On the origin of high piezoresponse in $\text{BiScO}_3\text{-PbTiO}_3$

L. Kodumudi Venkataraman*, Indian Institute of Science, India; A. N. Fitsch, European Synchrotron Radiation Facility, France; R. Ranjan, Indian Institute of Science, India

The Morphotropic Phase Boundary (MPB) based solid solution $x\text{BiScO}_3\text{-(1-x)PbTiO}_3$ has gained considerable importance in recent

years as a high temperature high performance ($T_c=450^\circ\text{C}$ and $d_{33}=460\text{pC}/\text{N}$) piezoelectric material. The MPB in this system is a mixture of tetragonal and monoclinic phases. Using high resolution synchrotron x-ray diffraction on poled and unpoled specimens in the MPB region, we have demonstrated that the most important factor responsible for giving anomalous piezoresponse is not primarily the co-existing phase fractions in the unpoled state; rather it is the considerably enhanced lattice polarizability of both the co-existing phases. The monoclinic phase fraction decreased by 20% on application of the field and the lattice parameters also revealed a 3-5 times more change for the composition exhibiting the highest d_{33} whereas the changes observed for other neighboring compositions were insignificant. The present results suggest low energy polarization rotation pathway towards the [001] direction in the (1-1 0) pseudocubic plane for the composition exhibiting the highest piezoelectric response.

S2: Multiferroic Materials and Multilayer Ferroic Heterostructures: Properties and Applications

Properties and Device Applications

Room: Coral A

Session Chair: Melanie Cole, U.S. Army Research Laboratory

2:00 PM

(EMA-S2-029-2013) Voltage Control of Magnetism in Multiferroic Heterostructures and Low-Power Devices (Invited)

N. Sun*, Northeastern University, USA

The coexistence of electrical polarization and magnetization in multiferroic materials provides great opportunities for realizing effective electric field control, or vice versa, through a strain mediated magneto-electric interaction effect in layered magnetic/ferroelectric multiferroic heterostructures. Strong magneto-electric coupling has been the enabling factor for different multiferroic devices, which however has been hard to achieve, particularly at RF/microwave frequencies. In this presentation, I will cover the most recent progress on novel layered microwave multiferroic heterostructures and devices. We will demonstrate strong magneto-electric coupling in novel microwave multiferroic heterostructures. These multiferroic heterostructures exhibit a giant electrostatically tunable magnetic field of 3500 Oe, and a high electrostatically tunable ferromagnetic resonance frequency range between 1.75~7.57 GHz. At the same time, we will demonstrate E-field modulation of anisotropic magnetoresistance, giant magnetoresistance and exchange bias at room temperature in different multiferroic heterostructures. New multiferroic devices will also be covered in the talk, including RF magneto-electric sensors, multiferroic voltage tunable bandpass filters, voltage tunable inductors, tunable bandstop filters, tunable phase shifters and spintronics.

2:30 PM

(EMA-S2-030-2013) Voltage Tunable Acoustic Resonance in Perovskite Thin Films (Invited)

N. M. Sbrockey*, G. S. Tompa, Structured Materials Industries, Inc., USA; T. S. Kalkur, University of Colorado at Colorado Springs, USA; M. W. Cole, U.S. Army Research Laboratory, USA; J. Zhang, S. P. Alpay, University of Connecticut, USA

Resonator devices are critical components in radio frequency (RF) communication, radar and wireless data applications. Materials which show voltage tunable, or voltage switchable acoustic resonance can simplify design and manufacture of RF systems, as well as enable frequency agile operation. This study is investigating RF resonator devices based on paraelectric $\text{Ba}_x\text{Sr}_{1-x}\text{TiO}_3$ (BST) and SrTiO_3 thin films. The ability to switch the resonator on/off, and to tune the resonance frequency using a low voltage control signal has been demonstrated for films prepared by both metal organic solution deposition (MOSD) and by metal organic chemical vapor deposition

(MOCVD). The BST and SrTiO₃ films were characterized by XRD, SEM and AFM, to correlate the material properties of the films with the electro-acoustic properties of the resonator. The electromechanical coupling efficiency is shown to depend strongly on the properties of the perovskite film.

2:45 PM

(EMA-S2-031-2013) Growth and Ferromagnetic Resonance Properties of Nanometer-Thick Yttrium Iron Garnet Films (Invited)

M. Wu*, Colorado State University, USA

Growth of nm-thick yttrium iron garnet films and ferromagnetic resonance (FMR) linewidth properties in the films will be reported. The films were grown on gadolinium gallium garnet substrates by pulsed laser deposition (PLD). Films in the 5-35 nm thickness range showed a (111) orientation and a surface roughness between 0.1-0.3 nm. The 10 nm films showed a 10 GHz FMR linewidth of about 6 Oe and a damping constant of 3.2×10^{-4} . The FMR linewidth increases with both the surface roughness and the surface Fe deficiency. Thicker films exhibit a smaller FMR linewidth and a lower damping constant.

3:00 PM

(EMA-S2-032-2013) Nonlinear dynamics of multiferroic cantilevers (Invited)

T. Onuta*, University of Maryland, USA

In the emerging hybrid field of spintronics and straintronics, multiferroic materials play an important role due to coexistence of ferromagnetism and ferroelectricity as well as their coupling. In heterostructured systems, strong magnetoelectric (ME) coupling is observed due to strain-mediated interaction across the interface between magnetostrictive and piezoelectric phases. We demonstrate read-write-read-erase cyclical mechanical-memory properties of all-thin-film multiferroic heterostructured cantilevers when a high voltage is applied on the PZT piezo-film. The device state switching process occurs due to the presence of a hysteresis loop in the piezo-film frequency response. The reference frequency at which the strain-mediated FeGa₂-based multiferroic device switches can also be tuned by applying a DC magnetic field bias that contributes to increase of the cantilever effective stiffness. The switching dynamics is mapped in the phase space of the device transfer function characteristic for such high piezo-film voltage excitation, providing additional information on the dynamical stability of the devices. We also show DC magnetic field or DC voltage-based state switching characteristics of an AC magnetically-driven multiferroic device for logic implementation.

3:15 PM

(EMA-S2-033-2013) Mechanism of microwave loss in practical high performance dielectrics (Invited)

N. Newman*, L. Liu, A. Matusевич, M. Flores, Arizona State University, USA

This work identifies the mechanism of microwave loss in practical high performance dielectrics, including those based on Ba(Zn_{1/3}Ta_{2/3})O₃, Ba(Zn_{1/3}Nb_{2/3})O₃, ZrTiO₄ and BaTi₄O₉/Ba₂Ti₉O₂₀. Dopants are added to these materials to improve the properties in order to (a) tune the temperature coefficient of resonant frequency to near zero, (b) reduce the loss tangent and (c) improve the manufacturability of the material by facilitating shorter annealing times. In this study, we use microwave resonators whose quality factors (Qs) are limited by dielectric loss to quantitatively measure the temperature (2-300 K) and magnetic field (0-9 Tesla) dependent loss tangent. These results, combined with pulsed Electron Paramagnetic Resonance (EPR) measurements, shows conclusively that microwave loss in transition-metal doped Ba(Zn_{1/3}Ta_{2/3})O₃ at cryogenic temperatures is due to resonant spin excitations of unpaired transition metal d-electrons in isolated atoms (light doping) or exchange coupled clusters (moderate to high doping); a mechanism that differs from the usual suspects. We also characterize and identify the factors that contribute to microwave loss at room temperature.

3:30 PM

(EMA-S2-034-2013) Material Advancement Needs for Efficient Pyroelectric Power Generation and Cooling (Invited)

S. Annapragada*, J. V. Mantese, T. D. Radcliff, United Technologies Research Center, USA

Direct energy-conversion devices are receiving significant attention stemming from a need for cleaner, efficient technologies. Pyroelectric-based power generation and cooling is one such technology, but until recently it has suffered from low efficiencies and power levels and has been restricted to infrared detection and imaging applications. New system-level innovations present an opportunity to provide direct cooling and generate significant electricity from wasted energy in the exhaust of vehicles and other combustion processes at improved efficiencies, enabling reduced use of fossil fuel. These innovations have the potential to cause game changes in transportation, industrial process, and military applications as a substitute for fossil fuel-based systems. Carnot efficiencies in excess of 50%, power densities in excess of 100 W/l and temperature lifts in excess of 10 K have been reported. However to compete with the current technologies, further innovations in materials engineering are required. This work investigates how a successful pyroelectric-based energy recovery and cooling system can be realized and identifies the material advances needed to make it a reality. Requirements for both future energy generation and cooling materials to make them practicable will be presented; including: thermal, mechanical, and electrical.

3:45 PM

(EMA-S2-035-2013) Giant Electrocaloric Effect in Relaxor Ceramic Materials for Dielectric Refrigeration

Z. Kutnjak*, B. Rozic, B. Malic, H. Ursic, J. Holc, M. Kosec, Jozef Stefan Institute, Slovenia; Q. M. Zhang, The Pennsylvania State University, USA

Materials with large electrocaloric effect (ECE) have the promise of realizing dielectric refrigeration which is more efficient and environmentally friendly compared to other techniques [1,2]. The electrocaloric effect (ECE) in a given material is related to the conversion of the electrical energy into heat and vice versa. It was shown recently by direct measurements that the large ECE is common in ceramic relaxor ferroelectrics [3,4] and that the electrocaloric responsivity is significantly enhanced in the proximity of the critical point similarly to the enhancement of the giant electromechanical response [5]. A review of recent direct measurements of the large ECE in thick ceramic ferroelectric multilayers, substrate-free thick films, thin films and antiferroelectrics will be given. It was found that the giant ECE is also common in these systems. [1] A. S. Mischenko et al., Science 311, 1270 (2006). [2] B. Neese et al., Science 321, 821 (2008). [3] R. Pirc, Z. Kutnjak, R. Blinc, Q.M. Zhang, Appl. Phys. Lett. 98, 021909 (2011). [4] S.-G. Lu, B. Rozic, Q. M. Zhang, Z. Kutnjak, B. Malic, M. Kosec, R. Blinc, R. Pirc, Appl. Phys. Lett. 97, 162904 (2010). [5] Z. Kutnjak et al, Nature 441, 956 (2006).

S7: Production Quality Ferroelectric Thin Films and Devices

Production Quality Ferroelectric Thin Films and Devices

Room: Coral A

Session Chairs: Glen Fox, Fox Materials Consulting, LLC; Geoff Brennecke, Sandia National Laboratories; Ronald Polcawich, U.S. Army Research Laboratory

4:00 PM

(EMA-S7-001-2013) Development of PZT based ferroelectric capacitor for mass-production ferroelectric RAM (FRAM) (Invited)

T. Eshita*, W. Wang, K. Nakamura, S. Mihara, FUJITSU SEMICONDUCTOR LIMITED, Japan; H. Yamaguchi, K. Nomura, FUJITSU LABORATORIES LIMITED, Japan

Ferroelectric Random Access Memory (FRAM) is a new non-volatile memory which has excellent electric properties of high writing speed and high switching endurance. FUJITSU SEMICONDUCTOR Ltd. has shipped both of embedded and stand-alone FRAM since 1999. In this presentation, we will show the key technologies sputter deposited and MOCVD (metal organic chemical vapor deposition) $\text{Pb}(\text{Zr,Ti})\text{O}_3$ (PZT) based capacitors for mass-production FRAM. Our PZT capacitors have evolved from 5-V operation 0.5- μm CMOS node to 1.8V operation 0.18- μm CMOS node. Interface control of the sputter-deposited PZT/electrode is found to be crucial for decreasing the operation voltages. In this purpose we have developed new buffer layers and annealing technique. In the MOCVD PZT based capacitor fabrication for high density FRAM, control of PZT/electrode interface is also essential to improve the surface morphology of PZT. The key issue for low voltage and high density FRAM is ensuring reliability such as charge retention with high switching endurance. With each FRAM generation, we have achieved high reliability with a 10-year guarantee.

4:30 PM

(EMA-S7-002-2013) Development of Process Technology for Ferroelectric Thin Film Application (Invited)

K. Suu*, ULVAC, Inc., Japan

Recently thin-film ferroelectrics such as $\text{Pb}(\text{Zr, Ti})\text{O}_3$ (PZT) and $(\text{Ba, Sr})\text{TiO}_3$ (BST) have been utilized to form advanced semiconductor and electronic devices including Ferroelectric memory (FeRAM), actuators composing gyro meters, portable camera modules, and tunable devices for smart phone applications and so on. Processing technology of ferroelectric materials is one of the most important technologies to enable the above-mentioned advanced devices and their productions. PZT sputtering and plasma etching has been proven for years as reliable production technology through FeRAM and MEMS production. In addition MOCVD and high-temperature plasma etching technologies are in the final stage toward next-generation device productions. Moreover, as applications to the next generation storage, the ferroelectric probe memory development for ultra-high density memories is also performed, and the epitaxial technology for the ferroelectric thin film is under development. In this paper, we will report our development results of ferroelectric thin film processing technologies including sputtering, MOCVD and plasma etching as well as manufacturing processes for FeRAM, MEMS (actuators, tunable devices) and ultra-high density probe memory.

5:00 PM

(EMA-S7-003-2013) Sputtered Nb-doped PZT Film with Giant Piezoelectricity for MEMS Applications (Invited)

Y. Hishinuma*, Y. Li, J. Birkmeyer, FUJIFILM Dimatix, USA; T. Fujii, T. Naono, T. Arakawa, FUJIFILM Corporation, Japan

Lead zirconate titanate (PZT) films are of great interest for MEMS devices including sensors, actuators, and energy harvesting because of

its large piezoelectric coefficient. Various deposition methods have been developed including sol-gel, sputtering, and CVD. However, to date, no thin films with sufficiently high piezoelectric properties with good compatibility to MEMS processes have been achieved. We have developed a method of forming PZT films on silicon substrates with a high piezoelectric coefficient using RF sputtering. Films have been formed on 6" wafers with thickness variation of less than +/-5% across the entire wafer with unusually high content of Nb dopant (13%) which results in x1.7 higher piezoelectric coefficient than sputtered PZT films previously reported. The x-ray diffraction patterns of our PZT film demonstrate that film is in a perovskite phase with (100) orientation which partly accounts for its high piezoelectric performance. One of the unique properties of our sputtered PZT film can be observed in the hysteresis loop shifted to the positive electric field, suggesting that the polarization axes have been aligned in a certain direction beforehand, making a post-deposition polarization process unnecessary. A displacement measurement using a diaphragm structure yielded $d_{31} = -250\text{pm/V}$. Additionally, 4-point cantilever bending measurement was conducted yielding $e_{31,f} = -25\text{C/m}^2$.

S9: Thin Film Integration and Processing Science

Novel Substrates

Room: Mediterranean B/C

Session Chair: Glen Fox, Fox Materials Consulting, LLC

2:00 PM

(EMA-S9-015-2013) PZT based PiezoMEMS for RF Systems (Invited)

R. G. Polcawich*, J. Pulskamp, T. Ivanov, S. Bedair, R. Proie, L. Sanchez, C. Meyer, US Army Research Laboratory, USA

This presentation will discuss several key aspects necessary to create devices for use in RF systems with a focus on switches, filters, and tunable inductors. Specific topics will include residual stress control, influence of texture control, and integration of lead zirconate titanate (PZT) thin film processing with multilayer Cu processing. Using chemical solution processing of PZT (52/48) thin films combined with surface and bulk micromachining, a wide array of devices can be created to facilitate performance improvements and/or enable new capabilities for RF systems including cellular phones, tactical radios, and radar systems. As a circuit control element, PZT actuated RF switches and relays have been demonstrated operating at voltages as low as a few volts while providing isolation better than -50 dB and insertion loss better than 0.3 dB from DC to 6 GHz. For signal filtering, PZT based resonators and filters offer devices exhibiting better than 60 dB of rejection with insertion losses better than 3 dB at VHF. Combining PZT actuators with a multilayer Cu process, extremely tunable inductors are possible achieving tuning ratios in excess of 2:1 in the range of a few GHz.

2:30 PM

(EMA-S9-016-2013) Sputtered PZT Thin Films on Copper Foils

J. Walenza-Slabek*, B. J. Gibbons, T. Ansell, Oregon State University, USA; R. G. Polcawich, U.S. Army Research Laboratory, USA

Lead zirconate titanate (PZT) thin films on copper foils were produced using RF magnetron sputtering and ex situ annealing in controlled atmospheres. The oxygen environment was controlled by combination of a forming gas atmosphere and use of a copper foil envelope, which buffered the oxygen partial pressure during heating and cooling. Films with low loss tangent (<5%) were produced with dielectric constants of ≈ 500 . No interfacial layer was detected in cross-sectional SEM imaging, however a second phase was observed on the surface. Spin casting and annealing a PbO sol-gel layer on the surface was found to eliminate this second phase. The remanent polarization was 20-35 $\mu\text{C}/\text{cm}^2$. The linear Rayleigh behavior, charac-

terizing the sub-switching AC field response of the domain walls, was determined. An analysis of the hysteresis according to the Preisach formalism is presented. The irreversible components of the dielectric constant and hysteresis are compared for films of varying thickness and processing conditions. Finally, cantilever energy harvesters were fabricated and tested. Device output as a function of frequency was compared with a model based on the Euler-Bernoulli beam equations. The resonant frequencies of the cantilevers, 20-40 Hz, were found to match the model well. Modeled peak-to-peak voltage was highly dependent on material parameters but typical values gave an expected output of 10-40 mV which match the observed values well.

2:45 PM

(EMA-S9-017-2013) The roles of solution chemistry, substrate, and pyrolysis temperature on the chemical heterogeneity in PZT films

J. Ihlefeld*, P. G. Kotula, B. D. Gauntt, G. L. Brennecke, D. V. Gough, E. D. Spörke, Sandia National Laboratories, USA

Recent investigations have revealed that Pb(Zr,Ti)O₃ films prepared via an inverted mixing order (IMO) chelate chemistry on Pt/ZnO/SiO₂/Si substrates possess improved ferroelectric and dielectric responses and that these responses are due to improved chemical homogeneity compared to those prepared on conventional Pt/Ti/SiO₂/Si substrates. In this presentation we have investigated the roles of solution chemistry, substrate metallization stack, and pyrolysis temperature on chemical homogeneity and the resulting properties. We will show that films prepared from traditional sol-gel chemistries possess chemical gradients regardless of substrate metallization stack and pyrolysis temperature. Films prepared from IMO chemistries do not possess chemical gradients when prepared on substrates devoid of titanium adhesion layers, but do possess gradients when a titanium adhesion layer is used. The resulting film crystallographic textures and ferroelectric properties will also be discussed. Sandia is a multiprogram laboratory operated by Sandia Corporation, a wholly owned subsidiary of Lockheed Martin Company, for the United States Department of Energy's National Nuclear Security Administration under contract DE-AC04-94AL85000.

3:00 PM

(EMA-S9-018-2013) Alternative Adhesion Layers for Noble Metal/Si substrates - Impact on PZT Thin Films for MEMS Devices (Invited)

P. Mardilovich*, J. Abbott, Hewlett-Packard Company, USA; C. Shelton, North Carolina State University, USA; W. Stickle, G. Long, Hewlett-Packard Company, USA; E. Patterson, K. Brookshire, B. Maack, S. Freyand, B. Gibbons, Oregon State University, USA

Zinc oxide based systems, ZnO, ZTO (ZnO:SnO₂), and IGZO (In₂O₃:Ga₂O₃:ZnO) were used as an adhesion layer between noble metals and an SiO₂/Si substrate. Effects of high temperature anneals were studied with respect to interaction of SiO₂ and ZnO-based systems. TEM, TEM-EDS, XRD, AFM and XPS depth profiling were used to understand the degree of material interaction, segregation, and crystallization after these heat treatments. Pt films deposited on ZnO, ZTO and IGZO annealed at temperatures up to 1000°C were used for deposition of PZT films by chemical solution methods. It was demonstrated that with these adhesion layers, the PZT performance could be as good as e₃₁f of 12 C/m². This high performing PZT was achieved due to the preferential <100> texture of PZT deposited on Pt with ZnO-based adhesion layers. Other application areas of ZnO-based adhesion layers will also be presented.

Controlling Phase Assemblage and Stoichiometry II

Room: Mediterranean B/C

Session Chair: Christopher Shelton, NCSU

4:00 PM

(EMA-S9-019-2013) Role of boundaries on the low-field magnetotransport properties of (La_{0.7}Sr_{0.3}MnO₃)_{1-x}(ZnO)_x nanocomposite thin films (Invited)

A. Chen, W. Zhang, Texas A&M University, USA; Z. Bi, Q. Jia, Los Alamos National Laboratory, USA; J. L. MacManus-Driscoll, University of Cambridge, United Kingdom; H. Wang*, Texas A&M University, USA

The role of boundaries including grain boundary (GB) and phase boundary (PB) on low-field magnetoresistance (LFMR) properties have been studied in La_{0.7}Sr_{0.3}MnO₃ (LSMO):ZnO vertically aligned nanocomposite (VAN) thin films. The LFMR of the nanocomposite films is greatly enhanced especially close the percolation threshold, due to the increased GB and PB effects. Interestingly, the LFMR and PB effect can be strongly tuned by both the deposition frequency and the secondary phase composition in the heteroepitaxial VAN films on SrTiO₃ substrates. And the LFMR and PB of the polycrystalline nanocomposite samples on sapphire substrates can be controlled by the doping composition but not the deposition frequency. These results demonstrate either GB or PB would enhance the LFMR and the enhanced LFMR by the network of both GB and PB can be achieved with the secondary phase content approaching the percolation threshold.

4:30 PM

(EMA-S9-020-2013) Effects of Pb-excess in Pb(Zr_{0.52}, Ti_{0.48})O₃, PZT(52/48), Thin Films for Use in Multilayer Actuators

L. M. Sanchez*, Army Research Laboratory, USA; G. Fox, Fox Materials Consulting LLC, USA; I. Takeuchi, University of Maryland, USA; R. G. Polcawich, Army Research Laboratory, USA

(001) oriented Lead Zirconate Titanate, PZT, films at the (52/48) Zr/Ti ratio has shown substantial improvements in properties. During the annealing PZT (52/48), lead (Pb) is volatilized from the films leading to a non-stoichiometric state and a deformation in the PZT unit cell which ultimately reduces the electrical properties. To remedy this issue, a percentage of Pb-excess is added to the PZT solution prior to deposition to compensate for the Pb that is lost during the thermal treatment. In the opposite case where there is an excess of Pb in the final film, the Pb atoms create conduction pathways leading to shorting and breakdown of devices. An initial study of using 8%, 10%, and 15% Pb-excess in the solution, showed that by using 10% Pb-excess 88% improvements in cantilever deflection were observed at 2V and 105% improvement at 10%. Problems with device breakdown at higher voltages were reported in other PZT MEMS devices. This study thoroughly examines the effects of the Pb-excess in the PbTiO₃ seed layer with percentages of 0%, 10%, 15%, 20%, and 30% and PZT (52/48) with Pb-excesses of 0%, 3%, 5%, 8%, and 10% combined in varying ratios. The x-ray diffraction (XRD), electrical properties, and displacement of cantilevers will be analyzed to determine effects of Pb-excess on orientation and film properties.

4:45 PM

(EMA-S9-021-2013) Influence of the precursor chemistry on the formation of the perovskite phase in PMN-PT thin films

A. Veber*, Institut "Jozef Stefan", Slovenia; S. Kunej, Institut "Jozef Stefan", Slovenia; M. Spreitzer, Institut "Jozef Stefan", Slovenia; A. Vorobiev, S. Gevorgian, Chalmers University of Technology, Sweden; D. Suvorov, Institut "Jozef Stefan", Slovenia

This work examines the synthesis and characterization of Pb(Mg_{1/3}Nb_{2/3})O₃-PbTiO₃ (PMN-PT) thin films prepared on Pt(111)/TiO₂/SiO₂/Si substrates using the sol-gel method for FBARs sensor applications. In order to determine the influence of the coordination chemistry on the formation of the perovskite the condi-

tions of the reagents were systematically varied. Various sources of Mg- and Pb-precursors were applied to reduce the concentration of the undesired pyrochlore phase that forms in addition to the perovskite phase. A pyrochlore-free PMN-PT film was formed when the steric hindrance of the Pb precursor was increased. Thus, Pb(PVP)₂ and Pb(AcAc)₂ were shown to be effective in the formation of pyrochlore-free thin films. It was observed that during the direct casting of the film on the Pt (111) substrate the film grows preferentially in the (100) direction. A predominant change in the growth direction from (100) to (111) was achieved by the initial casting of a thin, TiO₂ undercoat. The prepared films were dense and crack-free. The phase composition of the thin films was characterized by means of X-ray diffraction (XRD) and infrared spectroscopy (FT-IR), whereas the morphology and the thickness of the thin films were studied with scanning electron microscopy (SEM). The relative permittivity and dielectric losses were found to be 1600 and 0.12, respectively.

5:00 PM

(EMA-S9-022-2013) Control of Crystallographic Texture and Surface Morphology of Pt/TiO₂ Templates for Enhanced PZT Thin Film Performance

A. Fox*, Oregon State University, USA; G. Fox, Fox Materials Consulting LLC, USA; B. Gibbons, Oregon State University, USA; S. Trolier-McKinstry, Penn State University, USA

Optimized processing conditions for Pt/TiO₂ templating electrodes for {001} textured lead zirconate titanate (PZT) films were investigated. Titanium deposited by dc magnetron sputtering yields [0001] texture on a thermally oxidized Si wafer. It was found that the extent of this texture depends on the deposition time, pressure, power, and the chamber pre-conditioning. When oxidized, titanium yields [100] oriented rutile. This seed layer has a lattice mismatch of 6.2% in the [001] direction and 4.6% in the [010] direction with Pt. As a result, it was possible to achieve strongly oriented [111] Pt. The quality of the orientation and surface roughness of the TiO₂ and the Ti directly affect the achievable Pt texture and surface morphology. A 300 nm Ti layer deposited at 10 W/cm² and 2 mTorr yielded a rocking curve full width at half maximum (FWHM) of 4.4° and a RMS roughness of 0.6 nm. Increased thickness resulted in lower FWHM (3.3°) and increased roughness (1.1 nm). Thicker Ti yields a Pt layer with higher FWHM (1.9°) than thinner Ti (1.5°), however the surface roughness of the Pt correlates with that of the underlying Ti. Further details on the relationship between processing and achievable texture and surface morphologies will be presented.

5:15 PM

(EMA-S9-023-2013) Peculiarities of PZT Films Produced by Different Technologies for MEMS

N. Korobova*, S. Timoshenkov, V. Vodopyanov, National Research University of Electronic Technology, Russian Federation

Lead-zirconate-titanate (PZT) is a typical ferroelectrical material with outstanding properties. The preparation behavior of PZT composite films comprised of Si, SiO₂, Pt, PZT and Pt for MEMS applications was investigated. The choice of precursors can affect the microstructures and properties of the product, so in this paper we compared the crystallization behavior of PZT films derived from different precursors, stressing the influence of experiment conditions. Dense PZT films were prepared by electrophoretic deposition method (EPD), using commercial powder PZT precursor and metal alkoxide components for the same composition. Some specific comments were underlined about structure of PZT films. The PZT films were crack-free and have good morphology. The PZT films with perfect perovskite structure have excellent piezoelectric property. Ferroelectric hysteresis loops are measured, and the remnant polarization (Pr) of the PZT films was about 25mC/cm² and the coercive field (EC) is about 27kV/cm. In the radio-frequency (RF) region, the dielectric constant is about 350 and the dielectric loss is less than 0.01.

S10: Ceramic Composites for Defense Applications

Nano-composites

Room: Pacific

Session Chair: Edward Gorzkowski, Naval Research Laboratory

2:00 PM

(EMA-S10-001-2013) Dielectric Film Development for Naval Pulse Power Applications (Invited)

P. Armistead*, Office of Naval Research, USA

The Navy envisions moving to platforms with increased capability to handle a wide variety of energy demands electrically. This will require the use of large capacitors for storage, conditioning, and pulse power applications. Though the Navy does not have the extreme weight and temperature constraints found in many aeronautics applications, ships handle a lot of power and are of finite size so energy density and cost are drivers for energy storage devices. The ONR Dielectric Materials basic research program has focused on developing processable dielectric materials for high energy density wound film capacitors for pulse power applications. In this talk, we will present the device and materials requirements for some Navy energy storage applications and then discuss some promising areas of research including ferroelectric polymers, multi-layered dielectrics, and composite dielectrics. For the composite dielectrics we will present the strengths and weaknesses of this approach based on computational studies and present some experimental results.

2:30 PM

(EMA-S10-002-2013) Piezoelectric and Dielectric Enhancement of New Nano-structured Ceramics with High Density of Heteroepitaxial Interface by MPB Engineering (Invited)

S. Wada*, University of Yamanashi, Japan

Barium titanate (BaTiO₃, BT) and potassium niobate (KNbO₃, KN) (BT-KN) nano-structured ceramics with artificial morphotropic phase boundary (MPB) structure were successfully prepared by solvothermal method at temperatures below 230 deg. C. Various characterizations confirmed that the BT-KN nano-structured ceramics exhibited BT/KN molar ratio of 1, a porosity of around 30 % and heteroepitaxial interface between BT and KN. Their apparent piezoelectric constant d₃₃* was estimated at 136 pC/N, and was three times larger value than that of the 0.5BT-0.5KN dense ceramics. The concept proposed in this study can be a new way to create piezoelectric ceramics with artificial MPB region. Moreover, this method is very universal and applied into various functional materials such as magnetic, conductive, semi-conductive, and optical materials in addition to dielectric, piezoelectric and ferroelectric materials. In the future, we will develop various new materials with heteroepitaxial interfaces on the basis of the concept.

3:00 PM

(EMA-S10-003-2013) Polymer-MOF Composites for Dielectric Materials

L. N. Appelhans*, Sandia National Laboratory, USA

Improvement in dielectric performance is a key challenge to increase energy density of polymer-based capacitors. Polymer-inorganic nanocomposites have shown promise as high performance dielectric materials and can exhibit superior properties relative to dielectrics based on ceramics or polymers alone. However, difficulty in controlling nanoparticle dispersion and agglomeration is detrimental to electrical properties. The use of metal-organic frameworks as the filler component of the composite introduces a wide variety of new materials with unique structures, properties, and surface functionalities that may result in improved dielectric properties of MOF-polymer composites relative to inorganic-polymer composites. This work examines the use of metal organic frameworks (MOFs) as the filler phase in

polymer-MOF composite dielectric materials. Comparison of composite dielectric permittivity and breakdown strength to polymer alone will be presented, as well as the influence of particle size and loadings on the electrical properties of the composites. Sandia National Laboratories is a multi-program laboratory managed and operated by Sandia Corporation, a wholly owned subsidiary of Lockheed Martin Corporation, for the U.S. Department of Energy's National Nuclear Security Administration under contract DE-AC04-94AL85000.

3:15 PM

(EMA-S10-004-2013) Synthesis and Characterization of Nanoparticle/Nanocrystalline Barium Titanate and PLZT for Functional Nanoparticle-Polymer Composites

C. DiAntonio*, T. Monson, M. Winter, T. Chavez, P. Yang, Sandia National Laboratories, USA

Attractive for numerous technological applications, ferroelectric oxides constitute an important class of multifunctional compounds. Intense experimental efforts have been made recently in synthesizing, processing and understanding functional ferroelectric nanostructures. This work will present the systematic characterization and optimization of barium titanate and lead lanthanum zirconate titanate nanoparticle based ceramics. The nanoparticles have been synthesized using several solution and pH-based synthesis processing routes and employed to fabricate polycrystalline ceramic and functional nanocomposite/nanostructured components. The dielectric and ferroelectric properties of these various components have been gauged by impedance analysis and electromechanical response and will be discussed. Sandia National Laboratories is a multi-program laboratory managed and operated by Sandia Corporation, a wholly owned subsidiary of Lockheed Martin Corporation, for the U.S. Department of Energy's National Nuclear Security Administration under contract DE-AC04-94AL85000.

Piezo-composites/Extreme Environments

Room: Pacific

Session Chair: Charles Stutz, AFRL/MLPS

4:00 PM

(EMA-S10-005-2013) Composite Electronic Materials for Capacitive Devices (Invited)

C. Randall*, Penn State University, USA

Given the importance of phase connectivity in dielectric materials, we will review a number of novel concepts that are being explored for new materials. This includes ceramic-polymer composites with filler structuring that minimizes space-charge and enhances dielectric breakdown. We also consider core-shell microstructure in alkali-niobate dielectrics that have high temperature characteristics suitable for power capacitors. We also consider space charge enhanced ionic conductors for supercapacitor applications.

4:30 PM

(EMA-S10-006-2013) Bi(Zn_{0.5}Ti_{0.5})O₃ – BaTiO₃ Composites for Pulsed Power Applications

E. Gorzkowski*, M. Pan, Naval Research Laboratory, USA; G. Brennecke, H. Brown-Shaklee, Sandia National Laboratories, USA

In previous research freeze-casting was used to construct ceramic-polymer composites in which the two phases are arranged in an electrically parallel configuration. By doing so, the composites exhibit dielectric constant (K) up to two orders of magnitude higher than that of composites with ceramic particles randomly dispersed in a polymer matrix. This technique has been successful with both an aqueous and camphene based ceramic slurry that is frozen uni-directionally to form templates such that ceramic aggregates are aligned in the temperature gradient direction. Freeze-casting is a versatile processing technique that has been demonstrated to work with many ceramic systems. In this paper we will discuss the continued study of freeze-

cast processing of composites based around non-saturating Bi(Zn_{0.5}Ti_{0.5})O₃ – BaTiO₃ ceramics for use in high power capacitor applications. The processing parameters, composite dielectric properties, and composite microstructure will also be presented.

4:45 PM

(EMA-S10-007-2013) Investigation of Tunable Bulk Microwave Dielectrics

E. Furman*, B. A. Jones, S. E. Perini, M. T. Lanagan, Pennsylvania State University, USA; S. Kwon, W. Hackenberger, R. Sahul, TRS Technologies, Inc, USA

Tunable microwave bulk dielectrics are of great interest in developing high power phased array antennas and phase shifters, tunable metamaterials, and pulse forming nonlinear transmission lines. To achieve high power and high tunability we have focused on developing Barium Strontium Titanate (BST) and Barium Strontium Zirconate Titanate (BSZT) doped and undoped ceramic dielectrics with high breakdown strength and reliability. To achieve high breakdown strength we prepared dielectrics with the reduced grain size and minimized porosity. One mol. % Mn doping lead to 33% increase in Q for BST ceramics compared to the undoped samples. Composite BST-magnesium oxide and BST- magnesium titanate were prepared with good quality factor (highest Q of 385 at 3.7 GHz) and having moderate dielectric constant (k in the range of 185 to 414). The highest tunability of 85% at 160 kV/cm was obtained in BSZT ceramics which tend to have higher dielectric constant than the BST ceramics. In nominally single phase ceramics, porosity effectively acts as a second phase leading to a substantial reduction in the breakdown strength. Monte Carlo modeling of the effect of porosity on the breakdown strength and Weibull modulus of ceramics will be presented. The model indicates the importance of the ratio of pore size to sample size.

5:00 PM

(EMA-S10-008-2013) Bio-dielectric Hybrid Films for Capacitor Applications

D. Joyce*, Air Force Research Laboratory, USA; F. Ouchen, N. Venkat, S. R. Smith, University of Dayton Research Institute, USA; K. M. Singh, UES, Inc., USA; J. G. Grote, Air Force Research Laboratory, USA

DNA-based bio-dielectrics incorporating sol-gel have potential utilization for energy storage applications. Salmon DNA hybrid films incorporating sol-gel have increased dielectric constants and environmental stability compared to DNA only films. Based on the University of Arizona's research into DNA/sol-gel, thin film devices were made and characterized showing stability in dielectric values and reliability in voltage breakdown measurements, attaining values consistently at 300 v/um. Dielectric characterization will continue investigating frequency and temperature dependence.

S12: Recent Developments in High Temperature Superconductivity

Superconductor Applications II—Large-Scale and Hybrid Energy Storage and Machine Technologies

Room: Indian

Session Chair: Haiyan Wang, Texas A&M University

2:00 PM

(EMA-S12-030-2013) Superconductivity: Rising to the Energy Challenges (Invited)

Q. Li*, Brookhaven National Lab, USA

Superconductors offer powerful opportunities for increasing capacity, reliability, and efficiency of the electricity grid. The mismatch between variation of renewable energy resources and electricity demand makes it necessary to capture electricity for later use. Developing affordable, large-scale energy storage systems would be a

game-changing advance for the grid. Superconducting magnet energy storage systems (SMES) use magnetic fields in superconducting coils to store energy with near zero energy loss, and have instantaneous dynamic response. Superconducting coils can also provide a lower cost alternative to the rare-earth permanent magnet or geared systems for high power (> 10 MW) direct-drive wind turbines. In this presentation, I will discuss the major challenges for energy applications of superconductivity, followed by highlighting several application projects currently being carried out at Brookhaven Lab in collaboration with leading superconducting wire manufacturers and power system industry.

2:30 PM

(EMA-S12-031-2013) Compensation for Fluctuating Output of Solar Photovoltaic and/or Wind Power with a Hybrid Energy Storage System Composed of MgB₂ SMES and Hydrogen Storage Systems (Invited)

M. Tsuda*, D. Miyagi, Tohoku University, Japan; T. Hamajima, Hachinohe Institute of Technology, Japan; T. Shintomi, Nihon University, Japan; Y. Makida, KEK, Japan; T. Takao, Sophia University, Japan; M. Kajiwara, Iwatani Corporation, Japan

Efficient use of natural energy such as solar photovoltaic and wind energy is very important to realize a sustainable society in the future. However, integrating a large amount of fluctuating solar photovoltaic and wind energy into the utility grid causes various adverse effects on the reliability of the utility grid. Some energy storage systems are required to use the natural energy efficiently and adapt the output power of the natural energy sources to a power demand. The output power of the solar photovoltaic and wind energy sources can be separated into short cycle and long cycle components. We investigated the suitable compensation method for fluctuating output of solar photovoltaic and/or wind power with a hybrid energy storage system composed of MgB₂ SMES for the short cycle component and a hydrogen storage system with fuel cell, electrolyzer, and hydrogen storage tank for the long cycle component. Use efficiency of the natural energy was greatly influenced by the input-output control methods of SMES, fuel cell, electrolyzer that depended on the amount of electricity supplying to the utility grid.

3:00 PM

(EMA-S12-032-2013) Winding Technology of Fully-Superconducting Induction/Synchronous Machine for Next Generation Automobile Application (Invited)

T. Nakamura*, S. Misawa, H. Kitano, H. Shimura, T. Nishimura, N. Amemiya, Kyoto University, Japan; Y. Itoh, M. Yoshikawa, T. Terazawa, IMRA Material R&D Co., Ltd, Japan; N. Okumura, IAISIN SEIKI Co., Ltd., Japan

This paper will report on the development status of high temperature superconducting induction/synchronous machine (HTS-ISM) for next generation automobile. Winding technology for the realization of fully-superconducting HTS-ISM is mainly reported in this paper. Our target temperature is around 77 K in order to maintain the higher cooling efficiency of the cryocooler. Sumitomo's DI-BSCCO tapes are currently utilized for the windings, because of their longitudinal homogeneity of critical current and the slower take-off of the electric field vs. current density curve (n-value) compared to that of YBCO tapes. The appropriate n-value of the windings is important for the effective introduction of the flux-flow (nonlinear dissipative) state to the optimal operation of the HTS-ISM in the variable speed control mode. Rotor windings are so-called squirrel-cage type, and three-phase stator windings are realized by means of the racetrack-shaped double pancake coils. Especially, design technique of the stator windings, which takes into account the allowable bending radius, critical current degradation in the stator (iron) core, is explained in detail. Experimental and analysis results of the DC current transport properties and AC losses of the developed windings are reported and discussed.

3:30 PM

(EMA-S12-033-2013) Applications Using High Temperature Superconducting Tapes

C. Rey*, Tai-Yang Research Co., USA

High temperature superconductors (HTS) are now being applied to a wide variety of electric utility applications including: transformer, cables, and fault-current limiters. Barriers into these commercial utility markets have been difficult to surmount for several reasons but costs remain the primary challenge. Other applications where space, weight, and performance are stronger incentives have had better success achieving limited market penetration. Tai-Yang Research Company of Tallahassee, FL has developed two HTS based products that rely on the reduced weight and higher performance provided by HTS materials. The first is a cryogenic quick connect and disconnect used by the US Navy for their HTS degaussing and HTS mine sweeping systems. These cryogenic quick disconnects operate with cryogenic fluid flow at operating temperatures ranging from ~ 50-70 K. These cryogenic electrical connectors can carry several thousand amps without excessive heating and can be used in other applications such as power cables. The second application that TYRC is developing is a "trapped flux" or "induced field" magnet (Patent No. 6,925,316) fabricated using coated conductor technology. These trapped flux coils are being used as possible high field insert coils in NMR magnets. These trapped flux magnets are incredibly simple to fabricate and have a wide variety of potential uses.

3:45 PM

(EMA-S12-034-2013) Development of Superconducting and Cryogenic Power Systems and Impact for Aircraft Propulsion (Invited)

T. Haugan*, Air Force Research Laboratory, USA; D. Latypov, Berrie Hill Research Co., USA

This paper will report on the development and status of superconducting and cryogenic power systems for aircraft propulsion, and how such systems are expected to impact capabilities and benefits. The use of new technologies such as hybrid-electric or electric drive, lightweight batteries, and fuel cells are increasingly being incorporated into automotive power systems to increase fuel efficiencies. Although not well known, these technologies are also being implemented with similar benefits in 2 and 4 passenger aircraft. The components of MW-class superconducting power systems will be reviewed, including generators and motors, power transmission cables, superconducting magnetic energy storage (SMES) devices, power electronics including inverters, and cryogenic technologies. Cryogenic power systems have unique properties such as very low weights and ultra-high efficiencies > 98%, which are expected to provide new capabilities and potential significant benefits such as reduced fuel burns > 70% for commercial aviation aircraft.

4:15 PM

(EMA-S12-035-2013) SMES for Wind Energy Systems

A. Paul Antony*, D. T. Shaw, State University of New York at Buffalo, USA

Wind energy will grow rapidly because of the increasing concern on global climate change. However, increasing penetration of wind power presents significant operational challenges in ensuring grid security and power quality due to inherent wind-resource variability. This paper addresses the integration of large wind farms into the grid through the beneficial role of superconducting magnetic energy storage (SMES) systems. The last few years have seen an expansion on both application and market development strategies for SMES. Although originally conceived as a load-leveling device for nuclear power plants, today's utility-industrial realities emphasize other applications of SMES in the development of wind energy. In the industrial section, concerns about power quality and stability have driven the development of a market for micro-SMES devices for load-leveling applications. The paper reviews the recent history of SMES, in-

cluding those made by American Superconductor's HTS SMES connected to a scaled grid in Germany and the micro-SMES in Wisconsin, Japan's SMES for hydrogen fuel cells, as well as the recent E-ARPA's proof-of-concept SMES for competing with lead-acid batteries. The aim of this paper is to influence the optimal design and configuration of SMES for land and offshore wind power generation and to propose a roadmap for the resolution of technical barriers related to the integration of wind energy to the electric grid.

S13: Body Energy Harvesting for Intelligent Systems

Body Energy Harvesting

Room: Indian

Session Chairs: Wolfgang Sigmund, University of Florida;
Seungbum Hong, Argonne Nat Lab

4:30 PM

(EMA-S13-001-2013) A New Approach to Multifunctional Lead-free Piezoelectric Films Coupled with Ultra-Thin Flexible Metal Foil Substrates for Implantable Smart Medical Devices; Sensors and Energy Harvesters (Invited)

S. Kim*, A. Leung, E. Greenstein, Brown University, USA; S. Kim, D. Kim, Auburn University, USA; A. I. Kingon, Brown University, USA

The objective of this research is to demonstrate the new approach for enlarging the sensing capacity and the power generation of implantable medical sensors and energy harvesters without any complicated MEMS process via cost effective chemical solution-derived biocompatible (Na,K)NbO₃ (NKN) piezoelectric films coupled with conducting flexible metal foil substrates. By far, the vast majority of piezoelectric medical devices is fabricated using the complicated MEMS process and is generally required precious noble metal electrodes. Use of ultra thin flexible metallic foil substrates (~ 25 μm), however, is potentially beneficial for the fabrication of large-area and complicated-shaped devices without MEMS process. In addition, the metallic foil substrate can act as an electrode with stringent process

control. Flexible metal foils coated with high quality bio-compatible piezoelectric films can also be easily laminated onto various substrates and easy to make the diaphragm structure or complicated device shape that have broad impacts on implantable medical device fabrication with high performances. In this research, we will mainly focus on the materials and the device issues, but will provide a proof-of-concept for mass-producible process with detailed technical steps.

5:00 PM

(EMA-S13-002-2013) Piezoelectric and Electroactive Strain Harvesters for Wearable and Implantable Sensor Applications (Invited)

B. Wardle*, Massachusetts Institute of Technology, USA; M. Kim, KRIS, Republic of Korea; Q. Zhang, Pennsylvania State University, USA

Harvesting energy from the human body enables wireless and sustainable operation of biomedical devices. Piezoelectric materials produce electrical charge or voltage across them when a mechanical stress or strain is applied, or vice versa, and similarly-designed harvesters can be realized using electroactive polymers. Mechanical to electrical transduction enables such materials to convert biomechanical energy from human activities into useful electrical energy. For example, piezoelectric elements such as PZT and PVDF have been integrated beneath a standard running sneaker's removable insole to scavenge energy during human walking. Sufficient power from large-amplitude, low frequency sources found in the human body run contrary to miniaturization due to well-known scaling rules. New results from modeling and testing piezoelectric-based low-frequency harvesters include the intriguing finding that maximum power is independent of piezoelectric coupling. Model-experiment correlation is useful in better understanding of piezoelectric vibration energy harvesting performance at both materials- and systems-levels, with the ultimate goal of highly efficient biomedical energy generators for wearable and implantable applications. Recent work on nanostructured electroactive polymer bender systems will also be highlighted, as an intriguing (due to the match between body harvesting and the compliant, high-strain, and low-frequency nature of these systems) and perhaps overlooked alternative for body harvesting.

Author Index

* Denotes Presenter

A

Abbott, J.	71
Acosta, M.	47
Adamo, C.	64
Aguirre, B.	39, 48
Aguirre, B.A.	48
Ahn, C.*	33
Ahn, G.	43
Akhtar, M.*	40
Aksel, E.	30, 45
Alberga, M.	63
Albuquerque, E.*	43
Alexe, M.	34
Allendorf, M.D.*	49
Alpay, S.	46
Alpay, S.P.	68
Amani, M.*	28, 43
Amann, A.	53
Amemiya, N.	74
Amemiya, N.*	51
Ando, A.	40
Andrew, J.S.*	54
Anjunyan, H.	50
Annapragada, S.*	69
Ansell, T.	47, 70
Ansell, T.*	68
Anwar, F.	48
Aoyagi, R.*	52
Appelhans, L.N.*	72
Arakawa, T.	70
Arbiol, J.	38
Arcon, D.	54
Armistead, P.*	72
Awaji, S.	29
Ayon, A.	41
Azough, F.	56
Azzam, M.H.	48

B

Baca, J.	38
Backhaus-Ricoult, M.*	63
Bae, S.	42
Baker, A.	33
Balke, N.	64
Bao, S.	53
Barbero, E.	56
Barnes, P.	51
Barnes, P.N.	56
Barrera, D.	49
Barrett, C.A.*	30
Bartolomé, E.	38
Bashaihah, S.S.	53
Bassiri-Gharb, N.	64
Bauer, E.	59
Bäurer, M.	36
Beanland, R.	25
Bedair, S.	70
Beekman, C.	64
Bell, N.	39
Beltran, H.	28
Ben, L.	51
Berbano, S.S.*	32
Berry, J.J.*	49
Besselink, R.	64
Bhalla, A.*	52
Bharadwaja, S.	60
Bhatnagar, A.	34
Bi, Z.	30, 71
Bianchetti, M.	28

Biancoli, A.	52
Biegalski, M.	64
Birdwell, A.	28
Birdwell, A.G.	43
Birkmeyer, J.	70
Blea, M.A.	41, 52
Blendell, J.	60
Blendell, J.E.	35, 61
Bock, J.A.*	63
Booth, J.*	62
Borges, R.	53
Bosse, J.	27, 34, 48
Bosse, J.*	28
Bowman, K.J.	35, 61
Bréard, Y.	50
Bregadiolli, B.	44
Brennecka, G.	57, 61, 73
Brennecka, G.L.	43, 52, 58, 60, 67, 71
Brisigotti, S.	65
Brogli, G.*	28
Brookshire, K.	71
Brown, D.	43, 67
Brown-Shaklee, H.	63, 73
Brown-Shaklee, H.J.	52, 67
Brown-Shaklee, H.J.*	41, 52
Brunke, L.*	42
Brunke, L.B.	43
Budi, M.	54
Bulovic, V.	44
Burch, M.	58
Burch, M.J.*	42
Burke, J.L.	42, 43
Burrell, A.	58
Burrell, A.K.	59
Butee, S.P.	53
Bux, S.*	49

C

Caillat, T.*	50
Calandro, B.	64
Calvin, C.	48
Cann, D.	47
Cann, D.P.	40, 52, 68
Cantoni, C.*	59
Carman, G.*	34
Carter, J.	36
Carter, J.J.*	30
Chan, H.M.*	26
Chase, J.	50
Chavez, F.	54
Chavez, J.J.	48
Chavez, T.	73
Cheaito, R.	63
Chen, A.	30, 60, 71
Chen, C.*	34
Chen, L.	39
Chen, L.*	60
Chen, S.	41
Chen, Y.	29, 56
Cheng, S.R.	49
Cheng, T.	26
Cheung, J.	31
Chi, M.	64
Chin, M.	28
Chin, M.L.	43
Cho, I.	33
Cho, J.	41, 42
Choi, E.M.	30
Choi, Y.	43
Christen, H.M.*	64

Chu, B.*	39
Civale, L.	58, 59
Civale, L.*	59
Clem, P.*	38
Cole, M.W.	68
Coleman, E.	56
Coll, M.*	38, 65
Collings, T.	51
Collings, W.E.	66
Combe, E.	56
Contreras-Guerrero, R.	27
Cordoncillo, E.	28
Cross, L.	39
Crowne, F.J.	43
Cruz-Campa, J.	48
Cruz-Campa, J.L.*	48
Cubeda, V.	65
Culp, S.*	49

D

da Silva, L.R.	43
Dameron, A.A.	49
Damjanovic, D.*	52
Dang, F.	57
Daniels, J.	35
Daniels, J.*	35
Daryapurkar, A.	55
Davis, R.J.	49
Dawson, J.	51
Deepak, N.	53
Deepak, N.*	54, 61
Denis, L.M.*	31
Deutscher, G.	38
DiAntonio, C.*	73
Dias, A.*	53
Dickey, E.	63
Dickey, E.A.	42
Dickey, E.C.	58
Dillon, S.J.*	26
Dittmann, R.	44
Dong, S.	47
Dorjpalam, E.	33
Dorpalam, E.	60
Drew, D.*	44
Drofenik, M.	54
Droopad, R.	27
Dubey, M.	28, 43
Duda, J.C.	63
Duquette, D.	60
Dynys, F.	50

E

Ebbing, C.R.	43
Eblen, M.*	27
Edney, C.	38, 39
Edwards, D.*	63
Ehmke, M.C.*	35
Elizabeth, P.A.	37
Emergo, R.	38
Eom, C.B.	66
Eshita, T.*	70
Evans, J.T.*	28

F

Fancher, C.	60
Fancher, C.M.*	61
Farrar, A.K.	64
Ferekides, C.*	48

Ferguson, I.*48
 Ferreira, P.J.60
 Ferreira, S.R.49
 Finkel, P.*66
 Finstad, T.55
 Firdosy, S.50
 Fitsch, A.N.68
 Fjeld, H.*55
 Fleurial, J.49, 50
 Flores, M.69
 Foley, B.M.*63, 67
 Folkman, C.M.66
 Follman, J.67
 Forrester, J.31
 Forrester, J.S.30, 43, 44, 45, 68
 Forrester, J.S.*67
 Foster, M.49
 Fox, A.*72
 Fox, G.71, 72
 Frank, D.39
 Franzen, S.60
 Freeman, C.51
 Freer, R.*56
 Freyand, S.71
 Fujii, T.70
 Fulco, U.L.43
 Funahashi, R.56
 Funahashi, R.*50
 Furman, E.*73

G

Galtsyan, E.29
 Gao, G.F.49
 Gao, H.30
 Gao, J.35
 Gao, P.64, 66
 Gao, P.*30, 37
 Garcia, R.60
 Gascoin, F.50, 56
 Gauntt, B.D.71
 Gazquez, J.38, 65
 Genette, T.49
 Geng, L.D.27
 Gevorgian, S.71
 Ghosh, D.*36
 Gibbons, B.71, 72
 Gibbons, B.J.63, 70
 Gibbons, B.J.*57
 Ginley, D.S.49
 Glaum, J.31, 35
 Glaum, J.*47
 Goda, K.51
 Gonzales, E.48
 Gopalan, P.55
 Gorfman, S.25
 Gorzkowski, E.*73
 Gough, D.49
 Gough, D.V.39, 71
 Goyal, A.*38
 Graham, J.T.43, 67
 Graham, J.T.*60
 Grasso, G.*65
 Greenstein, E.75
 Grin, Y.*55
 Grishin, I.28
 Grote, J.G.73
 Guilmeau, E.50
 Guo, H.36
 Guo, Y.35, 37
 Guzmán, R.38
 Gyergyek, S.54

H

Haberkorn, N.59
 Hackenberger, W.73
 Hamajima, T.74
 Han, B.33
 Han, H.36
 Han, J.41
 Han, Y.*67
 Haneda, H.57
 Harding, J.51
 Hardy, V.50
 Harmer, M.P.26
 Harrington, S.A.30
 Harris, D.T.42
 Harris, D.T.*58
 Haruyama, J.*39
 Haugan, T.38, 42, 51
 Haugan, T.*74
 Haugan, T.J.43
 Haugan, T.J.*42
 Hauser, A.62
 Hayakawa, N.*41
 He, J.34
 Hebert, S.*56
 Hellstrom, E.*66
 Hellstrom, E.E.66
 Henriques, A.J.67
 Henriques, A.J.*43
 Hesse, D.34
 Higashikawa, K.29
 Hishinuma, Y.*70
 Hoffman, M.31, 35, 47
 Hoffmann, M.J.*36
 Holc, J.69
 Hong, K.33
 Hong, S.43
 Hong, W.32
 Hopkins, P.E.41, 63, 64, 67
 Hoshina, T.32
 Howe, J.64
 Hsu, J.W.49
 Huang, C.50
 Hudak, N.39
 Huey, B.64
 Huey, B.D.28
 Huey, B.D.*27, 34, 48

I

Ihlefeld, J.34, 57, 61
 Ihlefeld, J.*64, 71
 Ihlefeld, J.F.31, 41, 43, 58, 60, 63, 67
 Iijima, Y.29
 Imai, H.57
 Inoue, M.29
 Inoue, N.40
 Itoh, Y.74
 Ivanov, T.70
 Iwasaki, K.41
 Iwata, Y.51
 Izumi, T.29
 Izumi, T.*29

J

Jagodic, M.54
 Jang, M.61
 Janka, O.49
 Jankovic, S.66
 Jarmon, D.49
 Jeon, Y.57
 Jeong, S.39

Jia, Q.58, 71
 Jia, Q.X.*30, 59
 Jiang, J.34, 66
 Jin, Y.M.*27, 47
 Jiten, C.46
 Jo, J.39
 Jo, W.44, 61
 Jones, B.A.73
 Jones, J.L.30, 31, 36, 43, 44, 45, 58, 67, 68
 Jones, J.L.*61
 Jones, W.42
 Joyce, D.*73
 Jung, J.*37
 Jung, Y.42

K

Kagomiya, I.45, 46
 Kajdos, A.62
 Kajiwara, M.74
 Kakimoto, K.46
 Kakimoto, K.*45
 Kalem, V.*55
 Kalkur, T.S.68
 Kametani, F.66
 Kampe, S.L.47
 Kaneko, R.45
 Kaplan, W.D.*26
 Karlicek, R.F.*48
 Kato, K.*57
 Kauzlarich, S.49
 Keeble, D.25
 Keeney, L.53, 54, 61
 Keyawa, N.50
 Khatri, N.D.29
 Kim, B.61
 Kim, C.51
 Kim, D.36, 75
 Kim, H.34
 Kim, H.*41
 Kim, I.39
 Kim, J.33, 36, 41, 51
 Kim, J.*36
 Kim, M.39, 75
 Kim, S.39, 75
 Kim, S.*33, 43, 75
 Kim, Y.34, 43
 Kingon, A.I.75
 Kishio, K.59
 Kiss, T.*29
 Kitagawa, S.40
 Kitahara, T.52
 Kitano, H.74
 Klie, R.F.27
 Ko, S.60
 Kobayashi, K.45
 Kobayashi, N.P.56
 Kocic, L.66
 Kodumudi Venkataraman, L.*68
 Koley, G.30
 Kolosov, O.28
 Kolte, J.*55
 Koo, H.42
 Korobova, N.*72
 Kosec, M.69
 Koster, G.64
 Kotula, P.G.71
 Kováč, J.51
 Kováč, P.51
 Kowalski, B.*33
 Koyanagi, K.51
 Kracum, M.26
 Kral, K.*29

Parilla, P.A.	49	Rijnders, G.	64	Singh, G.*	31
Park, C.	41, 42	Rijnders, G.*	64	Singh, K.C.*	46
Park, H.	36	Rindfleisch, M.	51	Singh, K.M.	73
Park, S.	33	Rindfleisch, M.A.	66	Siqueira, K.	53
Parker, S.	56	Rivas, M.	27	Small, L.	60
Patterson, E.	47, 57, 71	Robinson, D.	61	Smith, A.*	67
Paul Antony, A.*	74	Rödel, J.	61	Smith, S.R.	73
Paunovic, V.	40, 66	Rodriguez, J.*	27	Snyder, J.	49
Pelloquin, D.	56	Roedel, J.*	44	Snyder, R.	41
Pemble, M.E.	53, 54, 61	Roelofs, A.*	65	Soares, J.	53
Peng, X.	51	Rogoy, M.*	60	Solovyov, V.*	38
Peng, Z.	53	Ronning, F.	59	Song, G.	67
Perejon, A.	54	Rossetti, G.	46	Song, J.*	39
Perez-Maqueda, L.A.	54	Rossetti, G.A.*	25	Song, K.	41
Perini, S.E.	73	Rouco, V.	38	Song, X.	41
Perkins, J.D.	49	Roy, S.	53	Song, X.*	56
Piccardo, R.	65	Rozic, B.	54, 69	Šouc, J.	51
Pierce, B.*	43	Ruff, A.	62	Spencer, M.G.	30
Pilania, G.	46			Spoerke, E.	48, 49
Pimentel, A.	48	S		Spoerke, E.*	39
Poeppelmeier, K.*	25	Sachet, E.	37	Spoerke, E.D.	48, 71
Pojprapai, S.*	45	Sachet, E.*	60	Spreitzer, M.	71
Pokale, G.B.*	53	Safa-Sefat, A.	59	Sreenivasulu, G.	54
Polak, M.	51	Sahu, S.	31	Srinivasan, G.*	54
Polcawich, R.G.	70, 71	Sahul, R.	73	Starr, J.D.	54
Polcawich, R.G.*	70	Saito, K.	31	Stavila, V.	49
Polomoff, N.	27	Saito, T.	29	Stemmer, S.*	62
Polyanskii, A.	66	Sakata, A.	36	Stickle, W.	57, 71
Ponomareva, I.*	47	Salem, D.R.	39	Studer, A.	45
Prades, M.	28	Sales, B.C.	59	Studer, A.J.	35
Prasertpalichat, S.*	40	Salguero, T.T.	30	Sudarshan, T.S.	30
Prieto, H.	48	Sanchez, C.A.	48	Sumption, M.	51
Priya, S.	32	Sanchez, L.	70	Sumption, M.D.*	66
Proie, R.	70	Sanchez, L.M.*	71	Sun, N.*	68
Przybysz, J.X.	31	Sanders, T.	61	Suu, K.*	70
Pudasaini, P.*	41	Sbrockey, N.	30, 56	Suvorov, D.	71
Puig, T.	38, 65	Sbrockey, N.M.*	68		
Pulskamp, J.	70	Schaefer, B.*	31	T	
		Schelhas, L.	34	Tagantsev, A.K.*	46
Q		Schlom, D.G.	64	Tai, K.	26
Qiao, Q.*	27	Schmidt, M.	53	Takagi, H.	40
Qing, R.*	32	Schrade, M.	55	Takahashi, H.	56
Qu, W.	33	Schrettle, F.	62	Takao, T.	74
		Schwartz, J.	64	Takato, M.*	31
R		Sebastian, M.P.	42	Takeda, H.	32
Radcliff, T.D.	69	Sehirlioglu, A.	33, 50	Takeda, K.	32
Raengthon, N.*	52	Seidel, J.*	33	Takeuchi, I.	62, 71
Raghavendra, N.	56	Seifikar, S.*	64	Takeuchi, I.*	57
Rajagopalan, R.	33	Selvamanickam, V.*	29	Talvacchio, J.*	31
Rajashekhar, A.	60	Seo, I.	61	Tan, X.*	32, 36
Raju, K.	53	Seo, I.*	61	Tang, M.*	37
Ramesh, R.*	25	Seo, S.	33	Tarantini, C.	66
Ramprasad, R.*	46	Seshadri, S.B.	43, 44, 67	ten Elshof, J.E.*	64
Randall, C.	67	Seshadri, S.B.*	68	Tenne, D.	64
Randall, C.*	39, 73	Shannon, S.C.	67	Terazawa, T.	74
Randall, C.A.	32, 33, 45, 63	Sharma, P.A.	41	Thomas, E.L.	56
Ranjan, R.	26, 68	Sharma, V.	46	Thomas, E.L.*	41
Rao, B.*	26	Shaw, D.T.	74	Thomas, P.A.	36, 68
Rao, W.	26	Shelton, C.	71	Thomas, P.A.*	25
Rasic, G.	64	Shelton, C.T.*	37	Thong, C.J.	51
Ratcliff, M.M.	42	Shi, J.	38	Tidrow, S.*	40
Ravi, V.	50	Shimoyama, J.	59	Timoshenkov, S.	72
Reaney, I.M.*	62	Shimura, H.	74	Timuçin, M.	55
Reichart, J.N.	42	Shintomi, T.	74	Tobita, H.	29
Ren, X.*	35, 53	Shiohara, Y.	29	Togano, K.	65
Ren, Z.	37	Siemons, W.	64	Tolbert, S.	34
Rey, C.*	74	Sigdel, A.K.	49	Tolson, J.T.	30
Rhee, K.*	42	Sigmund, W.	32	Tompa, G.S.	30, 68
Rheinheimer, W.	36	Sigmund, W.M.	37	Tompa, G.S.*	56
Ricart, S.	38	Simons, H.	47	Tomsic, M.*	51
Rickman, J.M.	26	Sinclair, D.*	51	Tomsic, M.J.	66
		Singh, A.K.*	30	Torres, M.	56

Author Index

Triamnak, N.*	.52	Wang, H.*	.71	Yan, L.	.30		
Trolrier-McKinstry, S.	.63, 72	Wang, J.	.35, 49	Yan, Y.*	.32		
Trolrier-McKinstry, S.*	.60	Wang, W.	.70	Yang, H.*	.62		
Tropeano, M.	.65	Wang, X.	.38	Yang, O.	.40		
Tsai, C.	.60	Wang, Y.	.62	Yang, P.	.73		
Tsai, C.*	.39	Wang, Y.U.	.47	Yang, Y.	.53		
Tsuda, M.*	.74	Wang, Y.U.*	.26, 45	Yao, Y.	.29, 53		
Tsurumi, T.*	.32	Wang, Z.	.42	Ye, L.	.34, 48, 64		
Tumino, A.	.65	Ward, D.	.48	Ye, S.	.38, 65		
Turney, J.	.49	Wardle, B.*	.75	Yimmirun, R.	.52		
U						Yokota, T.	.52
Uchikoba, F.	.31	Waser, R.*	.44	Yoo, K.	.36		
Uddin, M.	.30	Watanabe, K.	.29	Yoon, S.*	.41, 42		
Uhl, D.	.49	Weber, W.J.	.67	Yoshikawa, M.	.74		
Ursic, H.	.69	Wee, S.	.38	Yoshimoto, M.	.51		
Usher, T.*	.45	Weiss, J.	.66	Yoshizumi, M.	.29		
Uthaisar, C.	.45	Weiss, J.D.	.66	Young, S.E.	.32		
V						Yu, Q.	.57
Vailionis, A.	.64	West, A.R.	.28, 54, 55	Yu, Z.	.26		
Valanoor, N.	.31	West, A.R.*	.63	Z			
Valov, I.	.44	Whatmore, R.W.	.54, 61	Zakutayev, A.	.49		
Veber, A.*	.71	Whatmore, R.W.*	.53	Zavelkink, A.	.49		
Veldhuis, S.A.	.64	Wheeler, J.	.39	Zhang, J.	.32, 68		
Venkat, N.	.73	Widjonarko, N.E.	.49	Zhang, P.	.54, 61		
Viehland, D.	.66	Winter, M.	.73	Zhang, Q.	.75		
Vier, D.C.	.43	Withers, R.L.	.35	Zhang, Q.M.	.69		
Vlad, R.	.38	Wong, B.	.49	Zhang, W.	.71		
Vo, T.	.49	Wong-Ng, W.	.41	Zhang, X.	.60		
Vodopyanov, V.	.72	Woodward, D.	.25	Zhang, Y.	.26, 58, 66, 67		
Von Allmen, P.	.49	Wu, J.*	.38	Zhang, Y.Y.	.59		
Vorobiev, A.	.71	Wu, M.*	.69	Zhao, Z.	.60		
Vyas, V.	.27	Wu, Q.	.26	Zhou, C.	.35		
W						Zhou, J.	.26, 45
Wada, S.	.57	X				Zhou, N.	.26
Wada, S.*	.72	Xi, X.*	.59	Zhou, X.	.48		
Walenza-Slabe, J.*	.70	Xiao, D.	.53	Zhu, J.*	.53		
Wang, A.	.44	Xiong, J.	.30	Zhu, Y.	.58, 60		
Wang, H.	.30, 39, 59, 60, 62	Xu, A.	.29	Zou, G.	.59		
		Xue, D.	.35	Zou, G.*	.58		
		Y				Zubia, D.	.48
		Yamaguchi, H.	.70				
		Yamamoto, A.	.59				
		Yamamoto, H.*	.58				